Department for Environment Food & Rural Affairs

Department for Business, Energy & Industrial Strategy

Met Office
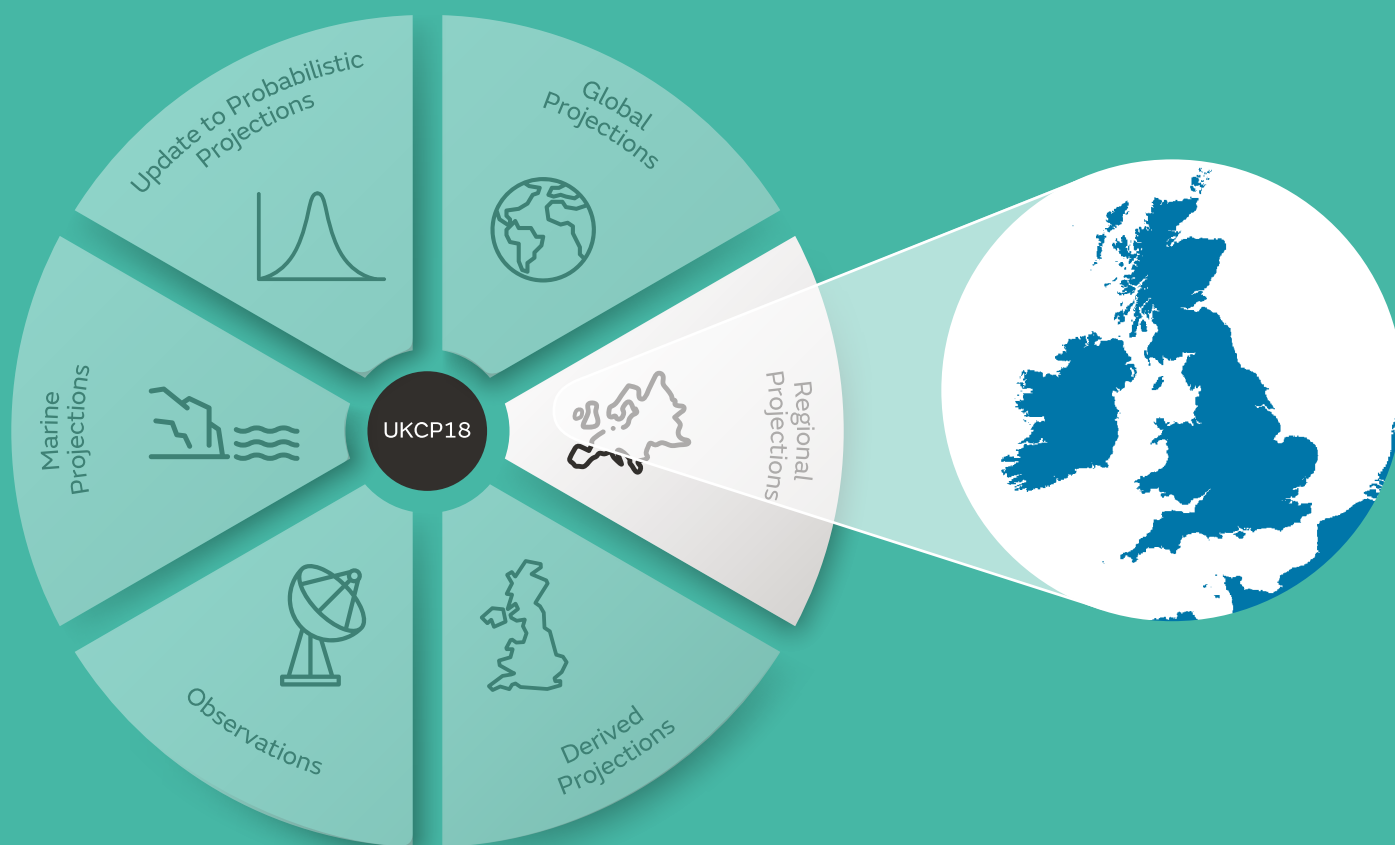**Hadley Centre**

Environment Agency

UKCP Convection-permitting model projections: Science report
September 2019

Author: Elizabeth Kendon

Co-authors: Giorgia Fosser, James Murphy, Steven Chan, Robin Clark, Glen Harris, Adrian Lock, Jason Lowe, Gill Martin, Jenny Pirret, Nigel Roberts, Mike Sanderson, Simon Tucker
Internal reviewers: Mike Bush, Richard Jones, Cath Senior
External reviewers: Brian Hoskins, Erik Kjellström, Christoph Schär, Bart Van den Hurk

Version 1.0

Contents

Non-technical summary

This report describes a new addition to the UKCP18 climate projections. For the first time internationally, a climate model at a resolution on a par with operational weather forecast models, is being used for national climate scenarios. This model allows us to examine the risk of extreme weather events in local areas for the coming decades.

> " **We are able to describe how climate change will impact the types and extremes of weather for your local area.** "

Global and regional climate models have typical resolutions of 60-300km and 10-50km, respectively. The new 2.2km "convection-permitting" model (CPM), by comparison, represents a step forward in our ability to simulate small scale behaviour seen in the real atmosphere, in particular atmospheric convection, and the influence of mountains, coastlines and urban areas. As a result, the CPM provides access to credible climate information on hourly timescales, important for small-scale weather features that affect flooding in summer, and also on local (kilometre) scales, improving our understanding of climate change in cities. Although the new data can provide information on small-scale weather events in the future, it should not be confused with an operational weather forecast, which provides information on weather that is likely to be experienced in the next few days. Instead the CPM provides a set of plausible projections of climate change for the UK if we follow a high emission pathway. In particular, it provides information on the local effects of changes in the types of weather that may be experienced in the future.

The new CPM projections are an addition to the UKCP18 toolkit, the land component of which consists of three Strands of information. Strand 1 provides updates to the UKCP09 probabilistic predictions, Strand 2 provides a new set of global model projections and Strand 3 provides downscaled regional climate model (RCM) projections. Projections from Strands 1, 2 and the 12km RCM projections from Strand 3 were released in November 2018 (Murphy et al., 2018). The 2.2km CPM projections are a new addition, which should be used in combination with these other Strands of information. In particular, the wider sampling of uncertainties in Strands 1 and 2 should be considered. Taken together the UKCP18 projections replace the previous UKCP09 scenarios. The CPM provides information at similar frequencies (daily and hourly) and spatial resolution as the UKCP09 weather generator. However, the CPM is based on a realistic physical representation of relevant climate processes, rather than relying on statistical relationships based on past observations. The UKCP18 website (https://www.metoffice.gov.uk/research/collaboration/ukcp) contains links to general advice on how to use the UKCP18 projections (Fung et al., 2018), and specific advice for previous users of UKCP09 (Fung and Gawith, 2018).

The new projections build on previous studies, which have shown that CPMs are able to represent hourly rainfall characteristics, including extremes, much more realistically than conventional climate models run at coarser spatial scales (Kendon et al 2014). However, the high cost of the simulations means that until now CPM results were based only on a single model projection of future climate change. Therefore, it has not been possible to assess uncertainties in the climate change signal at these scales. UKCP18 is the first time an ensemble of climate simulations has been carried out at convection-permitting resolution. The ensemble consists of 12 projections, run at 2.2km resolution. Each projection represents a plausible realisation of the future climate assuming no curbs on greenhouse gas emissions, with the ensemble members differing due

to natural climate variability and uncertainty in the global model physics. The CPM ensemble therefore gives an indication of uncertainties in future changes on kilometre and hourly scales for use in risk assessments, providing locally relevant information to inform decision making. However, we note that uncertainty in the convection-permitting model physics itself has not been sampled nor has information from other international climate models. The CPM ensemble therefore underestimates uncertainties.

The CPM projections provide data for the UK, for three 20-year periods (1981-2000, 2021-2040 and 2061-2080) under a high emission scenario RCP8.5. The 12 ensemble members are driven by the Strand 3 12km RCM ensemble. The CPM is based on the Met Office operational UK weather forecast model (UKV), which has been extensively tested for use in that context. The CPM shares many of the same model physics settings as the 12km RCM, but with some notable differences particularly in how convection is represented. Details on the model are provided in Section 2. Results presented here focus on temperature and precipitation, but some other variables including soil moisture, snow, cloud and lightning have also been considered.

Summary findings

Present-day model performance

- The CPM better simulates several aspects of present-day climate, which is verified by comparing the model results with observations of the real world. This leads to improved confidence in its ability to project the effects of future changes to aspects of our weather relating to extreme events at local and hourly scales. Here we examine how well the CPM represents the present-day climate compared to the driving 12km RCM (Section 3). We mainly consider temperature and precipitation, including extremes such as hot summer days and heavy downpours.

- In winter, the RCM is too cold in the north of the UK and too warm in the south, whilst the CPM gives better agreement with observations. The CPM also better represents cold winter days and the number of intense cold spells in the north UK in the present-day. In summer, the CPM is warmer than the RCM, giving better agreement with observations in the north but not in the south where it has a tendency for hot days to be too hot. These model differences are likely due to differences in the representation of snow (less lying snow in the CPM in winter), cloud (less cloud in the CPM) and the tendency for soil to be drier in the CPM.

- The CPM gives a significantly better representation of how rainfall varies day-to-day and hour-to-hour. In particular, rainfall is too persistent in the RCM, which leads to too much overall rainfall. There are fewer wet days in the CPM in better agreement with observations, although the CPM has too few wet days in the far south in summer. The CPM better simulates heavy rainfall in winter and over mountains. In summer, away from mountains, there is a tendency for heavy events to be too heavy in the CPM, resulting in poorer agreement with observations than the RCM. In common with climate models more generally, the RCM is unable to capture short intense downpours that can lead to flash flooding. Such events are more realistically captured in the CPM, although again they tend to be too heavy. These improvements in the CPM are due to the better representation of convection, and also of mountains and coastlines.

Climate change projections

- The CPM results do not change the UKCP18 headline message of a greater chance of warmer wetter winters and hotter drier summers across the UK in future (Lowe et al, 2018). For 2061-80, under a high emission scenario (RCP8.5), the CPM ensemble suggests winters will be warmer by 1.8-3.3ºC[1] and wetter by 16-42%, whilst summers will be hotter by 3.6-5.0ºC and drier by 16-46%. In general the CPM reinforces the results from the 12km RCM, projecting similar overall changes to UK climate. However the CPM results do provide new information in terms of winter mean precipitation changes, changes in extremes and changes at local scales (Section 4, Table 5.1).

- Mean temperature increases everywhere and in all seasons in future, with the greatest increases occurring in the south. The CPM ensemble shows increases in hot summer days (3.7-6.8ºC[1] increase by the 2070s under RCP8.5) and the frequency of hot spells, reinforcing the results of the RCM. In winter, there is a smaller increase in temperature over Scotland in the CPM compared to the RCM, with a smaller increase in the temperature of cold winter days and a smaller decrease in the frequency of intense cold spells. These differences are likely related to differences in lying snow, with a greater decrease in lying snow in the future in the RCM.

- Average winter precipitation increases in future, with the possible exception of northern Scotland where decreases are possible. We find that the CPM shows much greater increases than the RCM (27% compared to 16% increase[2]), due to greater increases in the number of wet days. This may be because it rains so often in the present-day in the RCM that there is little scope for this to increase further, although more research is needed to investigate this. Also the better representation of convective showers and their movement inland in the CPM may be a factor.

- Average summer precipitation decreases in future in the CPM ensemble, again with the possible exception of northern Scotland. The average changes are broadly consistent between the CPM and RCM ensembles, but the underlying changes in rainfall on a day-to-day and hour-to-hour basis are quite different. In particular, it rains less often in the future, but the rain is heavier when it does – and this shift to more intense rainfall in summer is more pronounced in the CPM projections. These changes in rainfall are primarily driven by increased moisture in the atmosphere with warming, leading to heavier rainfall, which is captured by both the CPM and RCM. However, local processes within the storms themselves can amplify increases, and these are only represented in the CPM projections.

- Hourly precipitation extremes increase in future. The CPM shows increases of 25%[3] in the precipitation associated with an event that occurs typically once every 2 years. RCM projections for hourly extremes are considered unreliable.

Use of projections

- The release of the CPM projections provides further capability to the UKCP18 suite of climate projection tools. The CPM provides information on changes in hourly rainfall and for local areas that can be used in local decision making, for example information on urban flooding for contingency planners. However, the CPM and RCM ensembles sample a narrower range of uncertainty than the UKCP18 Strand 1

---

[1] The range quoted corresponds to the UK-average of the 2nd lowest to 2nd highest responses across the 12-member CPM ensemble.
[2] UK-average of the central response across the 12-member ensemble
[3] UK-average of the central estimate across the 12-member CPM ensemble

(probabilistic) or Strand 2 (global model) projections. This is because they are driven exclusively by variants of a recent configuration of the Met Office Hadley Centre global model, and currently lack information from other international climate models, in contrast to Strands 1 and 2. Users need to balance the improvements the CPM offers against the fact that not all uncertainties are sampled. Where possible, users should use the new CPM projections in combination with other UKCP18 products that provide a wider sampling of uncertainty.

- The CPM results largely reinforce results from the RCM in terms of UK seasonal mean changes. One possible exception is for changes in winter precipitation where the CPM suggests greater increases compared to the RCM. Research is ongoing to understand the complex drivers behind this, but initial analysis suggests that projections based on conventional coarser resolution climate models may underestimate "upper-end" responses in winter mean precipitation (Section 5), although studies with other CPMs are needed to confirm this.

- For temperature, there is no evidence to suggest that the CPM projections are more or less plausible than those from the RCM. In some cases there are differences in the projections between the models, notably for temperature changes over Scotland in winter. In this case, although the CPM gives better agreement with observations, it has a less sophisticated treatment of lying snow, and so we do not have greater confidence in its projections. Thus for temperature changes, we recommend usage of information from Strand 1 and 2 given the more comprehensive view of uncertainties, except where fine spatial detail is required.

- The CPM projections are expected to be the primary source of information for users interested in daily rainfall extremes in summer or changes on hourly timescales. For these the CPM projections are considered more plausible, due to the better representation of convection and local processes in storms in the CPM. However, there are still deficiencies, as many convective storms occur on scales smaller than 2.2km in reality. Further research is needed to assess the importance of these deficiencies for future projections. Projections of hourly rainfall change from conventional climate models are unreliable. Coarser resolution models also likely underestimate increases in summer rainfall intensity, with implications for flood risk assessment.

- The CPM is expected to better represent changes over cities, due to the higher spatial resolution and use of a more sophisticated urban scheme, although more work is needed to confirm this. Also over mountains and coastlines, the added spatial detail provided by the CPM may be important for some users.

- We have confidence that the UKCP18 projections provide significant improvements on UKCP09, and additions of new capability. Nevertheless, there are still limitations in our ability to project 21st century weather and climate. For example, although the CPM provides a big step forward in representing small scale behaviour in the real atmosphere, there are still deficiencies. Also all projections are conditioned on the chosen scenario of future greenhouse gas emissions (RCP8.5) and the particular models and methodologies we employ in UKCP18. Supporting guidance documentation is being developed with the purpose to guide users through the new projections.

1 Introduction

The UKCP18 land projections replace the previous UKCP09 scenarios, taking into account subsequent feedback from users and developments in modelling capability. The new projections consist of three Strands. Strand 1 provides updated probabilistic projections, which incorporate new information (notably from the latest CMIP5 generation of international climate models). These are a direct replacement for the probabilistic projections that formed the centrepiece of UKCP09. In addition, UKCP18 includes two new products (Strands 2 and 3), consisting of time series of climate model output, without the extensive statistical postprocessing required to produce Strand 1. These are provided in response to user requests for flexible datasets consisting of a wider range of climate variables with full spatial and temporal coherence, capable of supporting a range of impacts assessments. Strand 2 provides a new set of global model projections including a 15-member perturbed parameter ensemble (PPE) of the Hadley Centre global model HadGEM3-GC3.05 (hereafter GC3.05-PPE) and a 13-member multi-model ensemble of CMIP5 models (hereafter CMIP5-13). GC3.05-PPE is higher resolution than the global simulations that formed the core of UKCP09, in particular 60km grid spacing compared to 300km, as well as including several model improvements. Strand 3 provides downscaled regional climate model (RCM) projections, with a 12-member ensemble with a 12km grid spacing for Europe. The UKCP18 Land Projections Part 1 report (Murphy et al, 2018) describes and compares projections from Strands 1, 2 and 3. This Part 2 report presents results from a 12-member ensemble with a 2.2km grid spacing for the UK, which form a second component of Strand 3. These simulations are termed "convection-permitting" because convective storms are explicitly represented on the model grid, providing new capability for advice on projected changes at very fine spatial and temporal scales. This new 2.2km convection-permitting model (CPM) ensemble is compared with the 12km RCM, and guidance is provided on the interpretation and use of these projections in the context of the other Strands of information from UKCP18.

1.1 Recap of UKCP09 and drivers for UKCP18

The UK Climate Projections UKCP09 (Jenkins et al, 2009) were the first set of UK scenarios developed to support risk assessments, providing quantitative estimates of uncertainty in future climate change. In addition to probabilistic projections, UKCP09 provided a set of regional projections using a 25km grid spacing. These consisted of an 11-member perturbed parameter ensemble of RCM simulations for Europe, supporting applications requiring detailed impacts information at local to sub-national scales. For example the 25km projections were used in assessments of drought (Burke et al, 2010), river flows (Prudhomme et al, 2012), water availability (Sanderson et al, 2012), flood frequency (Kay and Jones, 2012), and effects on the electricity and rail networks (McColl et al, 2012; Palin et al, 2013). It was necessary to use the RCM simulations if time-series of spatially consistent future projections were required, and UKCP09 users were encouraged to use the RCM simulations in conjunction with the broader sampling of uncertainties contained in the probabilistic projections.

A weather generator (Jones et al, 2010) was also provided in UKCP09, which was driven by change factors sampled from the projections. The weather generator provided time series information at the hourly and 5km scale, but only utilizing 25km scale climate change information. Thus any climate change processes specific to local or hourly scales (for example greater increases in hourly precipitation extremes due to local storm feedbacks, Lenderink and van Meijgaard, 2008) were not represented in the weather generator output.

Since UKCP09 there have been substantial model developments leading to better simulations of regional climate variability in the European/North Atlantic sector. In particular, in the Met Office Unified Model there has been a major revision to the dynamical core (Wood et al, 2014), numerous improvements to parameterisations of sub-grid scale processes (Walters et al, 2017), and replacement of the ocean and sea-ice models (Williams et al, 2018). Dynamical coupling between the stratosphere and troposphere, which may influence changes in the winter storm track, is now more accurately represented through an increase in vertical levels in the global model. Also an increase in horizontal resolution using a 60km grid spacing globally has led to a better representation of synoptic weather systems compared with the 300km global simulations in UKCP09. Regional climate models are now commonly run at 12km resolution (Giorgi et al, 2009) giving a better representation of mountains, land-sea contrast and mesoscale circulations. In addition, the advent of very high resolution (km-scale) climate models since UKCP09 has enabled a more physically realistic representation of convection and for the first time a plausible estimate of climate change on hourly scales (Kendon et al, 2014), as well as information on local scales representing for instance urban effects (Argueso et al, 2014). These recent developments in modelling capability are a major driver for the new UKCP18 projections (Williams et al, 2018).

A guidance document (Fung and Gawith, 2018) is available which provides advice on UKCP18 for UKCP09 users, including which data products have been updated and which are new. This document will be updated following release of the UKCP18 CPM results, to provide guidance on how these new results should be used alongside previous UKCP09 outputs. In particular, the pros and cons of using the CPM results as a replacement to the UKCP09 weather generator output will be outlined.

1.2 Key results from UKCP18 Land Projections report

The updated probabilistic projections from Strand 1, the global projections from Strand 2 and the 12km regional projections from Strand 3 are presented in the UKCP18 Land Projections report (Murphy et al, 2018). The report provides detailed information on the methodologies and new climate models used, as well as an evaluation of historic performance and projections of future variability and change for the UK. Here we summarise the key results.

Strand 2 consists of a 15-member perturbed parameter ensemble GC3.05-PPE, augmented by a 13-member multi-model ensemble CMIP5-13. In general GC3.05-PPE members perform well in comparison to CMIP5-13 models when assessed across a range of key atmospheric variables globally, including temperature, precipitation, humidity, circulation and radiation fields. For Europe, GC3.05-PPE members all show a cold bias in winter. The median bias is considerably larger than that of CMIP5-13, being greatest over northern Europe and much smaller (less than 2ºC) over the UK. The magnitude of the cold bias varies between members, and is affected by several factors (Murphy et al, 2018). All members show a negative bias (of varying magnitude) in longwave heating from clouds, while in some members the cold bias is exacerbated by a relatively weak Atlantic Meridional Overturning Circulation (AMOC), or (in two members) weaker than observed average westerly flow over the North Atlantic and Europe. A further factor is a slight cooling in global mean surface temperature that occurs during the second half of the 20th century, which manifests in most GC3.05-PPE members and in all seasons of the year. This contrasts with a warming in observations, and is probably related to the large-scale effects of anthropogenic aerosol forcing, which is relatively strong in the relevant members. For other seasons the two Strand 2 ensembles show similar temperature biases. GC3.05-PPE is also too wet in winter (as is CMIP5-13) whilst showing too little precipitation over central and southern Europe in summer.

In terms of interannual variability the Strand 2 ensembles perform comparably, and for UK precipitation variability the GC3.05-PPE members typically perform better. The GC3.05-PPE members give quite realistic simulations of the North Atlantic storm track, which is important for driving climate variability and extremes across Europe. In particular the number of storms tracking across the UK is quite well captured in GC3.05-PPE, being only slightly higher than reanalysis values in the ensemble-mean (see Fig. 3.17 of Murphy et al, 2018), with a spread of modest positive or negative biases between members. In comparison, CMIP5-13 members also give a range of biases in storm numbers over the UK, but with a larger positive bias in the ensemble-mean.

The Strand 3 12km regional projections consist of a 12-member PPE, hereafter RCM-PPE. This uses a limited area configuration of the GA7.05 atmospheric model spanning Europe (HadREM3-GA705) and is driven by 12 of the 15 GC3.05-PPE members. The RCM-PPE is first evaluated for the historical period (1981-2000). For seasonal mean temperature and precipitation, the RCM-PPE captures the observed spatial contrasts, with the impact of the downscaling showing clear orographic effects. In particular, high precipitation amounts over mountain areas of the UK are represented with substantial skill. RCM-PPE has higher precipitation than GC3.05-PPE, leading to a broad-scale wet bias in winter but improvements in dry biases over central and southern Europe in summer. For the latter region, however, there is an overestimation of interannual temperature variability in warm summer months, possibly due to errors in local soil moisture feedbacks. The RCM-PPE has increased cloud cover compared to the driving GC3.05-PPE, which acts to reduce the cold bias over northern Europe.

In general, large-scale patterns of bias in RCM-PPE follow those of GC3.05-PPE, reflecting the strong control exerted by the driving model (and consistent with the aim of our one-way nesting approach). It is on finer spatial scales and shorter time-scales that added value of the downscaling is apparent. In particular, the simulation of cold daily extremes in winter is improved in the RCM-PPE compared to the driving GC3.05-PPE (with cold biases in the north and over high-elevation regions and warm biases along the south coast reduced). Also daily precipitation extremes are better captured, especially in winter, with substantial reductions in the dry bias found in GC3.05-PPE over UK mountainous regions. Benefits of enhanced resolution are seen especially in coastal areas and regions of high orography, both for extreme events and in the climatological average.

In terms of future changes, Strand 1 results are derived from large samples of potential outcomes, and are formally constrained by observations. This allows them to be interpreted as probabilistic estimates, conditional upon the climate modelling inputs and statistical methods used to produce them. On the other hand, Strands 2 and 3 provide limited sets of individual projections with full spatial and temporal coherence. They are intended for impacts assessments and the development of storylines. The GC3.05-PPE members simulate relatively high levels of globally averaged warming, lying mostly above the range of changes in CMIP5-13 and towards the upper end of the Strand 1 probability distribution (Murphy et al, 2018). This appears to be related to the occurrence of strong positive cloud feedbacks in GC3.05-PPE. The levels of warming in the GC3.05-PPE simulations suggest that most members possess values of climate sensitivity (the equilibrium response to a doubling of CO_2) above 4.5ºC, lying outside the IPCC likely range of 1.5-4.5ºC, but below the IPCC unlikely level of 6ºC.

Strand 1, Strand 2 and Strand 3 projections are provided for the RCP8.5 scenario. (Strand 1 probabilistic projections are also provided for SRES A1B and RCP2.6, 4.5 and 6.0, and additional synthetic data derived from the Strand 2 global projections are provided for RCP2.6 and for changes consistent with 2ºC and 4ºC levels of global warming). Strand 1 provides the broadest uncertainty ranges, whilst Strand 3 shows the

narrowest uncertainty ranges since the other Strands contain information from multi-model simulations alongside the relevant PPE results. For the UK, the average change in temperature for 2061-80 under RCP8.5 is 2.4ºC, 2.7ºC and 3.1ºC in winter and 3.1ºC, 4.2ºC and 4.8ºC in summer, for the central estimate from Strands 1, 2 and 3, respectively. For winter, Strand 1 reveals potential outcomes below 1ºC at the lower end and above 4ºC at the upper end. Corresponding numbers for summer are below 1ºC and above 5ºC. Such extreme responses are not represented in Strands 2 or 3 in winter, but high-end responses in summer are similar in Strands 2 and 3. For precipitation, the projections show a shift to wetter winters and drier summers across the UK. The central estimate for UK average change in precipitation is 16%, 14% and 17% in winter and -23%, -22% and -26% in summer, for Strands 1, 2 and 3, respectively. Uncertainty ranges show that modest reductions in precipitation (up to 10%) are possible in winter, whilst increases in summer precipitation are also plausible (high-end changes from Strand 1 give a UK average value of +2%).

In winter there is a high degree of overlap between the GC3.05-PPE and CMIP5-13 ensembles of Strand 2, but this is not the case in summer. In particular, GC3.05-PPE samples a stronger UK summer warming signal, with temperature changes largely above the CMIP5-13 ensemble-mean and Strand 1 median value. In addition, all GC3.05-PPE members simulate a reduction in summer precipitation over northern Europe and the UK, whilst some CMIP5-13 members project an increase. This difference appears to be in part explained by GC3.05-PPE members simulating larger increases in the summer North Atlantic Oscillation. As a consequence of this difference, there is a greater tendency for summer precipitation reductions in Strand 3 (UK-average high-end changes are +2%, -6% and -17% for Strands 1, 2 and 3), since this is built entirely from a PPE that produces a consistent drying signal across its members.

Strands 2 and 3 provide information on future changes for a wide range of climate indicators, including extremes on fine spatial and temporal scales. For example for daily extremes, GC3.05-PPE shows substantial warming for cold winter days (1st percentile of daily mean temperature distribution) over the northern UK (of up to 9ºC in places, with high end changes exceeding 10ºC). The intensity of hot summer days (99th percentile of daily mean temperature distribution) also increases everywhere (by about 6ºC, with high end changes up to 9ºC in the south). For precipitation, there is a general shift towards heavier events. In winter, extreme precipitation increases are larger than the corresponding changes in the mean. In summer, GC3.05-PPE shows a consistent drying in the mean, yet daily precipitation extremes can still increase (high-end changes in summer extremes show increases across much of the UK except the far south).

There is a high degree of consistency between the RCM-PPE and the driving GC3.05-PPE in terms of future changes, both for changes in long-term averages of temperature and precipitation and for changes in extremes. A few differences are apparent though. For example, the substantial warming of cold winter days over the northern UK in GC3.05-PPE is reduced in the RCM-PPE, which may relate to reduced cold biases in the RCM. In general, the consistency at the national scale between the RCM-PPE and its driving simulations is an expected consequence of the design of the RCM simulations, and supports use of RCM-PPE results to add value to analysis of detailed impacts at local to regional scales.

A comparison of annual warming and precipitation changes for the UKCP09 and UKCP18 probabilistic projections (from Strand 1) for regions of the UK are provided in the overview report (Lowe et al, 2018). In general UKCP18 gives slightly smaller temperature increases than UKCP09 for the same scenario, and greater reductions or smaller increases in precipitation, although the differences depend on location. Despite the differences, there is considerable overlap between the two sets of projections over land, with uncertainty ranges being broad in both cases.

1.3 Motivation for new 2.2km projections

Global and regional climate models have typical grid spacing of 60-300 km and 10-50 km respectively. In UKCP18, the global and regional projections from Strand 2 and 3 (described in the Land Projections report, see above) use models at the high resolution end of these ranges. At these standard resolutions, climate models rely on a parameterization scheme to represent the average effects on the atmosphere of convection, which cannot be represented explicitly on the grid. This simplification is a known source of model error (Dai, 2016, Stephens et al, 2010), that leads to deficiencies in the daily timing of convection (Brockhaus et al, 2008) and an inability to represent hourly extremes (Hanel and Buishand, 2010, Gregersen et al, 2013). Very high resolution models (order 1km grid spacing) are able to represent convective storms explicitly on the model grid, without the need for such a parameterization scheme. Such models are termed "convection-permitting" because larger storms are permitted, although they may not be well resolved, whilst smaller showers are still not well represented. Convection-permitting models (CPMs) are now standard in short-range weather forecasting, where they have been shown to give a much more realistic representation of convection, better forecast skill, and can be used to forecast localised high-impact rainfall not captured at coarser resolution (Done et al, 2004, Lean et al, 2008, Roberts and Lean, 2008, Weisman et al, 2008, Weusthoff et al, 2010). In particular, 2.2km models have been run in numerical weather prediction (NWP) for several years (e.g. in the Met Office Global and Regional Ensemble Prediction System for the UK, MOGREPS-UK, Tennant 2015), where they are routinely verified against observations. This shows that these models perform well in a range of weather regimes.

The high computational cost of CPMs has been a barrier to their deployment in climate studies. However, a number of these studies have been performed during the past few years, providing opportunities to assess the capabilities of CPMs in relation to climate change applications. The first multi-year climate change simulations at convection-permitting resolution, for a region of the UK, were carried out by Kendon et al, (2014); with similar studies for Sydney Australia (Argueso et al, 2014), the Alps (Ban et al, 2015), Germany (Fosser et al, 2017), the USA (Liu et al, 2016) and Africa (Kendon et al, 2019). CPMs do not necessarily better represent daily mean precipitation (Chan et al, 2013) but they have significantly better hourly rainfall characteristics with improved representation of the diurnal cycle of convection (Ban et al, 2014), the spatial structure of rainfall and its duration-intensity characteristics (Kendon et al, 2012, Lind et al, 2016), and the intensity of hourly precipitation extremes (Chan et al, 2014, Ban et al, 2014). All of these characteristics are typically represented poorly in conventional climate models. Kirchner-Bossi et al (submitted) also showed CPM added-value in representing extreme wind regimes, with improvements in summer likely related to the better representation of convective processes.

In addition to the improved representation of convective-phenomena, CPMs also give a better representation of orography and local surface features such as urban areas and soil moisture variability. This is expected to provide added value to projections of urban temperature (Argueso et al, 2014, 2015). It also leads to an improved representation of the climate over mountainous regions (Knote et al, 2010, Rasmussen et al, 2014), with the potential for improved snow cover at high elevation.

The advent of convection-permitting climate models since UKCP09 provides a new opportunity for UK climate projections, allowing us to provide credible estimates of changes in convectively-driven phenomena, such as hourly rainfall extremes and severe wind gusts, and in regions of strong spatial heterogeneities, such as mountains and urban areas (Kendon et al, 2017). For the UK, Kendon et al (2014) found substantial

future increases in the intensity of hourly summer rainfall extremes in a 1.5km CPM simulation, that were not captured in a coarser 12km simulation in which convection was parameterised. Ban et al (2015) found a similar result for the Alpine region when considering future changes in an extreme intensity metric (90th percentile of wet hours, their Fig. S6), however decreases were found for an equivalent percentile of all hours, due to significant future decreases in the frequency of wet hours. Other studies have suggested that hourly extremes may intensify more than expected simply from scaling increased atmospheric moisture with warming (Lenderink and van Meijgaard, 2008), due to local storm feedbacks captured by CPMs. CPMs also have the potential to provide added value to projections of wind (Belusic et al, 2018, Kirchner-Bossi et al, submitted), hail and lightning (Kendon et al, 2017).

The research summarised above reflects the current status of CPMs as a promising but relatively new addition to the set of modelling tools available for use in climate change simulations. Current CPMs still contain biases that may limit their credibility in some respects. In particular, their inability to fully resolve showers (see above) leads to a tendency for heavy rainfall to be too intense. This is because individual updraughts get represented on too large a scale with insufficient turbulent mixing (Kendon et al, 2012, Fosser et al, 2015). Nevertheless they provide a step change in our ability to represent deep convection and an opportunity to examine the importance of representing local storms for future climate projections.

The impact of new estimates of future changes in rainfall intensity from CPMs for sewer design was demonstrated in Dale et al (2016). In particular, the CPM rainfall changes were higher than existing UK climate change allowances, with implications for increased flooding. However, these results were based on a single model projection of future climate change and more CPM experiments are needed to assess the robustness of the findings. This has been a key limitation of convection-permitting climate modelling to date, with only single model projections for different regions available, and so it has not been possible to assess uncertainties in the climate change signal at the convection-permitting scale.

As a step towards addressing this, UKCP18 is providing the first ensemble of climate simulations at convection permitting scale. In particular, an ensemble of 12 projections at 2.2km resolution for the UK have been run, driven by the Strand 3 12km RCM-PPE. Although no perturbations have been applied directly to the CPM (the same CPM is used for all members), the different boundary conditions will drive differences in the fine-scale projections. For the first time, this will support an estimate of uncertainty in future changes at convection-permitting scale, given uncertainty in the larger-scale conditions. This will provide information on UK projections at local and hourly scales that helps to inform risk assessments and decision making.

In addition to the UKCP18 approach, work is also underway under the CORDEX-Flagship Pilot Study (FPS) on "Convective phenomena at high resolution over Europe and the Mediterranean" (Coppola et al, 2018) and under the Horizon 2020 European Climate Prediction System (EUCP) project (Hewitt and Lowe, 2018) to carry out coordinated CPM experiments across Europe. This will provide multi-model information on changes at convection-permitting scale, which will complement the UKCP18 CPM ensemble and provide a first indication of the relative importance of CPM structural uncertainties (which are uncertainties due to different parameterisation schemes or model architectures). A first model-intercomparison study at convection-permitting scale (Berthou et al, 2018) suggested that the added value of CPMs in representing present-day precipitation is robust to CPM structural uncertainties. In particular, two CPMs, using different dynamical cores and parameterisation packages, showed qualitatively similar differences in present-day precipitation characteristics compared to 12km models.

Finally, it should be emphasized that our confidence in CPM projections is strongly controlled by the ability of the driving global model to represent relevant large-scale processes and changes in large-scale circulation patterns, since the local weather is constrained by the larger-scale environment. In particular, the large-scale circulation in the CPM remains fairly close to that of the driving model (due to the small domain size), and local detail can be provided by the CPM only to the extent that it is consistent with this. Thus CPM results will reflect larger-scale errors in the global model. In UKCP18, the CPM ensemble is driven by perturbed parameter variants of the Hadley Centre global model (HadGEM3-GC3.05) at 60km resolution, via a 12km intermediate nest. As discussed in Section 1.1, this model gives a significantly better simulation of regional climate variability in the European/North Atlantic sector compared to the previous generation of climate models as used in UKCP09. Notable biases include a cooling in global average surface temperature between ~1950 and ~1980 in most members, and a significant cold bias in winter surface temperatures over northern Europe. The GC3.05-PPE members have been screened from a wide range of possible parameter combinations based on their historical performance in representing large-scale patterns compared to observations. Their global performance is competitive with a screened subset of CMIP5 models that is also included in Strand 2.

1.4 Report outline

In Section 2, this report describes the new convection-permitting ensemble, including a summary of the evidence supporting the chosen CPM resolution and experimental design. In Section 3, we assess the historical performance of the CPM and compare this against the 12km RCM. This provides the evidence base to establish the credibility of the new ensemble of convective-permitting climate projections. Section 4 presents the convection-permitting UK projections of future variability and change under the RCP8.5 scenario. We focus primarily on metrics of temperature and precipitation, and highlight where the CPM projections provide new information on future changes compared to the 12km RCM. Section 5 provides a summary table giving an overview of present-day biases and future changes in the CPM compared to the RCM, and our understanding of any differences in terms of the key processes that are represented differently in the CPM. Guidance on the use of the CPM projections in light of other information from UKCP18 (Strands 1, 2 and the 12km RCM) is also provided in Section 5. Finally, we provide a summary and forward look to future potential updates and planned work (Section 6).

2 Methods

2.1 Overview

UKCP18 is the first time internationally that an ensemble of climate projections has been carried out at convection-permitting scale for use in national climate scenarios. This therefore represents a step forward in our ability to quantify uncertainties in future changes at local and hourly time scales. However, it also represents a major cost in terms of computing resource. Before embarking on the final ensemble simulations, work was therefore carried out to determine the optimal resolution, model configuration and experimental design for the CPM ensemble. In particular, for a given computer resource, increasing model resolution (within the convection-permitting regime) comes at the cost of shorter simulations, a smaller domain or a smaller ensemble size. Thus the scientific benefits of increased resolution, within the convection-permitting definition, were assessed and balanced against user needs.

The CPM configuration is based on the Met Office operational UK-Variable resolution (UKV) model, which has been extensively tested within NWP trials (Bush et al, 2019). Previous CPM climate simulations (Kendon et al, 2014) were based on an older UKV configuration, and therefore it was important to test the recent model configuration in climate length runs and confirm that improvements seen in NWP were realised on longer timescales. We also tested other recent developments including the use of "Easy Aerosol", in which time series of aerosol properties and cloud droplet number concentration are prescribed (Stevens et al, 2017), in order to replicate approximately the aerosol forcing simulated in the driving global model (cf. Section 2.4).

The CPM and chosen experimental design are outlined in the following sub-sections, along with a brief summary of evidence supporting the choice (further details can be found in Fosser et al, submitted). Key considerations were scientific credibility, utility for stakeholders and computational performance.

2.2 Choice of convection-permitting resolution

Before embarking on the final CPM ("production") ensemble, test simulations were performed to determine the optimal CPM resolution (Fosser et al, submitted). In particular three different convection permitting resolutions (4km, 2.2km and 1.5km) were assessed in terms of their representation of precipitation, weighed against the additional computational cost of higher resolution (2.2km is 5.5 times and 1.5km 14 times more expensive than 4km).

The test simulations span the UK, for a 12 year period (March 1996 to June 2008, with three months discarded as spin-up) and were driven by the recent European Centre for Medium-Range Weather Forecasts Re-Analysis, ERA-Interim (Dee et al, 2011). The latter allows assessment of the CPM performance when provided with a quasi-observational time series of the atmospheric circulation at its lateral boundaries, largely free of the biases typically present in global climate models (GCMs). The test simulations were done with Met Office Unified Model version 10.1 (UM10.1), using the version of the NWP UKV model that was operational in 2015 (for more details see Fosser et al, submitted). The CPMs were also assessed against a 12km RCM. The latter is a limited-area version of the Global Atmosphere GA7 configuration of the Met Office Hadley Centre Global Environmental Model HadGEM3 (Walters et al, 2019), similar to the GA7.05 configuration used for the Strand 2 and 3 projections (see Section 2.4). This comparison provided an opportunity to compare CPM performance against a regional model that includes convective parameterisation, and is typical of RCMs used previously to provide downscaling information in national climate scenarios.

The 4km model was found to realise many of the benefits of convection-permitting resolution. In particular, the rainfall fields are more realistic in terms of the spatial structures and hourly evolution, compared to convection-parameterised models. However there are some key deficiencies at convection-permitting resolution that are notably worse at 4km, namely the tendency for the heaviest events to be too intense (Fig. 2.2.1), convective showers to be too "clumpy" and persistent, and delays in the initiation of convection (Fig. 2.2.2). These deficiencies are particularly apparent in summer when convection is more prevalent, and relate to the fundamental problem of updraughts being too strong across a 4km grid square. The use of a restricted convection scheme at 4km, which allows explicit convection when showers are large enough but activates a parameterisation to represent the effects of weaker convection (Roberts 2003), did not significantly alter the performance of the 4km model (Fosser et al, submitted). This is because the version of the scheme used was tuned, in operational forecasting, to allow the explicit representation of small storms by imposing a high degree of restriction on the parameterised convection.

The 2.2km model was found to perform similarly to the 1.5km model in terms of hourly precipitation metrics (Figs 2.2.1 and 2.2.2), with the benefit of considerably lower computational cost. In particular, for a given computer resource and ensemble size, it is possible to run three 20-year time slices at 2.2km resolution, whereas at 1.5km resolution extended climate simulations would not be possible, leaving a set of shorter case-study experiments (for example a set of ~40 simulations of selected seasonal events) as the only option. Longer simulations, or more time slices, are also possible at the cost of reducing ensemble size. From the standpoints of both scientific robustness and utility for stakeholders, a simulation of minimum length of 10 years (ideally longer) is needed, as this allows more robust derivation of impacts-relevant metrics such as extremes. Also the larger the ensemble size, the more it is possible to characterise uncertainty. Therefore, taking into consideration both scientific credibility and utility to stakeholders, 2.2km resolution was selected as the optimal resolution for the UKCP18 production ensemble. This allowed an ensemble size of 12 members, and the use of 20-year time slices for 3 periods (present-day, mid-21st century and end-of-21st century).
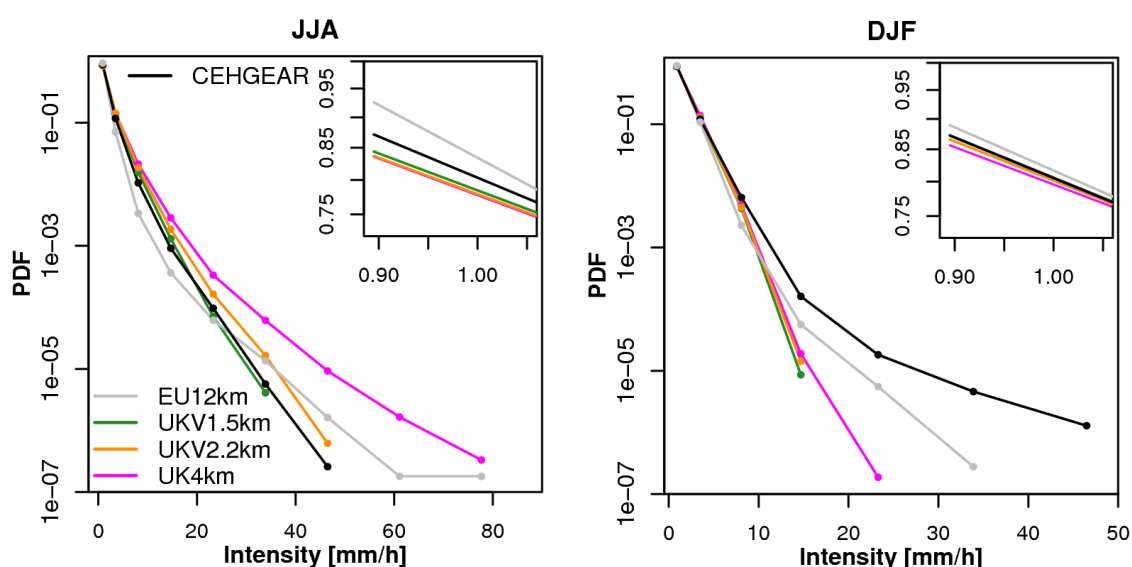

Figure 2.2.1. Impact of convection-permitting model resolution on precipitation intensity. Cumulative probability distribution of hourly precipitation intensity, for wet values >0.1mm/h for summer (left) and winter (right). Results represent the probability of exceeding the relevant intensity level, for data pooled across Great Britain, and are shown for the 1.5km (green), 2.2km (orange), 4km (pink) and 12km (grey) models and the CEHGEAR 1hr gauge observational dataset (black, Lewis et al, 2018, see also Table 3.1). The insert shows a zoomed in version of the distribution for low intensities, using a linear scale on the vertical axis. For all datasets precipitation has been regridded onto the 12km grid of the regional model (EU12km).
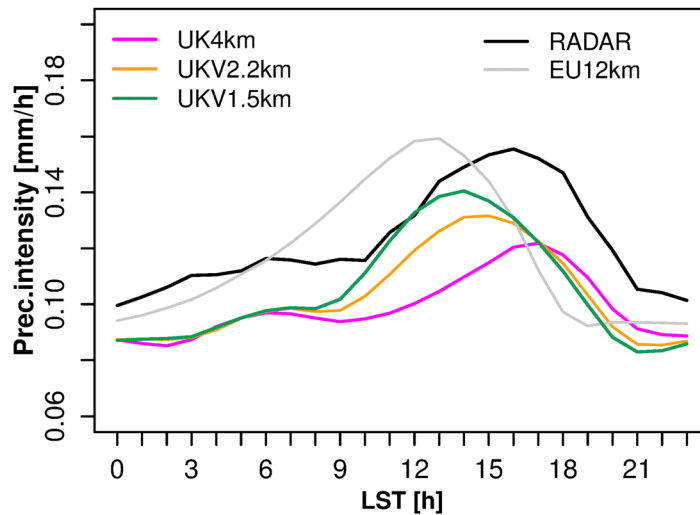
Figure 2.2.2. Impact of convection-permitting model resolution on the diurnal cycle of precipitation. Diurnal cycle of summer precipitation intensity for Great Britain in the 1.5km (green), 2.2km (orange), 4km (pink) and 12km (grey) models and the NIMROD radar dataset (black, Harrison et al, 2000), all remapped onto the 12km grid.

2.3 The 2.2km convection-permitting model

The 2.2km model is based on a recent operational NWP configuration (that was made operational in November 2016) at UM10.6, but with the addition of various changes to support its use in climate runs. This configuration is different from the version of the UKV (at UM10.1) that was used for the test simulations in Section 2.2, with the upgraded physics shown to give improved correspondence with observations (see below). The configuration is close to the operational Regional Atmosphere 1 mid-latitude configuration (Bush et al, 2019) and hence is termed "HadREM3-RA11M". Its horizontal grid spans the UK at 2.2km resolution, with a rotated pole set at 37.5ºN and 177.5ºE (the pole is chosen so that the grid's equator runs through the centre of the model domain). It includes a variable resolution rim (consistent with the operational UKV domain), with a fixed grid spacing outer region at 4km in the corners and 2.2km x 4km rectangles at the edges (the area outside the solid lines in Fig 2.3.1), a uniform 2.2km grid spacing inner region and a variable resolution area between the two (between the solid and dashed lines). This transition zone is characterised by rectangular grid cells in which grid length varies from fine to coarse resolution in one direction, using a constant stretching factor as described in Tang et al (2013). The smoothly-varying grid in the transition zone helps to reduce boundary artefacts affecting the interior of the domain, such as the fragmentation of fronts, which has been linked to insufficient frequency of updating at the boundaries (Tang et al, 2013). Moreover, it helps the initiation of showers before entering the fixed high-resolution part of the domain, by making the transition more gradual and by adding a larger "spin-up" region at a lower cost than if the whole grid is at 2.2km fixed resolution (Tang et al, 2013). The model uses a terrain-following hybrid-height vertical coordinate, with 70 vertical levels (with an upper lid at ~40km) and a Charney-Philips staggered grid. The model time step is 60 seconds, which is shorter than that used in the NWP operational 2.2km model (75 or 100 seconds) so as to improve numerical stability.

The 2.2km model configuration uses the semi-implicit semi-Lagrangian ENDGame (Even Newer Dynamics for General atmospheric modelling of the environment, Wood et al, 2014) dynamical core. This solves the non-hydrostatic, fully-compressible deep-atmosphere equations of motion. The new dynamical formulation leads to improved numerical accuracy and stability (Walters et al, 2017). The 2.2km model includes a two-stream radiation scheme (Edwards and Slingo, 1996) and an extensive set of parameterizations

describing the land surface (Best et al, 2011), boundary layer (Lock et al, 2000, with revisions described in Boutle et al, 2014) with 3-dimensional Smagorinsky (1963) turbulent mixing, and mixed-phase cloud microphysics (based on Wilson and Ballard, 1999, but with extensive modifications). The latter includes prognostic rain, which allows the three-dimensional advection of rain mass mixing ratio. This improves precipitation distributions in the vicinity of mountains, especially at the smaller grid spacing used in convection-permitting configurations (Lean et al, 2018, Lean and Browning 2013). Due to sub-grid inhomogeneity, clouds will form before the overall grid-box reaches saturation, and this is still true for kilometre-scale grid boxes (Boutle et al, 2016). The 2.2km model uses the Smith (1990) cloud scheme to determine the fraction of the grid-box that is covered by cloud, and the amount and phase of condensed water in these clouds. The microphysics scheme then determines whether any precipitation has formed. The 2.2km model includes a new mass conservation scheme (Zerroukat and Shipway 2017), which is applied to all atmospheric moisture tracers and removes the excess of moisture spuriously generated by the higher order semi-Lagrangian advection scheme (typical mass errors of ~1e-3 %). It uses the Joint UK Land Environment Simulator (JULES, Best et al, 2011) to model processes at the land surface and in the sub-surface soil. This includes the CO_2 impact on plant stomata, which affects evaporation fluxes. It also includes the new Met Office Reading Urban Surface Exchange Scheme (MORUSES), which uses two tiles to represent roof and street canyon facets, with the surface parameters determined from the morphology and materials properties of relevant cities (Porson et al, 2010). MORUSES gives a better representation of urban surface energy balance than the simpler one-tile urban scheme used in the 12km RCM (Murphy et al., 2018), capturing the phasing and the amplitude of the diurnal cycle of surface sensible heat flux more accurately when compared with observations.

Tests were carried out to determine the optimal settings for the 2.2km ensemble, within the limits of recent NWP operational configurations. In the recent operational UKV configuration (at UM10.6, from November 2016), the free-tropospheric mixing length was reduced (thereby decreasing the amount of mixing between convective updraughts and the surrounding air) and revised stochastic perturbations in potential temperature and moisture were introduced (which act to inject random noise into the boundary layer and so aid the triggering of convection) compared to the older configuration. These differences were expected to lead to earlier convective initiation and more widespread showery activity, overcoming deficiencies of the older model version (Hanley et al, 2015). A mass conservation scheme (Zerroukat and Shipway, 2017) was also introduced, which has the benefit of reducing high precipitation intensities, while increasing low intensity precipitation previously underestimated by the model. Climate length tests confirmed that these combined changes gave improved correspondence between simulated and observed distributions of hourly precipitation (Fig. 2.3.2, with more details in Fosser et al, submitted), hence the recent operational configuration at UM10.6 (blue line in Fig 2.3.2) was selected as the basis for the 2.2km production ensemble.

The 2.2km model used in UKCP18 (HadREM3-RA11M) has some differences compared to the NWP configuration. In particular, it uses Brooks Corey (1964) instead of Van Genuchten (1980) soil hydraulics, in order to correct an error which meant that vertical moisture transport through the soil was too slow. Also, excess moisture in HadREM3-RA11M is moved down (instead of up) as soil layers become saturated. The 2.2km model uses JULES with the topography based rainfall-runoff model TOPMODEL (Beven and Kirkby, 1979) instead of the Probability Distributed Model (PDM, Moore 2007) hydrology scheme. TOPMODEL is a more complex scheme that represents soil moisture heterogeneity throughout the soil column, including aspects such as a water table and the capability to estimate wetland fractions (Best et al, 2011). The HadREM3-RA11M model uses the simpler zero-layer snow scheme (with no explicit model layers to

represent snow) rather than the new multi-layer snow scheme (Best et al, 2011). The reason for this is that the newer snow scheme had not previously been tested in convection-permitting climate simulations and also it was not possible to run ERA-Interim driven simulations using the multi-layer scheme (as some input data was not available). Finally there are changes to radiative forcing settings, to ensure forcing of the CPM is consistent with the GC3.05-PPE simulations in Strand 2.

The CPM HadREM3-RA11M shares the majority of its main physical components with the 12km RCM used in Strand 3 (HadREM3-GA705, described in the Part 1 report). However, there are some notable differences. In particular, the mass flux convection parameterisation (Gregory and Rowntree 1990) is used in the RCM, but is switched off in the CPM. To represent turbulent mixing in strongly sheared areas such as the edges of convective updrafts, the CPM interactively blends the three-dimensional Smagorinsky-Lilly subgrid turbulence diffusion scheme (Brown et al, 1994, based on Lilly 1962 and Smagorinsky 1963) with the one-dimensional vertical boundary layer scheme used in the RCM (Lock et al, 2000, Boutle et al, 2014). The cloud scheme used is also different: the RCM uses the prognostic cloud scheme PC2 (Wilson et al, 2008) whilst the CPM uses the Smith (1990) scheme (since PC2 has not yet been implemented in mid-latitude convection-permitting UM operational forecast configurations). Both models use the same cloud microphysics scheme (Wilson and Ballard, 1999), and include the effect of sub-grid variability in the warm-rain scheme (Boutle et al, 2014). However, there are a few differences in the coefficients used in the cloud microphysics (e.g. in the ice particle mass-diameter relationship), and importantly prognostic graupel. This represents a second category of ice with higher densities and fall speeds found in convective cloud (Forbes and Halliwell, 2003), which is included in the CPM but not the RCM. The prognostic graupel is a prerequisite for the inclusion of a lightning flash rate prediction scheme. This scheme included in the CPM is described by McCaul et al (2009), and has been shown to produce useful forecasts in convection-permitting models (Wilkinson and Bornemann 2014). Prognostic graupel in the CPM is added to the snowfall output diagnostics but is not seen by JULES, and so is not included in the snow pack. The latter setting follows current operational practice and was recommended due to the tendency for the convection-permitting model to produce too much small graupel, which if included in the snow pack would lead to an overestimation of lying snow. We note a complete representation of frozen precipitation in CPMs and its interaction with the land surface (for example, the continuing potential for local non-conservation in the semi-Lagrangian dynamics, the treatment of graupel formation, its interception by vegetation canopies and the density of new frozen precipitation falling into the snow pack) is still the subject of on-going research. In contrast, all ice precipitation in the RCM (which in this model is diagnosed uniquely as snow, with no graupel category) is seen by the land surface. In terms of the representation of the snow pack, the RCM uses the new multi-layer snow scheme (Best et al, 2011) whereas the CPM (see above) does not. Both of these factors contribute to differences in simulated snow cover between the CPM and RCM, discussed in section 3. Finally, as also noted above, the RCM uses the simpler one-tile urban scheme rather than MORUSES.
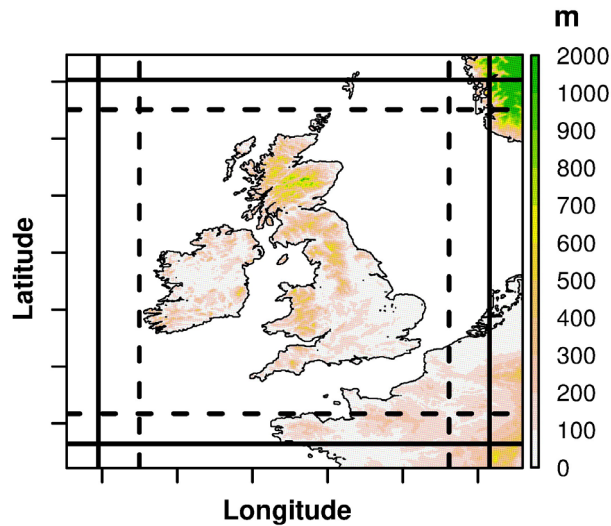
Figure 2.3.1. 2.2km model domain. CPM domain, including variable resolution rim. Colours show 2.2km model orography.
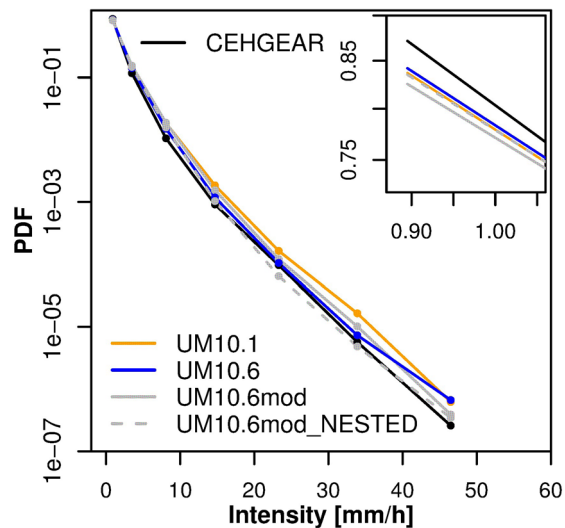
Figure 2.3.2. Impact of 2.2km configuration and nesting strategy on precipitation intensity. Probability distribution of hourly precipitation intensity, for wet values >0.1mm/h for summer, for UM10.1 (orange) and UM10.6 (blue) configurations and for the CEHGEAR gauge observations (black). "_mod" (grey) is a modified version with earlier boundary layer and mixing settings, run to test the impact of changes from UM10.1 to UM10.6. "_NESTED" (dashed) is the result on including an intermediate 12km nest. UM10.6, with an intermediate nest, is the selected configuration for the production ensemble. The precipitation has been regridded onto the 12km scale, and then the probability of exceeding the relevant intensity level calculated for all data pooled across Great Britain.

2.4 Design of 2.2km experiments

The 2.2km model is driven at its lateral boundaries in a one-way nesting approach, using a time series of three-dimensional wind components, potential temperature, Exner pressure, dry density and moisture prognostics (including mixing ratios of water vapour, liquid and ice). These variables are introduced (from archived files) every 3 hours from the relevant Strand 3 12km RCM member, and applied to the CPM across a 24-point relaxation zone (which is the outer part of the 55-point variable resolution rim described in Section 2.3). The 12km RCM spans Europe and is in turn driven at its lateral boundaries by the relevant GC3.05-PPE member. The CPM simulation evolves freely in its internal domain, from which the 24-point rim is removed for all analysis presented here. Prescribed daily fields of SST and sea-ice cover are supplied from the driving global simulation. Following NWP standard practice, the only inland water body included in the

CPM land-sea mask is Lough Neagh in Northern Ireland (the temperature of which is given by the SST of the closest global model sea point). Other lakes are considered as land grid-boxes, a fraction of which is defined as water.

The use of a 12km intermediate nest (as opposed to driving the CPM directly from the 60km global simulation) was found to significantly improve biases both in the intensity distribution (Fig. 2.3.2, Fosser et al, submitted) and mean summer precipitation (Fig. 2.4.1). This may be explained by the propagation or spin-up of events entering the UK domain being impeded when there is a large resolution jump at the boundary (60km in GCM to 4km in variable resolution rim). The use of an intermediate nest provides smaller scale variability that helps initiate precipitation structures closer to the model boundaries. Running a 12km ensemble comes with significant computing cost implications, in particular it reduces the CPM ensemble size that can be afforded by about 5. Nevertheless, it was decided to use the intermediate nest, motivated by improvements in CPM driving data outlined above, plus the recognition that the 12km RCM itself would be a useful product to users in the first phase of UKCP18 (Murphy et al, 2018), notably through its ability to provide 100-year continuous time series data at enhanced resolution compared to the Strand 2 output. The 12km RCM projections can also be compared with EURO-CORDEX models (Jacob et al, 2014), which may be useful both to UKCP18 users as well as the international EURO-CORDEX community.

The driving GCM ensemble consists of perturbed parameter variants of HadGEM3-GC3.05, which uses GA7.05 for the atmospheric model. This is close to the Global Atmosphere 7 (GA7) configuration (Walters et al, 2019), but includes a number of updates (see Appendix D of Murphy et al., 2018), including the Liu et al, (2008) parameterisation of the spectral dispersion of cloud droplets, and an update to the refractive index of black carbon (Bond and Bergstrom, 2006). Since GC3.05 does not include a carbon cycle component, the GC3.05 PPE members were run with prescribed CO_2 concentrations, using different concentration pathways for each member to replicate the range of outcomes projected from Strand 1 for the RCP8.5 scenario (Murphy et al, 2018). The spread of outcomes from GC3.05 therefore contains contributions from internal variability, uncertainties in the modelling of physical processes, and uncertainty in the globally-averaged effects of carbon cycle feedbacks. In Strand 3, each 12km RCM and corresponding 2.2km CPM member inherits the CO_2 pathway prescribed in its driving Strand 2 global simulation.

The 12km RCM is a limited area configuration of the GA7.05 atmospheric model (HadREM3-GA705) spanning Europe. The RCM-PPE consists of 12 members, each with parameter perturbations as in the corresponding GC3.05 member. Only 12 out of the full 15 GC3.05-PPE members in Strand 2 were downscaled due to affordability. The selection of the 12 members is detailed in Murphy et al (2018), and was based on historical performance, as well as maximising the spread of sampled parameter values. The same 12 members were then downscaled to 2.2km over the UK to give a 12-member CPM ensemble (hereafter CPM-12).

Given the structural differences between the CPM (HadREM3-RA11M) and the driving global and regional models (Section 2.3), it was not possible to mirror the full set of RCM parameter perturbations in the CPM. Therefore, it was decided not to implement any parameter perturbations in the CPM, using the same version of the model for each ensemble member. Thus CPM-12 samples uncertainties exclusively through its driving data, arising from internal climate variability and parametric uncertainties in the physics of the driving models. CPM-12 underestimates uncertainty in changes at local scales, since parametric uncertainties in its local processes and feedbacks (e.g. uncertainty in soil moisture parameters) are not sampled. More widely, the CPM and RCM ensembles also underestimate uncertainties because they are driven exclusively by variants of the Met Office Hadley Centre model (GC3.05), and currently lack

information from other international climate models. Nevertheless, the present ensemble represents a significant step forward, since previous CPM information has been limited to individual climate change simulations lacking any uncertainty context.

The CPM simulations were run in three 21-year time slices (1980-2000, 2020-2040 and 2060-2080), using a 360-day calendar. For the latter two time slices, the projections correspond to the RCP8.5 scenario, which is a high emissions "business-as-usual" scenario assuming unmitigated greenhouse gas emissions. This scenario was chosen as it provides an upper estimate of expected changes, with the benefit of a high signal-to-noise ratio that is helpful in justifying use of the results to infer changes for other scenarios using scaling approaches. Initial conditions were taken from the corresponding points of the driving 12km RCM simulations. The first year of each CPM time slice was used as a spin-up period, to allow fine-scale circulations and land surface properties (particularly soil moisture in the root zone) to reach approximate equilibrium. This was achieved, with only small residual adjustments in soil moisture at the deepest level for some members, and no evidence of residual drift in soil moisture at surface levels, after this point. The use of a mid-century time-slice was motivated by user needs, as this represents a period that is within, or close to, the time horizon of most users. The late 21st century time-slice is relevant to planning activities related to long-term infrastructure decisions. It also has the benefit of a greater signal to noise ratio: it is easier to identify changes above natural variability at the end of the century, which makes it possible to infer changes for earlier periods (as well as for lower forcing scenarios, as discussed above) using scaling approaches.

In each CPM member, the applied changes in radiative forcing were the same as in the driving GC3.05-PPE and RCM-PPE members from Strands 2 and 3. After 2005, the changes in greenhouse gas forcing included the member-specific CO_2 concentration pathways mentioned above. The CPM uses the same volcanic, solar and ozone forcing as the GC3.05 simulations. In the case of ozone, there was a year offset in the ozone concentrations for the periods 1980-89 and 2020-30. This error, which was also present in the driving RCM, was assessed as leading to a very small error in the total forcing of <0.4%. It was decided not to include the GLOMAP-mode aerosol scheme as an interactive component in either the RCM or CPM. This was due both to its computational expense and a lack of previous experience of how the scheme performs in climate simulations at high resolution. However, aerosol radiation and cloud effects simulated by the relevant GC3.05 member were approximately replicated in the RCM and CPM. This was achieved by saving monthly spatial fields of shortwave and longwave optical properties (absorption, extinction, scattering and asymmetry) and cloud droplet number concentration, and then prescribing these as a time series in the RCM and CPM simulations for use in their calculations of time-varying radiative forcing. In a global model, Stevens et al (2017) showed that this ("Easy Aerosol") approach replicates quite well the aerosol forcing found in interactive simulations, and tests using GC3.05 supported this conclusion. It should be noted, however, that the use of monthly mean fields results in the smoothing out of daily variability in aerosols.

Present-day land cover in the CPM is defined from the high-resolution Centre for Ecology and Hydrology land cover dataset (Fuller et al, 1994), which uses Institute of Terrestrial Ecology (ITE) Landsat-derived cover types over Great Britain, and from the International Geosphere-Biosphere Programme (IGBP) dataset for the rest of the UK. There are two urban tiles (distinguishing between street canyons and roofs) for use with the MORUSES urban scheme as well as an urban morphology ancillary, which gives information on building height and width. This differs from the RCM which uses IGBP data to define the present-day land cover throughout the domain, and has a single urban tile. Past and future changes in land use are represented by prescribing a time-varying component due to anthropogenic disturbance, consistent with the Strand 2 GCM and Strand 3 RCM (Murphy et al, 2018). The time-dependent disturbance fraction is

taken from the harmonised land-use LUH2 v2h dataset (at 0.5 degree resolution, Hurtt et al, 2011) used in CMIP5 simulations. It is used to modify the observed present-day land cover distribution. In particular changes in crops and pasture from LUH2 v2h were mapped into changes in the combined coverage of C3 and C4 grasses at the expense (addition) of clearing (planting) a corresponding fraction of trees and shrubs. Changes are implemented in such a way as to preserve the observed proportions of C3 and C4 grasses, and proportions of needleleaf, broadleaf trees and shrubs. Urban, ice and bare soil remain fixed at the prescribed present-day values. Although the methodology applied is the same, RCM and CPM land use changes can differ through time because the present-day vegetation fraction is taken from different datasets. In particular, when calculating land use changes for grid boxes where there is no forest for the present day, we cannot transition to forest for this grid box (as we don't know the broadleaf, needleleaf, shrub ratio) or indeed transition from forest (as there is already none). Since the occurrence of grid boxes with no forest is more common for the RCM/GCM (based on IGBP) than for the CPM (based on ITE) this can lead to slightly different future land use changes.

An additional simulation was produced using ERA-Interim reanalyses (rather than GC3.05) to drive the RCM standard member (ERAI-RCM-STD), which was in turn downscaled using the CPM (hereafter ERAI-CPM-STD). This simulation allows the downscaling properties of the RCM and CPM to be assessed, free from biases in the large-scale driving conditions from the GCM. Thus biases in RCM-STD and CPM-STD can be partitioned approximately into a component inherited from the driving global model and a component arising from regional and local errors in the downscaling models. The ERAI-CPM-STD simulation was run from 1981-2001. Sea surface temperatures and sea-ice extents were prescribed from analyses of observations (Reynolds et al, 2002). Aerosol properties are prescribed in a similar manner to that above, but using a standard historical forcing dataset developed for CMIP6 (Stevens et al, 2017). Subsequent to the hindcast simulation having being run, it was discovered that there was some double counting of aerosols in the upper troposphere. In particular, some upper tropospheric aerosol was incorrectly included in the stratospheric aerosol (volcanic forcing) dataset, which was used to create inputs to the "Easy Aerosol" scheme. The impact of this double counting equates to a net top of the atmosphere warming of ~0.06Wm^{-2}, and is therefore deemed to be negligible.
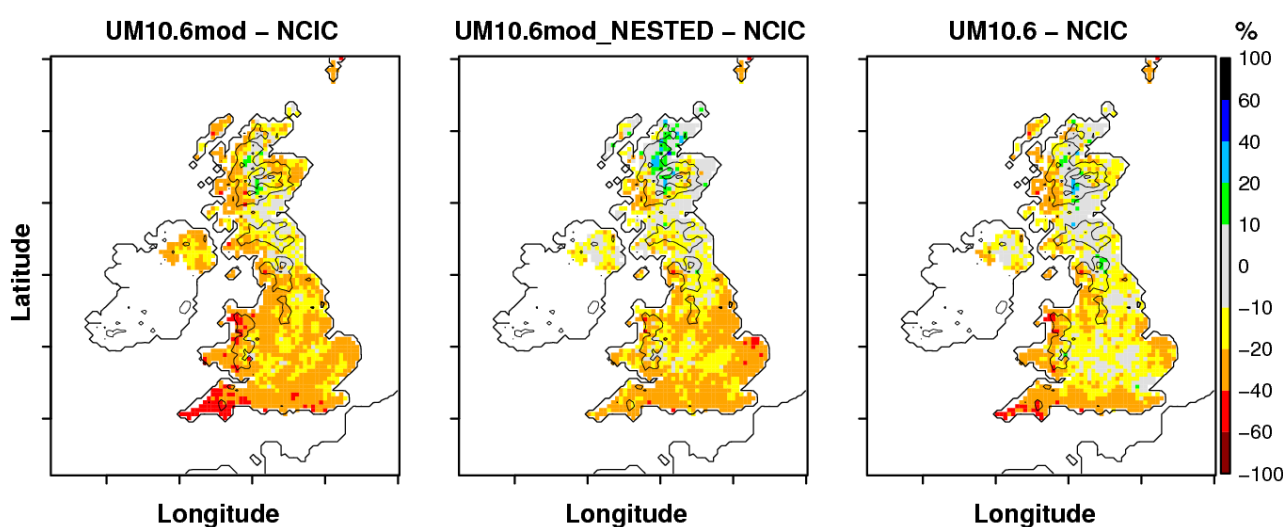
Figure 2.4.1. Impact of intermediate 12km nest on mean precipitation. Biases in summer mean precipitation (%) in the 2.2km model with respect to NCIC observations for the (left) UM10.6 configuration with modified settings, (centre) UM10.6 configuration with modified settings and a 12km intermediate nest, and (right) the UM10.6 configuration without an intermediate nest.

2.5 Summary

UKCP18 is the first time a convection permitting model (CPM) has been used for national climate scenarios. It represents a step change in climate modelling capability, allowing us to provide information on changes at kilometre and hourly scales. The CPM configuration is based on the Met Office operational UK weather forecast model (UKV), which has been extensively tested for use in weather forecasting. Climate length tests were carried out prior to UKCP18, to determine the optimal resolution and model configuration. Taking into consideration both scientific credibility and utility to stakeholders, 2.2km resolution was selected as the optimal resolution for the UKCP18 CPM ensemble. This allowed an ensemble size of 12 members and simulations for three 20-year periods (1981-2000, 2021-2040 and 2061-2080).

The UKCP18 CPM ensemble (CPM-12) is driven by the 12km regional climate model perturbed parameter ensemble (RCM-PPE) from Strand 3. The CPM shares many of the same model physics settings as the 12km RCM, but with some notable differences. In particular, the convection parameterisation is switched off in the CPM, which also uses a different cloud scheme and includes prognostic graupel, required for its lightning prediction scheme. The CPM also uses a simpler snow scheme, but a more sophisticated urban scheme, compared to the RCM. No parameter perturbations are applied in the CPM, with the same version of the model used for all 12 ensemble members. The CPM ensemble samples uncertainties arising from internal climate variability and uncertainties in its driving data due to parametric uncertainties in the physics of the driving models. However, it does not include uncertainty in the convective-scale model physics itself, nor does it sample information from other international climate models.

The CPM projections correspond to the high emission scenario RCP8.5. The forcings are the same as in the driving RCM-PPE from Strand 3, which is in turn driven by the global model ensemble GC3.05-PPE from Strand 2. An additional simulation was also produced using ERA-Interim reanalysis (rather than GC3.05) to drive the RCM standard member which in turn was downscaled by the CPM. This simulation allows the RCM and CPM downscaling performance to be assessed, free from biases in the global model.

3 Evaluation of historical period

3.1 Overview

This section provides the evidence base to establish the credibility of the new ensemble of convective-permitting UK projections. This involves two main steps. The first is to assess the performance of the CPM as a specific downscaling tool, in the absence of large-scale errors that might be inherited from the driving global model in climate scenario simulations. As explained in section 2.4, we perform this aspect of the assessment using ERAI-CPM-STD. This is a simulation of 1981-2001 driven by ERA-Interim reanalyses of observations, via an intermediate nest using the corresponding regional model simulation, ERAI-RCM-STD. If the reanalysis-driven CPM cannot produce an acceptable simulation of impact-relevant variables, at both national and local scales, it would not be justified to provide CPM-based climate scenarios. This would apply, irrespective of the level of performance achieved in GCM-driven simulations. Accordingly, we start section 3.2 with an evaluation of climatological surface air temperature and precipitation patterns simulated by ERAI-CPM-STD. In subsequent material we also include assessment of selected metrics of temperature and precipitation extremes. By comparing ERAI-CPM-STD with ERAI-RCM-STD we highlight the downscaling benefits of enhanced resolution and explicit convection in the former. In addition, comparison with CPM-STD, the corresponding GCM-driven simulation, allows us to illustrate the relative contributions of biases from internally-generated errors, compared to those inherited from the driving global model.

The second key step is assessment of biases in CPM-12, the ensemble of CPM scenario simulations driven from GC3.05-PPE global simulations via RCM-PPE members. This is critical, since CPM-12 is the "production" ensemble that will be used in impacts applications, and also because biases can vary between different CPM-12 members due to differences in the driving simulations. The assessment of CPM-12 considers 1981-2000, and includes comparison to the driving 12km RCM-PPE. We focus on selected metrics of precipitation and temperature, from seasonal means to daily and hourly extremes. Other variables including snow, cloud, soil moisture and lightning are also examined. The report does not survey all variables of interest to users, and additional material on CPM evaluation for other variables will be provided in journal papers.

The evaluation presented here is primarily carried out at the 12km scale to allow comparison with the RCM-PPE. In this case, the 2.2km CPM data is averaged onto the RCM grid using area-weighted regridding, with land and sea points regridded separately to avoid any combination of land and sea data in coastal regions. We would not expect the CPM-12 to depart significantly from the RCM-PPE for seasonal mean variables on large-spatial scales, and indeed large departures would be inconsistent with the assumptions of the one-way nesting approach adopted here. Some differences may arise due to differences in the representation of convective, cloud, snow and urban processes, which may feedback on the large-scale. However, it is on fine spatial and temporal scales where we primarily expect added-value from the CPM. Thus we examine daily and hourly extremes, and also at the 2.2km scale, added fine-scale detail from the CPM.

We use several observational datasets, ranging from monthly to hourly time scales. These are summarised in Table 3.1, with the data also regridded to 12km for comparison with the models. The climatological baseline period for the models is December 1980 to November 2000. For the observational datasets, we use the same 20-year period where possible; otherwise, we use 20 years that maximise the overlap with the model years; or where records are shorter than 20 years, we use all available data. For CEHGEAR, we

use all 25 years of the available hourly precipitation observations, since instances of missing data reduce the effective record length below 25 years. It should be noted that we would not expect correspondence between the observations and the CPM-12 or RCM-PPE simulations on a day-to-day or season-to-season basis. This is because the regional models produce simulated realisations of internal climate variability, rather than actual forecasts of events: they are not initialised from observations, and use modelled rather than observed time series of lateral boundary conditions. However, their emergent climatological characteristics, such as 20-year averages or the typical intensity of selected types of extreme event, can be evaluated against corresponding observational metrics. One exception to this is ERAI-CPM-STD and ERAI-RCM-STD (see above). These simulations are supplied with time series of information on the observed atmospheric state at the lateral boundaries of the European model, and are also driven by observed sea surface temperatures (SSTs). They can therefore be assessed in terms of their ability to reproduce specific historical events, as well as evaluated in a climatological sense. This is because these simulations are expected to capture a sequence of large-scale weather patterns that is similar to observations. However, the precise timing and location of related events of interest, such as occurrences of extreme regional precipitation, can still be expected to differ in detail. This is because the prescribed lateral boundary forcing does not fully constrain the generation of local variability within the RCM or CPM domains.

Variable	Time scale	Dataset	Data span	Grid	Comments and Reference
Surface air temperature	Daily mean	NCIC	1960-present	5km	Based on meteorological station observations (Perry et al, 2009). The number of stations varies between 400 and 600, depending on the year.
Precipitation	Daily	NCIC	1958-present	5km	Gauge-based dataset (Perry et al, 2009). There are typically between 2500 and 5000 daily rain gauges, depending on the year, although with fewer stations before 1961. Rain gauge observations are affected by systematic measurement undercatch due to multiple factors including snow, wind blow losses and exposure of the gauge. Gauges may also miss localised events entirely and there is a tendency for gauges to be sited in valleys rather than at the tops of mountains. Biases vary with season and location, and are largest at high elevations. The systematic undercatch varies between 4% and 50%, with an average estimate of 20% (Kotlarski et al, 2014, Rajczak and Schar, 2017). No correction for this undercatch has been applied here.
Precipitation	Hourly	CEH-GEAR1hr	1990-2014	1km	Gauge-based dataset (Lewis et al, 2018). This is based on 1900 quality controlled hourly rain gauges (although the number used ranges from 295 to 1372 gauges on any given day, due to missing data or quality issues). The gridded hourly data is obtained by disaggregating the Centre for Ecology and Hydrology Gridded Estimates of Areal Rainfall (CEH-GEAR) daily gridded dataset using the hourly gauges. An average storm profile was used to disaggregate the daily dataset, where the nearest hourly gauge was >50km away. This process of disaggregation results in a discontinuity in the diurnal cycle at 09Z (when the daily data recording period starts). As for the daily gauges, the hourly gauges are expected to underestimate the intensity of heavy events, and the same caveats as for the daily dataset apply, with even greater sampling errors due to fewer hourly gauges. Additional error will also be introduced by the disaggregation step, associated with distance to the nearest gauge (low gauge density in Scotland and south-west England gives greater distances there).

Variable	Time scale	Dataset	Data span	Grid	Comments and Reference
Precipitation	Hourly	NIMROD RadarNet	2003-2017	5km	Radar dataset (Harrison et al, 2000). Precipitation is estimated from reflectivity measurements. There are known to be errors due to radar calibration, ground clutter, beam attenuation, and assumptions in the reflectivity-precipitation rate relationship. Heavy rainfall tends to be underestimated, and uncertainties are significant for hail. The radar network provides good spatial coverage over the southern UK, but poorer coverage over northern UK. There are some spurious high totals and these have been removed here by setting all data >100mm/h averaged over a 12km box to missing (corresponding to 0.0004% of UK data; 63 mm/h is maximum value observed by gauges over UK). In general the radar data provide reliable information on the spatial patterns and temporal characteristics of rainfall, but we would have lower confidence in the absolute rainfall amounts especially for intense events.
Falling snow	Days of falling snow per month	NCIC	1971-2011	5km	Based on meteorological station observations (Perry et al, 2005). A day is reported even if there is only one observation of snow (or sleet). There are typically 400 to 500 stations recording snow up to the 1990s, but with the number of stations declining thereafter. Gridding of snow data is problematic, and these gridded products are no longer updated operationally due to the diminishing network size.
Lying snow	Days of lying snow per month	NCIC	1961-2011	5km	Meteorological station observations (Perry et al, 2005). Based on observer deciding that the ground is more than half covered in snow. There are typically 400 to 500 stations recording lying snow from 1961 to the 1990s, but a subsequent fall to approximately 100 stations currently. Gridding of snow data is problematic, and these gridded products are no longer updated operationally due to the diminishing network size.
Cloud and surface radiation	Monthly mean	CLARA-A2	1982-2015	0.25°	Based on Advanced Very High Resolution Radiometer (AVHRR) measurements from National Oceanic and Atmospheric Administration (NOAA) and European Organization for the Exploitation of Meteorological Satellites (EUMETSAT) polar-orbiting satellites (Karlsson et al, 2017). Original visible radiances were inter-calibrated and homogenised using Moderate Resolution Imaging Spectroradiometer (MODIS) data. Prior to 1992 there was only one instrument available, leading to more missing data; it is more complete over Europe from 1992, and better again from 2002. Cloud detection biases for period October 2006-December 2009 are about 13% compared to Cloud-Aerosol Lidar and Infrared Pathfinder Satellite Observation (CALIPSO) Cloud-Aerosol Lidar with Orthogonal Polarization (CALIOP) observations.
Soil moisture	Daily mean	WFDEI-JULES	1979-2012	0.5°	Simulation of land-surface properties by JULES, forced by the WATCH Forcing Data methodology applied to ERA-Interim reanalysis (WFDEI, Weedon et al, 2014) meteorological dataset. WFDEI is based on ERA-Interim reanalysis data, but includes bias correction using monthly gridded surface observations. This dataset is considered as a proxy for observed soil moisture.
Lightning	Flashes per day	ATDnet	2009-present	Point data	Met Office long-range very low-frequency lightning location system, Arrival Time Difference Network (ATDnet, Anderson and Klugmann, 2014). Relies on detection of electromagnetic fields produced by lightning, providing the location and time of every flash. ATDnet system mainly records cloud-to-ground (but not intra-cloud) lightning (Enno et al, 2016). ATDnet suffers from interference due to the height of the ionosphere, and so periods of nocturnal lightning are not detected (Bennett et al, 2011). The detection efficiency of ATDnet goes up every few years as the hardware is upgraded, so observations from the last few years (2014-2018) only are used here. The point data have been aggregated to a 12km grid for comparison with the model output here.

Table 3.1. Observational UK datasets used in the evaluation of the RCM and CPM simulations.

3.2 Seasonal mean performance

The performance of the RCM and CPM standard members (RCM-STD and CPM-STD) in representing seasonal mean temperature in winter and summer is shown in Figs 3.2.1-3.2.2. We focus on the standard member, since a corresponding ERA-Interim driven experiment is available, allowing an assessment of the extent to which biases in the RCM and CPM are inherited from the driving GCM. In winter, RCM-STD is too cold in the northern UK and too warm in the south (by up to 1ºC in each case), with similar biases in ERAI-RCM-STD. These biases are considerably reduced in the CPM. In summer RCM-STD is too cold, but these biases are reduced or (in some areas) reversed in ERAI-RCM-STD, suggesting they are largely inherited from the driving global model. The CPM is generally warmer than the RCM, especially in the south UK, leading to reduced biases in CPM-STD but a warm bias in ERAI-CPM-STD. These differences in seasonal mean temperature are in part explained by the CPM having less cloud than the RCM in all seasons and different cloud optical properties (see Section 3.5). These cloud differences are likely due to the different cloud schemes used in the CPM and RCM, and the fact that the cloud fraction tends to be more discretely closer to 0 or 1 in each CPM grid square because the grid squares are smaller. Differences in winter may also relate to the different treatment of graupel and different snow schemes, with less lying snow being a factor in explaining the warmer temperatures in the CPM in the northern UK (see Section 3.5).

For precipitation, there is a wet bias in RCM-STD in winter which is reduced in CPM-STD (UK-average root-mean-square RMS error of 36% reduced to 20% in CPM, Fig. 3.2.3). Biases are also further reduced in ERAI-CPM-STD (RMS error of 12%), showing that much of the wet bias in the CPM is inherited from the driving model. In summer, biases are again considerably lower in the CPM (UK-average RMS error of 25% in RCM-STD reduced to 16% in CPM-STD, Fig. 3.2.4). In particular, the wet bias in RCM-STD over the northern UK is reduced in CPM-STD, but the CPM has a tendency to be too dry in the far south. The ERAI driven simulations show a similar result, but with reduced biases in general. Although ERAI-CPM-STD gives lower biases across the UK as a whole compared to ERAI-RCM-STD, it does show a marked dry bias along western and southern coasts. We note that these biases are with respect to rain gauges (Table 3.1), which are known to suffer from systematic measurement under-catch (of typically about 20%, but varying between 4% and 50%, with larger errors in winter because of snow and at high elevations because of wind exposure, Rajczak and Schar 2017) and sampling uncertainties (over mountains the siting of gauges mostly in valleys leads to an underestimate). These deficiencies however are not expected to (fully) account for the wet bias in the RCM, but may contribute to the greater apparent bias in winter. This bias, and the improvement seen in the CPM, is linked to the representation of rainfall occurrence (see Section 3.3).

In terms of the fine-scale information (panel d in Figs 3.2.1-3.2.4), the 2.2km model adds spatial detail over mountainous regions for both temperature and precipitation. For temperature, the typical RMS magnitude of the small scale signal[4] over the UK is similar to that found for the CPM minus RCM differences at the 12km scale. For precipitation, the typical RMS difference over the UK is larger for the CPM minus RCM differences, however the small scale signal can dominate in some specific locations, particularly in regions of high elevation.

---

[4] Defined as the difference between the raw 2.2km and aggregated 2.2km results, where aggregated results are produced by averaging over 5x5 grid boxes.
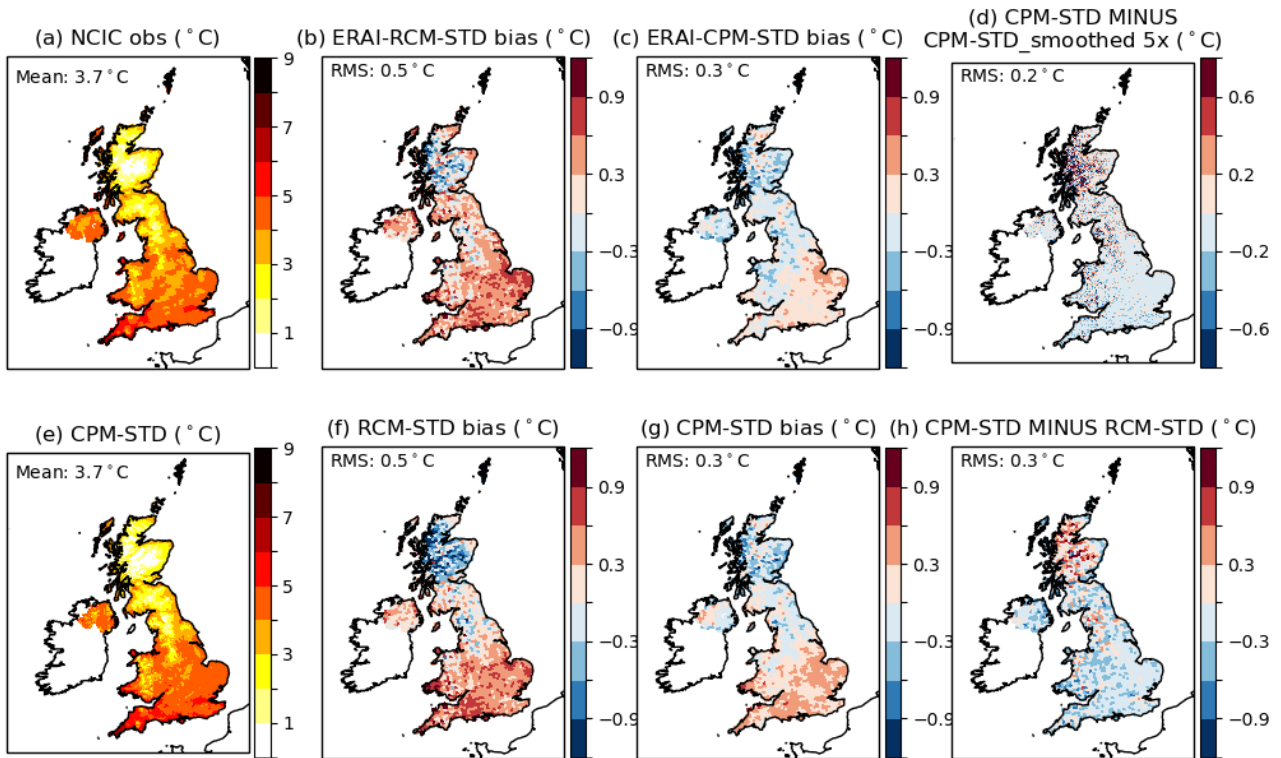
Figure 3.2.1. Observed and simulated winter mean temperature. Mean temperature in winter in the (a) NCIC observations at 12km scale and (e) CPM-STD at 2.2km scale during 1981-2000. Biases (ºC) at the 12km scale in the (b) ERAI-RCM-STD, (c) ERAI-CPM-STD, (f) RCM-STD and (g) CPM-STD. (d) CPM added spatial detail (2.2km minus 2.2km-smoothed-to-12km, which equates to averaging over 5x5 2.2km grid boxes) and (h) the difference between the CPM-STD and RCM-STD at 12km. The UK-averaged (a,e) mean value or (b-d,f-h) Root Mean Square (RMS) error is indicated.
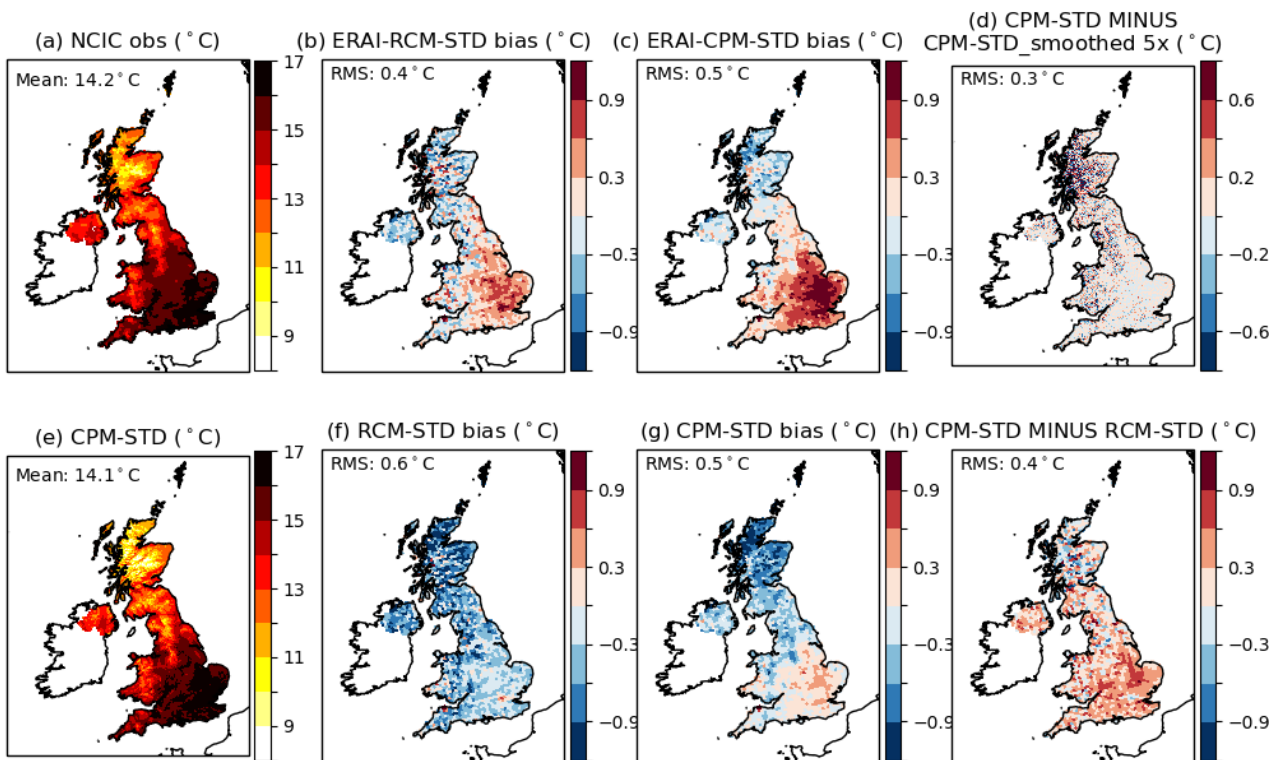
Figure 3.2.2. Observed and simulated summer mean temperature. As Fig 3.2.1 but for mean temperature in summer.
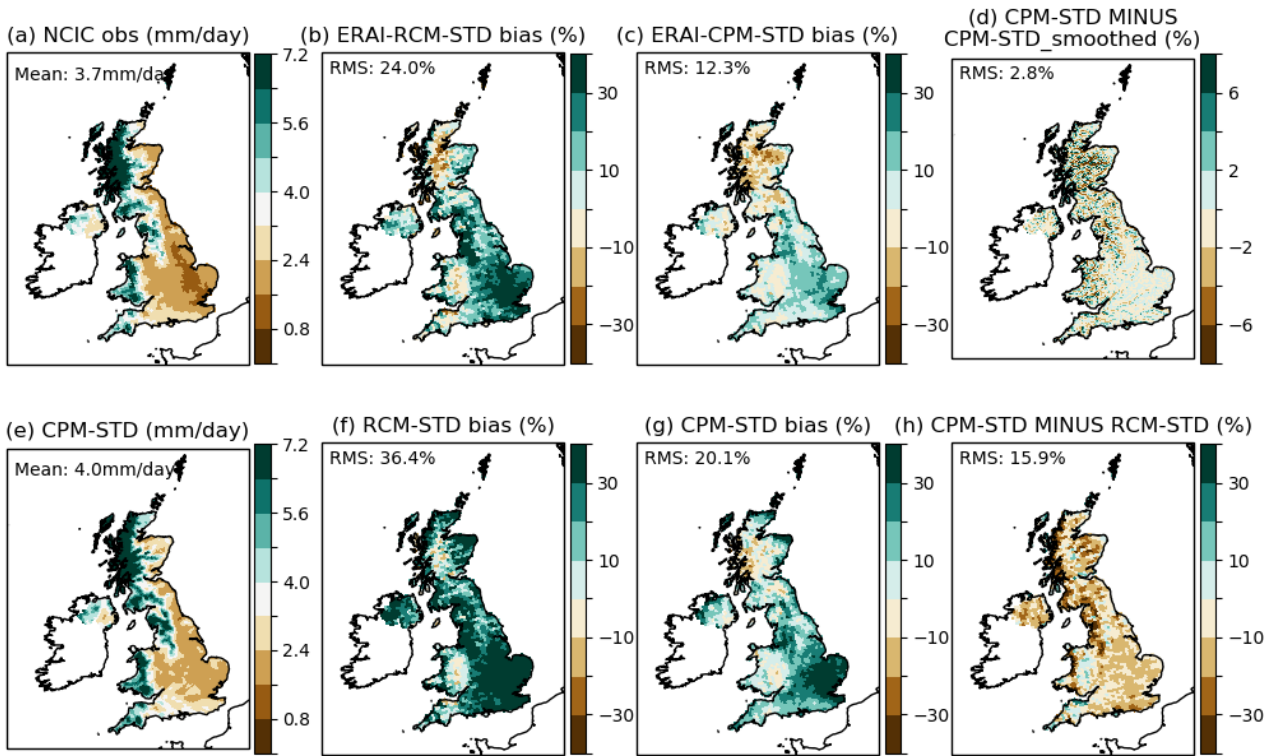
Figure 3.2.3. Observed and simulated winter mean precipitation. As Fig 3.2.1 but for mean precipitation in winter.
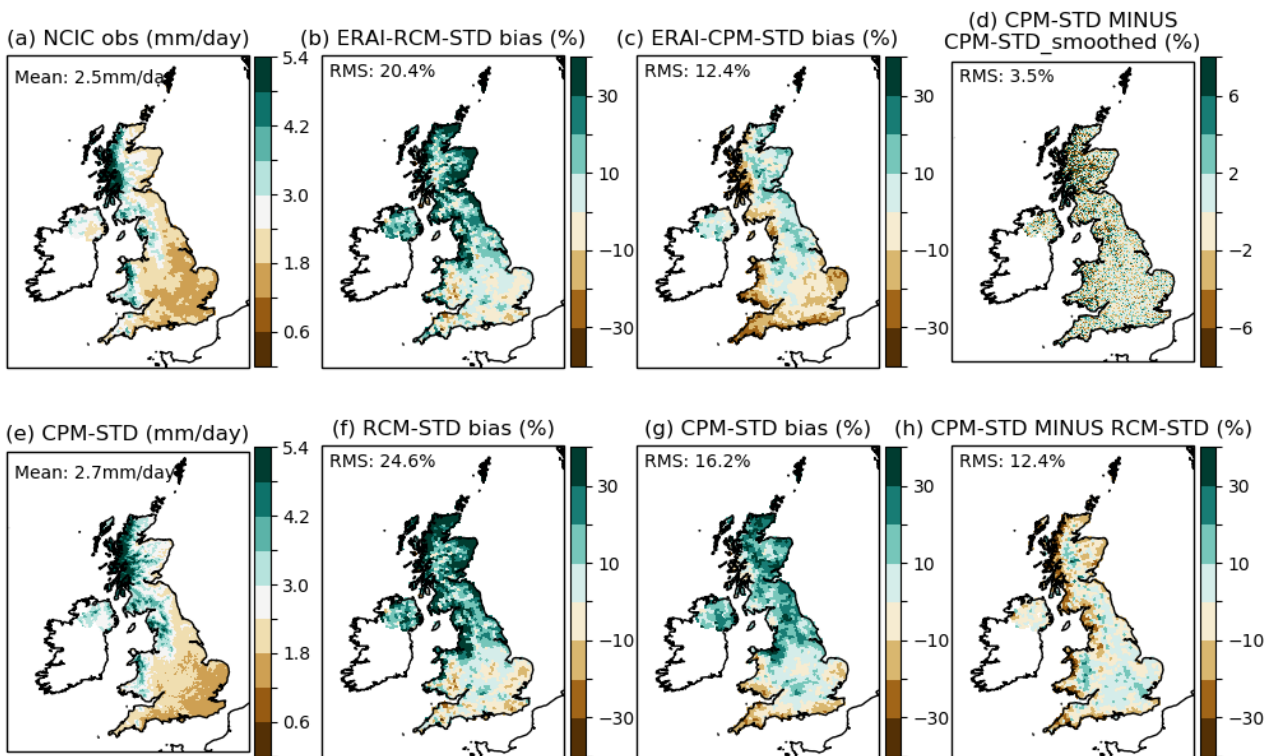
Figure 3.2.4. Observed and simulated summer mean precipitation. As Fig 3.2.1 but for mean precipitation in summer.

3.3 Daily variability

In this section we consider the performance of CPM-12 compared to the driving RCM-PPE in representing daily variability of temperature and precipitation. We focus mainly on ensemble-averaged biases from the GCM-driven simulations, as these are the simulations that will be used in impact applications. It is therefore appropriate to consider a measure of performance across the whole ensemble, that accounts for regional errors arising both from the global model boundary forcing, as well as from internal errors generated within the RCM and CPM domains. However, we also discuss biases from the ERA-interim driven simulations, which provide a direct validation of the RCM and CPM standard member as specific regionalisation tools, independent of biases in the driving global models. For temperature we consider cold winter days (1st percentile of the distribution of daily average winter temperatures) and hot summer days (99th percentile of the distribution of daily average summer temperatures); whilst for precipitation we consider the frequency and intensity of precipitation, as well as wet days (99th percentile of the daily precipitation distribution) in winter and summer.

Figure 3.3.1 shows that cold winter days are too cold in the RCM especially in the north (UK RMS error of 1.7ºC). In contrast, cold winter days are too warm in the CPM (UK RMS error of 1.0ºC), but the bias is reduced. The results in Fig 3.3.1 are for the ensemble mean; individual members show similar results except for one member, where both CPM and RCM are too warm, with greater biases in the CPM. The biases are also seen in the ERA-interim driven simulations (not shown), suggesting that the biases are inherent to the downscaling models. We note that the cold bias in GC3.05-PPE over northern Europe is smaller over the UK (Section 1.2), and does not play a major role in the biases in cold winter days here.

Hot summer days are largely too cold in the RCM-PPE and CPM-12 ensemble-averages (UK RMS errors of 0.8ºC and 0.6ºC respectively, Fig 3.3.1); this is also true for all but two of the individual ensemble members. These biases are largely inherited from the driving global models. The ERA-interim driven simulations (ERAI-RCM-STD and ERAI-CPM-STD, not shown), show that the CPM gives a better representation of hot summer days over the northern UK than the RCM, but not in the south where hot summer days tend to be too hot (by up to 1.5ºC). Drier soils in the CPM (Section 3.5) may be a contributing factor to the latter bias.

In terms of daily precipitation, RCM-PPE has a tendency for too many wet days, in winter and summer, which is considerably improved in CPM-12; although over the far south of the UK the CPM has too few wet days in summer (Figs. 3.3.2-3.3.3). ERAI-driven simulations show similar results (with biases of 5.4% in ERAI-CPM-STD compared to 18.7% in ERAI-RCM-STD in winter, and 12.2% compared to 16.6% in summer) confirming the reduced biases in CPM-12 reflect improved performance in the CPM (and not just a compensation of errors). Fig 3.3.4 shows absolute biases in wet day frequency in winter, showing that in the RCM there is a tendency for too much continuous generation of rain particularly over the mountains, but also in the south-east. In the CPM, rainfall is less frequent particularly over the mountains, in much better agreement with the observations.

The CPM also shows some improvement in wet-day intensity, although this is more modest (Figs. 3.3.2-3.3.3). The RCM tends to underestimate rainfall intensity over mountains, which is improved in the CPM; however in regions remote from major orographic influences, there is a tendency for the CPM to overestimate rainfall intensity by about 10%. Biases are very similar in ERA-interim driven simulations (not shown) indicating that these biases are inherent to the downscaling models. For heavy daily precipitation (99th percentile of all days) in winter, the RCM underestimates the intensity over mountains, but typically overestimates it elsewhere. These biases are reduced in the CPM (UK RMS error is reduced from 19% in

RCM-PPE to 16% in CPM-12, and similarly from 20% in ERAI-RCM-STD to 16% in ERAI-CPM-STD). In summer, biases are similar in the CPM, but with a tendency for the CPM to overestimate the intensity of heavy daily events (UK RMS error of 18% in CPM-12 compared to 16% in RCM-PPE, and similarly 17% in ERAI-CPM-STD compared to 16% in ERAI-RCM-STD). In both seasons, and in both models, wet biases in heavy precipitation are reduced in the STD member when driven by ERA-interim compared to GC3.05, suggesting wet biases are in part inherited from the driving global simulations. In addition, we note that the tendency for the models to overestimate heavy rainfall intensity (in the CPM in summer and in both models in winter away from mountains) is likely to be less in reality, due to the NCIC gauge observations tending to give an underestimate (Table 3.1).
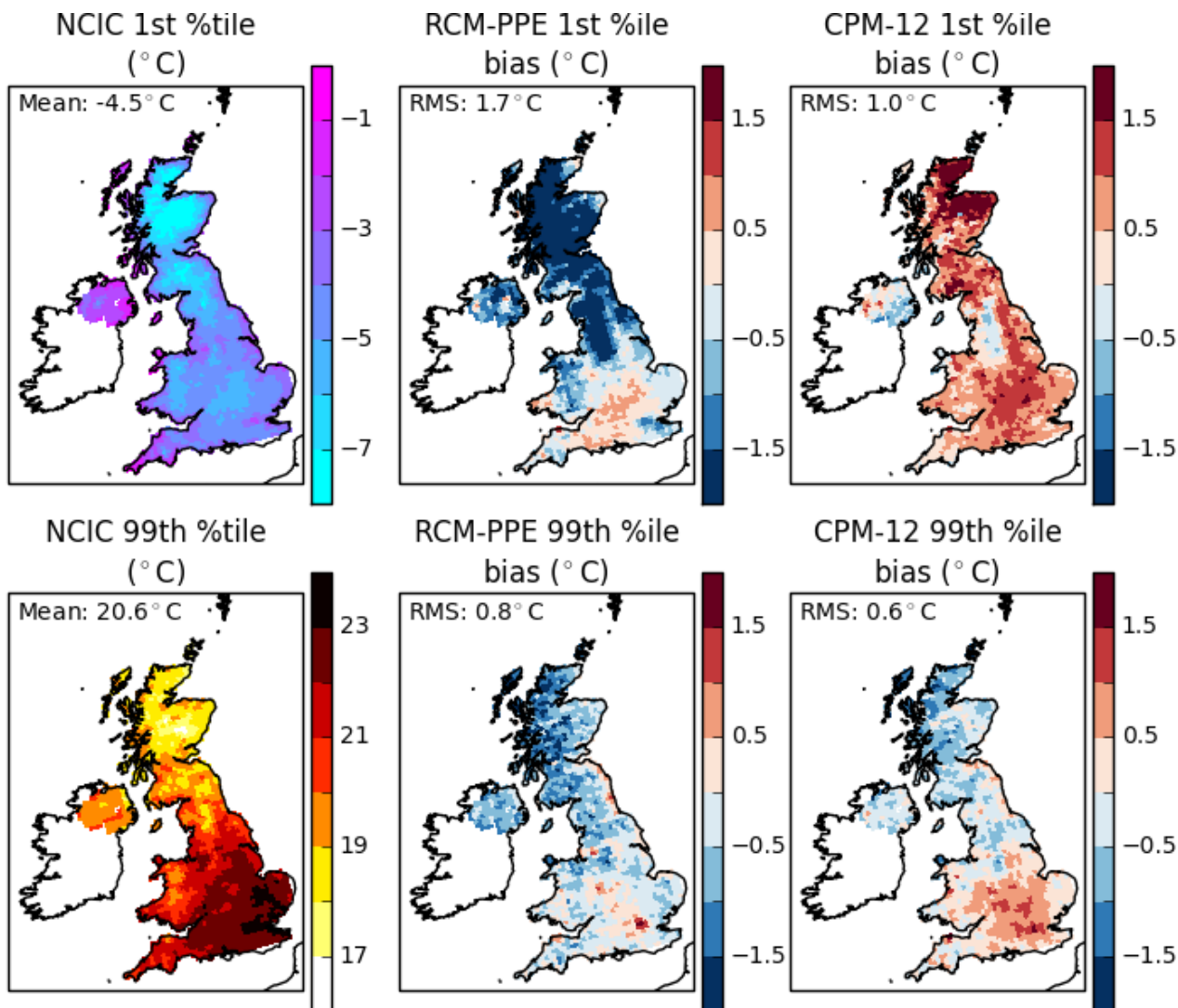
Figure 3.3.1. Observed and simulated daily temperature extremes in winter and summer. Left panels show the 1st percentile of daily average temperature in winter (cold days) and the 99th percentile in summer (hot days) in the NCIC observations during 1981-2000. Centre and right panels show biases (ºC) in the ensemble-average simulated values for the corresponding metrics, from the 12-member RCM-PPE and CPM-12 respectively. Daily data was regridded to the 12km scale in all cases. The UK-averaged (left panels) mean value or (centre, right panels) Root Mean Square (RMS) error is indicated.
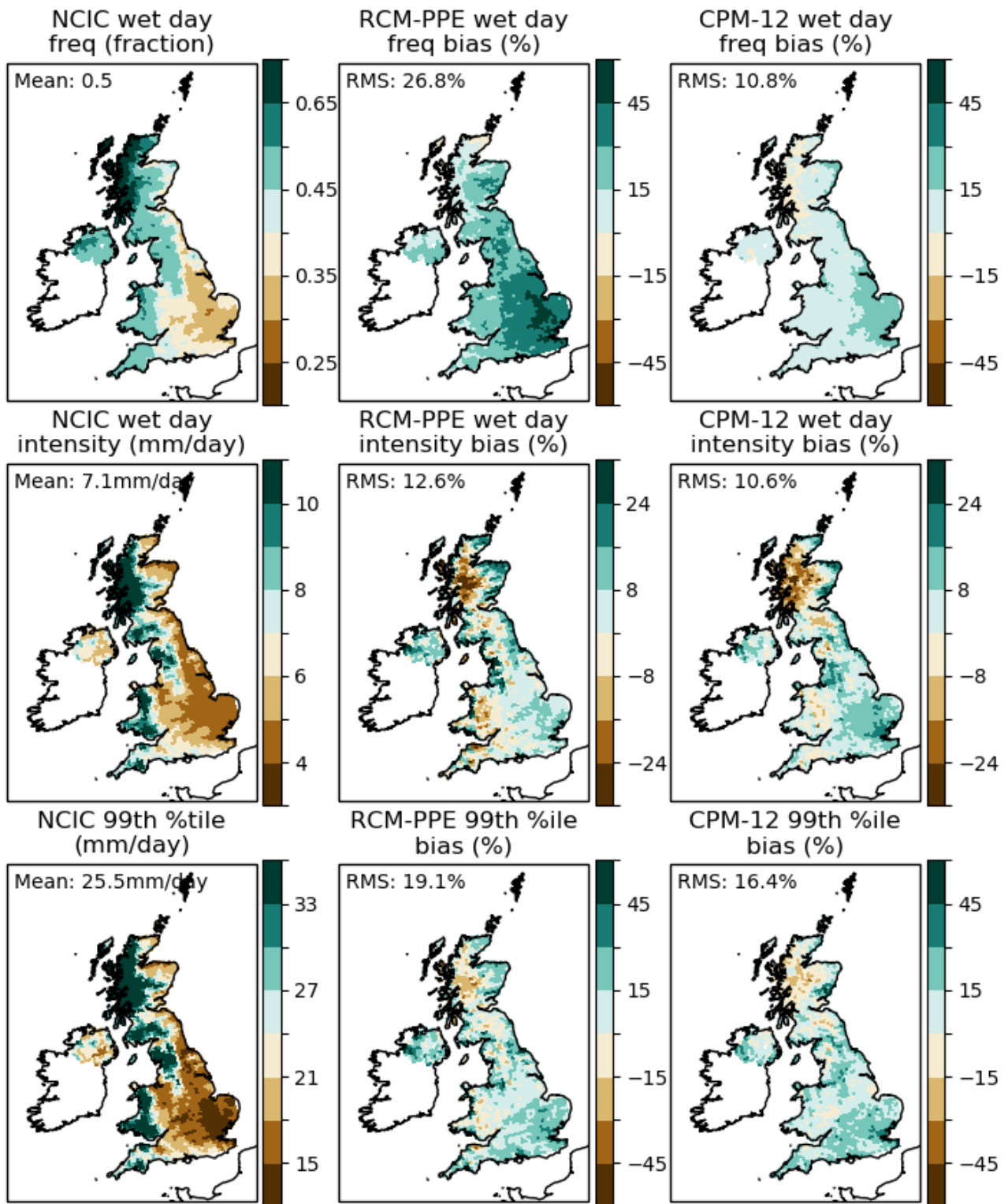
Figure 3.3.2. Observed and simulated daily precipitation in winter. Left panels show wet day frequency, mean wet day intensity and heavy daily precipitation (99th percentile of all days) in winter in the NCIC observations during 1981-2000. Centre and right panels show biases (%) in the ensemble-average simulated values for the corresponding metrics, from the 12-member RCM-PPE and CPM-12 respectively. Wet days are days with greater than 1mm accumulation of precipitation, and daily precipitation data was regridded to the 12km scale in all cases. The UK-averaged (left panels) mean value or (centre, right panels) Root Mean Square (RMS) error is indicated.
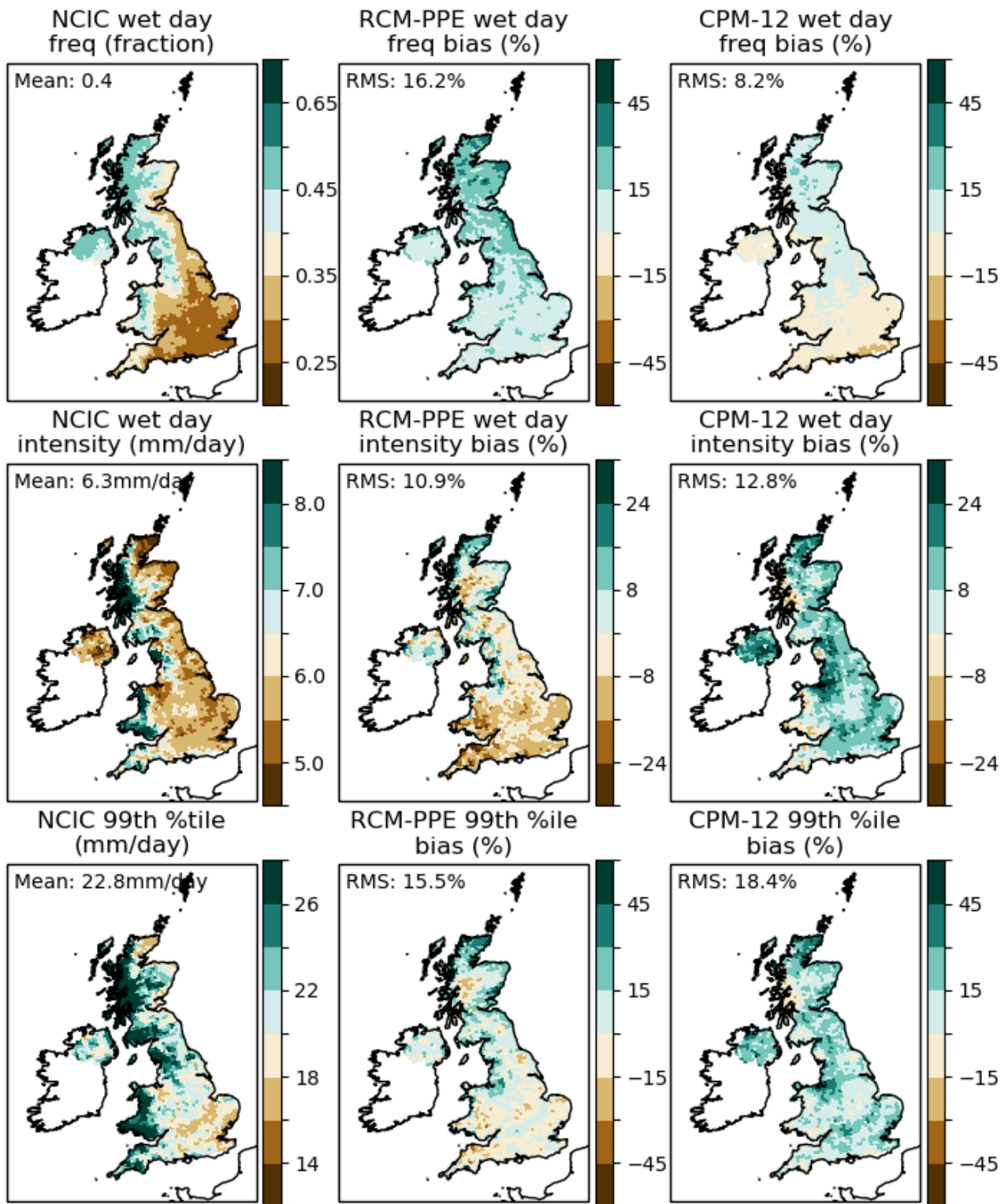
Figure 3.3.3. Observed and simulated daily precipitation in summer. As Fig 3.3.2 but for daily precipitation metrics in summer.
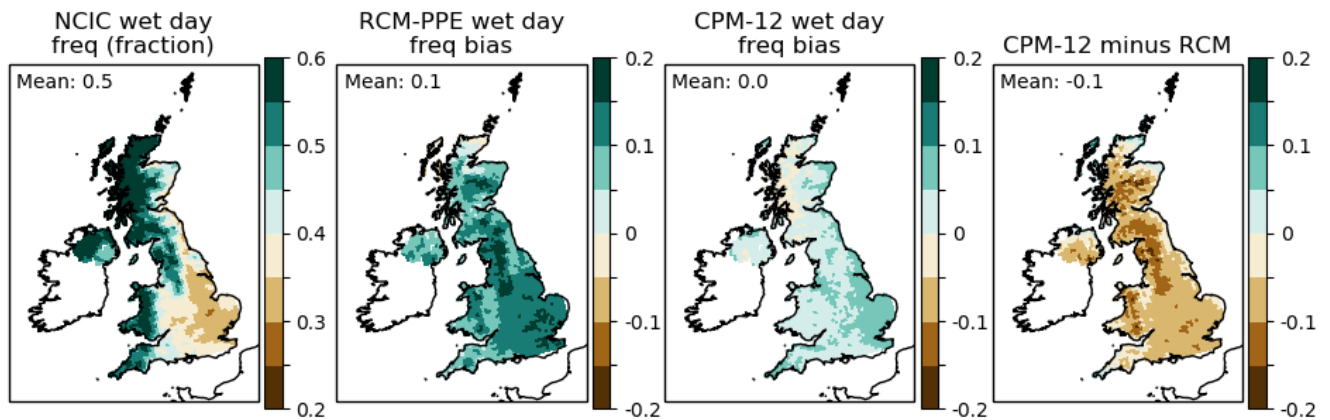
Figure 3.3.4. Wet day frequency in winter. As Fig 3.3.2 top, but showing absolute (instead of percentage) biases in wet day frequency (expressed as a fraction of number of wet days/all days). Also shown (right) is the difference in the ensemble-average values for CPM-12 minus RCM-PPE.

3.4 Hourly precipitation variability

Previous studies have suggested that it is for precipitation events that occur on hourly timescales where we may expect the greatest added value from convection-permitting models, so we now explore the performance of CPM-12 versus RCM-PPE in representing hourly precipitation variability. Hourly precipitation extremes are evaluated in Section 3.5.

On hourly timescales, RCM-PPE has too frequent but too low intensity rainfall, which is a common deficiency in convection-parameterised models (Figs. 3.4.1-3.4.2). In CPM-12, this is considerably improved, although the ensemble does underestimate wet-hour frequency over much of Wales and southern England in summer, and there is now a tendency for rainfall to be too intense. We note that the RCM biases in rainfall frequency (RMS error of ~40%) are greater than the differences between the gauge and radar datasets. This is similarly true for both CPM and RCM biases in rainfall intensity in summer (RMS errors of 22% and 25%), however in winter model biases in rainfall intensity are similar to the observational uncertainty given by the difference between the two datasets used here and less significant. Figs. 3.4.3-3.4.4 show results for high percentiles of the hourly distribution, including all hours, where the 99.5[th] percentile corresponds to about 10 hourly events per season, whilst the 99.95[th] percentile corresponds to about 1 hourly event per season. The RCM underestimates the intensity of these events, whilst the CPM overestimates. These biases are outside of observational uncertainty in summer with an RMS error of 30% in CPM-12 for the 99.95[th] percentile (but not in winter for the UK as a whole). However we note that both observational datasets are likely to underestimate localised intense events (Table 3.1) and so this comparison is likely to overestimate any bias in the CPM.
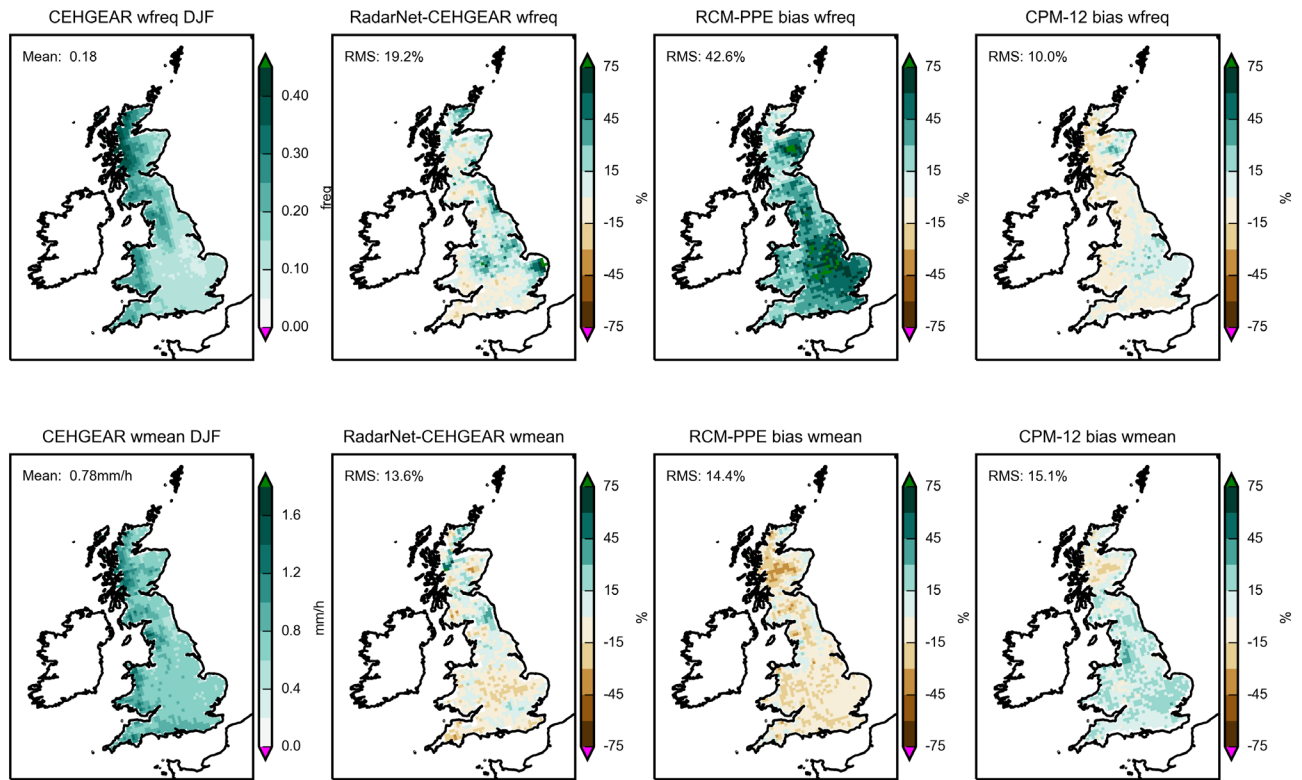
Figure 3.4.1. Observed and simulated hourly precipitation variability in winter. (Top) Wet hour frequency and (bottom) wet hour intensity in winter in the (left) CEHGEAR gauge observations, (centre left) RadarNet minus CEHGEAR observational differences (%), and biases (%) in the ensemble-average simulated values with respect to the gauge observations for the (centre right) RCM-PPE and (right) CPM-12. The gauge observations correspond to 1990-2014, radar observations to 2003-2017, and the model results to 1981-2000. Wet hours are hours with greater than 0.1mm accumulation of precipitation, and hourly precipitation data was regridded to the 12km scale in all cases. The UK-averaged mean value (for gauge observations) or UK-Root Mean Square value (for differences and biases) is indicated in each panel.
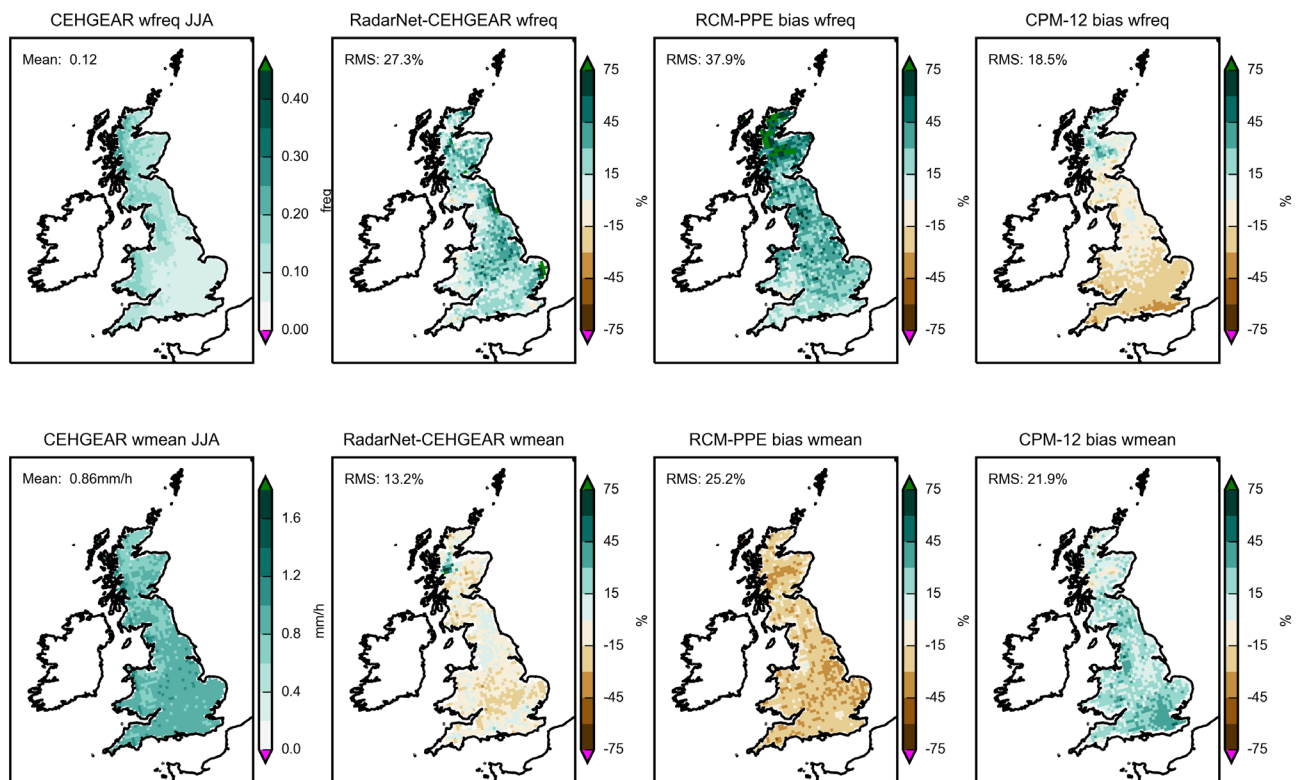
Figure 3.4.2. Observed and simulated hourly precipitation variability in summer. As Fig. 3.4.1 but for summer.
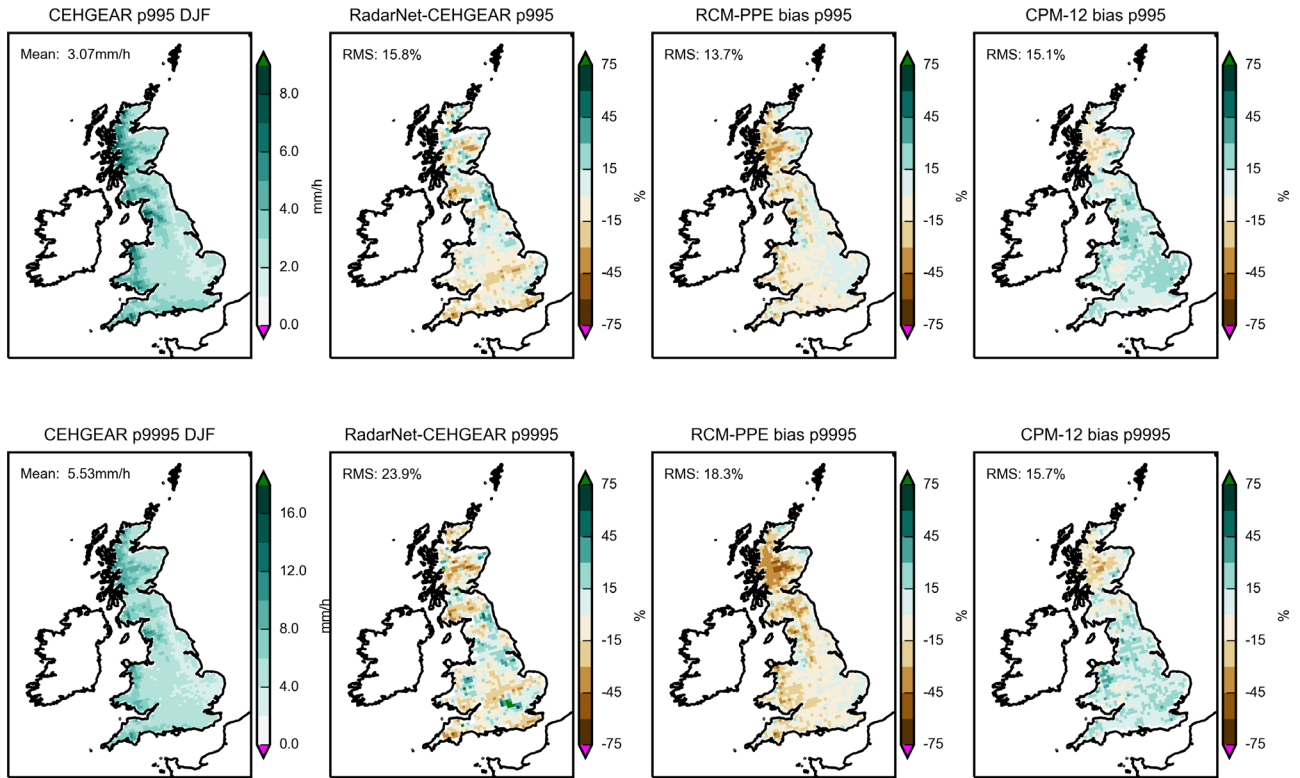
Figure 3.4.3. Observed and simulated heavy hourly precipitation in winter. As Fig 3.4.1 but for the (top) 99.5th and (bottom) 99.95th percentile of hourly precipitation (including all hours) in winter.
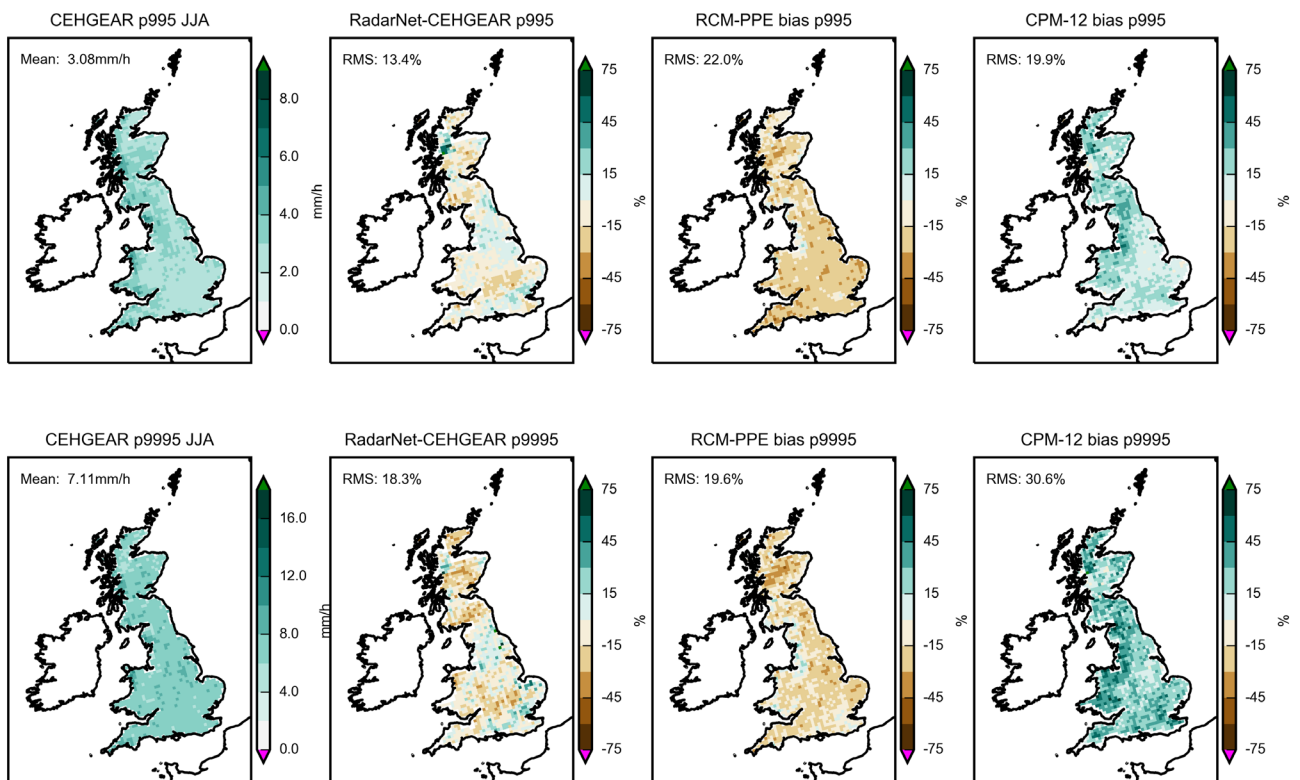
Figure 3.4.4. Observed and simulated heavy hourly precipitation in summer. As Fig 3.4.1 but for the (top) 99.5th and (bottom) 99.95th percentile of hourly precipitation (including all hours) in summer.

The CPM is found to give a better representation of the diurnal cycle of precipitation compared to the RCM (Fig. 3.4.5). In particular a later afternoon peak and secondary morning peak is seen in the CPM in SON in good agreement with the radar. In JJA, there is some improvement in the CPM, with a delay in the initiation of convection and a later decay, but the CPM peak is still too early compared to the observations. We note that revised stochastic perturbations in the boundary layer were introduced in the latest operational NWP configuration (on which the CPM is based, Section 2.3) with the aim of actually achieving an earlier initiation of convection, since this was found to be too late in NWP case studies. It is perhaps surprising that the greatest improvement in the diurnal cycle in the CPM is in autumn, rather than summer when a greater proportion of the rainfall is convective. The most likely explanation is that explicit convection tends to kick off too readily when there is sufficient solar heating (although convective initiation is still more realistic than in the parameterised model). This will tend to happen earlier in the morning in the summer than the autumn, with convection becoming more intense. In the autumn, convection will tend to be more delayed and perhaps organise more because of stronger shear which helps it to persist rather than die out when the sun gets weaker. We note that the diurnal cycle for the gauge data is not shown in Fig. 3.4.5 since the diurnal cycle is not reliable due to the construction of this dataset (hourly data is created by disaggregating daily data from 09Z to 09Z+1 day).
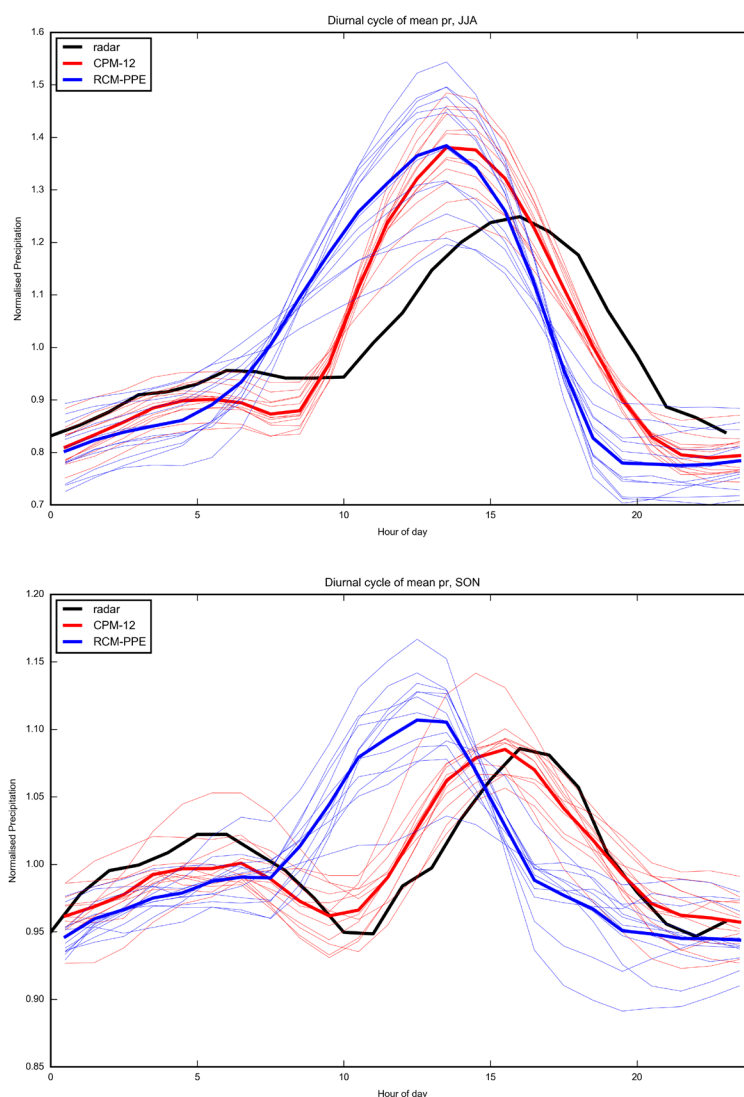
Figure 3.4.5. UK-average diurnal cycle of precipitation. Results are shown for RadarNet radar observations (2003-2017) and the RCM-PPE and CPM-12 (1981-2000; ensemble-average is thick and individual members are thin lines), for (top) JJA and (bottom) SON. Plotted is the average precipitation for the given hour of the day normalised by the average precipitation for all hours.

Figure 3.4.6 evaluates the shape of the distribution of hourly precipitation events, for all four seasons. The highest contributions to the total precipitation come from moderate intensity events, rather than the more numerous low-intensity events. The results again show the tendency of CPM-12 to overestimate hourly intensities, with too many high intensity events compared to the gauge observations (in the majority but not all CPM-12 members) in summer. In all seasons, however, CPM-12 performs better than RCM-PPE in capturing the observed distribution of hourly intensities. The RCM ensemble tends to underestimate the number of high intensity events and overestimate the number of low intensity events, with too few dry hours. In general, biases in the ERA-Interim driven CPM and RCM simulations are similar to those in the corresponding GCM-driven simulations, indicating the biases are inherent to the regional models themselves.
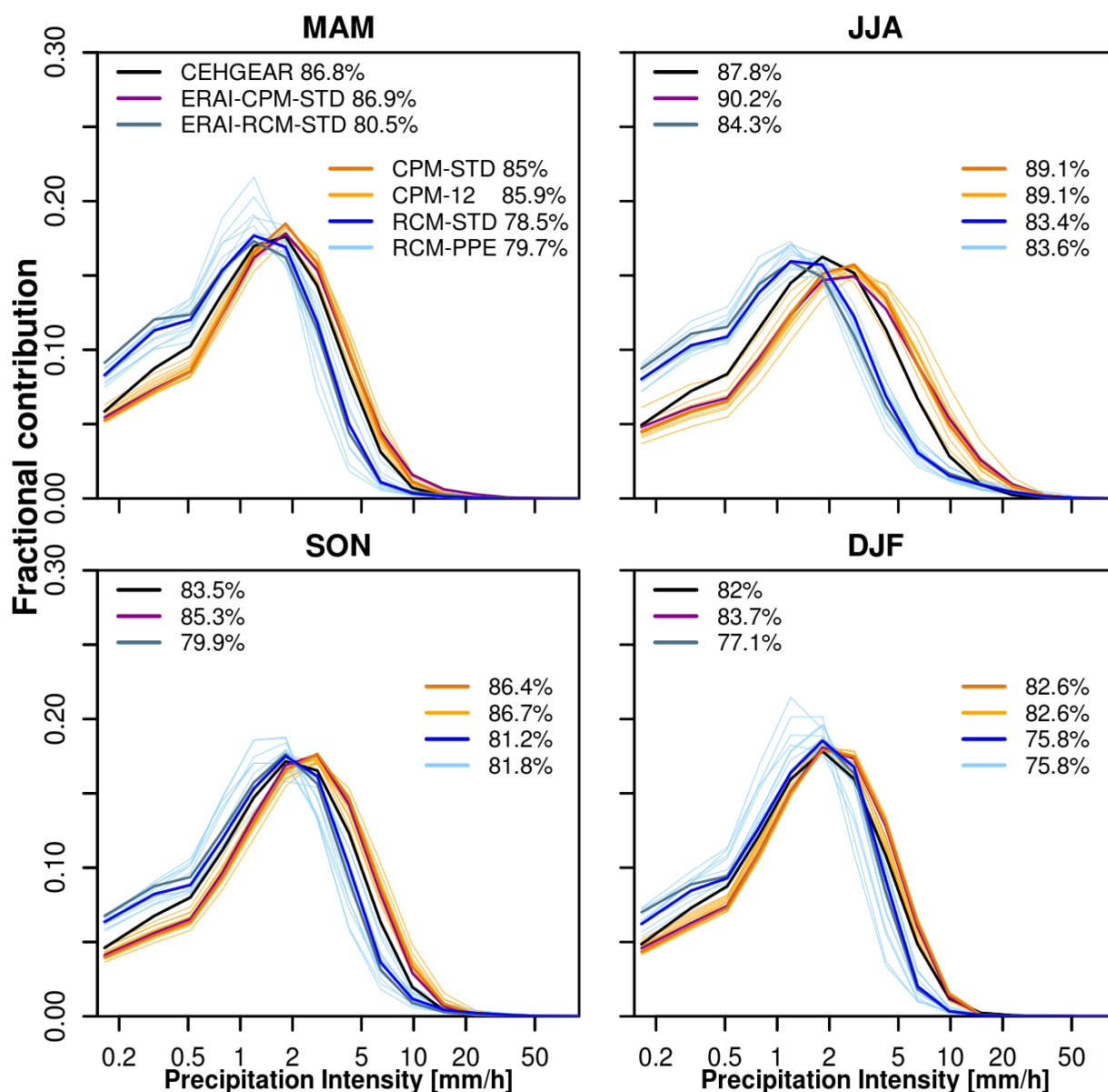
Figure 3.4.6. Fractional contribution of hourly precipitation intensities to total precipitation. Plotted is the fractional contribution of hourly precipitation events within 17 different intensity bins to total UK rainfall, for wet events only (>0.1mm/h), in different seasons. The contributions were calculated by assigning each wet hour from every 12km UK grid box to the relevant intensity bin, and multiplying the number of counts in each bin by the average intensity; these contributions are then divided by the total precipitation across all bins to give the fractional contribution. Results are shown for the (black) CEHGEAR gauge observations (1990-2014), (purple) ERAI-CPM-STD, (turquoise) ERAI-RCM-STD, (orange) CPM-12 and (blue) RCM-PPE (1981-2000). The percentage of dry hours (in %) are indicated in the figure legends. Intensity bin boundaries are: 0.1, 0.23, 0.41, 0.62, 0.95, 1.4, 2.2, 3.4, 5.1, 7.8, 11.9, 18.1, 27.5, 42.0, 63.9, 97.4,148 and 500 mm/h.

The joint precipitation-amount and duration distribution of events across Great Britain (Fig 3.4.7 – 3.4.8) shows evidence of the improved representation of hourly rainfall characteristics in the CPM compared to the RCM. In summer, the RCM has a tendency for too little short-duration rainfall and too much longer-duration low-intensity rainfall. Biases are similar in the ERAI-RCM-STD and RCM-STD, suggesting they are inherent to the RCM itself. These biases are considerably improved in the CPM, but this has a tendency for too much short-duration higher-intensity rainfall. Similar results are also seen in winter, although the excess in short-duration high-intensity rainfall is less pronounced than in summer, resulting in better overall agreement between the CPM and the gauge observations in this season. These results indicate that convective showers over the UK in winter are well captured by the CPM (with convection still occurring but less prominent than in summer). Overall, the results are consistent with those shown in earlier CPM studies (Kendon et al, 2012, Kendon et al, 2014). Some overestimation of intense events by the CPM is expected due to the fact that, at 2.2km grid spacing, the model is unable to fully resolve convection (Section 1.3).
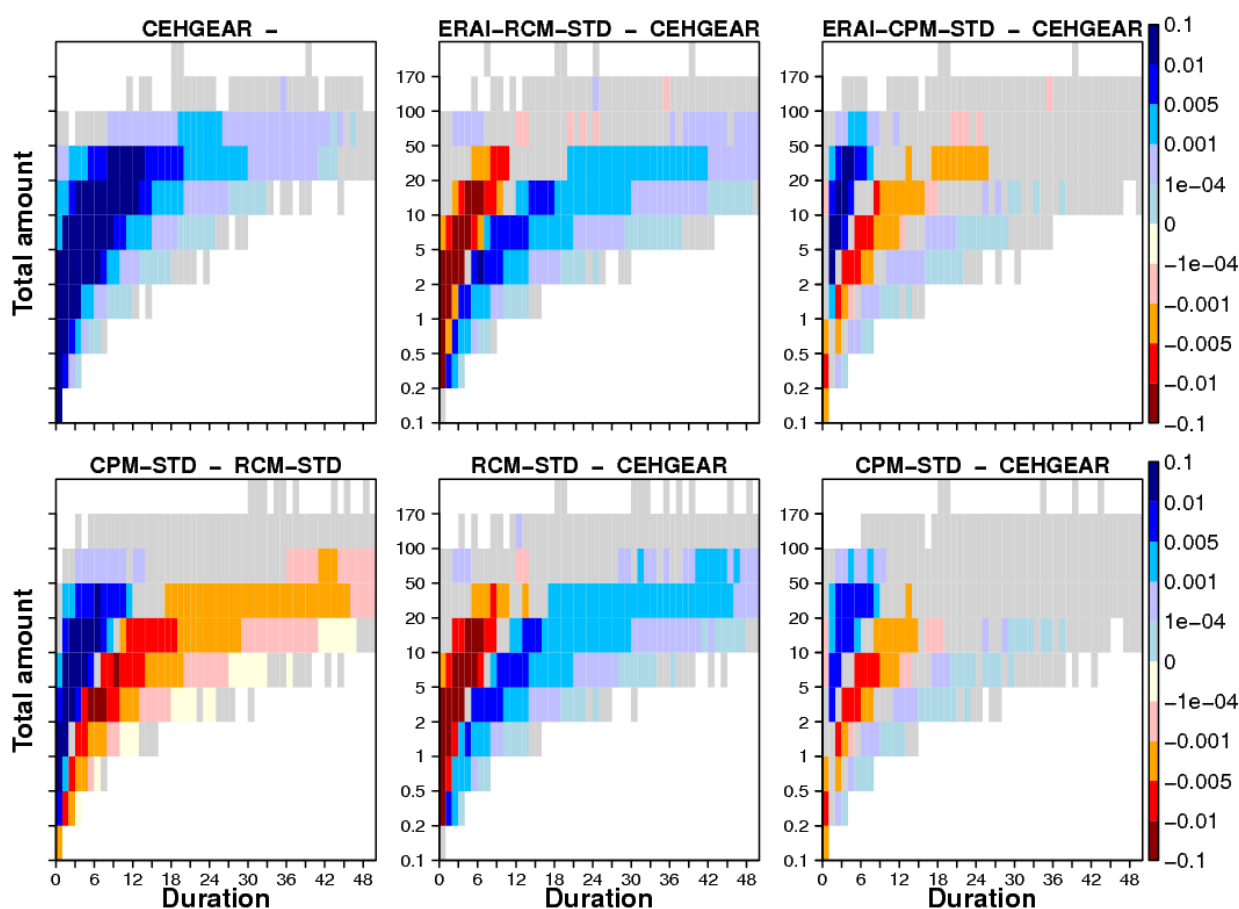
Figure 3.4.7. Precipitation amount and duration of summer rainfall events. Plotted is the fractional contribution of each amount-duration bin to the total precipitation in the (top left) CEHGEAR gauge observations; biases for the (top centre) ERAI-RCM-STD, (top right) ERAI-CPM-STD, (bottom centre) RCM-STD and (bottom right) CPM-STD; and (bottom left) differences between CPM-STD and RCM-STD. Amount is the total precipitation accumulated over the event, where events are continuous periods of precipitation exceeding 0.1mm/h, for all grid cells over Great Britain. Fractional contribution is given by (joint probability of a given amount-duration bin) x (mean bin precipitation amount) / (total precipitation over all bins). Model biases that are not significant at the 1% level are masked in grey. Significance is tested using a 1000 member bootstrap applied to the CEHGEAR (1990-2014) observations and to the model simulations (by choosing years at random with replacement from the full 20 or 25 year time series) to give 1000 estimates of the model bias. The bias is significant if the 0.5-99.5th confidence interval does not overlap zero.
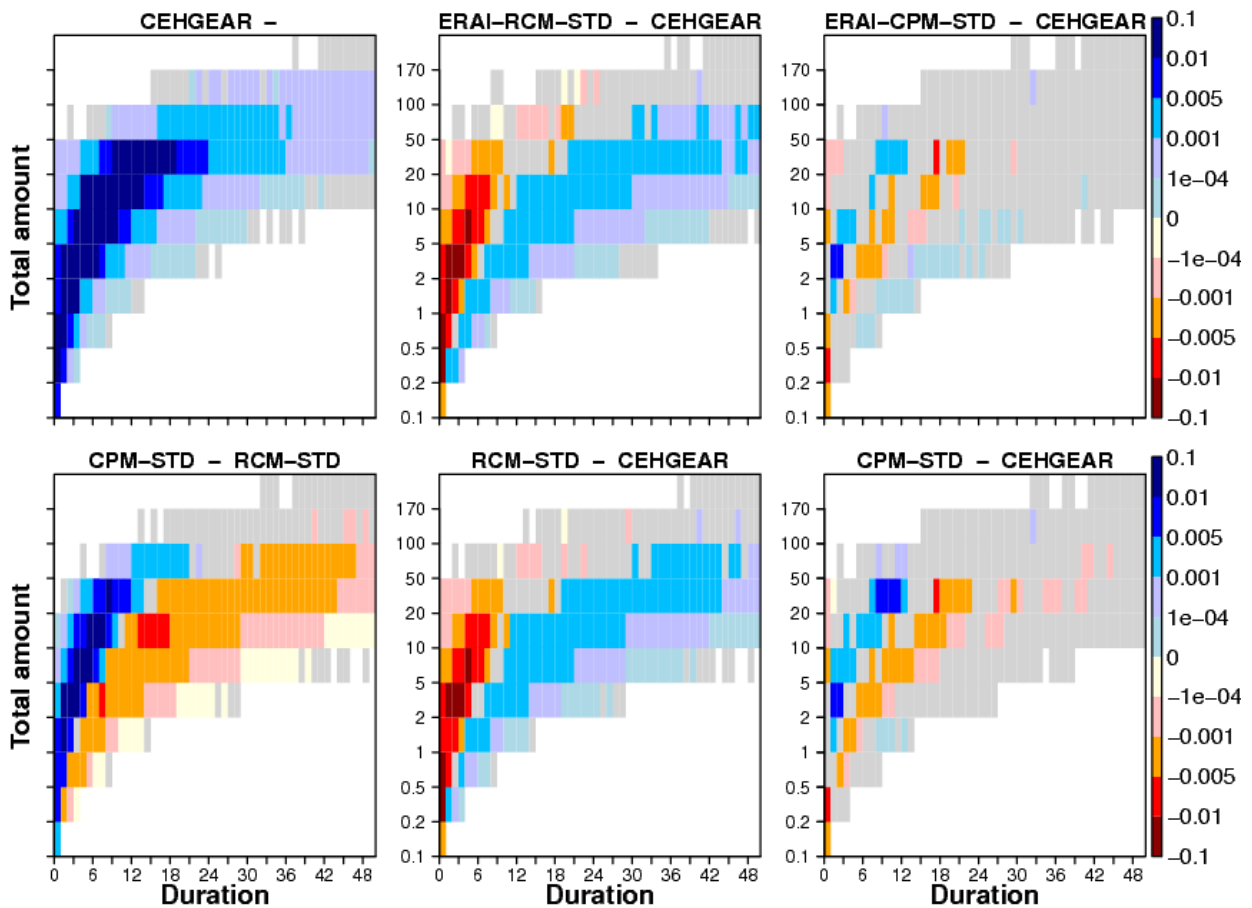
Figure 3.4.8. Precipitation amount and duration of winter rainfall events. As Fig 3.4.7 but for winter.

3.5 High impact events

Extreme hourly precipitation

To characterise the extreme tail of the hourly precipitation distribution, we fit a Generalised-Pareto Distribution (GPD) to extremes of daily maximum hourly precipitation selected using Peak-Over-Threshold (POT) methodology (Coles, 2001; Chan et al, 2014). In particular, extremes are values exceeding the 99.5[th] percentile of all daily-maximum hourly values for annual analysis or the 99.0[th] percentile for seasonal analysis. This corresponds to a sample size of almost 2 events per year, or almost 1 event per season, at each grid box. The use of daily maximum hourly values ensures only one event is selected on a given day, and is a simple method of accounting for time dependence in the data. At each grid box, we fit a GPD normally with L-Moments and compute the 2-year return level. In the case of the radar data there are a few spurious high values (in excess of 100 mm/h at the 12km scale, Table 3.1) and these were removed before fitting the GPD. Choice of the appropriate threshold for eliminating "bad" data is not easy and is a balance between minimising the removal of valid high values and minimising contamination with spurious values. For the gauges the maximum observed value over the UK is 63mm/h at the 12km scale, but gauges will miss localised intense showers and so hourly extremes will be underestimated. Therefore 100m/h was chosen as an estimate of the valid upper limit for the radar, but some contamination of the data with spurious values will remain.

In addition to a grid-point analysis, we also carry out a regional frequency analysis following Hoskins and Wallis (1993) in order to allow a more robust calculation of return levels for higher return periods (see Appendix A for details). For this we divide the UK into three sub-regions (NW, NE and S UK, see Fig 3.5.1), chosen to be approximately uniform in terms of their precipitation climatology. In this analysis of the extreme tail, we primarily use the gauge observations to evaluate model performance, given the known deficiencies of the radar in measuring intense events (Table 3.1) and the spurious high values in the radar data, but also acknowledge that gauges miss localised heavy precipitation.

2-year return levels of annual extremes are higher for the CPM than the RCM, with the CPM tending to overestimate the 2-year return level compared to the gauge and radar observations (Fig. 3.5.1). However, as noted above, both the gauge and especially the radar datasets have deficiencies in their representation of localised intense extremes (the gauges are expected to give an underestimate due to undercatch or the event being missed entirely; whilst the radar suffers from beam attenuation as well as spurious high values, Table 3.1.). Some overestimation of intense events by the CPM is expected due to the fact that, at 2.2km grid spacing, the model is unable to fully resolve convection (Section 1).

Looking across a range of return periods for the 3 UK sub-regions (Figs. 3.5.2-3.5.4), it can be seen that although the CPM tends to overestimate hourly extremes, it gives a much better representation of the rate at which extremes increase with increasing return period ("growth-curve", i.e. slope of red and black lines agree). The growth curve is commonly used in hydrological modelling where it is a measure of the variability in flooding, but it is also important as it is indicative of the underlying extreme rainfall processes, and the extent to which the model is able to capture the relative increase in rainfall for the rarest events. The improvement in the CPM compared to the RCM in representing the growth-curve is true for the S-UK in all seasons and for the NE-UK in all seasons except DJF where it underestimates the growth-curve. In each of these cases, the growth curve is too steep in the RCM-PPE compared to gauge observations. For the NW-UK, the CPM overestimates extremes in summer only; in winter, it underestimates extremes and underestimates the growth curve. In this region, the RCM-PPE tends to underestimate extremes in winter (more so than the CPM) and spring, whilst in summer and autumn it has a too steep growth curve. The consequence of a too steep growth-curve is that although the RCM-PPE underestimates the 2-year return level (in most but not all ensemble members), it overestimates rare extremes (beyond 10-year return period) in summer and autumn, and in all seasons over the S-UK.

Comparing the CPM-STD and ERAI-CPM-STD results (Figs. 3.5.2-3.5.4) shows that the overestimation of extremes in the CPM is largely an inherent bias in the CPM, with similar biases for the ERA-Interim driven run (biases are actually slightly worse in spring, similar in summer and slightly reduced in autumn and winter for ERAI-CPM-STD). In the case of the RCM, ERAI-RCM-STD also shows similar results to RCM-STD (although in northern regions there is a shift to lower extremes in autumn), indicating that the tendency for the growth curve to be too steep is an inherent bias in the RCM.

Uncertainty in the GPD fit is shown in Figs. 3.5.2-3.5.4 for the standard member (dotted lines), which is indicative of the uncertainty in the fit for all ensemble members. This shows that uncertainty in the GPD fit is generally larger than the ensemble spread, suggesting that the differences between ensemble members are due, at least in part, to uncertainty in the sampling of extremes. Uncertainty in the GPD fit in the RCM is larger than that for the CPM, with this increasing considerably on moving to higher return periods.

This difference in behaviour at the extreme tail between convection-permitting and convection-parameterised models has been found previously, and relates to unphysical so called "grid point storms" in the 12km model. These events occur when the convection parameterisation is unable to remove enough of the convective instability and the model has to represent a storm on a grid square that is too large to be physically sensible for a single updraft. Grid point storms typically involve saturated conditions, and large amounts of large-scale and convective precipitation occurring simultaneously (Chan et al 2014, 2016) with unphysically large vertical velocities. They can be identified on visualising the heaviest hourly events in the RCM. In summer the heaviest event in the RCM-PPE is 121mm/h, corresponding to a single grid cell with an unphysically high value in excess of 100 mm/h, in the middle of a larger area of heavy rainfall (Fig 3.5.5). For the UK, the highest hourly total in observational records is 92 mm which was recorded on 12th July 1901 in Maidenhead, Berkshire, but this is for a single point location and such a high value when averaged over a 12km grid box is not plausible. The heavy rainfall event in the RCM is also seen in the CPM, but with a more realistic maximum intensity over the UK of 37 mm/h. The situation is similar for the heaviest event of 103 mm/h in the RCM-PPE in autumn (Fig 3.5.6). In contrast the heaviest events in CPM-12 of 72 mm/h in summer and 47 mm/h in autumn (Figs. 3.5.7-3.5.8) are associated with organised heavy events, with no evidence of single grid point saturation. We note that in all these events, the broader scale organisation of precipitation and sea level pressure patterns are similar between the CPM and RCM. Unphysical grid point storms in the RCM-PPE are likely to be the cause of the notable increase in ensemble spread for high return period estimates (reflecting the large uncertainty in the GPD fit) in RCM-PPE seen in Figs 3.5.2-3.5.4. We note that the screening out of unphysical grid point storms, potentially using the simultaneous occurrence of large amounts of convective and large-scale precipitation as a diagnostic, could be applied to the RCM data before fitting the GPD, which may improve the performance of the RCM in representing extremes. This has not been applied here, and would require careful evaluation to assess the validity of this approach and the resulting RCM return level estimates.
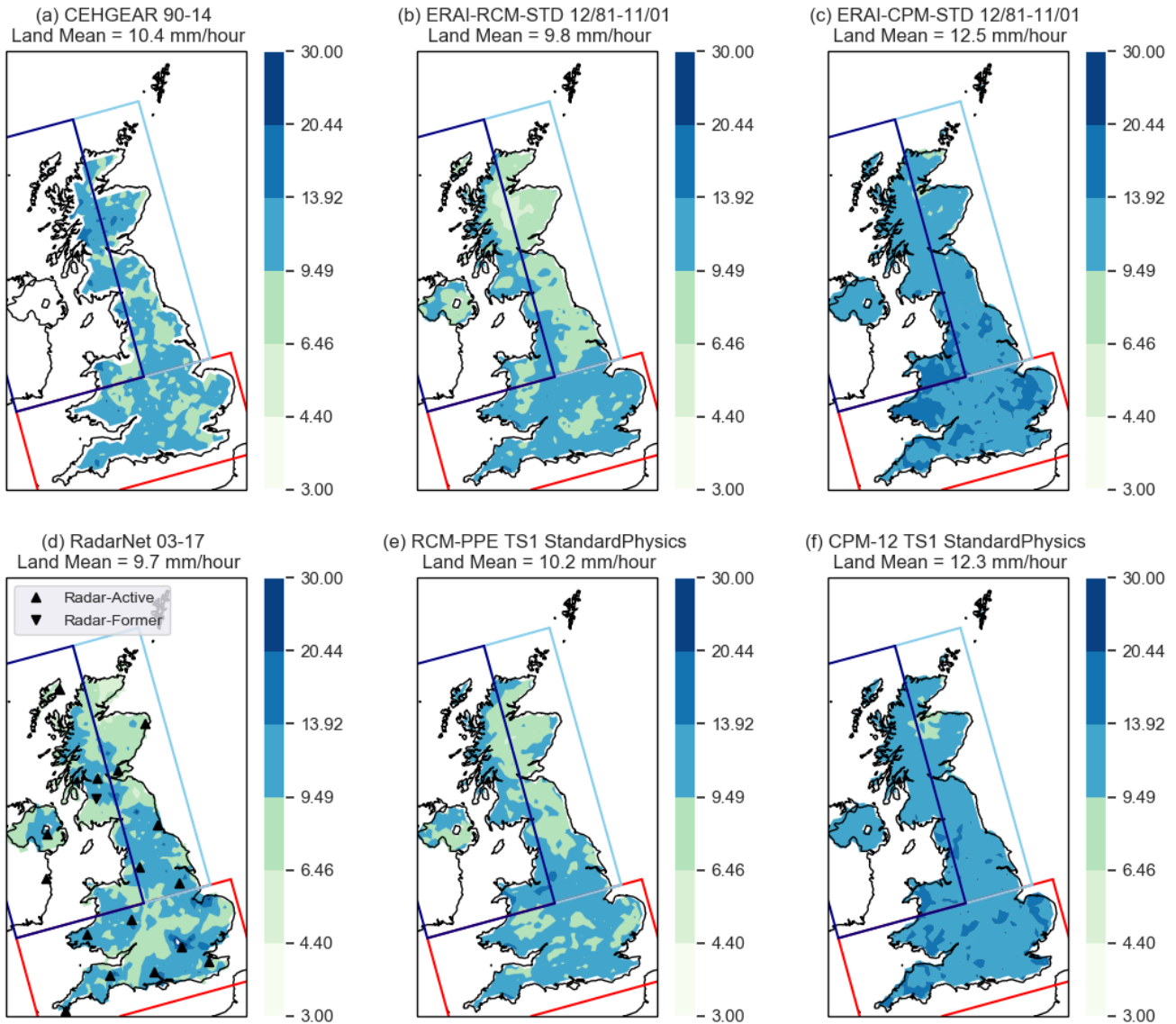
Figure 3.5.1. 2 year return level of daily maximum hourly precipitation. Shown are the return levels using data from all seasons for: observations from (a) CEHGEAR gauge dataset for 1990-2014 and (d) RadarNet radar dataset for 2003-2017; model estimates for (b) ERAI-RCM-STD and (c) ERAI-CPM-STD for Dec 1981 to Nov 2001; and (e) RCM-STD and (f) CPM-STD and for TS1 (Time slice 1, Dec 1980 to Nov 2000). All hourly precipitation data has been regridded to a common 12km grid before calculation of return levels. The NW, NE and S UK regions for the regional frequency analysis are shown. Also indicated in (d) are the sites of radar stations that are currently operational (radar-active) and radar sites that are in the UK network but are no longer providing data (radar-former).
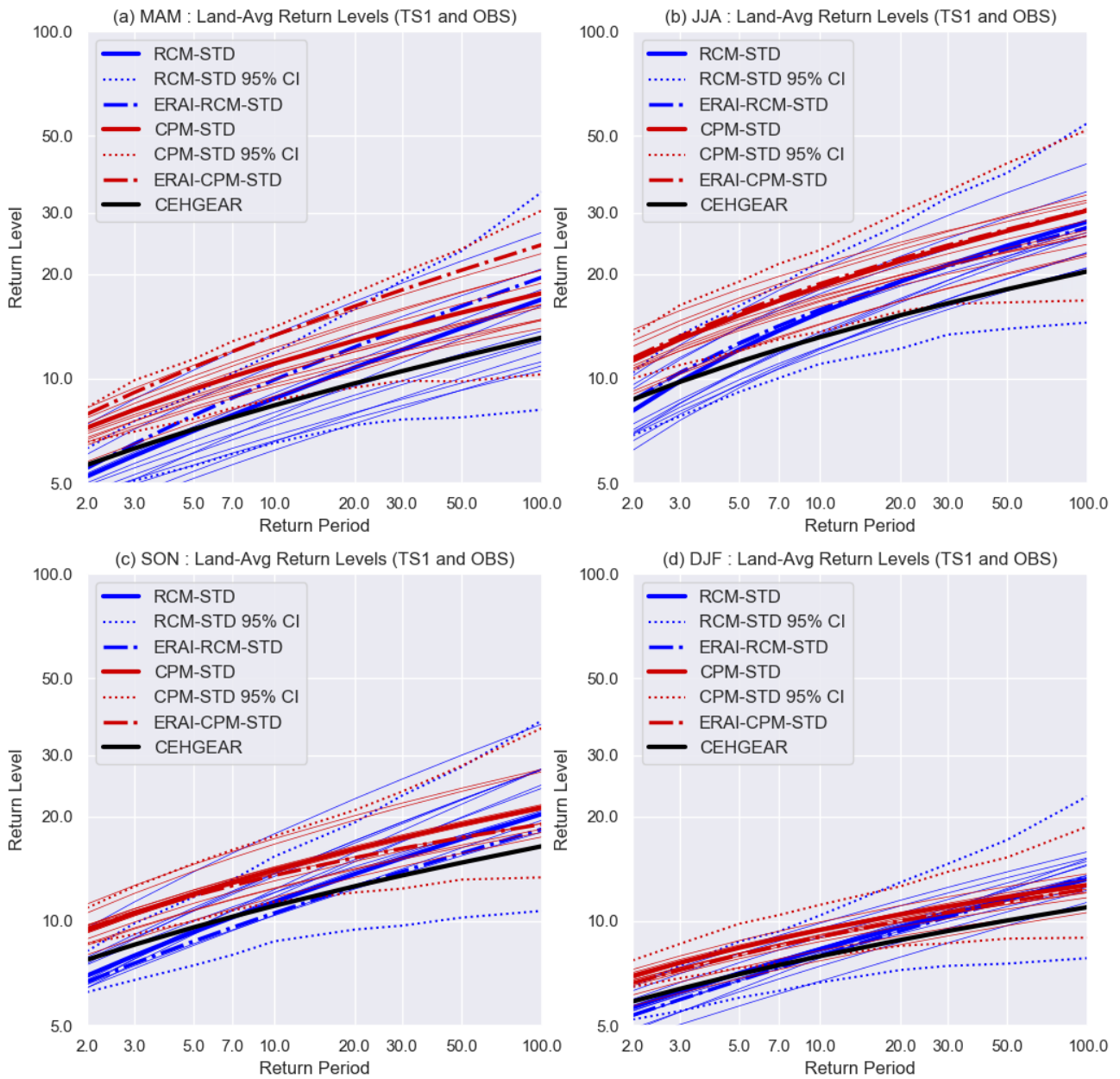
Figure 3.5.2. Southern UK average return level of hourly precipitation extremes. South UK average return level of daily maximum hourly precipitation as a function of return period, for individual seasons. Shown are the return levels (mm/h) for the CEHGEAR gauge observations (1990-2014); the twelve CPM-12 and RCM-PPE ensemble members (1981-2000), where the standard member CPM-STD and RCM-STD is shown in bold; and ERAI-CPM-STD and ERAI-RCM-STD. The regional average values have been calculated using the regional frequency analysis method. The 95% confidence interval in the GPD fit for the standard member is shown as dotted, and is calculated by generating random data from the original fit, refitting the GPD, and recomputing the return levels 1000 times.
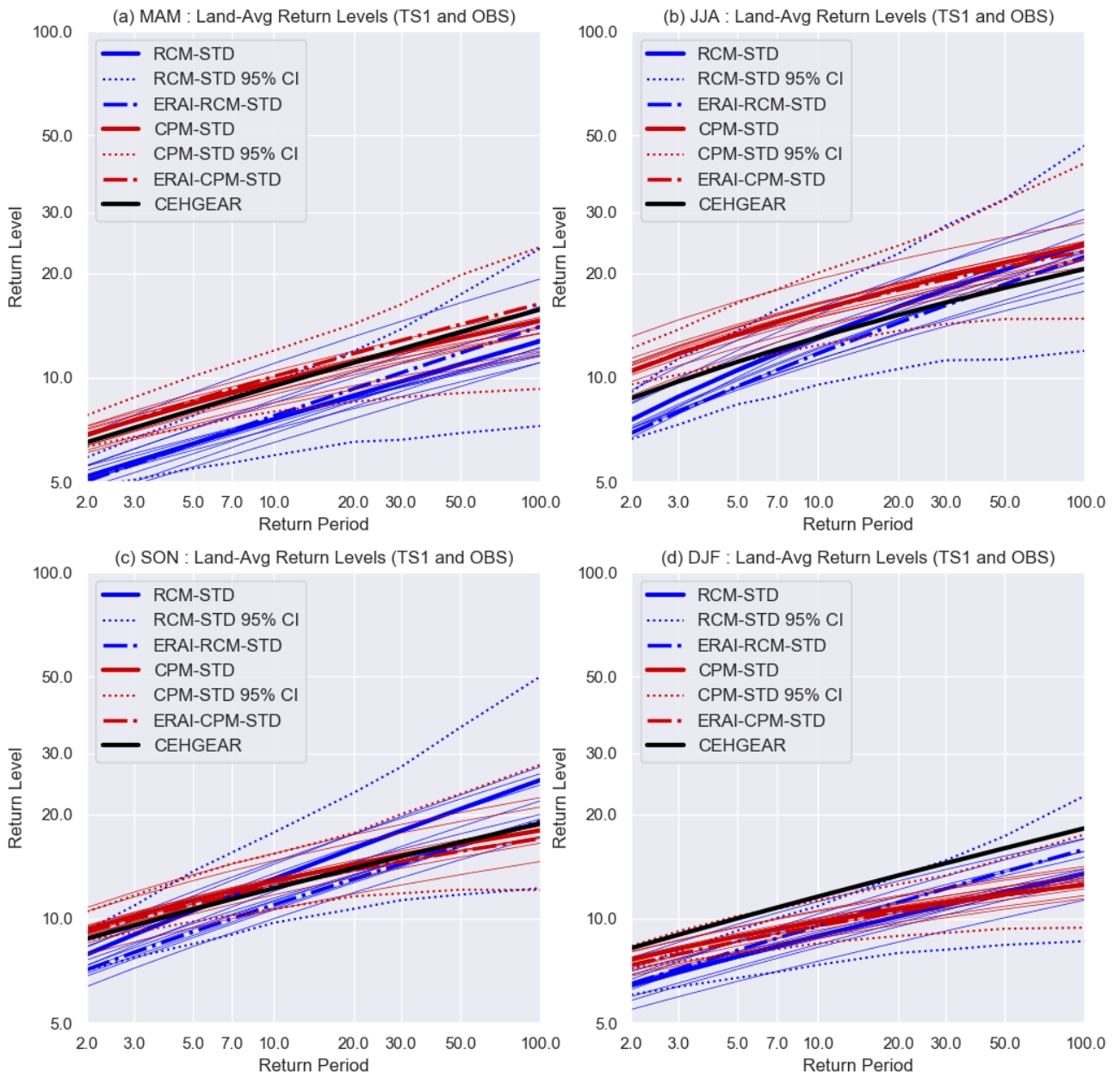
Figure 3.5.3. North-West UK average return level of hourly precipitation extremes. As Fig 3.5.2 but for NW region.
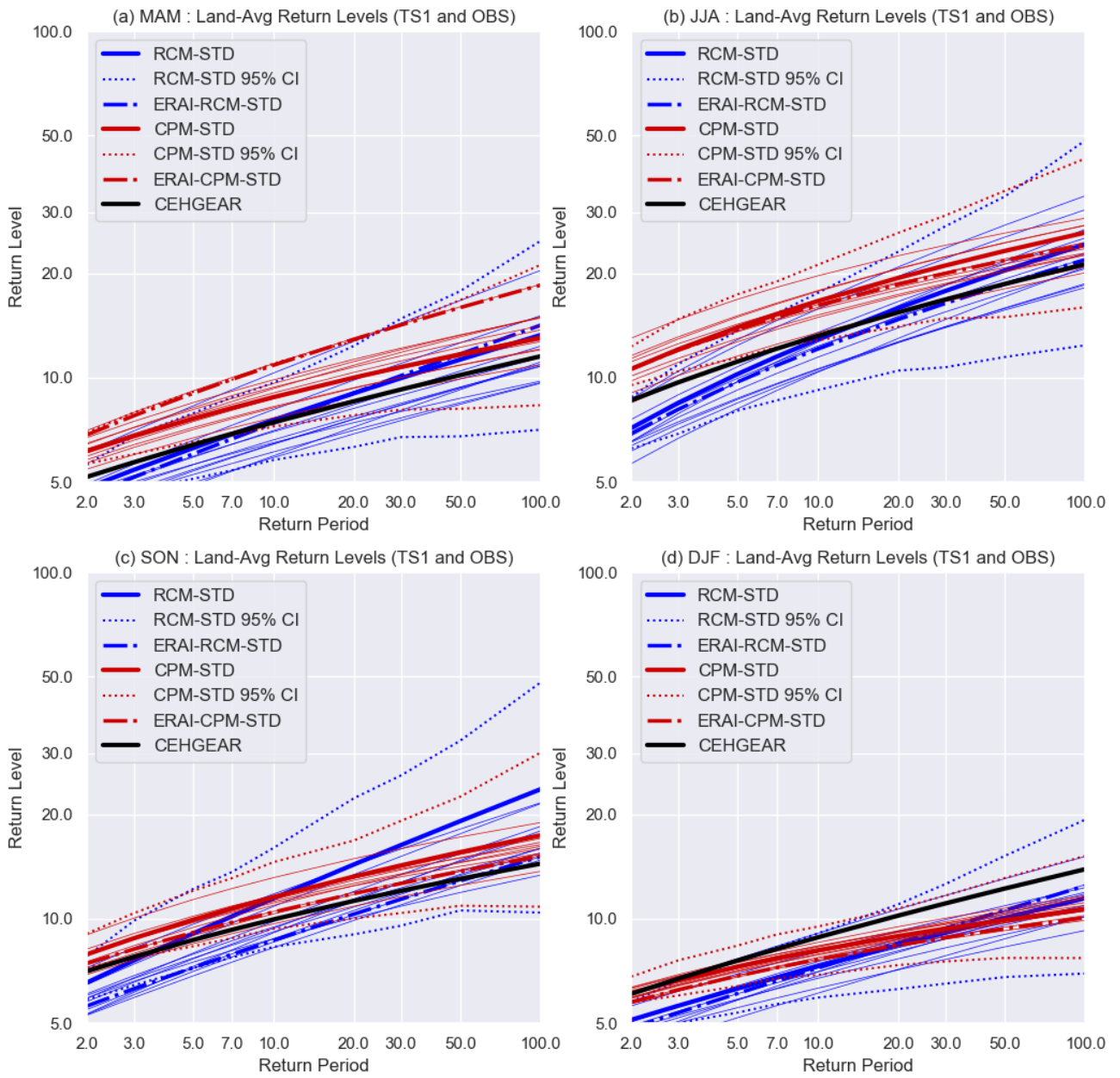
Figure 3.5.4. North–East UK average return level of hourly precipitation extremes. As Fig 3.5.2 but for NE region.
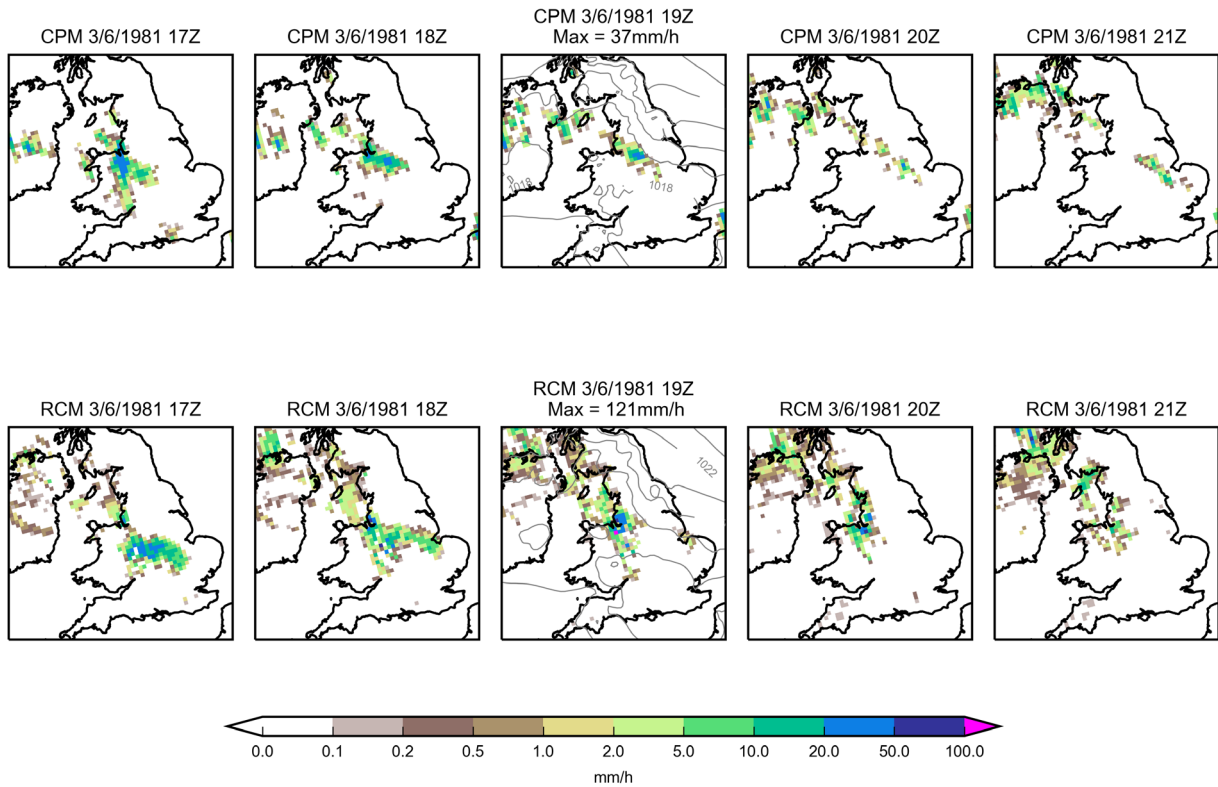
Figure 3.5.5. Heaviest summer hourly event in RCM-PPE. Hourly precipitation in the RCM and corresponding CPM member, for the heaviest hourly event across the UK in summer in the baseline period across the RCM-PPE. Precipitation is shown for the (centre) hour of the event, (left) 2 hours previous to and (right) 2 hours following the event. The maximum over the UK is indicated for the centre panel. Also contoured on the centre panel is the daily mean sea-level pressure on the day of the event in the RCM and CPM respectively.
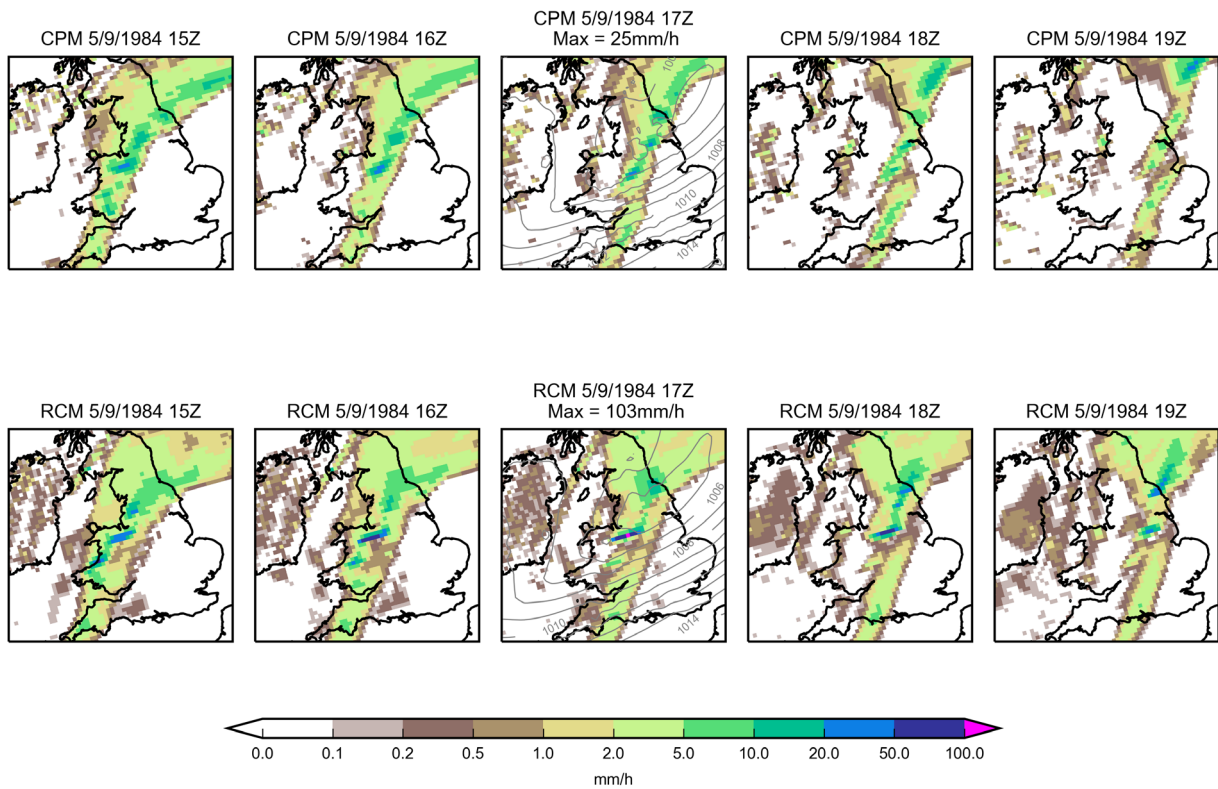
Figure 3.5.6. Heaviest autumn hourly event in RCM-PPE. As Fig 3.5.5, but for the heaviest hourly event across the UK in autumn across the RCM-PPE.
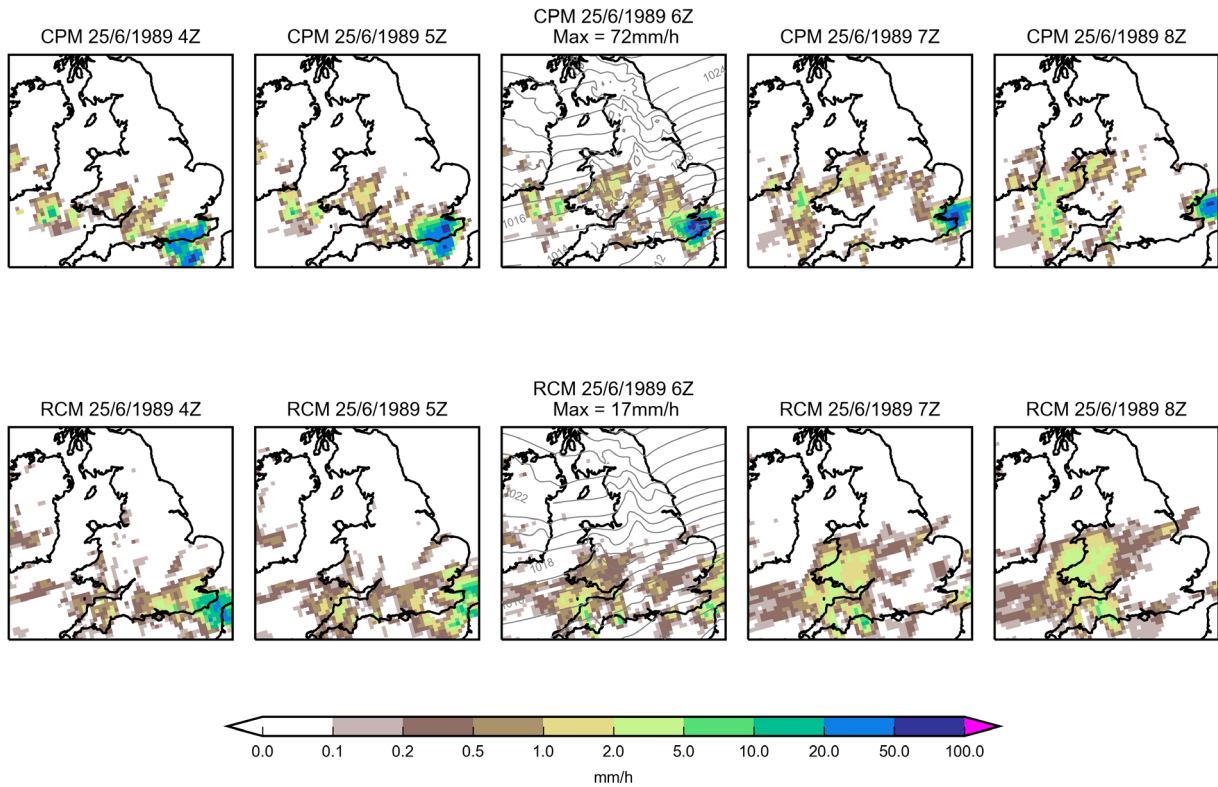
Figure 3.5.7. Heaviest summer hourly event in CPM-12. As Fig 3.5.5, but for the heaviest hourly event across the UK in summer across the CPM-12 ensemble.

Figure 3.5.8. Heaviest autumn hourly event in CPM-12. As Fig 3.5.5, but for the heaviest hourly event across the UK in autumn across the CPM-12 ensemble.

www.metoffice.gov.uk   Pg 48 of 153   Source: Met Office © Crown Copyright 2019

Figure 3.5.7. Heaviest summer hourly event in CPM-12. As Fig 3.5.5, but for the heaviest hourly event across the UK in summer across the CPM-12 ensemble.
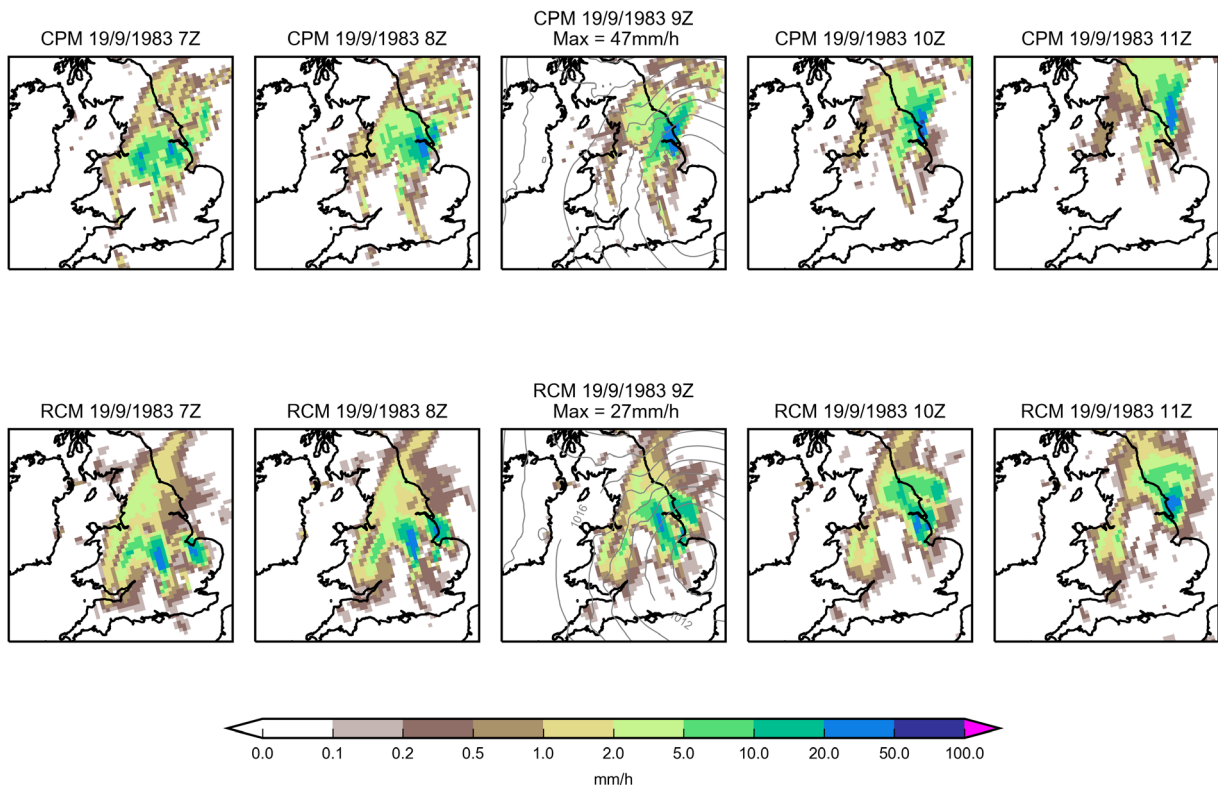
Figure 3.5.8. Heaviest autumn hourly event in CPM-12. As Fig 3.5.5, but for the heaviest hourly event across the UK in autumn across the CPM-12 ensemble.

Hot and cold spells

The Met Office issues high temperature warnings based on multi-day temperatures; the threshold for public health is typically around 30ºC for daily maximum surface temperature (Tmax). So here we define a hot spell as exceedance of this threshold for 2 or more days. Similarly for cold temperatures, the threshold is below +2ºC for daily average surface temperature for 2 or more days. Here we assess this, along with a more severe threshold of -2ºC to define "intense cold spells".

Cold spells are largely confined to Scotland and regions of high terrain (Fig. 3.5.9), where they are relatively common. There are too many cold spells lasting 2 days or more in both models compared to NCIC observations over low-lying areas, but this bias is reduced in ERA-Interim driven simulations. In general the CPM gives slightly worse agreement with NCIC than the RCM for the number of cold spells, but this is not the case for the number of intense cold spells. There are too many intense cold spells in the RCM, with the CPM giving better agreement with NCIC observations (Fig. 3.5.10-3.5.11).

We note that biases in the number of individual cold spells do not clearly correspond to biases in the intensity of cold winter days (Section 3.3). For example for the CPM, despite cold winter days being too warm, there are too many cold spells. In addition, the results above for the ERAI-driven simulations, suggest that biases in the global model have a significant role in leading to too many individual cold spells. However, biases in the regional models themselves (likely relating to snow, see below) are found to be more important for cold winter days (Section 3.3), and also any overall mean winter cold bias (Section 3.2). This difference can be explained by large-scale variability in weather patterns (inherited from the driving GCM), as well as any mean cold bias, being important for the frequency of individual cold spells. The fact that biases in the number of intense cold spells are lower in the CPM than RCM, is consistent with the CPM being warmer over the northern UK in winter than the RCM, both for the seasonal mean and cold winter days (Sections 3.2 and 3.3). In this case regional biases, as well as biases in large-scale variability are important.

Hot spells are largely confined to the south-east UK, with relatively few occurrences of daily maximum temperature exceeding 30ºC for 2 or more days in the present-day (Fig. 3.5.12). There is some suggestion that ERAI-CPM-STD overestimates the occurrence of hot spells in the south (with less of a bias in the equivalent ERAI-RCM-STD), but this is not significant given the small number of events. Looking across a range of thresholds and minimum spell lengths (Fig. 3.5.13), more generally we find CPM-12 shows better agreement with observations in the frequency of hot spells over the southern UK, with RCM-PPE tending to underestimate the number. The tendency for more hot spells in the CPM than RCM is consistent with the finding that the CPM is hotter in the southern UK in summer both for the seasonal mean (Section 3.2) and hot summer days (Section 3.3), and also the fact that soils are drier in the CPM than RCM (see below).

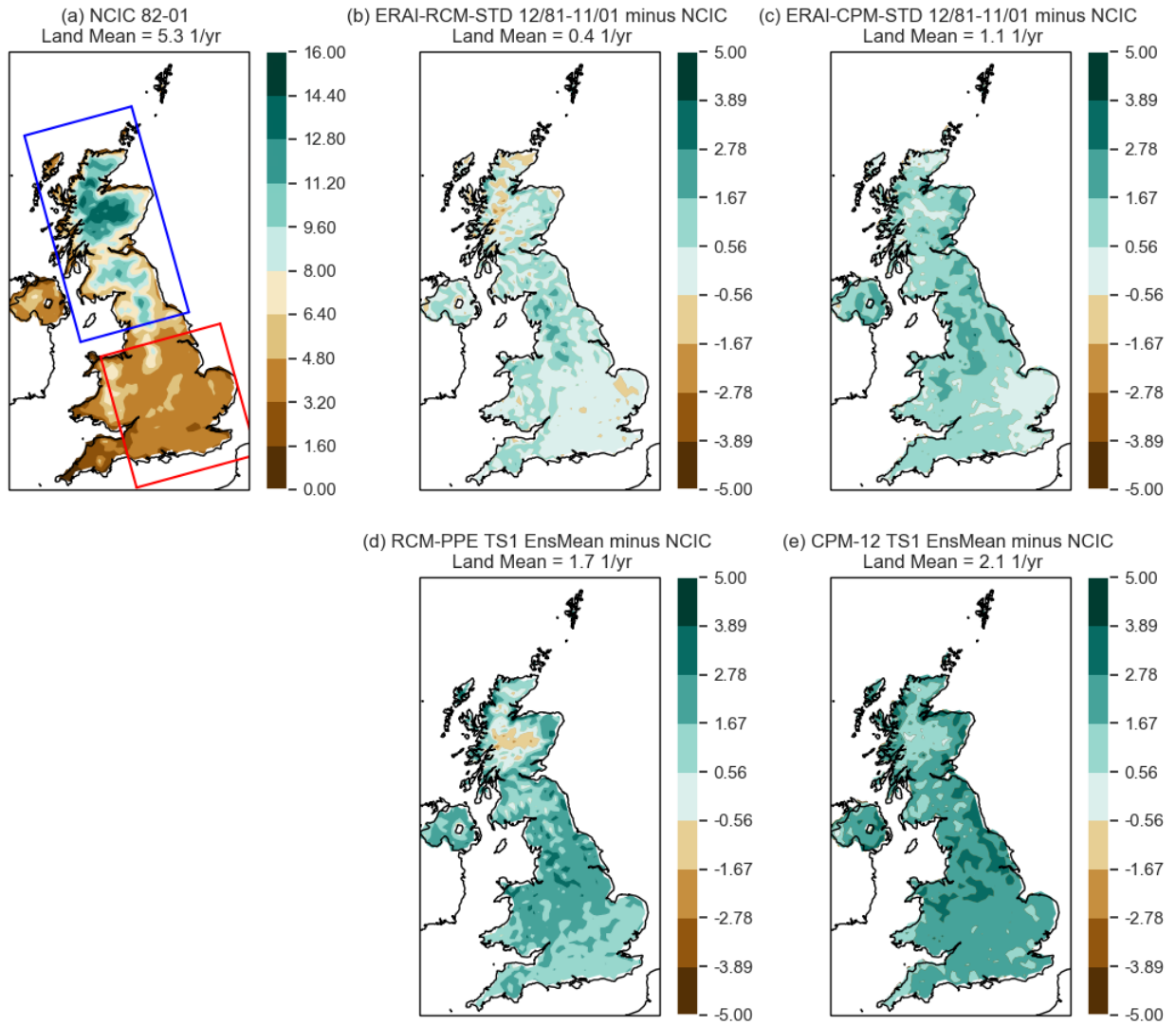# Present-Day : Freq_02+dy_Spells_tas_Below_2p0degC Independent

Figure 3.5.9. Observed and simulated cold spells. (a) Frequency of cold spells in NCIC observations (1982-2001) and model biases for (b) ERAI-RCM-STD and (c) ERAI-CPM-STD (Dec 1981- Nov 2001) and for (d) RCM-PPE and (e) CPM-12 ensemble means (TS1 = Dec 1980 – Nov 2000). Cold spells are defined as two or more consecutive days with daily mean surface temperature below +2°C. The UK-average biases are indicated in the panel titles.

Present-Day : Freq_02+dy_Spells_tas_Below_minus2p0degC Independent
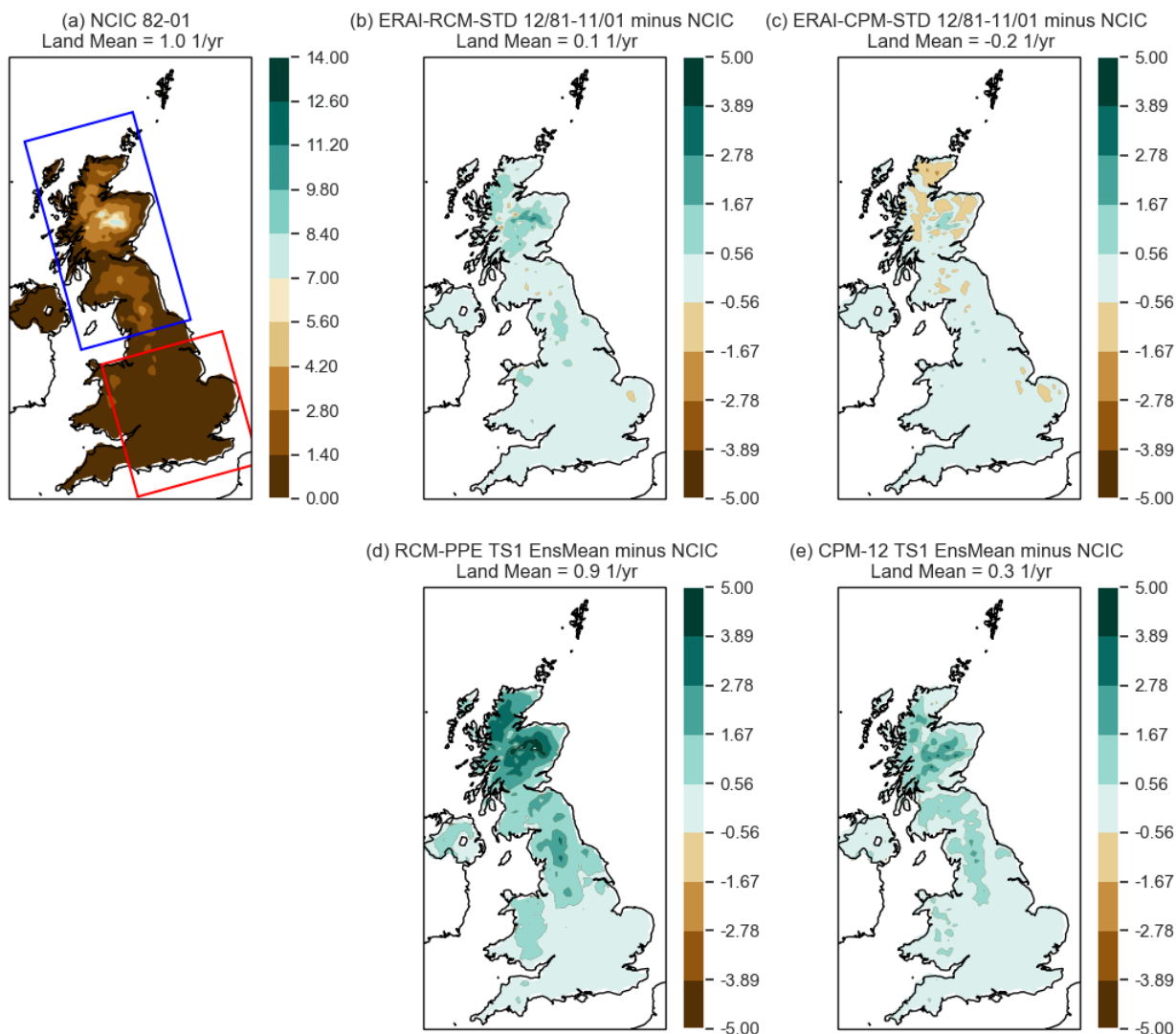
Figure 3.5.10. Observed and simulated intense cold spells. As Fig. 3.5.9, but for intense cold spells defined as two or more consecutive days with daily mean surface temperature below -2ºC.

tas NUK Cold Spells - Present Day
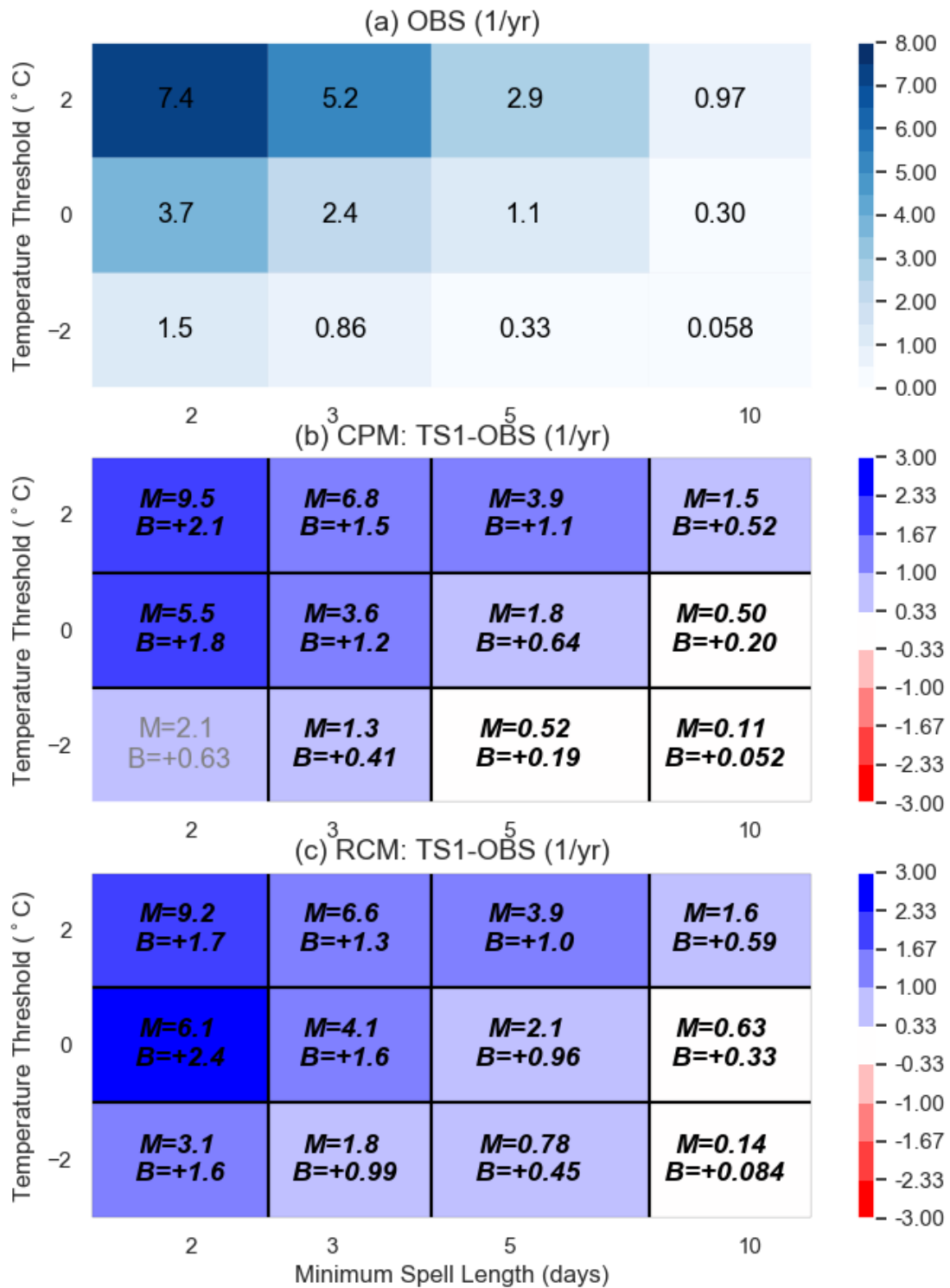
Figure 3.5.11. Frequency of cold spells over the northern UK. (a) Frequency of cold spells in NCIC observations (1982-2001) over the northern UK and (b/c) model biases for the CPM-12 and RCM-PPE ensemble means for Time Slice 1 (TS1, 1981-2000). Results are shown for cold spells defined using a range of daily mean surface temperature thresholds (-2°C, 0°C and +2°C) and minimum spell lengths (two, three, five, and ten days). The northern UK region is as defined in Fig 3.5.9. The mean frequency (M) in the model for the present-day is quoted, along with the bias (B). Differences that are significant compared to variability across the ensemble at the 5% level are indicated with a black border and bold black italic text.

Present-Day : Freq_02+dy_Spells_tasmax_Above_30p0degC Independent

(a) NCIC 82-01
Land Mean = 0.1 1/yr

(b) ERAI-RCM-STD 12/81-11/01 minus NCIC
Land Mean = 0.0 1/yr

(c) ERAI-CPM-STD 12/81-11/01 minus NCIC
Land Mean = 0.1 1/yr

(d) RCM-PPE TS1 EnsMean minus NCIC
Land Mean = -0.0 1/yr

(e) CPM-12 TS1 EnsMean minus NCIC
Land Mean = 0.0 1/yr
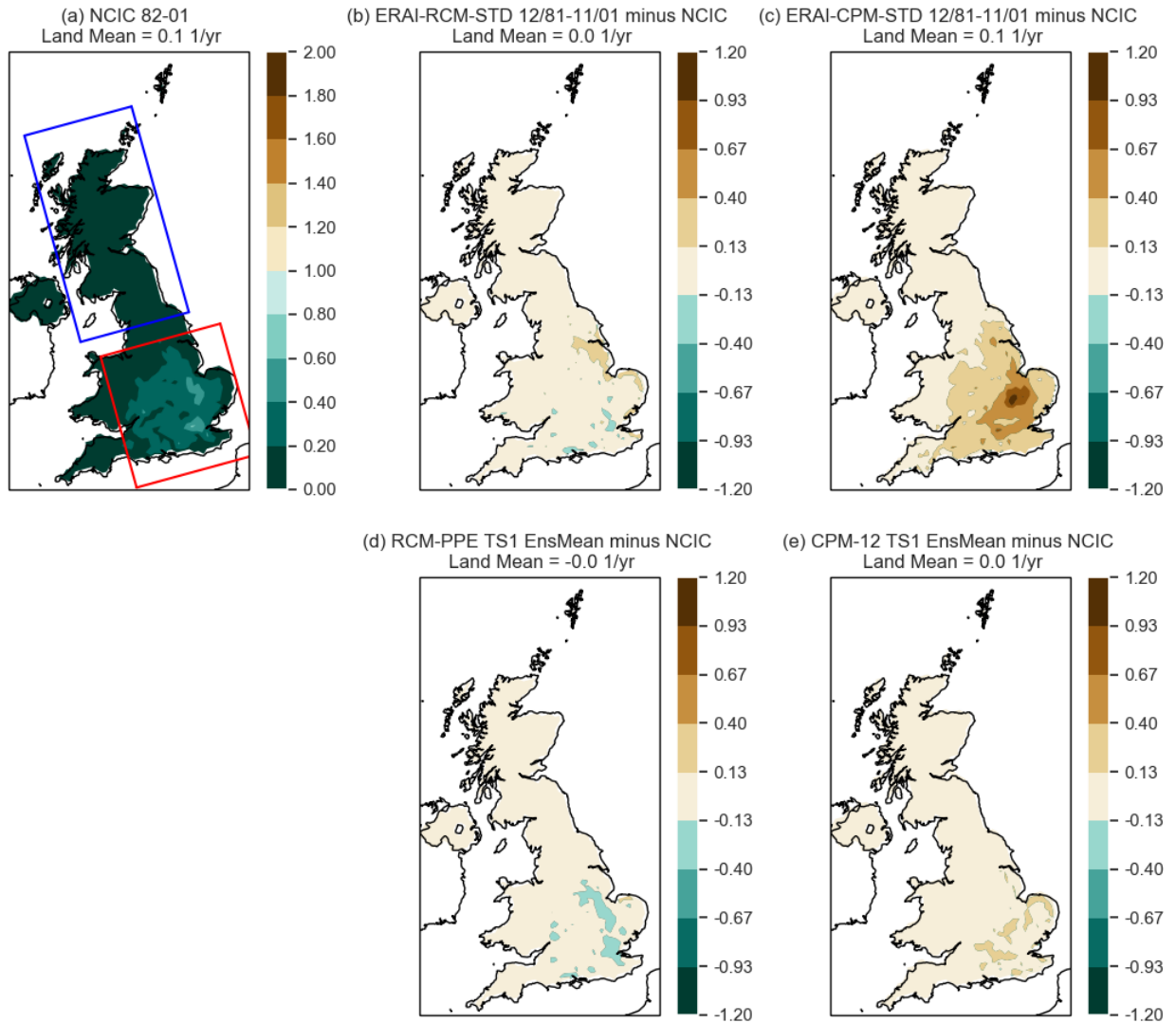
Figure 3.5.12. Observed and simulated hot spells. As Fig. 3.5.9 but for hot spells defined as two or more consecutive days with daily maximum surface temperature above +30°C.
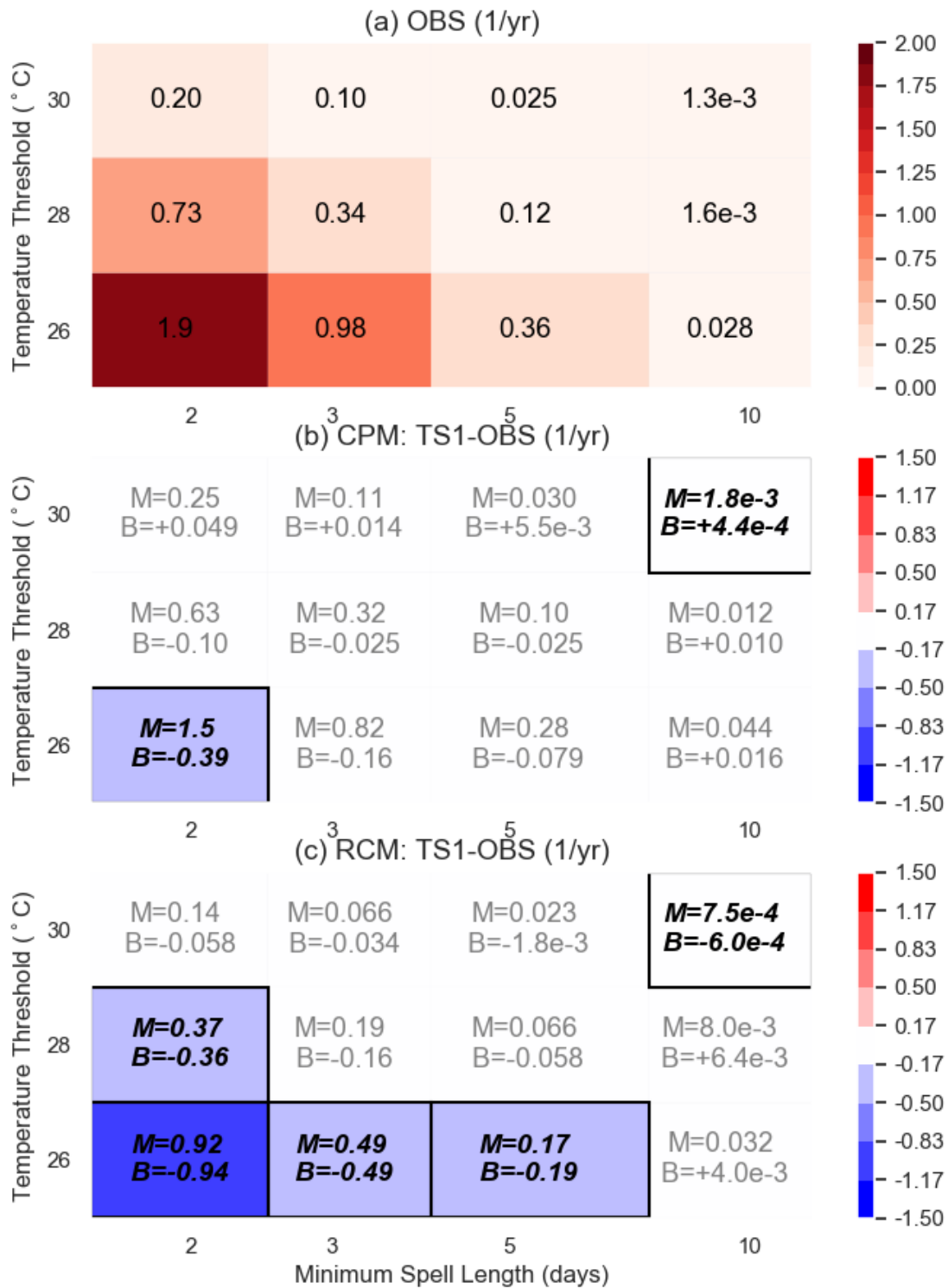
Figure 3.5.13. Frequency of hot spells over the southern UK. As Fig. 3.5.11 but for hot spells over the southern UK defined using a range of daily maximum surface temperature thresholds (26ºC, 28ºC and 30ºC) and minimum spell lengths (2, 3, 5, and 10 days). The southern UK region is as defined in Fig 3.5.9.

Soil moisture

We consider soil moisture in the top 1m of soil, as this determines the level of water stress for vegetation with shallow roots (such as grass), whereas vegetation with deeper roots (such as trees) is rarely substantially water-stressed in the UK. Maximum soil moisture occurs in January or February, following accumulation of water during autumn and winter; whilst minimum values occur in August or September, following depletion during spring and summer (Fig 3.5.14). Soil moisture varies across the ensemble members in RCM-PPE due to the variation of parameters in the land surface model physics (in particular the scaling factor for soil moisture is varied across the ensemble, which controls the critical and saturated soil moisture thresholds, Murphy et al, 2018). Soil moisture is very consistent across CPM-12 members as no parameter perturbations are applied.

Soil moisture is lower in CPM-12 than RCM-PPE. This is due to the more intense and intermittent nature of rainfall in the convection-permitting model, which is less effective at wetting the soil than the frequent lower-intensity rainfall in the convection-parameterised model. Here we use the WFDEI-JULES dataset (Table 3.1) as a proxy for observed soil moisture. It can be seen that compared to WFDEI-JULES soil moisture is slightly too low in CPM-12, but considerably too high in RCM-PPE for the majority of members (Fig 3.5.14). It is notable that the RCM-STD member (with the standard soil moisture parameter settings as used in CPM-12) gives reasonable agreement with WFDEI-JULES.
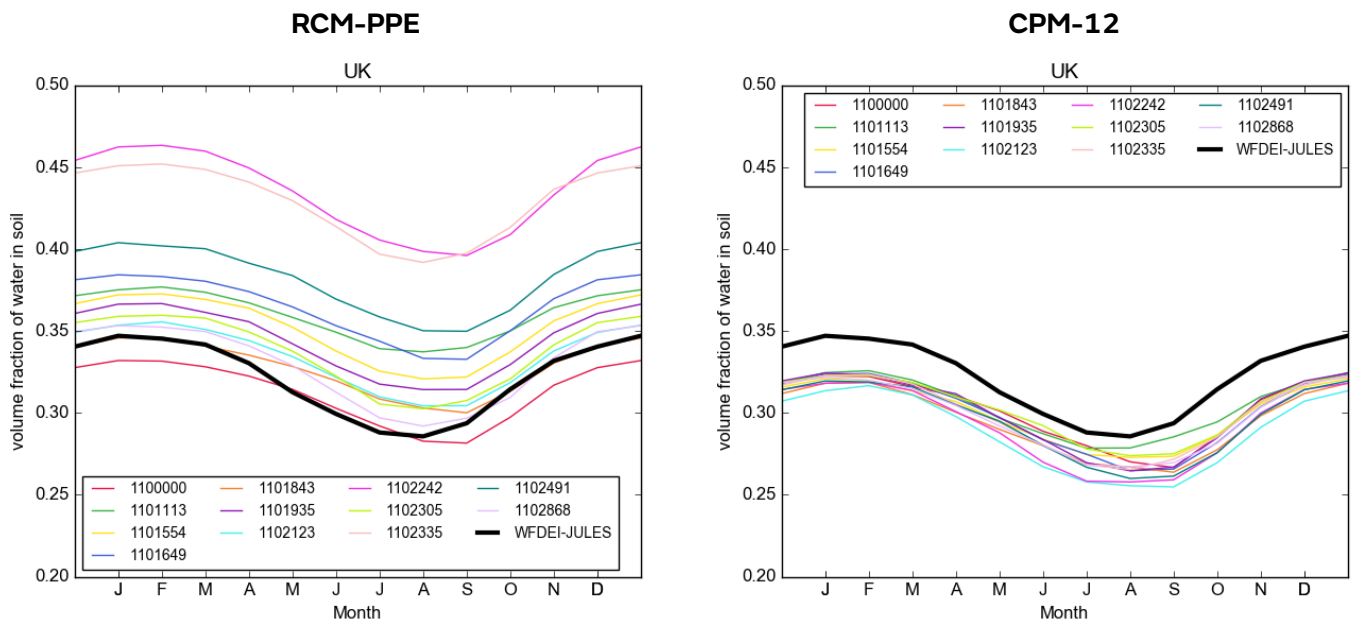
Figure 3.5.14. UK-average annual cycle of soil moisture in the top 1m of soil. Volume fraction of water in the soil (m^3/m^3) for (left) RCM-PPE and (right) CPM-12 ensemble members compared to WFDEI-JULES data, for the present-day (1981-2000). Colours correspond to the different ensemble members, with the STD member (1100000) shown in red.

Examining soil moisture in the southern and northern UK separately (Fig 3.5.15), it can be seen that soil moisture drops below the critical threshold from May to October over the southern-UK in CPM-12. This means that evaporation becomes soil-moisture limited in CPM-12 during summer, as supported by the WFDEI-JULES observational proxy. In RCM-PPE, by contrast, soil moisture is above the critical threshold year-round for the majority of members, with only a few members dropping below this threshold over the southern-UK during summer months. Overall, CPM-12 gives a better representation of soil moisture compared to RCM-PPE across the ensemble as a whole.
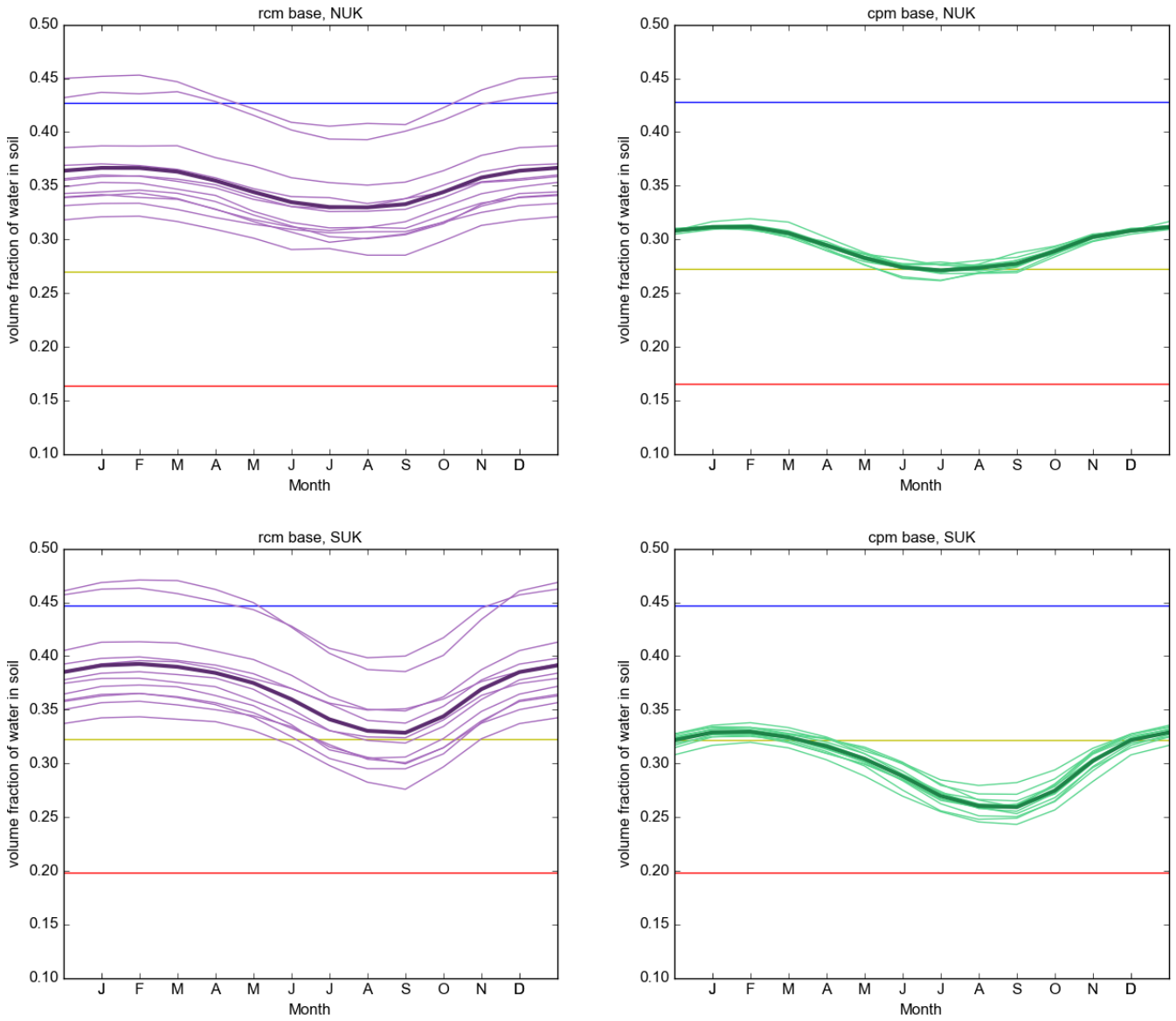
Figure 3.5.15. Annual cycle of soil moisture in the top 1m of soil, for the northern and southern UK. Volume fraction of water in the soil (m³/m³) for the (thin lines) individual ensembles members and (thick line) ensemble mean, for (left) RCM-PPE and (right) CPM-12, for the (top) northern-UK and (bottom) southern-UK. The blue line indicates soil moisture saturation; yellow line the critical point below which evapotranspiration becomes soil-moisture limited; and red line the wilting point.

Snow

Observations of the number of days of lying snow and the number of days of falling snow are available from NCIC (Table 3.1). To produce an equivalent metric for the models, a threshold needs to be applied to convert the daily model outputs of lying snow amount and snowfall rate to "yes/no" indicators of occurrence. This represents an uncertain choice, particularly in the case of lying snow, which is reported if the observer decides that the ground is more than half covered, rather than on the basis of a specific threshold in mm. A threshold of 0.02mm was used in UKCP09, and based on this choice, both the CPM and RCM substantially overestimate the number of days of lying snow and falling snow, although they both capture reasonably well the observed downward trend in lying snow through time (Figs. 3.5.16-3.5.17). The apparent biases in falling snow are worse in the CPM and those in lying snow are worse in the RCM.

However, the 0.02mm threshold may be too low for either variable, and a higher threshold of 0.5mm would give better agreement. It is also possible to look at correlations between the model snow outputs and the observations, to evaluate the temporal and spatial variability of snow in the models independent of any mean biases. The temporal correlation between the ERA-Interim driven simulation and NCIC observations for yearly winter snowfall values over Scotland is 0.45 for the CPM and 0.62 for the RCM; whilst for lying snow it is 0.78 for the CPM and 0.60 for the RCM. The spatial correlation between the ERA-Interim driven simulation and NCIC observations for winter-mean snowfall across UK grid boxes is 0.76 for the CPM and 0.75 for the RCM; whilst for lying snow is 0.73 for the CPM and 0.77 for the RCM. Thus both models do well at capturing the spatial variability in snow across the UK in winter. Winter-to-winter temporal variability in falling snow is better represented in the RCM, but for lying snow is better represented in the CPM.

Despite the difficulty in assessing model performance compared to observations, it is instructive to compare snowfall and lying snow between the CPM-12 and RCM-PPE, as the model differences are relevant to wintertime temperature biases. The CPM has more falling snow than the RCM in the present-day (in most but not all ensemble members, Fig. 3.5.18). Since the CPM has less overall precipitation (Section 3.2), the relative proportion of precipitation falling as snow is much higher in the CPM. This is due to a large degree to prognostic graupel, which is included in the CPM but not the RCM (Section 2.3) and is added to the snowfall output diagnostics. A large proportion of the snowfall in the CPM is found to be graupel, which has higher fall speeds and is able to reach the ground even when temperatures are too high for snow to reach the ground. The tendency of the RCM to have excessive drizzle production, arising from deficiencies in the parameterisation of convection, may also cause the RCM to have relatively less snow.

Despite there being more falling snow, there is considerably less lying snow in the CPM than RCM in the present-day (Fig. 3.5.19), which is true for all ensemble members (Fig. 3.5.17). This difference is likely related, at least in part, to the different treatment of graupel and the different snow schemes used. Firstly, prognostic graupel in the CPM is included in the snowfall diagnostics, but is not seen by JULES (Section 2.3) and thus is not added to the snow pack. Secondly, the zero-layer scheme used in the CPM does not properly insulate the surface (although snow does decrease the thermal conductivity of the surface layer) and as a result tends to melt snow too rapidly, therefore leading to lower overall snow depths in winter compared to the physically more comprehensive multi-layer snow scheme used in the RCM (Best et al, 2011). Preliminary analysis suggests that, of the two factors above, missing graupel in the snowpack is likely to contribute more to the difference in lying snow between the CPM and RCM, but does not fully account for the difference.

Less lying snow in the CPM is likely to be a major factor leading to the CPM being warmer at the surface than the RCM over the northern UK in winter (Section 3.2), through changes in the surface energy budget. In particular a reduction in snow cover reduces the surface albedo resulting in more absorbed shortwave radiation, and allows sensible heating from the ground into the lowest atmospheric layer (since snow acts as a thermal insulator). An overestimation of lying snow in both the CPM and RCM, but with greater biases in the RCM (as the validation here suggests), is consistent with both models showing a cold bias over Scotland in winter, but with greater cold biases in the RCM.
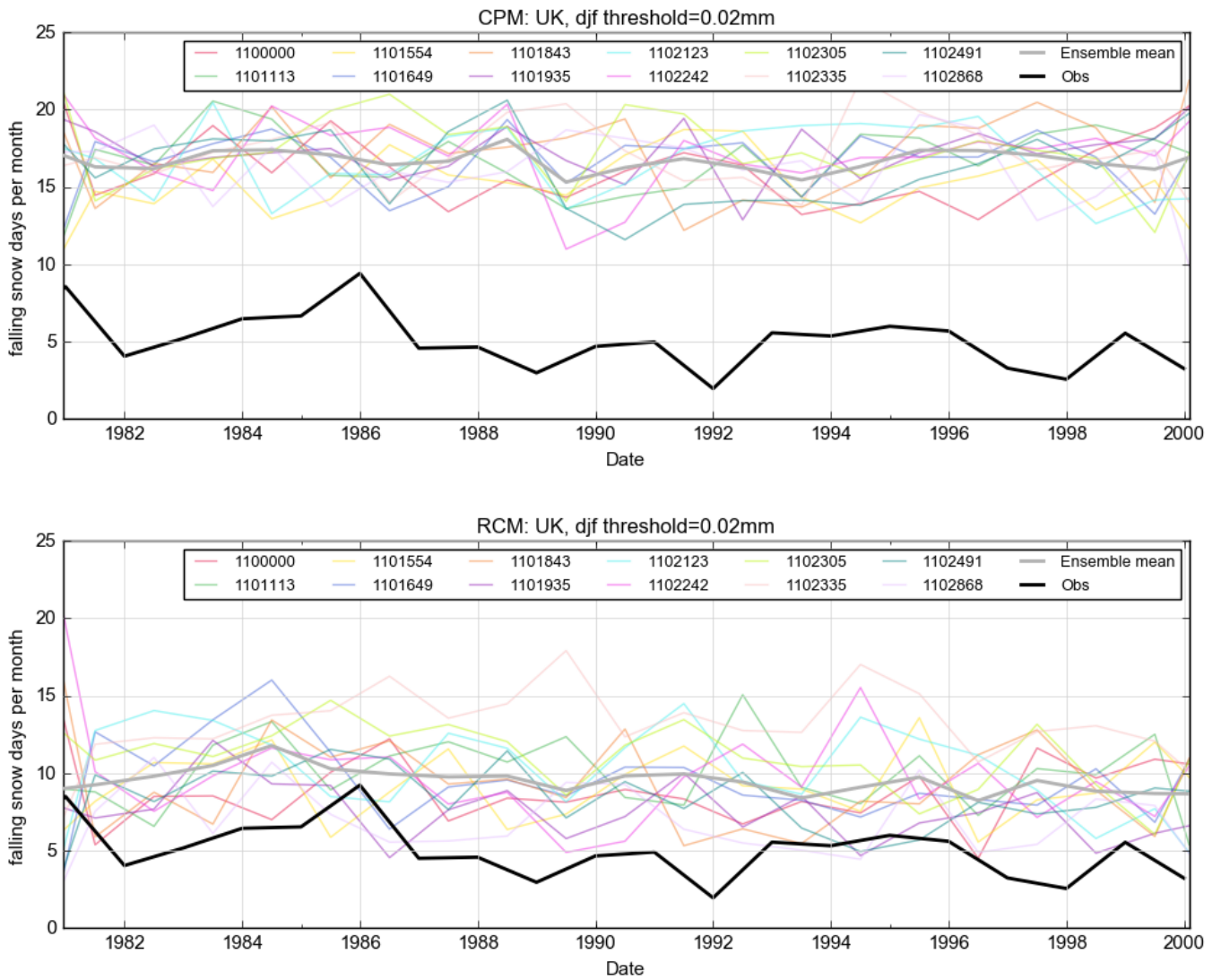
Figure 3.5.16. Observed and simulated UK-average number of days of falling snow. Yearly time-series are shown for NCIC observations, and for the individual ensemble members and ensemble-mean for the (top) CPM-12 and (bottom) RCM-PPE, for DJF. For the models a 0.02mm threshold in snowfall flux is used to define a day of falling snow.
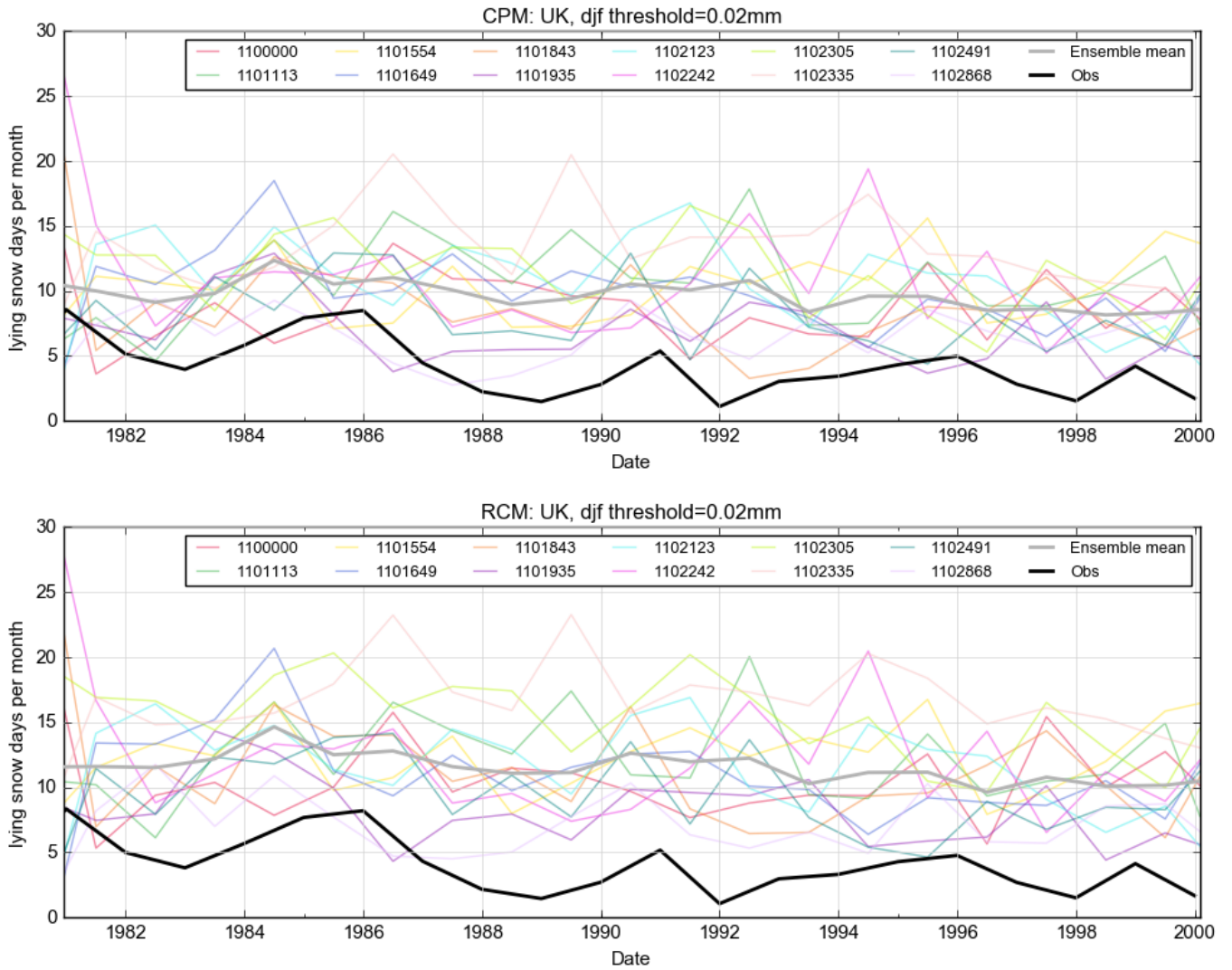
Figure 3.5.17. Observed and simulated UK-average number of days of lying snow. As Fig 3.5.16 but for lying snow. For the models a 0.02mm threshold in snow amount is used to define a day of lying snow.
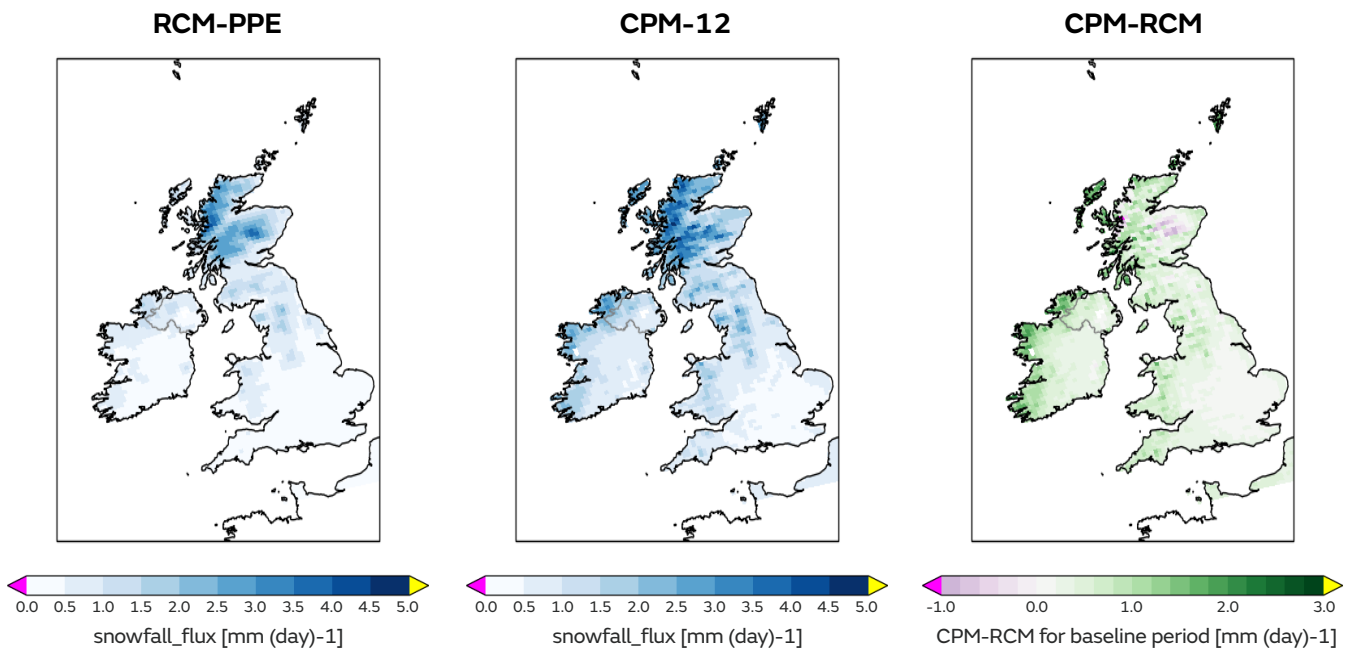
Figure 3.5.18. Mean snow fall in winter. Ensemble-averaged mean snowfall flux (mm/d) in (left) RCM-PPE, (centre) CPM-12 and (right) the CPM-RCM difference, for DJF 1981-2000.
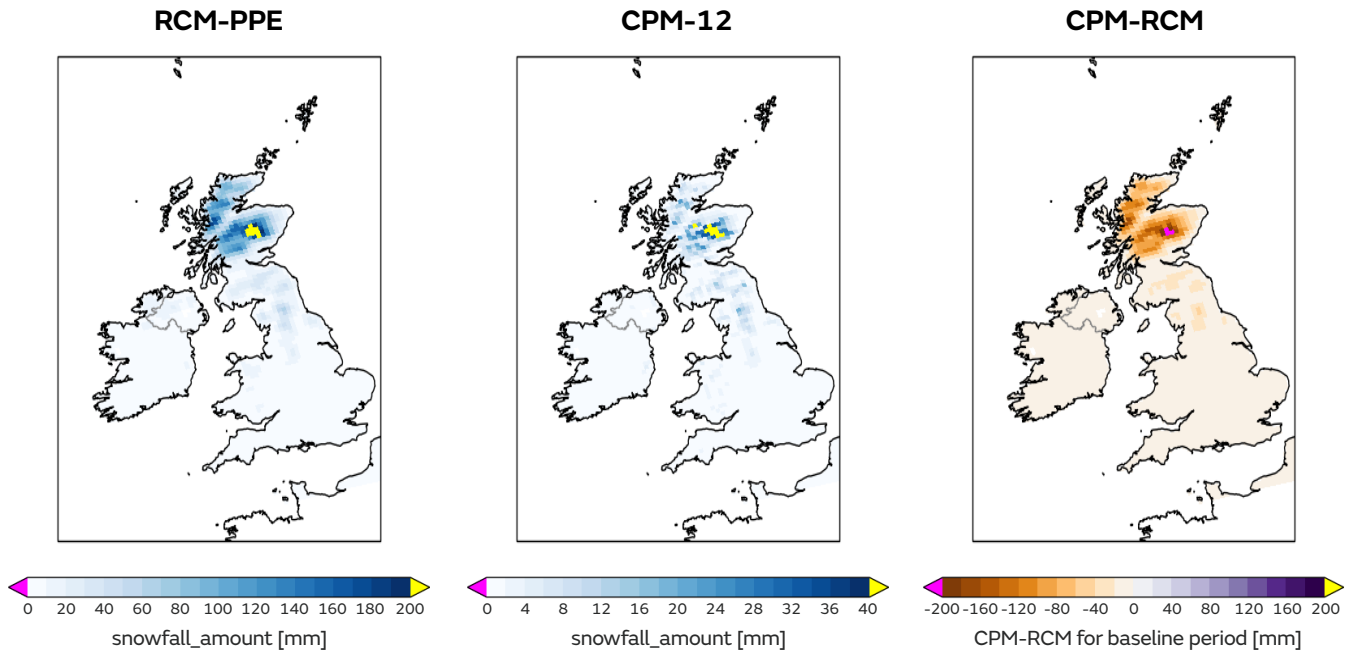
Figure 3.5.19. Mean snow amount in winter. Ensemble-averaged mean snow amount (kg/m²) in (left) RCM-PPE, (centre) CPM-12, and (right) the CPM-RCM difference, for DJF 1981-2000.

Cloud

There is consistently less cloud in the CPM than the RCM in all seasons. In winter, the CPM shows better agreement with the CLARA-A2 observations (Table 3.1) than the RCM both in terms of cloud cover and shortwave and longwave radiation (Fig 3.5.20). In this season, the RCM has too much cloud, and consistent with this, too little downward shortwave radiation at the surface and too much downward longwave radiation at the surface particularly over mountains. These biases are all reduced in the CPM.

In summer, the CPM has too little cloud cover compared to CLARA-A2 observations, with the RCM giving better agreement (Fig 3.5.21). However, these biases in cloud cover do not simply translate to greater biases in surface shortwave and longwave radiation. In fact, the CPM actually shows reduced biases in both the latter fields, with the RCM having too much downward shortwave and too little downward longwave radiation at the surface. This is explained by the fact that the impact of clouds on the radiation fluxes is not just controlled by the cloud cover (clt), but also the optical properties of the cloud which will be influenced by the cloud thickness and its vertical distribution. So although the RCM has about the right amount of cloud cover in summer, the clouds may not be reflective enough and too high (and hence are too cold with less long wave radiation).

These biases in radiation are consistent with the temperature biases shown earlier (Section 3.2). In particular in summer the CPM is warmer than the RCM, due to more downward longwave at the surface. In winter the CPM is cooler than the RCM in the south, due to less downward longwave at the surface.

The differences in cloud between the CPM and RCM are likely related to the different cloud schemes used in the different models, with the CPM using the Smith (1990) scheme but the RCM using the prognostic cloud scheme PC2 (Section 2.3).
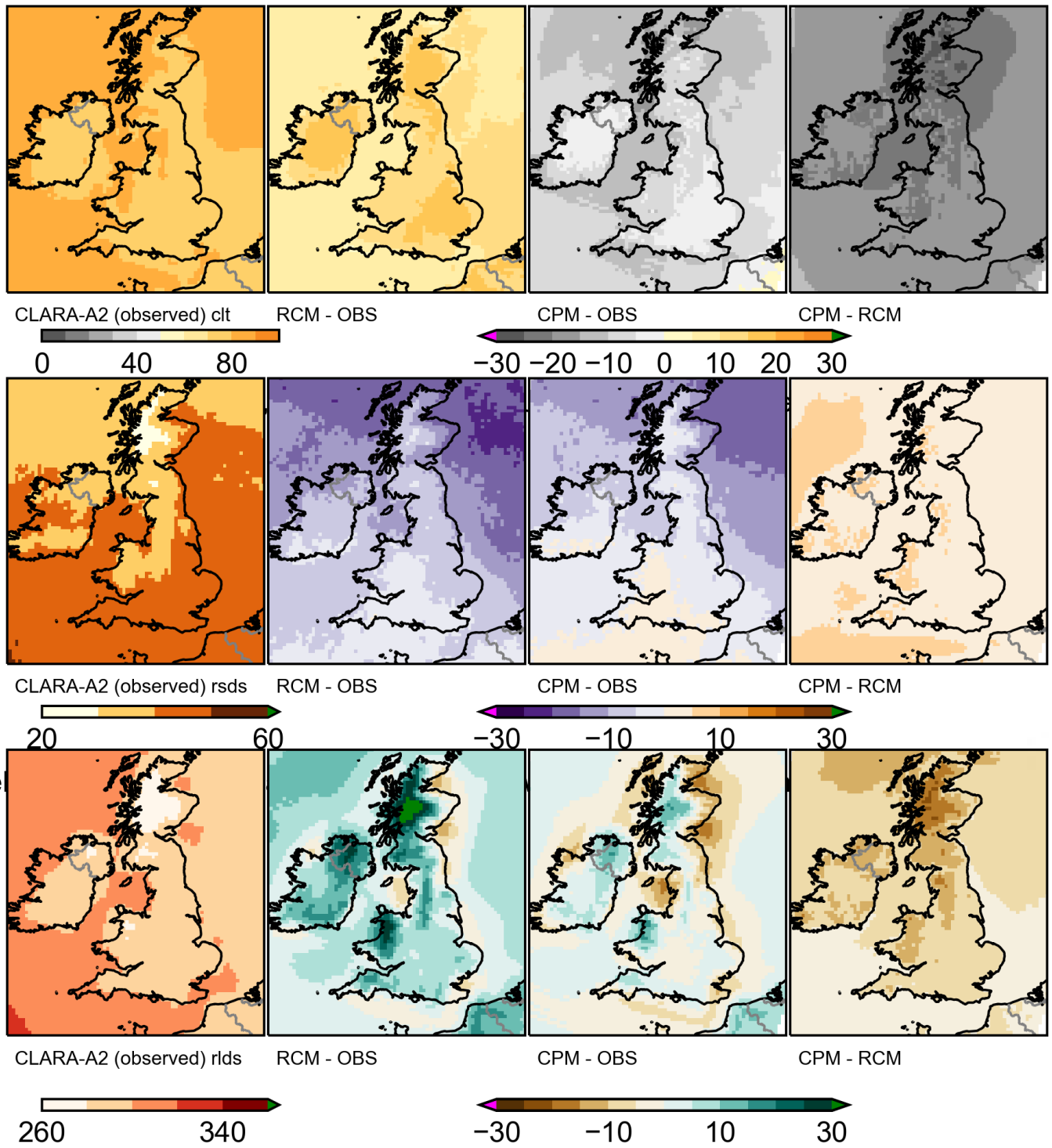
Figure 3.5.20. Observed and simulated cloud and radiative fluxes in winter. (Left) Observed cloud cover (clt, %), total downward shortwave radiation at the surface (rsds, Wm^{-2}) and total downward longwave radiation at the surface (rlds, Wm^{-2}) from the CLARA-A2 observations, for DJF. Biases compared to the observations for the ensemble-means of (centre left) RCM-PPE and (centre right) CPM-12; and (right) CPM minus RCM differences. The observational data corresponds to the 20-year period 1982-2002 and the model data to 1981-2000.
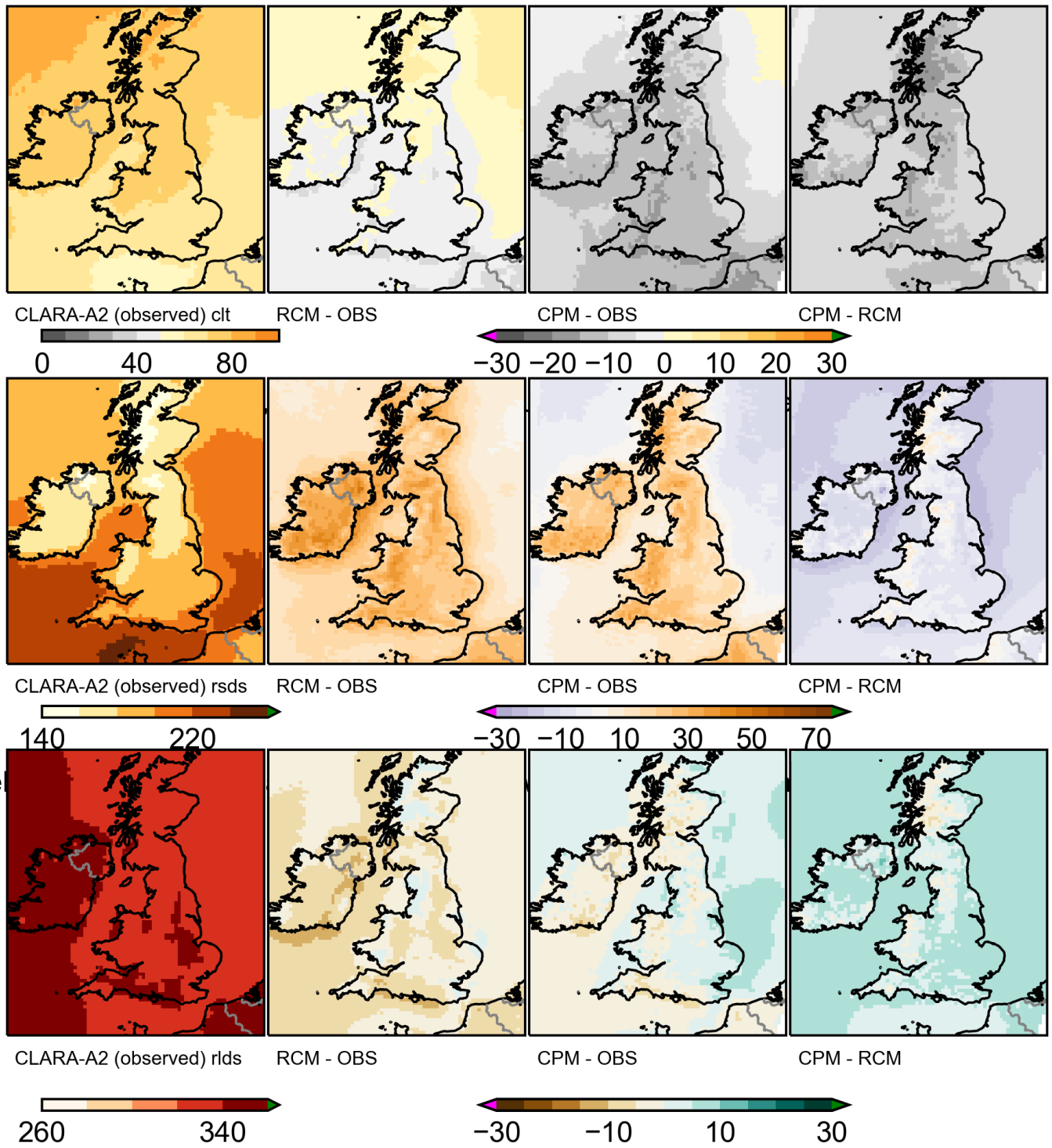
Figure 3.5.21. Observed and simulated cloud and radiative fluxes in summer. As Fig. 3.5.20 but for summer.

Lightning

Lightning is predicted in the CPM using the McCaul et al (2009) scheme, which requires a graupel prognostic that is included in the CPM but not the RCM (Section 2.3). The McCaul scheme has been shown to produce useful forecasts in convection-permitting operational NWP models (Wilkinson and Bornemann 2014). Evaluation of the lightning flash rate output from the CPM however is difficult because this includes both intra-cloud and cloud-to-ground lightning, whilst it is the latter component only that is typically of relevance to users and is measured by the ATDnet observations (Anderson and Klugmann, 2014; Table 3.1). In particular, Enno et al (2016) suggest that the ATDnet observations capture ~90% of cloud-to-ground lightning over the south of France, but only ~25% of intra-cloud lightning, which tends to have weaker signals. A further problem is that ATDnet suffers from interference due to the height of the ionosphere, which is lower at night (Bennett et al, 2011). As a result, there will be periods of nocturnal lightning which are not being detected in the observations.

For the above reasons, only a subjective evaluation of lightning output from the CPM can be made. Initial results suggest that the CPM overestimates lightning in winter but performs better in summer in terms of representing the UK-average occurrence rate, but with potential deficiencies in the spatial distribution of lightning. This is consistent with other studies showing that the McCaul et al (2009) scheme, which we use in the operational UKV model and the UKCP18 CPM-12 ensemble, overpredicts lightning in winter (Fierro et al, 2013) but does better in summer. Particularly poor model performance in winter may be due to the model discharging lightning too frequently from charged clouds, and also there is known to be too much graupel in the CPM (shown in NWP case studies) which contributes to the overestimation of falling snow in winter (Fig 3.5.16).

Further work is needed to evaluate the lightning output from the CPM and understand the causes of any deficiencies, before we can recommend use of this output by stakeholders.

3.6 Summary

We have assessed the performance of the CPM compared to the driving 12km RCM in representing present-day temperature and precipitation. We have also briefly examined high impact events, including hourly precipitation extremes, hot and cold spells, snow and lightning. This provides the evidence base to establish the credibility of the new CPM projections.

For temperature, the CPM generally shows better agreement with observations compared to the RCM. In winter, it shows a reduced cold bias in the north and reduced warm bias in the south, with reduced biases in cold winter days and the number of intense cold spells in the north UK (too many cold spells in the RCM). In summer, the CPM is warmer leading to reduced biases, except in the south of the UK where it is too warm. For hot summer days, biases are reduced in the north but the CPM is too hot in the south, although the number of hot spells is better represented in the CPM (with too few in the RCM). Differences in winter are explained by less cloud in the CPM than RCM, in better agreement with observations, and also considerably less lying snow due to missing graupel in the snowpack and the different (less sophisticated) snow scheme in the CPM. In summer, warmer temperatures in the CPM are explained in part by reduced biases in radiation fluxes (relating to differences in cloud radiative properties), although drier soils in the CPM may also contribute.

For precipitation, the CPM provides an improved representation of variability on daily and hourly timescales, leading to overall reduced biases in seasonal mean precipitation compared to the RCM. In winter, the wet bias in the RCM due to too persistent rainfall is considerably reduced in the CPM; this is similarly true in summer, although there is a tendency for too few wet days in the CPM in the far south. For heavy precipitation events, biases over mountains are reduced in the CPM (where the RCM underestimates precipitation intensity), however elsewhere the CPM tends to overestimate heavy precipitation intensity (although known deficiencies in observational estimates likely contribute to this). On hourly timescales, biases are considerably improved in the CPM, with precipitation too frequent, too low intensity and showing an unrealistic midday peak in the RCM. For hourly precipitation extremes, the CPM overestimates the 2-year return level but better captures how precipitation increases in moving to increasingly rare events; by contrast, the RCM tends to underestimate the 2-year return level, but overestimate rare extremes due to unphysical "grid point storms". The improved representation of precipitation variability in the CPM is due to the more realistic representation of convection and, in mountainous regions, the better resolution of topography. Some overestimation of the intensity of heavy events is expected due to the fact that, at 2.2km grid spacing, convection is not fully resolved.

This report does not survey all variables of interest to users. In addition to precipitation and temperature metrics, we briefly evaluate soil moisture, snow, cloud and lightning in the CPM. For soil moisture, lying snow and cloud radiative fluxes, CPM-12 generally shows reduced biases compared to RCM-PPE. For lightning, further work is needed to understand deficiencies in the CPM lightning output, with no equivalent lightning estimate available from the RCM. For CPM evaluation of other variables, including wind, additional material will be provided in journal papers.

4 Projections of future variability and change

4.1 Overview

In this section we present projected changes for the UK under high emission scenario RCP8.5, comparing results from CPM-12 with the driving RCM-PPE. A comparison of the RCM-PPE projections with those from Strands 1 and Strands 2 was presented in the Part 1 report (Murphy et al, 2018, Section 1.2). The main focus here is on surface air temperature and precipitation, with data from CPM-12 regridded to the 12km scale to allow comparison with RCM-PPE. We show changes between the 2061-80 and baseline (1981-2000) periods, as these will be greater than the nearer-term changes during 2021-40, and therefore easier to discern above natural climate variability. We firstly show seasonal mean changes, followed by information on changes in daily and hourly variability. We also consider examples of high impact events, such as precipitation extremes, hot and cold spells, soil moisture stress and snow. We note that in Section 5, a summary table is presented (c.f. Table 5.1) giving an overview of future changes in CPM-12 compared to RCM-PPE, and our understanding of any differences in terms of the key processes that are represented differently in the CPM.

The range of changes across each ensemble is represented by showing the 2nd lowest, central and 2nd highest member responses, calculated locally. These responses correspond approximately to the 10th, 50th and 90th percentiles of the ranked 12-member ensemble at each grid box (consistent with the approach used in Murphy et al, 2018). The maps should not be interpreted as examples of spatial patterns that may be simulated by an individual realisation (since the member selected at each grid point may differ), but instead give the best indication of uncertainty at each local grid point. In Appendix B, however, we also give examples of the projections from individual members with the 2nd lowest, central and 2nd highest UK mean responses, and these results are discussed briefly in the context of seasonal mean changes in Section 4.2. The uncertainty sampled across CPM-12 includes that arising from natural variability and parametric uncertainties in the physics of the driving models. However uncertainty in the convective-scale model physics itself is not sampled (Section 2.4).

4.2 Seasonal mean changes

Mean temperature increases everywhere and in all seasons. The UK-average central estimate of temperature change is 3.1°C in winter and 4.6°C in summer, with the greatest increases occurring in the south (Figs. 4.2.1-4.2.2). Mean temperature changes are broadly consistent between CPM-12 and RCM-PPE, as expected and assumed in the one-way nesting approach (Figs. 4.2.3-4.2.4). However, there are some local differences. Notably CPM-12 projects less of an increase in temperature over Scotland in winter than RCM-PPE. Differences in projected warming between an individual CPM member and its parent RCM are consistently negative, with the CPM showing a smaller increase ranging from typically 0.1-0.2°C to 0.3-0.4°C (upper and lower estimates in Fig. 4.2.3). These differences may be related to differences in lying snow (Section 4.5). In winter, UK-average differences between CPM-12 and RCM-PPE are almost zero, because smaller increases over Scotland in the CPM are in part compensated by a tendency for larger increases in temperature in the south-east UK. In summer, there is no consistent difference between the CPM and RCM members, and individual CPM members can give smaller or larger increases in temperature than their parent RCMs, with differences up to 0.3-0.4°C locally (Fig 4.2.4).

Winter precipitation increases in future across the UK, with the possible exception of northern Scotland. For the latter, RCM-PPE suggests decreases of up to 15-30%, while CPM-12 suggests decreases of up to 15% are plausible (for lower estimate of change, Fig. 4.2.5). Notably, CPM-12 shows greater increases in winter precipitation (UK-average central estimate of 27% increase in CPM compared to 16% in RCM), with the increase 20% higher for some members compared to their driving RCM (Fig. 4.2.7). We note that this difference between the CPM and RCM responses is less on averaging percentage changes over all land and sea points throughout the CPM domain (central estimate of 22% increase in CPM compared to 18% in RCM). This indicates that the greater precipitation responses seen in the CPM over land do not extend over the sea (c.f. Table 4.1). This substantially greater increase in projections of winter precipitation in the CPM has considerable implications for river flows and flood risk.

The difference found in the wintertime mean precipitation response between CPM-12 and RCM-PPE is in contrast with earlier CPM studies (Kendon et al, 2014, 2017), which showed the CPM following the driving model for changes in winter. The difference found here is not due to differences in mean circulation or humidity changes, with the basic seasonal-mean CPM response in these variables following the driving model. Instead, there are a number of possible explanations, as outlined below, although further work is needed to confirm these and analyse other potential contributions to the differences.

- **1) Influence of baseline.** In the present-day, winter mean precipitation is higher in the RCM than CPM over land and the coastal sea areas (although winter mean precipitation is lower over the North Atlantic to the northwest of the UK). This is linked to precipitation being more frequent in the parameterised convection model, with many fewer dry days/hours (Section 3.4). Given that total precipitation is higher in the RCM than in the CPM, processes leading to the local formation of precipitation must act more in the RCM (since the same moisture is being advected in through the lateral boundaries), with higher evaporation rates over sea in the RCM (Table 4.1). This is also true in the future climate, although with smaller relative differences between the models. In future, the greater increase in winter mean precipitation in the CPM over land is due to a greater increase in precipitation occurrence (Section 4.3), as well as a greater increase in the contribution from intense precipitation events (see point 2 below). Given the large number of wet days/hours in the baseline climate in the RCM, there is less scope for this to increase in the future (c.f. Figs 5.2 and 5.3 for relationship between present-day biases and future changes for seasonal mean precipitation). Indeed, we find that the number of wet days/hours over land actually decreases in the RCM in future over the eastern side of the UK (Section 4.3), in part offsetting the increased precipitation over the western side associated with orography (see point 2).

- **2) Role of orography.** The largest precipitation events (in terms of hourly or daily accumulations) mostly occur over orography in winter. It is these large events which are the main contributors to the total precipitation (rather than the much more numerous light events) and which show the largest future changes in actual contribution to total precipitation (Section 4.4). In the RCM it rains much more frequently over orography, with a tendency for too much continuous generation of rain over the mountains (Section 3.3, Fig 3.3.4). The CPM does not rain as frequently (although when it does, it does so with greater intensity), leading to lower mean precipitation on the upslopes in the present-day (Section 3.2). Given the more frequent nature of orographic precipitation in the RCM in the present-day, there is less scope for this to increase in future. In addition, the increases in precipitation contribution from the highest intensities over orography in future are greater in the CPM than RCM (Section 4.4).

- **3) Representation of convective showers.** Convection, although less prominent than in summer, still occurs in winter (in the form of convective showers and in association with cold fronts). In winter, convective showers are mainly triggered over the sea and then advected over land (convection makes up about 50% of the precipitation over the sea in winter in the RCM). The parameterised model represents these showers as broad areas of convective precipitation (and hence has a tendency for too many long-duration low-intensity events, Section 3.4). In the future, the warmer ocean and higher levels of atmospheric moisture will favour more triggering of convective showers (assuming other influences on convective instability, including the average lapse rate of atmospheric temperature, remain similar). This is seen in both the CPM and RCM, with a decrease in dry hours over the sea in future in both models (Section 4.4) and for the RCM an increase in the fraction of precipitation from the convection scheme over the sea (Fig 4.2.9). Over land in the RCM, however, there is an increase in dry hours that is largely related to a decrease in the frequency of lower intensity precipitation events, with convection becoming less favourable over northern and western regions in winter (Fig 4.2.9, possibly due to a longer time needed for the replenishment of moisture between events). The opposite is true in the CPM, where the decrease in dry hours over the sea also extends over the land, suggesting that convective showers are being advected inland (there is an increase in both smaller hourly events and larger hourly totals in the CPM over land). This is supported by initial analysis showing that the contribution to total precipitation from days with relatively little large-scale frontal activity (diagnosed using convective fraction in the RCM) is increasing in future in the CPM, and more than in the RCM. Thus the more realistic representation of the triggering and evolution of convection in the CPM may contribute to the different wintertime mean precipitation responses (which, away from orography, are small in absolute terms but significant in percentage change terms).

There are a number of possible reasons why different wintertime mean precipitation responses were not seen in earlier CPM studies for the UK. One reason may be the small domain size of the earlier CPM simulations, potentially resulting in convective events advected in at the boundary not being fully spun up over the UK. This would impact (2) above, since high terrain is mostly on the western side of the UK close to the inflow boundary in the older simulations. It would also impact the spin up of convective showers over the sea, and hence (3) above. In addition to the domain size, there have also been many changes to the model physics, which may explain the difference. For example, recent changes were made to the mixing settings and boundary layer perturbations in the weather forecast model that provided the basis for the CPM (Section 2.3), which tended to favour more convective showers.

In summer, precipitation is projected to decrease in the future, again with the possible exception of northern Scotland where small increases are possible (for upper estimate of change, Fig. 4.2.6). In general summer mean precipitation decreases are slightly greater in CPM-12 than RCM-PPE (UK-average central estimate of 28% compared to 26% decrease), with the lower estimate of the change (upper estimate of the decrease) showing decreases of 46% in CPM-12 compared to 41% in RCM-PPE. Fig. 4.2.8 shows that the decrease in the CPM can either be greater or smaller than its parent RCM, depending on member. Thus there is not a systematic shift in the ensemble responses in summer (unlike winter, cf. Fig. 4.2.7). The summer decreases in both CPM-12 and RCM-PPE ensembles are larger than those sampled by CMIP5 models, with little overlap between the ranges of change from the PPEs and CMIP5-13 for England (c.f. Fig 5.1).

Water budget components (mm/day)	Present-day (DJF 1981-2000)		Future change (DJF, 2061-80 minus 1981-2000)	
	CPM-12	RCM-PPE	CPM-12	RCM-PPE
Evaporation (domain average)	2.08	2.31	0.31	0.37
Evaporation over land	0.66	0.80	0.20	0.20
Evaporation over sea	2.81	3.08	0.36	0.47
Precipitation (domain average)	3.99	4.36	0.85	0.82
Precipitation over land	4.03	4.65	1.05	0.76
Precipitation over sea	3.96	4.22	0.74	0.84
Moisture flux convergence (domain average)	1.63	1.63	0.45	0.44
Residual (domain average)	0.28	*0.42*	0.09	*0.01*

Table 4.1. Components in atmospheric water budget for winter, as average over CPM-domain (excluding outer rim region). Also shown are averages over (British Isles) land and sea grid boxes, separately, for evaporation and precipitation. In italics is the residual, given by precipitation - evaporation - moisture flux convergence. Moisture flux convergence is calculated offline from column integrated moisture fluxes, using a finite differencing approach.

Water budget components (mm/day)	Present-day (JJA 1981-2000)		Future change (JJA, 2061-80 minus 1981-2000)	
	CPM-12	RCM-PPE	CPM-12	RCM-PPE
Evaporation (domain average)	2.00	2.07	0.07	0.05
Evaporation over land	2.32	2.39	-0.08	-0.02
Evaporation over sea	1.84	1.91	0.15	0.09
Precipitation (domain average)	2.17	2.37	-0.58	-0.62
Precipitation over land	2.71	2.89	-0.76	-0.75
Precipitation over sea	1.89	2.10	-0.48	-0.55
Moisture flux convergence (domain average)	0.16	0.14	-0.54	-0.55
Residual (domain average)	*0.01*	*0.16*	*-0.11*	*-0.12*

Table 4.2. As Table 4.1, but for summer.

For both mean temperature and precipitation, the seasonal mean fine-scale response in the CPM is considerably smaller than the differences between the CPM and RCM changes at the 12km scale (Figs. 4.2.3,4.2.4,4.2.7,4.2.8).

Tables 4.1 and 4.2 show the atmospheric water budget terms, and their future change, in winter and summer respectively. In both seasons, the mean moisture flux convergence over the CPM domain (and its future change) is very similar between the CPM and RCM, confirming that moisture entering and leaving the CPM domain is well constrained by the RCM. It should be noted that precipitation does not exactly equal evaporation plus moisture flux convergence (see residual in Tables 4.1 and 4.2), due to numerical errors in our estimation of moisture flux convergence. In particular, although moisture conservation is enforced internally in the CPM (Section 2.3), significant errors will arise in the offline calculation of moisture convergence (which uses a finite differencing approach) due to fine-scale structures in the winds. In terms of future changes, the greater increase in winter precipitation in the CPM over land (1.05 mm/day in CPM versus 0.76 mm/day in RCM) is not explained by greater increases in evaporation (with similar changes in evaporation over land in the CPM and RCM), and therefore instead is coming from greater increases in moisture flux convergence over land in the CPM (consistent with the advection of moisture from the sea). In summer (unlike in winter) evaporation is the dominant moisture source for precipitation over land, with the local recycling of moisture being important (although the extent to which showers, and local moisture recycling, occur may be conditioned by the large-scale circulation patterns, e.g. fewer showers where there is more dry continental flow). This is in contrast to winter, where showers over land may be more dependent on the advected moisture from the sea. In terms of future changes in summer, however, it can be seen that these are dominated by convergence changes, since evaporation hardly changes. In particular, there is a large decrease in moisture flux convergence (over the whole domain), resulting in the UK changing from a region of small positive moisture convergence to significant moisture divergence. These mean changes in summer are captured similarly by both the CPM and RCM (see Section 5 for further discussion).

Figures B1.1-B1.4 in Appendix B show examples of projected seasonal mean temperature and precipitation change from individual members. For summer and winter temperature, and summer precipitation, these show very similar results to the maps of the 2nd lowest, central and 2nd highest member responses calculated locally (Figs 4.2.1, 4.2.2, 4.2.6). This is true both in terms of the spatial variations and the uncertainty ranges. For winter precipitation, the uncertainty range in UK-average changes from individual member responses is smaller than from averaging the 2nd lowest or 2nd highest member responses locally (Figs 4.2.5). This is explained by the fact that the selection of low or high response members locally will measure uncertainty at each grid point independently, with small-scale natural variability always added to the uncertainty in the large-scale conditions. The spatial patterns of the individual member responses however are similar to the results in Figs 4.2.5, with greatest increases in the south. The UK-average changes from individual members similarly show the key result above that wintertime precipitation increases are larger in CPM-12 than RCM-PPE by about 10% for the central estimate. It should be noted when plotting individual member responses ranked by the UK mean response, it is possible for the central estimate to actually be higher than the high estimate locally. For example, this is visible for summer temperature change over the far north of Scotland in the RCM-PPE (Fig B1.2), where the member with a high UK mean response has a large warming in the south but a smaller warming in the north than the central member. For this reason, for the remainder of the report, we represent uncertainty by showing the 2nd lowest, central and 2nd highest member responses calculated locally, which gives the best indication of the full range of uncertainty (i.e. including from natural variability) at each local grid point.
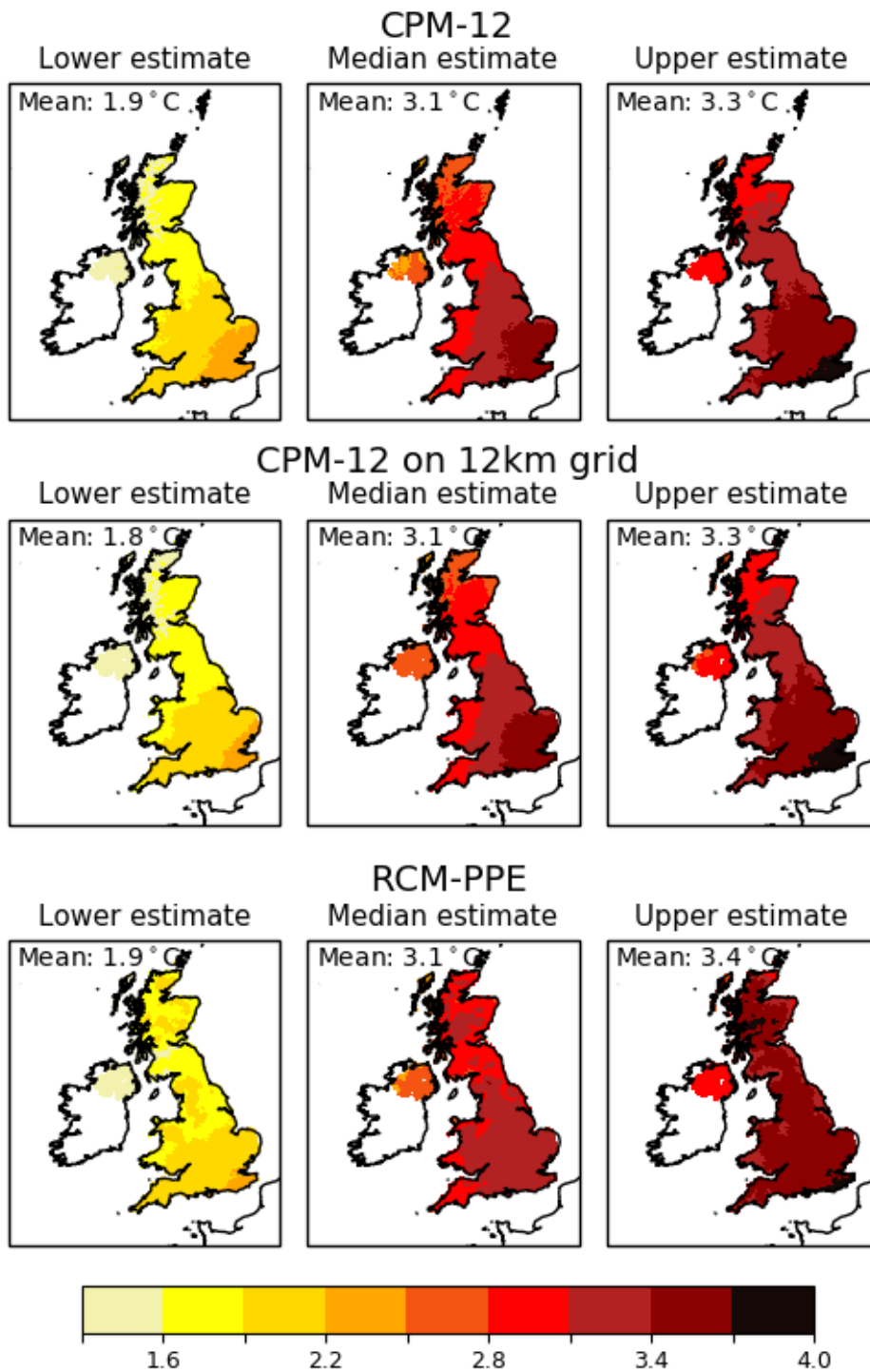
Figure 4.2.1. Future change in winter mean temperature. Changes for (left) 2nd lowest, (centre) central and (right) 2nd highest member locally, for (top) CPM-12 at native 2.2km resolution, (middle) CPM-12 regridded to 12km RCM grid and (bottom) RCM-PPE. Changes (in °C) correspond to the difference between the future (2061-2080) and baseline (1981-2000) periods. The regridding to 12km (middle) is done before calculation of responses and selection of low/high responses. The UK-averaged change is indicated in each panel.

TS3 MINUS TS1 seasonal mean tas jja tas (°C)
upper, median & lower estimates across PPE
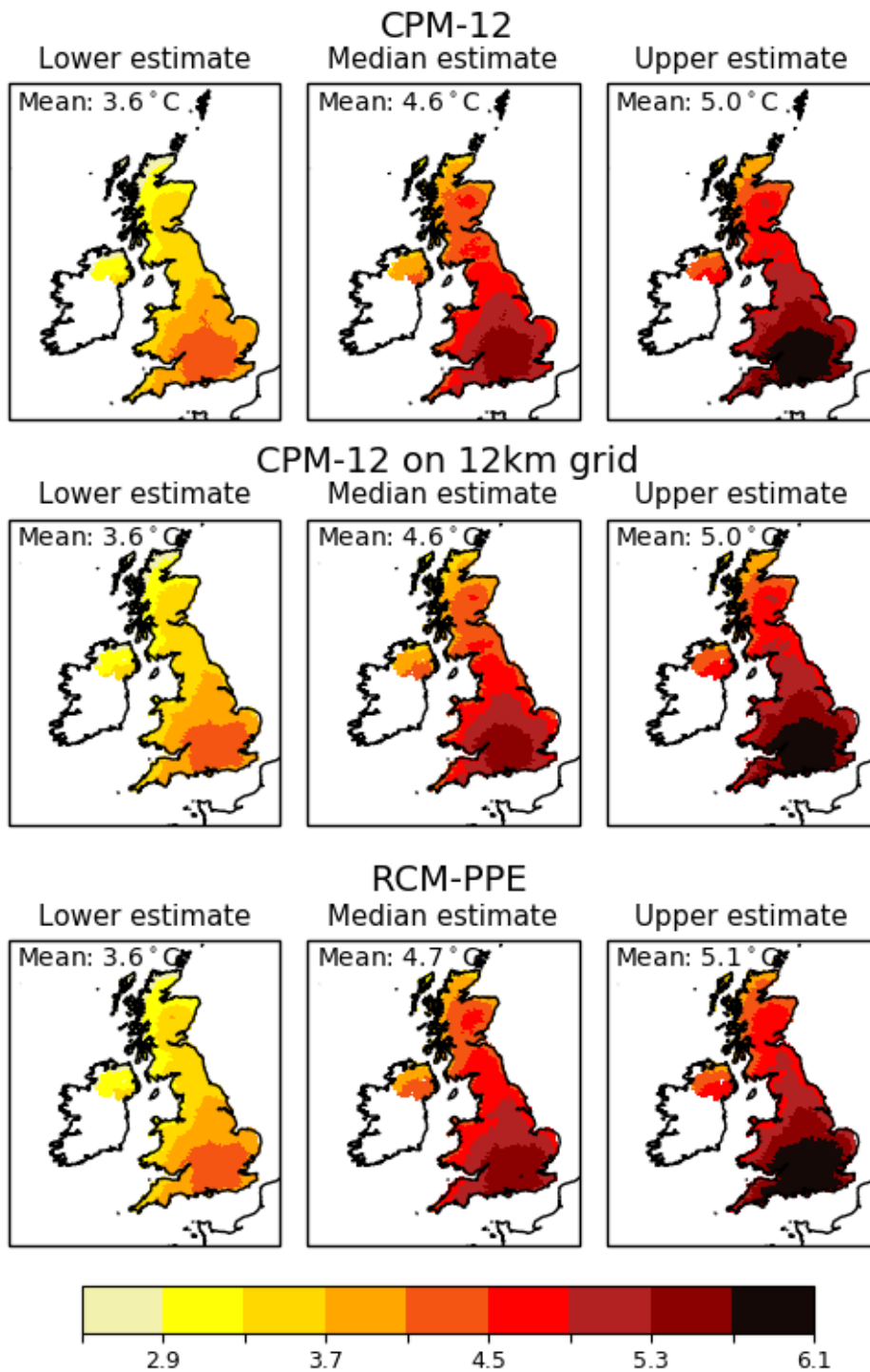
Figure 4.2.2. Future change in summer mean temperature. As Fig 4.2.1, but for summer.
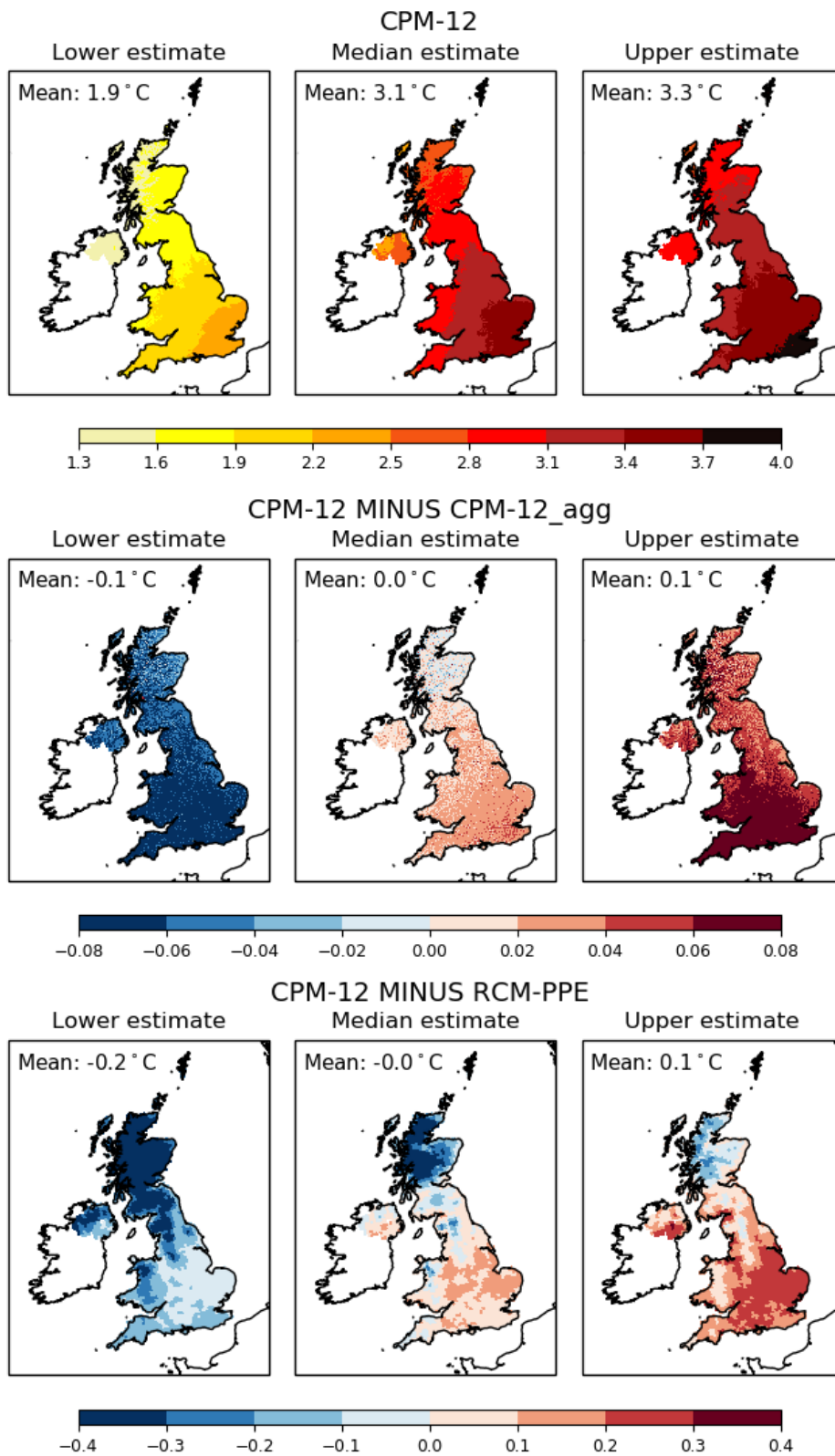
Figure 4.2.3. Impact of convection-permitting downscaling on future change in winter mean temperature. (left) 2nd lowest, (centre) central and (right) 2nd highest member estimates locally, for (top) future changes in CPM-12 at native 2.2km resolution, (middle) differences between the top row and the corresponding responses obtained when the relevant CPM-12 members are smoothed to the 12km horizontal resolution of the RCM (by averaging of data over 5x5 2.2km grid boxes) (bottom) CPM-12 at 12km scale response minus RCM-PPE response. The UK-averaged difference is indicated in each panel.
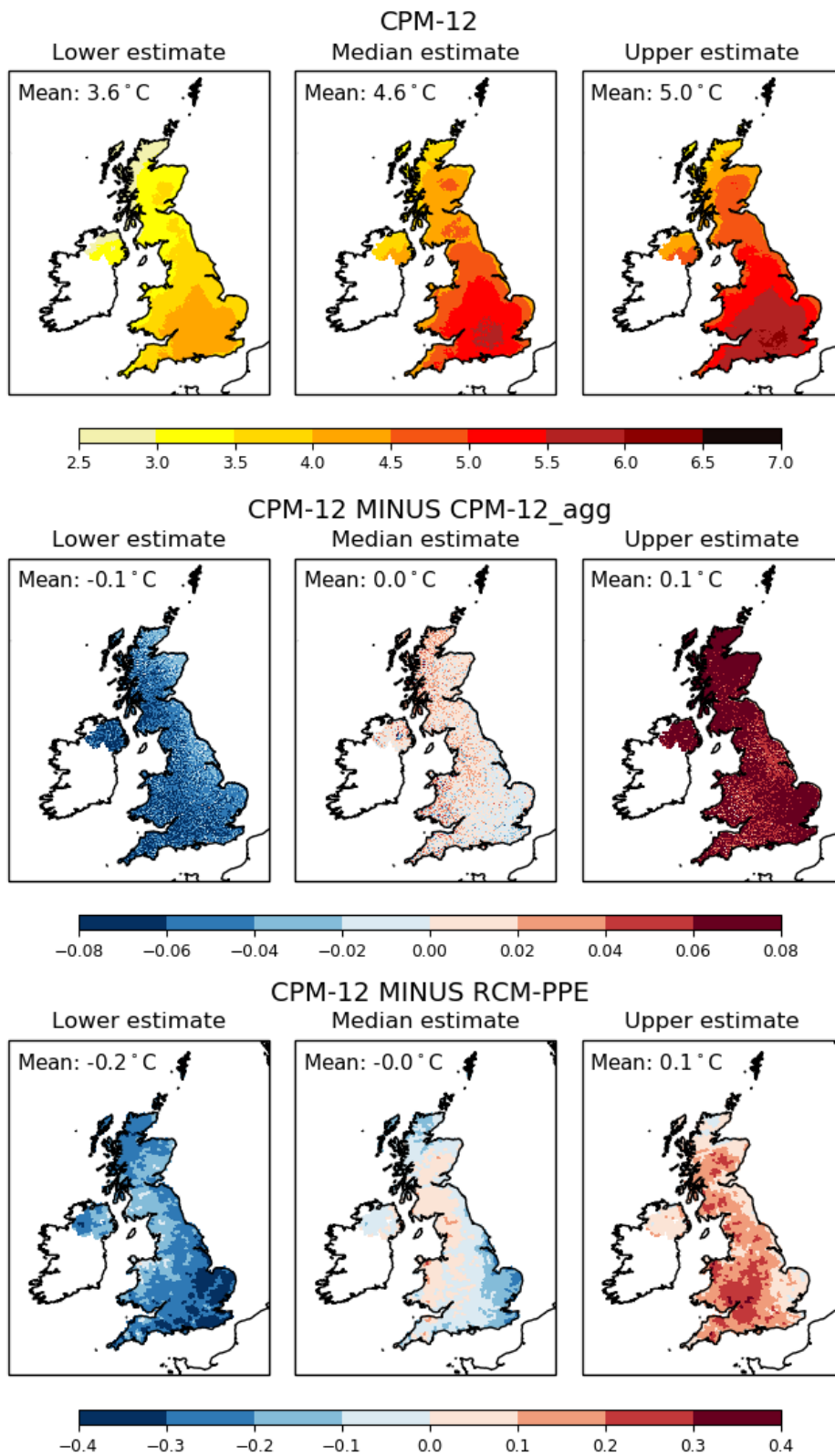
Figure 4.2.4. Impact of convection-permitting downscaling on future change in summer mean temperature. As Fig. 4.2.3 but for summer.

TS3 MINUS TS1 seasonal mean pr djf pr (%)
upper, median & lower estimates across PPE
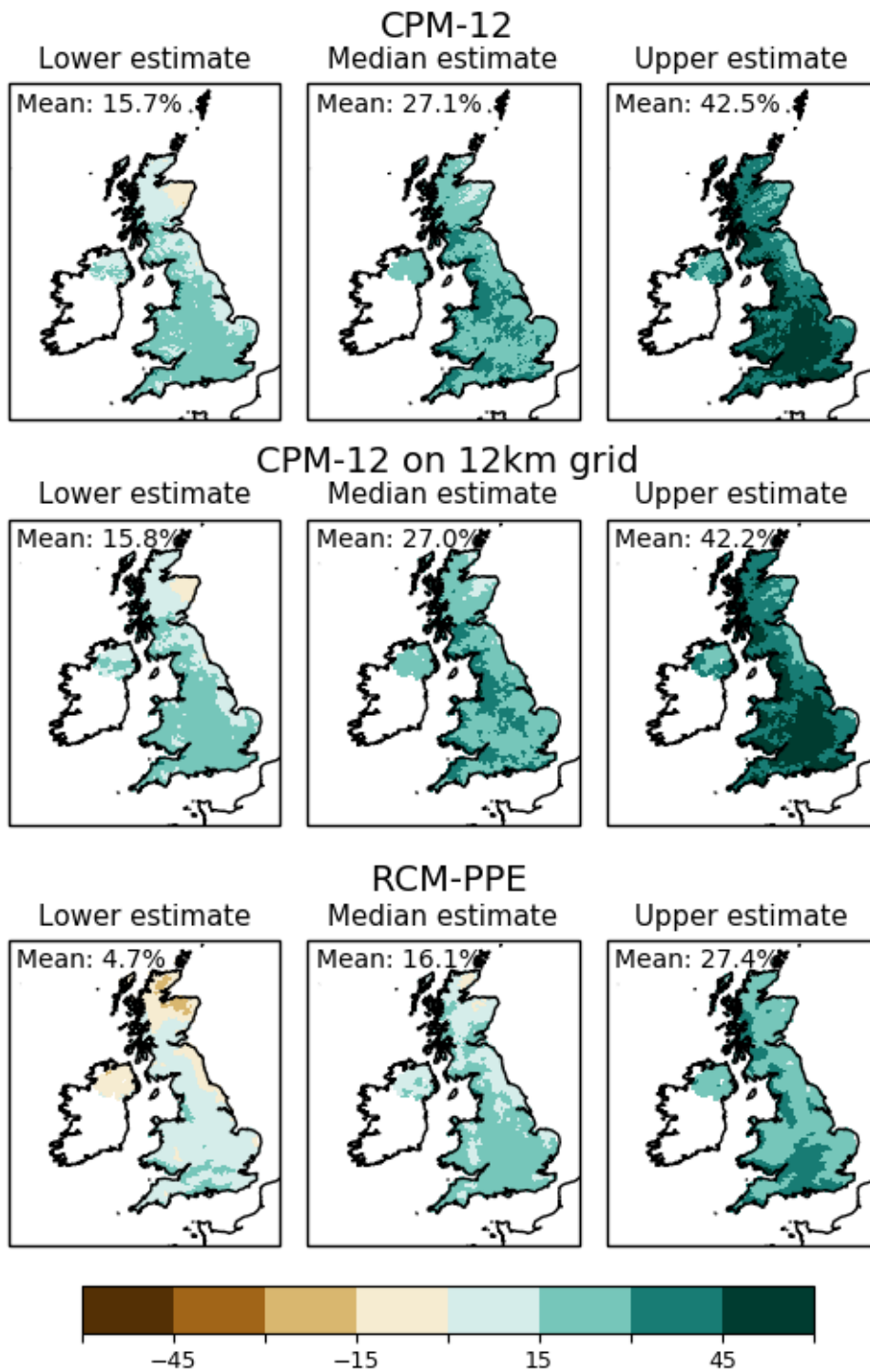
Figure 4.2.5. Future change in winter mean precipitation. As Fig 4.2.1, but for wintertime mean precipitation.
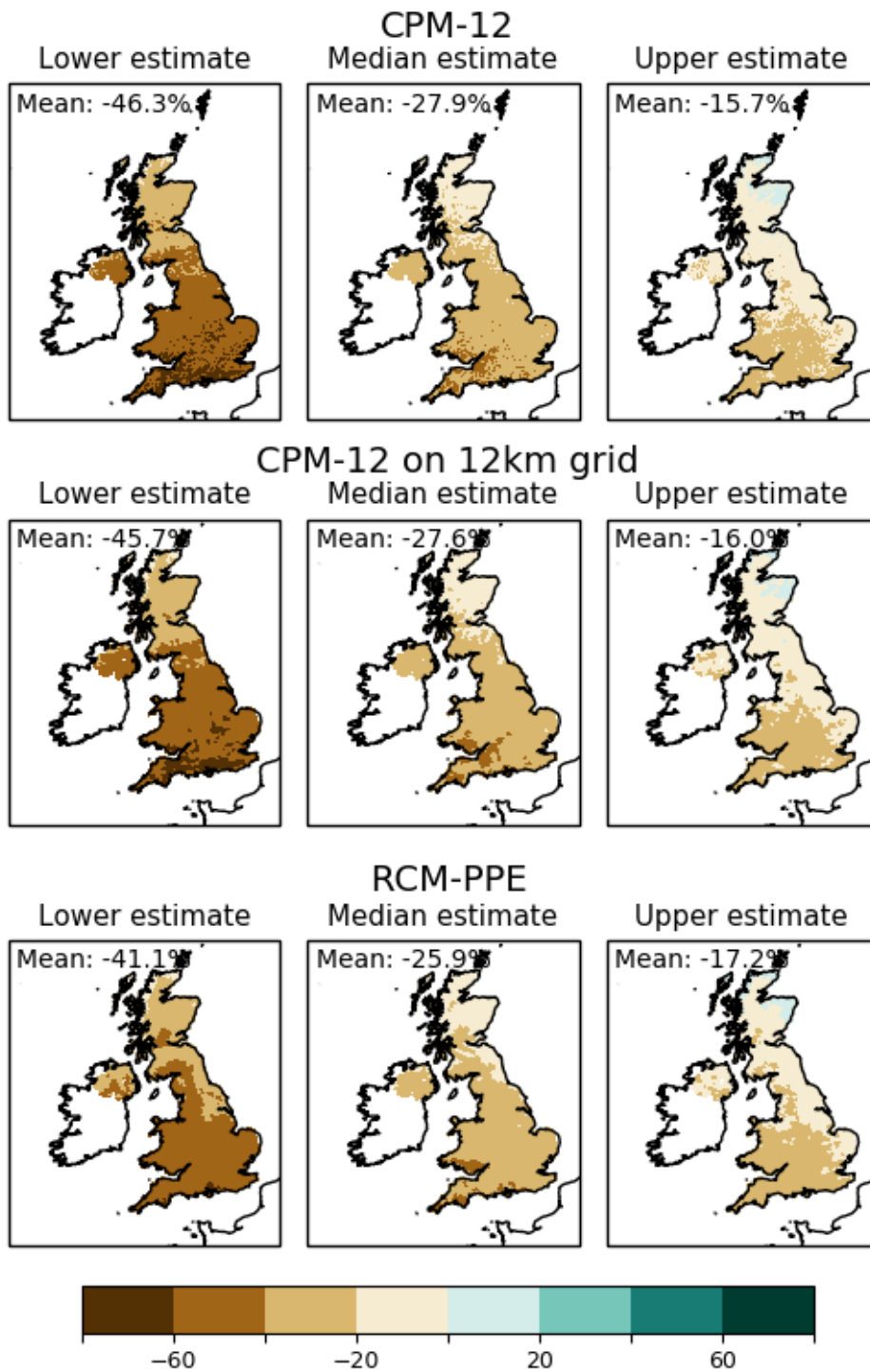
Figure 4.2.6. Future change in summer mean precipitation. As Fig 4.2.1, but for summertime mean precipitation.
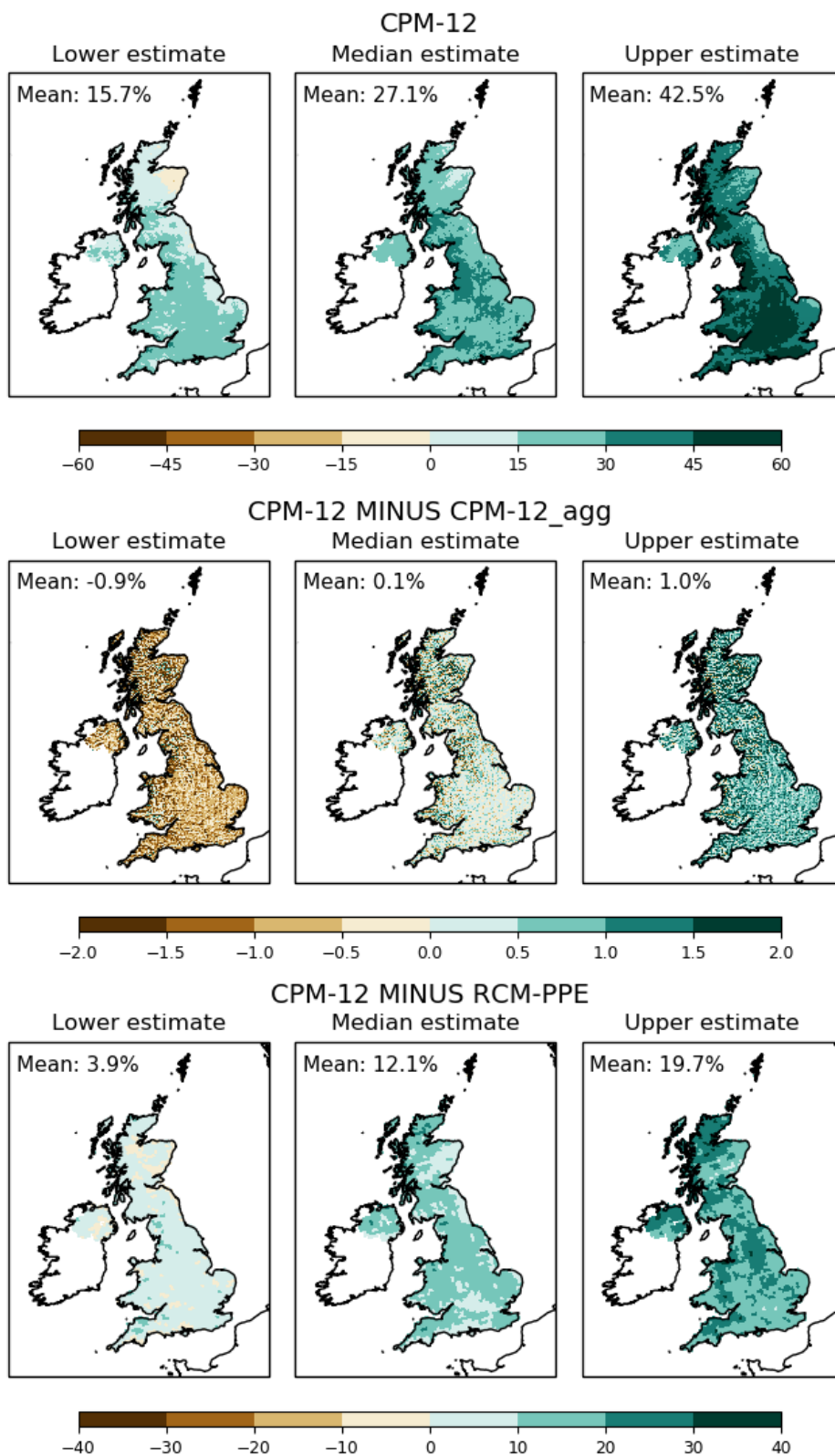
Figure 4.2.7. Impact of convection-permitting downscaling on future change in winter mean precipitation. As Fig. 4.2.3 but for winter mean precipitation.
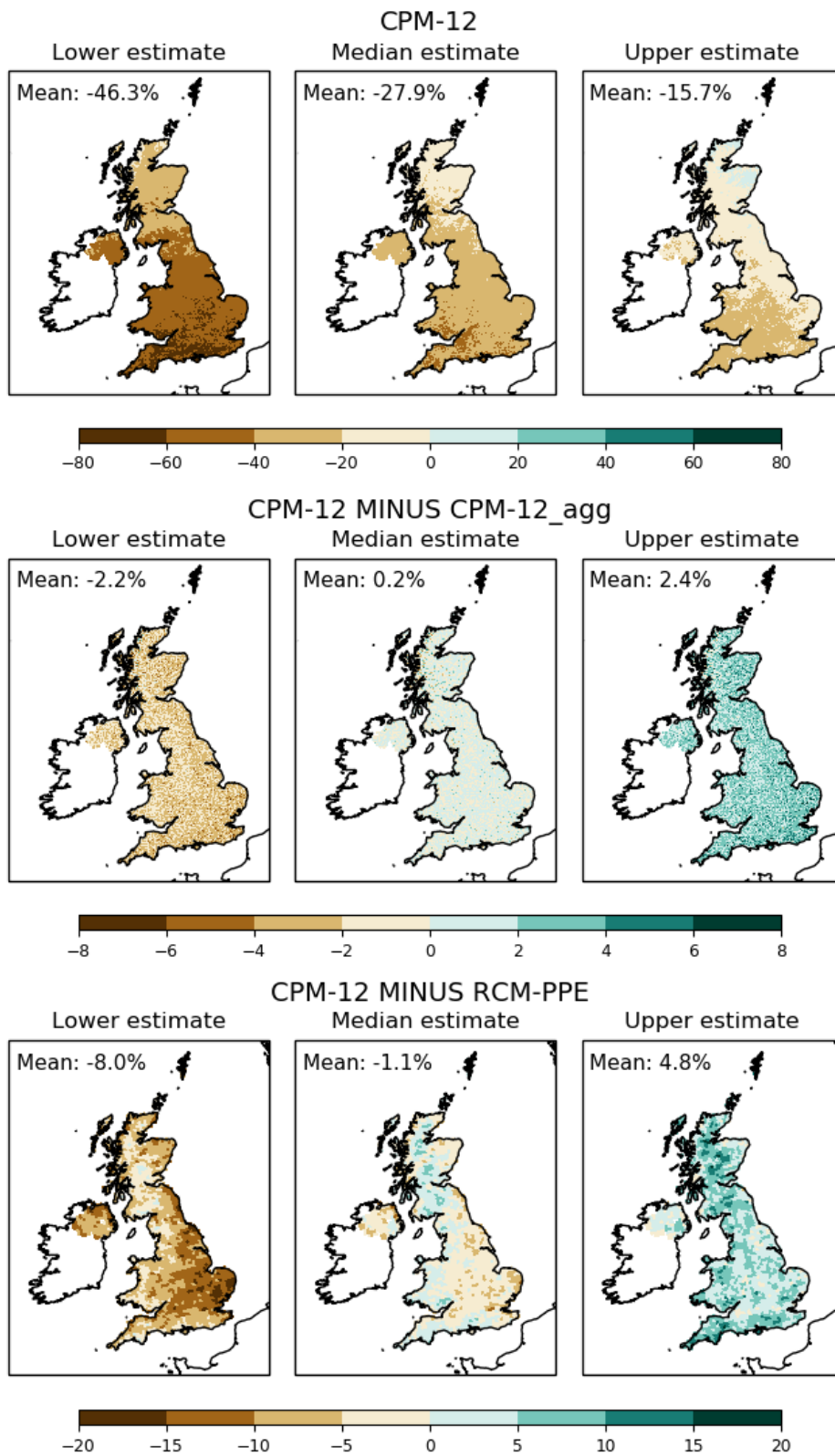
Figure 4.2.8. Impact of convection-permitting downscaling on future change in summer mean precipitation. As Fig. 4.2.3 but for summer mean precipitation.

JJA　　　　　**DJF**
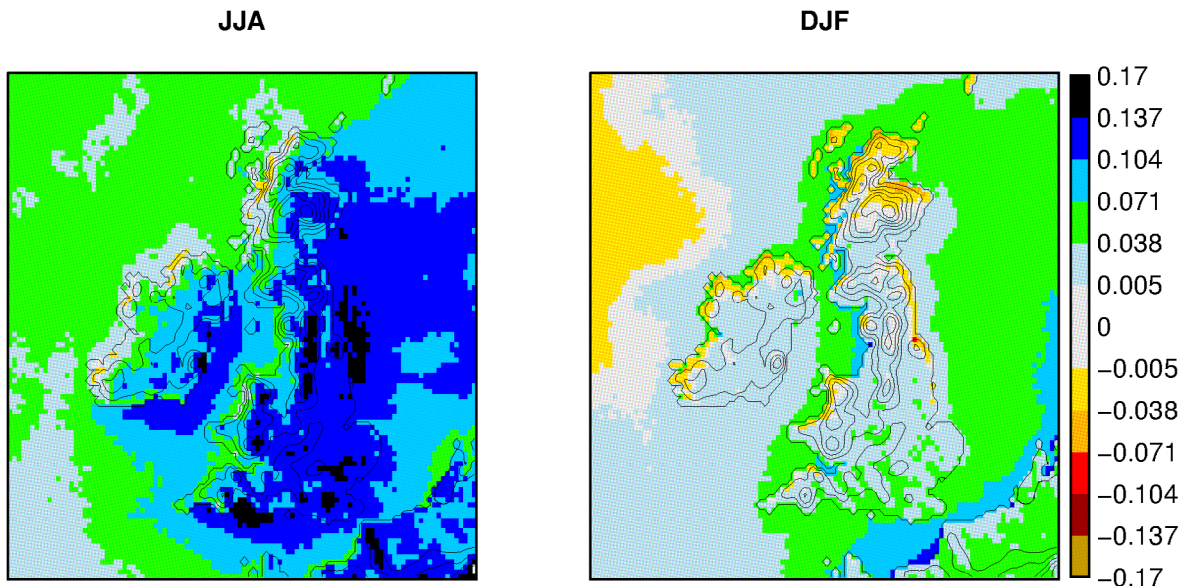
Figure 4.2.9. Future change in the convective fraction of precipitation in the RCM-PPE. Future change in the ensemble-average convective fraction in RCM-PPE for (left) summer and (right) winter. Convective fraction is given as the ratio of convective precipitation to total precipitation, as measured by the convection parameterisation scheme.

4.3 Changes at daily time scale

CPM-12 consistently shows less of an increase in temperature for cold winter days than RCM-PPE (UK average central estimate of 3.8ºC compared to 5.4ºC for all data at 12km scale, Fig 4.3.1), with responses being as much as 4ºC less over northern UK for some CPM-12 members compared to their RCM driving model. Over Scotland, the magnitudes of the differences between the CPM and RCM changes are considerably larger than the corresponding differences in the 20-year seasonal average changes (Section 4.2). It is likely that these differences between the CPM and RCM are related to differences in lying snow (Section 4.5).

For hot summer days, CPM-12 and RCM-PPE generally give consistent responses (UK average central estimate of 5.9ºC) with high-end increases of 7ºC or more in the south (Fig 4.3.2). Individual CPM-12 members can give a lower or higher response than their parent RCM, which may be due to parameter perturbations applied across the RCM ensemble not being mirrored in the CPM ensemble.

For daily precipitation, CPM-12 shows an increase in wet day frequency in winter that is not seen in the RCM-PPE (UK-average central estimate of 9.2% compared to 0.6% for data at 12km scale, Fig 4.3.3). Given present-day biases in RCM-PPE for wet day frequency, we have low confidence in RCM projected changes for this metric. The CPM-12 projected changes are considered plausible, given the much better representation of the baseline. More generally, we note that the skill of the simulated baseline, while an important consideration, is only one of (potentially) many physical factors to consider, when assessing the credibility of projected changes in a given variable. In particular, an understanding of the local and remote drivers of future change is also important. For example, we would expect both the RCM and CPM simulations to capture any future changes in wet-day frequency related to changes in the occurrence of mid-latitude weather systems inherited from the driving global simulations. However, as discussed previously in Section 4.2, a possible explanation for the differences in the downscaled responses may be more triggering of convective showers in a future warmer climate in the CPM. However, further work is needed to establish if this is the case.

Increases in wet day intensity in winter (central estimate of 17-18%, Fig 4.3.4) are in good agreement between CPM-12 and RCM-PPE, which may be explained by the increases being driven by increasing atmospheric moisture with warming – a process well captured by coarse resolution climate models. Thus, the greater increase in wintertime mean precipitation in CPM-12 shown earlier is due to the different changes in rainfall occurrence on the daily timescale. For heavy daily events in winter, increases in precipitation are slightly larger in CPM-12 (central estimate of 23% compared to 20%, Fig 4.3.5), with an upper estimate of changes of 38% compared to 34% (for data regridded to 12km scale for fair comparison with the RCM).

In summer, both CPM-12 and RCM-PPE show decreases in wet day frequency, with larger decreases in CPM-12 (UK average central estimate of 32% compared to 25% decrease, Fig 4.3.6). On the other hand, changes in wet day intensity are consistently more positive in the CPM (UK average central estimate of 5% increase in CPM but 3% decrease in RCM, Fig 4.3.7). Thus although changes in mean summer precipitation are similar between CPM-12 and RCM-PPE (see previous section), there are quite different underlying changes in intensity and occurrence. Given present-day biases in rainfall occurrence in RCM-PPE, and the improved representation of convective processes in the CPM, we have greater confidence in the underlying frequency/intensity changes in CPM-12 in summer. This is also supported by previous studies which have shown the tendency for a greater intensification of summer time rainfall in convection-permitting compared to parameterised models (Kendon et al, 2017).

For heavy daily events in summer, the central estimates suggest little change in the CPM and a slight decrease in the RCM (UK average of 0% and -6% change respectively, for data at 12km scale, Fig 4.3.8). The upper estimates of the change are 16% (CPM-12) compared to 8% (RCM-PPE) increase. Thus there is a greater tendency for heavy events to intensify in the CPM, consistent with the greater tendency towards increases in average summertime rainfall intensity.
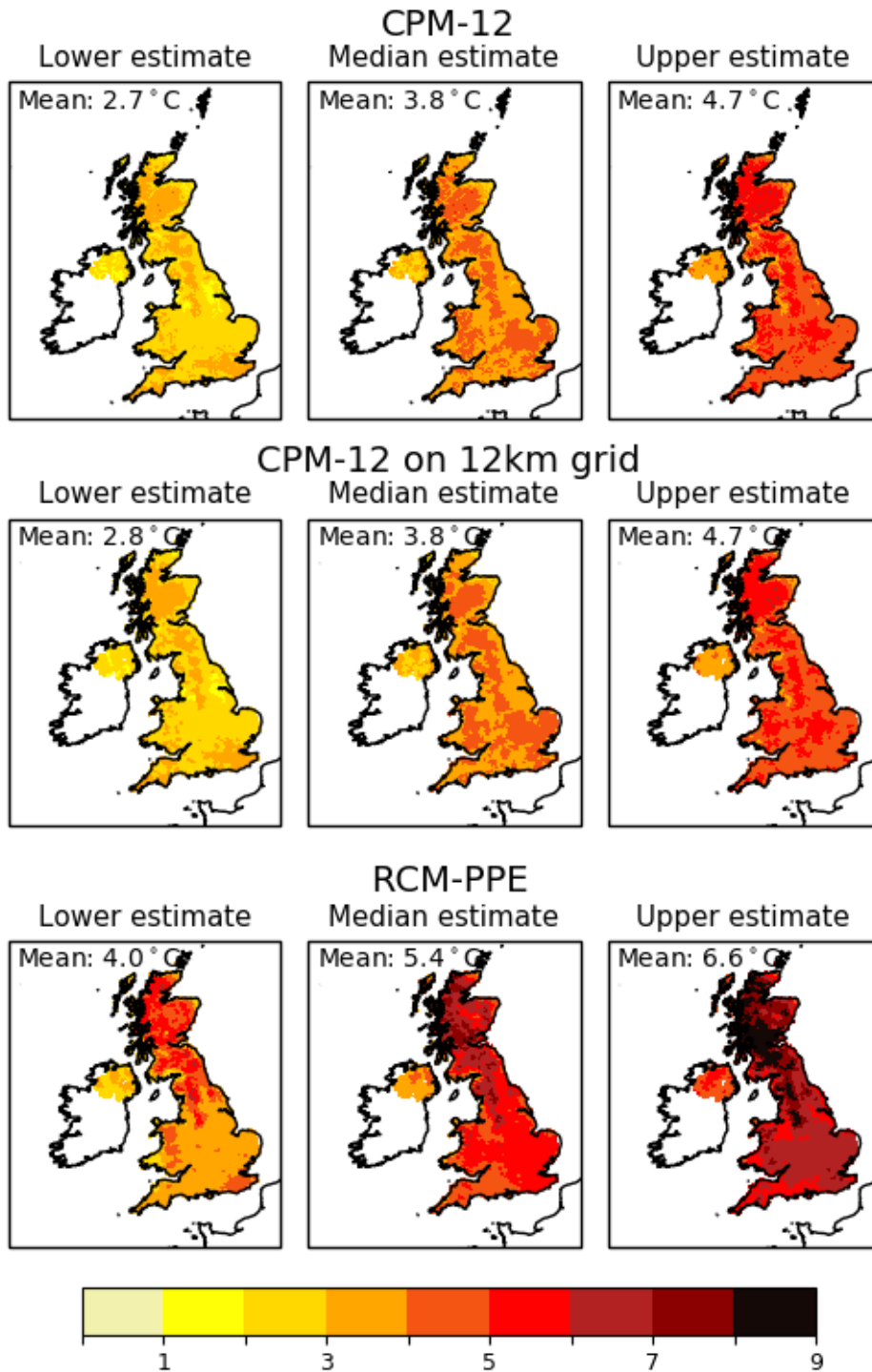
Figure 4.3.1. Future change in cold winter days. Changes for (left) 2nd lowest, (centre) central and (right) 2nd highest member locally, for (top) CPM-12 at native 2.2km resolution, (middle) CPM-12 regridded to 12km RCM grid and (bottom) RCM-PPE. Changes (in °C) correspond to the difference between the future (2061-2080) and baseline (1981-2000) periods. Cold winter days are defined as the 1st percentile of daily mean temperature in DJF. UK-average changes are indicated in each panel.
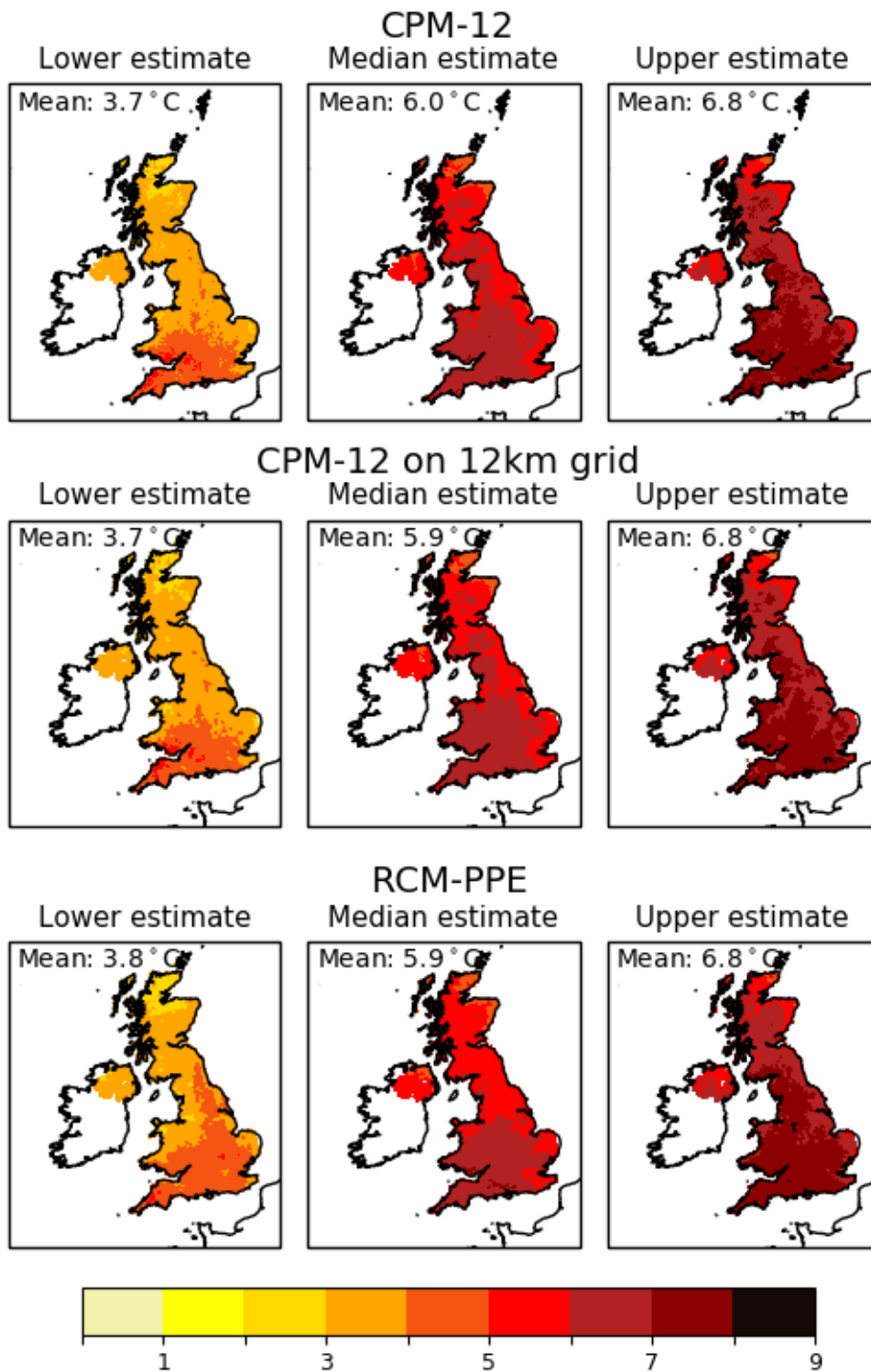
Figure 4.3.2. Future change in hot summer days. As Fig 4.3.1 but for future change in hot summer days. Hot summer days are defined as the 99th percentile of daily mean temperature in JJA.

TS3 MINUS TS1 Wet day (>1mm per day) frequency djf pr (%) upper, median & lower estimates across PPE

CPM-12

Lower estimate	Median estimate	Upper estimate
Mean: 3.0%	Mean: 9.2%	Mean: 16.7%

CPM-12 on 12km grid

Lower estimate	Median estimate	Upper estimate
Mean: 3.1%	Mean: 9.2%	Mean: 16.4%

RCM-PPE

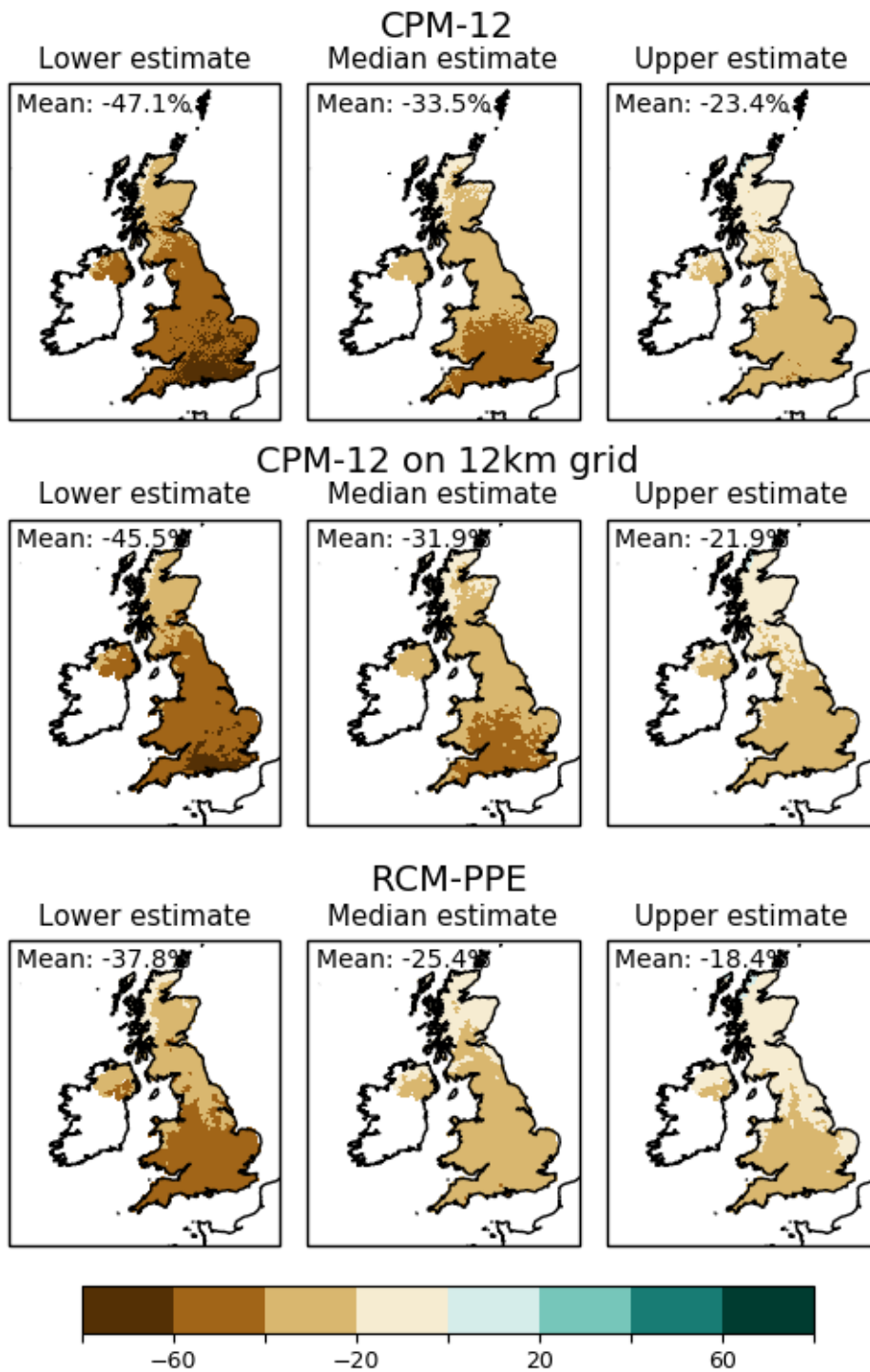| Lower estimate	Median estimate	Upper estimate
Mean: -4.5%	Mean: 0.6%	Mean: 5.5%
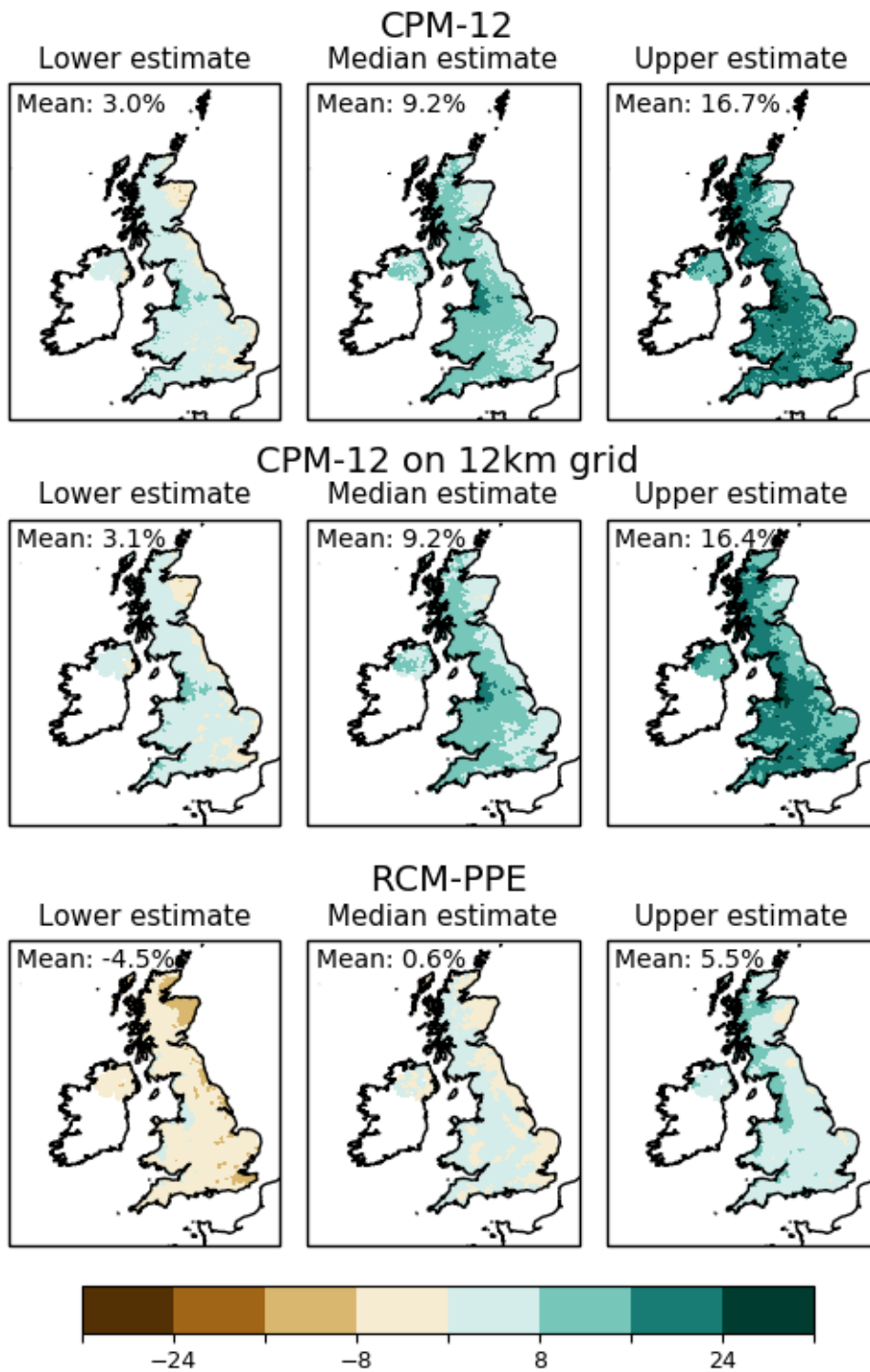
Figure 4.3.3. Future change in wet day frequency in winter. As Fig 4.3.1 but for future change in wet day frequency in winter. Wet days are defined as days with precipitation >1mm/d.
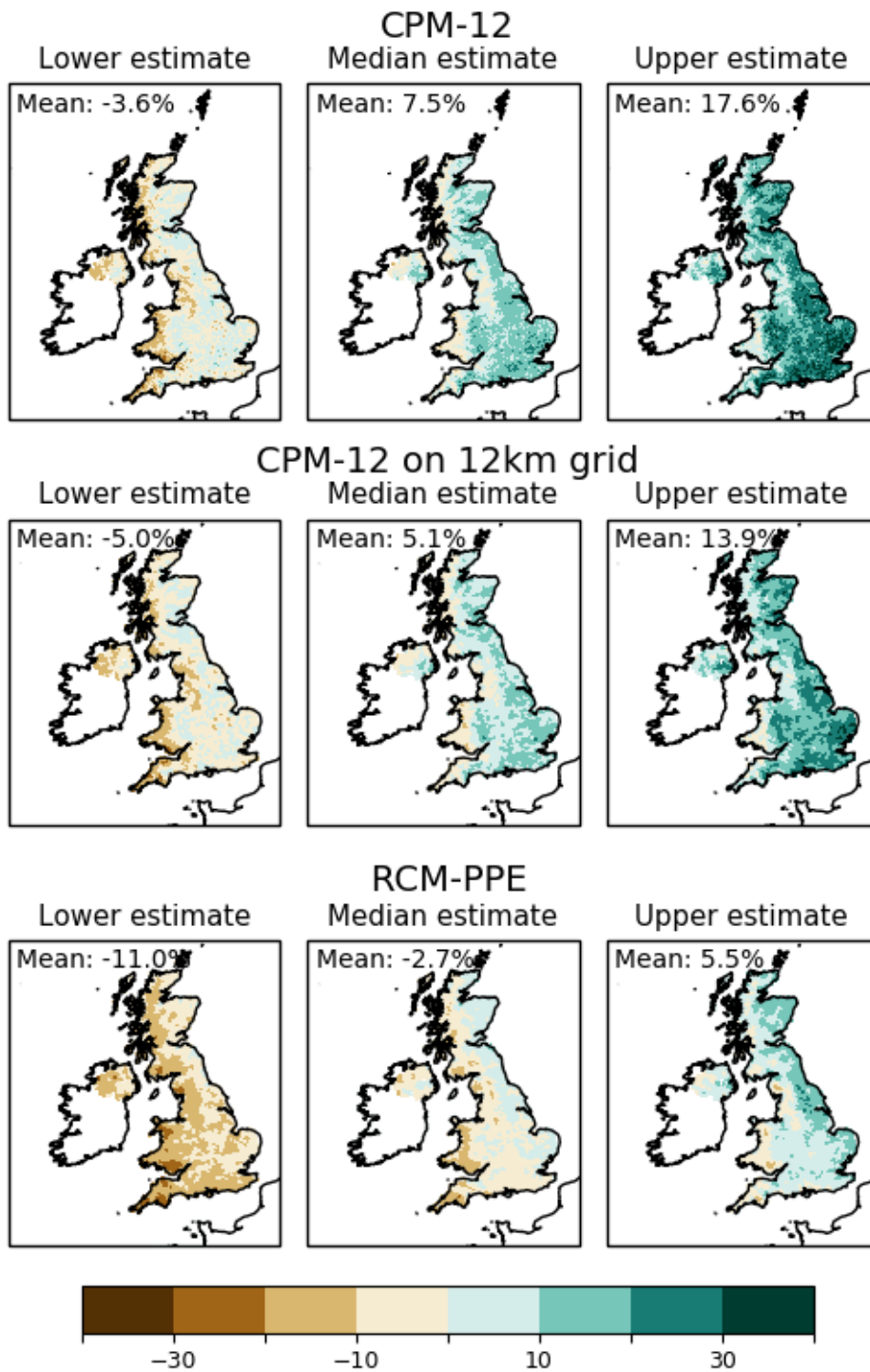
Figure 4.3.4. Future change in wet day intensity in winter. As Fig 4.3.1 but for future change in wet day intensity in winter. Wet days are defined as days with precipitation >1mm/d.
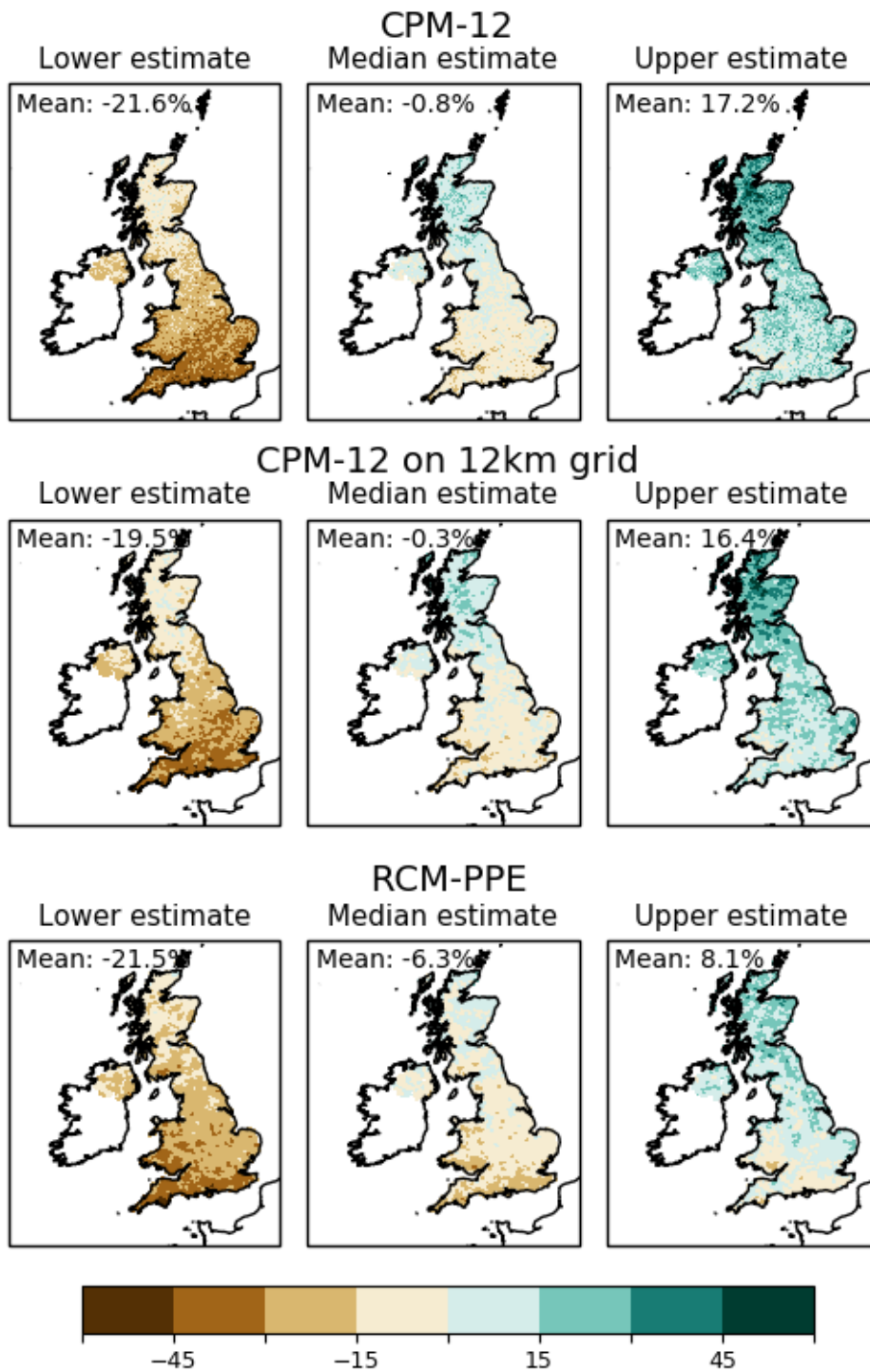
Figure 4.3.5. Future change in heavy daily events in winter. As Fig 4.3.1 but for future change in the 99th percentile of daily mean precipitation in DJF.

Figure 4.3.6. Future change in wet day frequency in summer. As Fig 4.3.1 but for future change in wet day frequency in summer. Wet days are defined as days with precipitation >1mm/d.

TS3 MINUS TS1 Wet day (>1mm per day) intensity jja pr (%)
upper, median & lower estimates across PPE

CPM-12

Lower estimate	Median estimate	Upper estimate
Mean: -3.6%	Mean: 7.5%	Mean: 17.6%

CPM-12 on 12km grid

Lower estimate	Median estimate	Upper estimate
Mean: -5.0%	Mean: 5.1%	Mean: 13.9%

RCM-PPE

Lower estimate	Median estimate	Upper estimate
Mean: -11.0%	Mean: -2.7%	Mean: 5.5%

−30   −10   10   30

Figure 4.3.7. Future change in wet day intensity in summer. As Fig 4.3.1 but for future change in wet day intensity in summer. Wet days are defined as days with precipitation >1mm/d.

Figure 4.3.8. Future change in heavy daily events in summer. As Fig 4.3.1 but for future change in the 99th percentile of daily mean precipitation in JJA.

4.4 Changes in hourly precipitation

Changes in hourly precipitation occurrence and intensity

In winter, CPM-12 shows a future increase in hourly precipitation occurrence (UK-average central estimate of 17% increase), which is not seen in RCM-PPE (2% increase, Fig 4.4.1). This is similar to the behaviour on the daily timescale. However, hourly precipitation intensity changes are greater in RCM-PPE (15% increase) compared to CPM-12 (10% increase, Fig 4.4.2). Both models suggest an increase in high percentiles of hourly precipitation in winter. For the 99.95th percentile of hourly precipitation (including wet and dry values, corresponding to ~1 event per season), the CPM-12 and RCM-PPE show similar changes (UK-average central estimate of 22% and 20% increase respectively) although the uncertainty range in changes across the ensemble is greater in RCM-PPE (Fig 4.4.3). The latter result is not surprising given that we are comparing a perturbed parameter ensemble (RCM-PPE) with an ensemble of models that only differ in their boundary conditions (CPM-12). However, we note that the large ensemble spread in changes in hourly precipitation extremes in the RCM-PPE (Section 4.5) is unlikely to be "real" uncertainty, and instead likely reflects unphysical grid point storms in the RCM.

In summer, CPM-12 shows a slightly greater future decrease in hourly rainfall occurrence (32% decrease compared to 28% decrease in RCM-PPE, Fig 4.4.4) and a greater future increase in hourly rainfall intensity (8% increase compared to 2% increase in RCM-PPE, Fig 4.4.5). These results are similar to those on daily timescales. For the 99.95th percentile of hourly precipitation in summer, both models project an increase, but decreases are possible especially in the south (for low-end changes, Fig 4.4.6). Notably, there are larger increases in high percentiles in CPM-12 compared to RCM-PPE (central estimate of 16% compared to 12%) consistent with the larger increase in summertime rainfall intensity. We note that this discrepancy between the models is less than in Kendon et al (2014), which showed increases in heavy summer rainfall in the CPM only. As in winter, the RCM-PPE shows a slightly greater uncertainty range in changes in summertime heavy events.

In both models, the largest relative increases in the 99.95th percentile actually occur in autumn (SON, Fig 4.4.7), unlike for heavy daily events where the largest increases occur in winter. In autumn, there are smaller decreases in hourly rainfall occurrence and larger increases in hourly rainfall intensity than in summer, and the intensity changes are consistent between the CPM and RCM. This change in the seasonality of heavy hourly rainfall may be explained by warming leading to an extension of the convective season and greater increases in moisture availability in autumn (c.f. Section 4.5). The central estimate of the change in the 99.95th percentile in autumn is similar between CPM-12 and RCM-PPE (30% and 32% increase), but the RCM-PPE shows a larger range of changes (the average low- and high-end changes are 11% and 57%, cf. 14% and 47% in CPM-12).
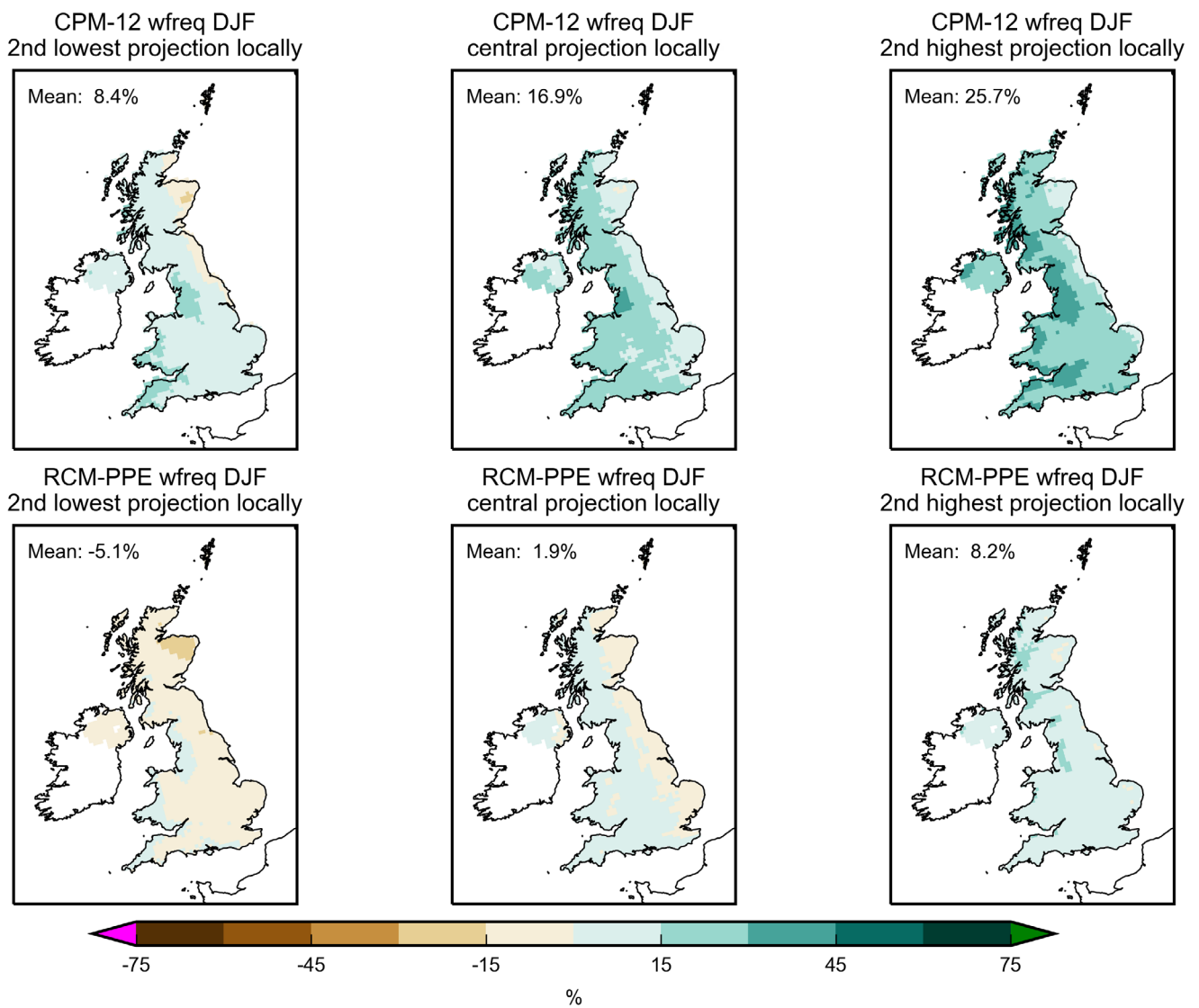
Figure 4.4.1. Future change in hourly precipitation occurrence in winter. Changes for (left) 2nd lowest, (centre) central and (right) 2nd highest member locally, for (top) CPM-12 regridded to 12km RCM grid and (bottom) RCM-PPE. Changes (in %) correspond to the difference between the future (2061-2080) and baseline (1981-2000) periods. Wet hours are defined as hours with precipitation > 0.1mm/h . UK-average changes are indicated in each panel.
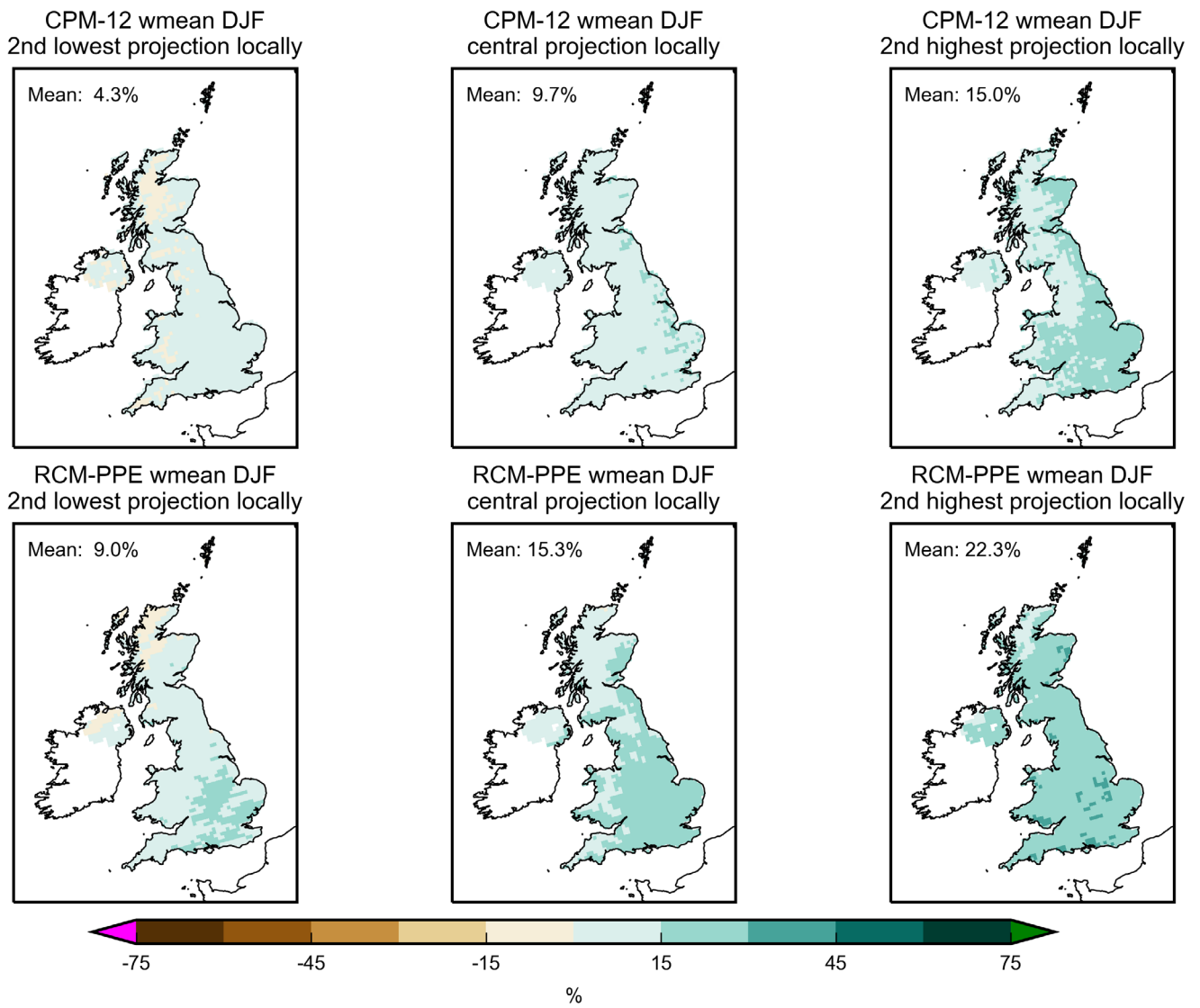
Figure 4.4.2. Future change in hourly precipitation intensity in winter. As Fig 4.4.1 but for hourly precipitation intensity.
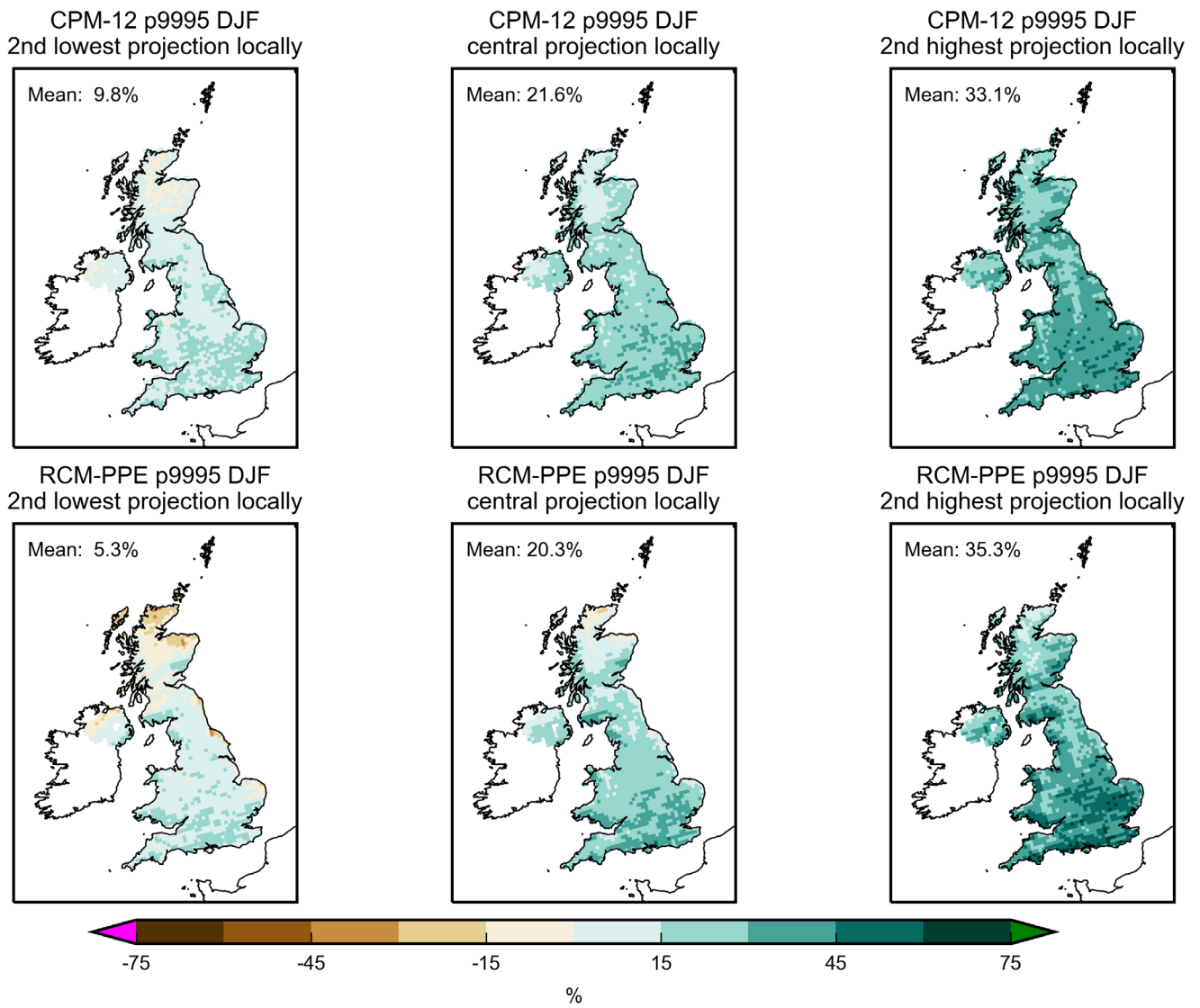
Figure 4.4.3. Future change in heavy hourly precipitation in winter. As Fig 4.4.1 but for heavy hourly precipitation defined as the 99.95[th] percentile of hourly precipitation (for all hours) in DJF.
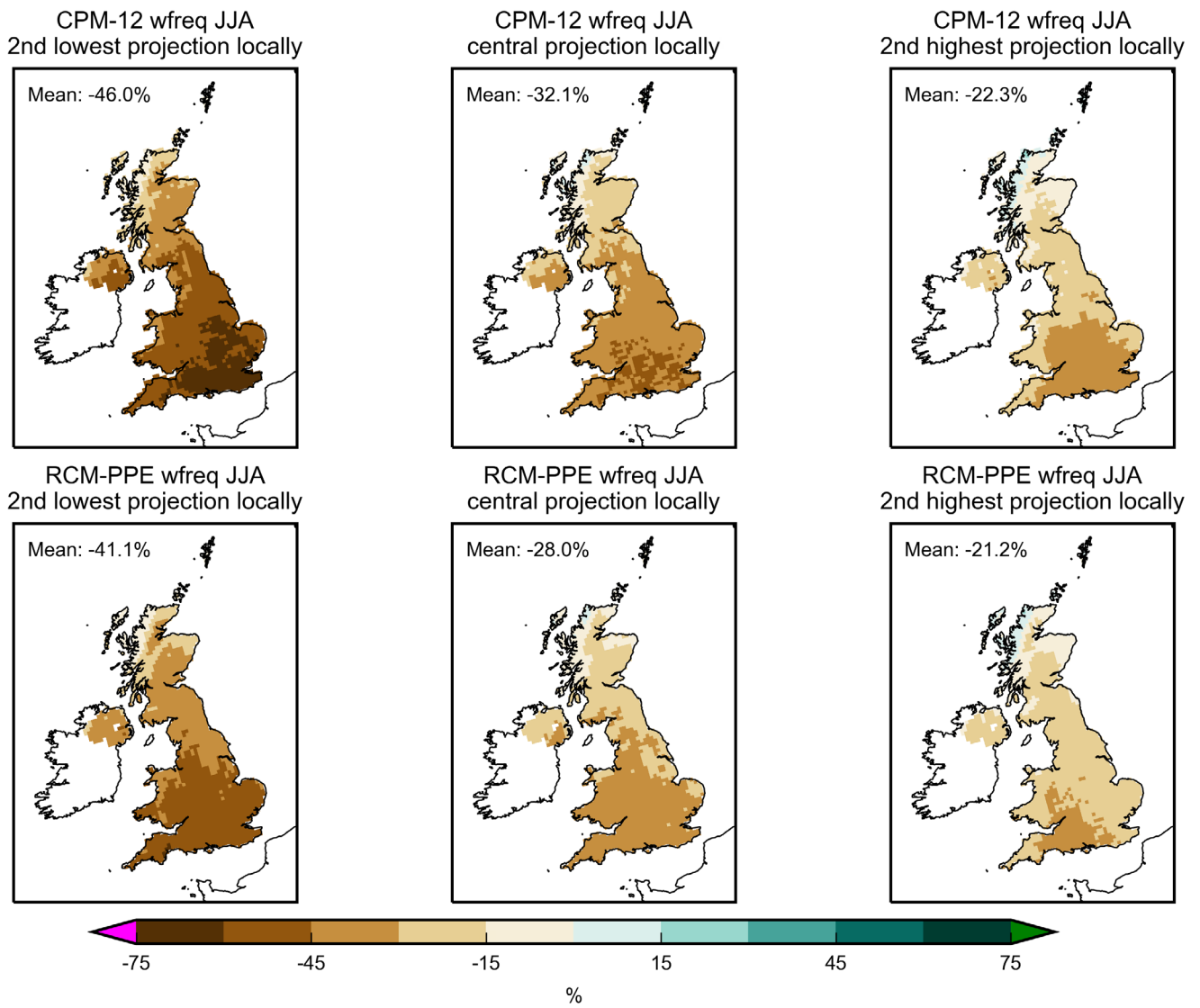
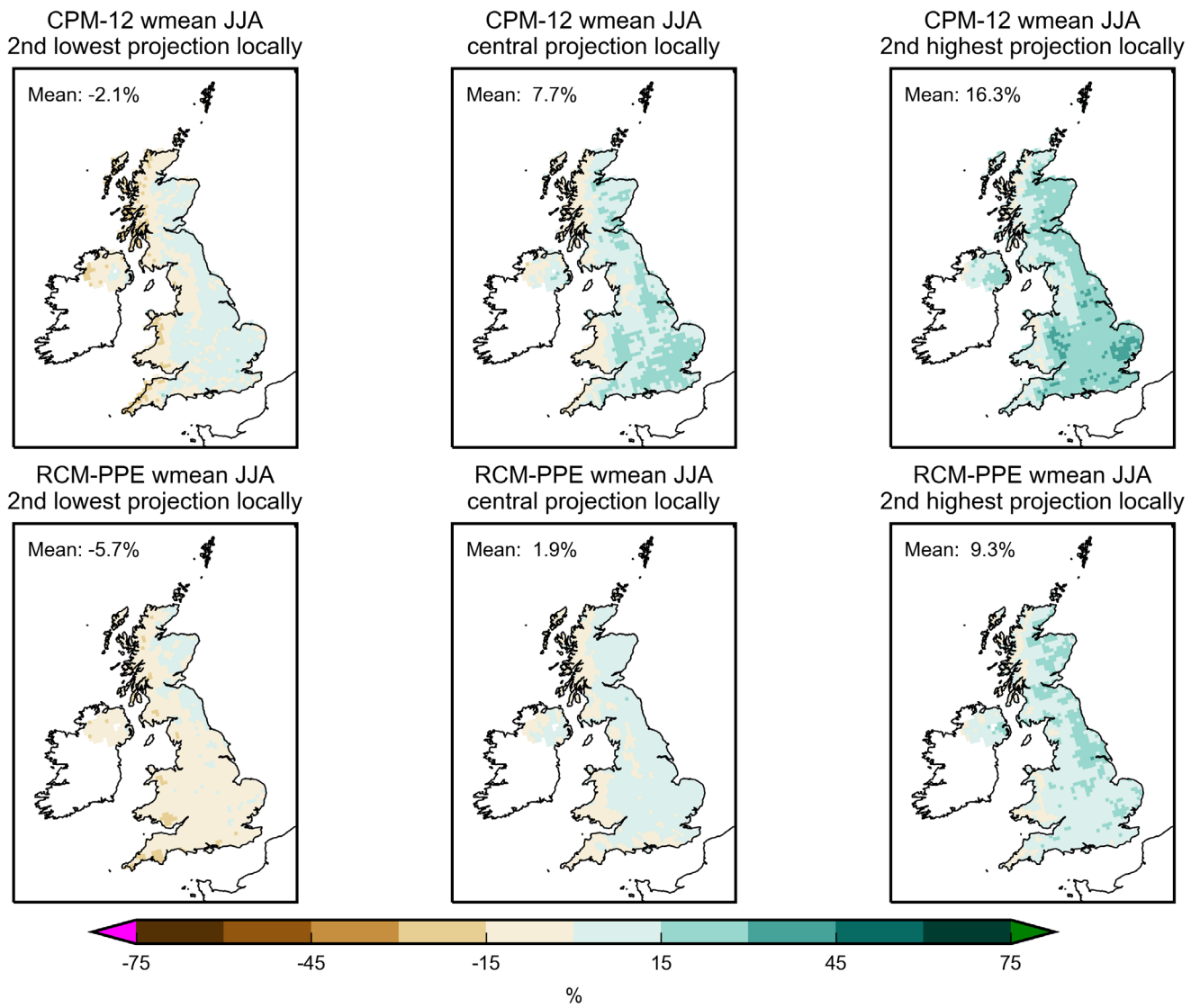**Figure 4.4.4.** Future change in hourly precipitation occurrence in summer. As Fig 4.4.1 but for summer.

Figure 4.4.5. Future change in hourly precipitation intensity in summer. As Fig 4.4.1 but for hourly precipitation intensity in summer.
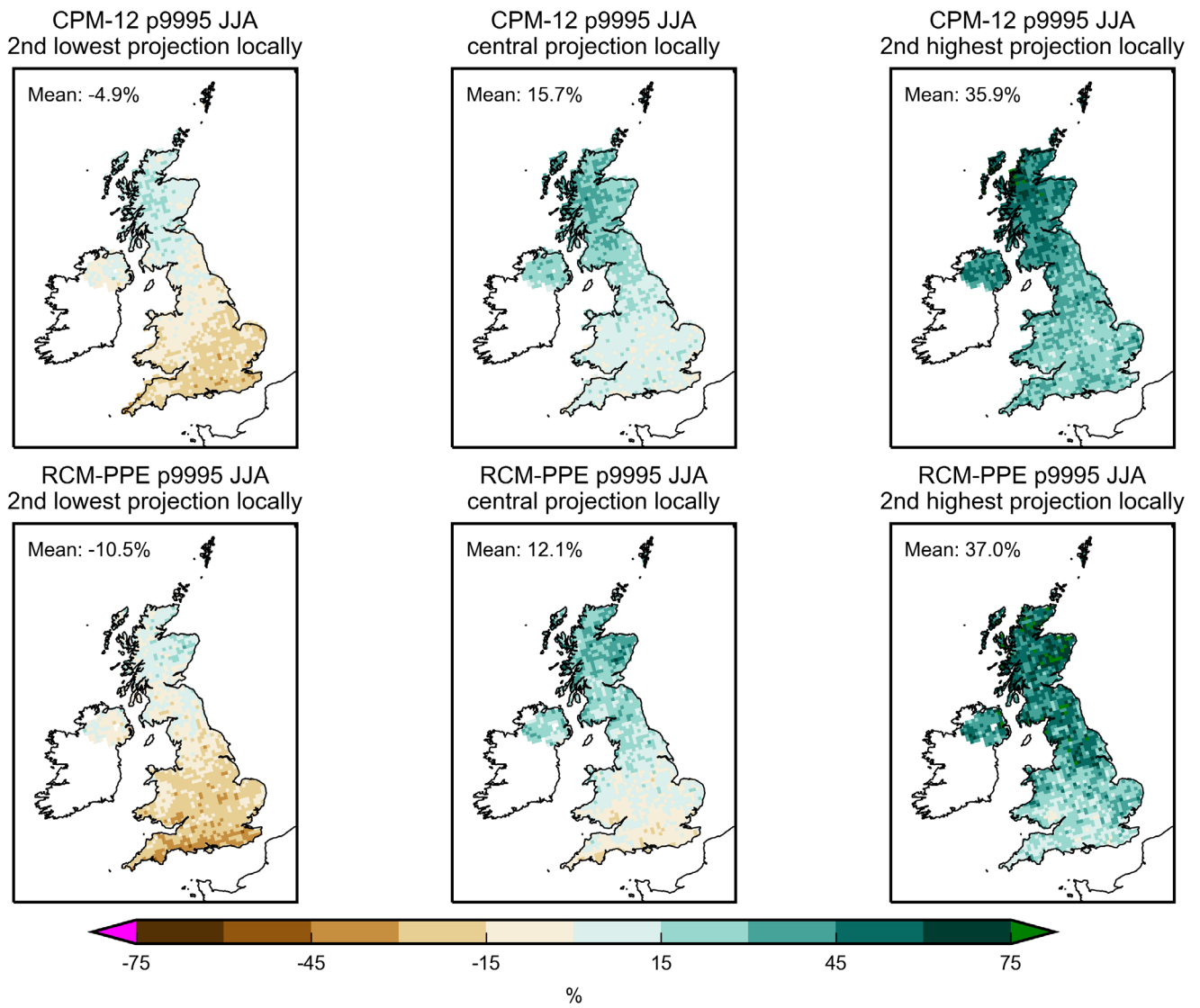
Figure 4.4.6. Future change in heavy hourly precipitation in summer. As Fig 4.4.1 but for heavy hourly precipitation defined as the 99.95th percentile of hourly precipitation (for all hours) in JJA.
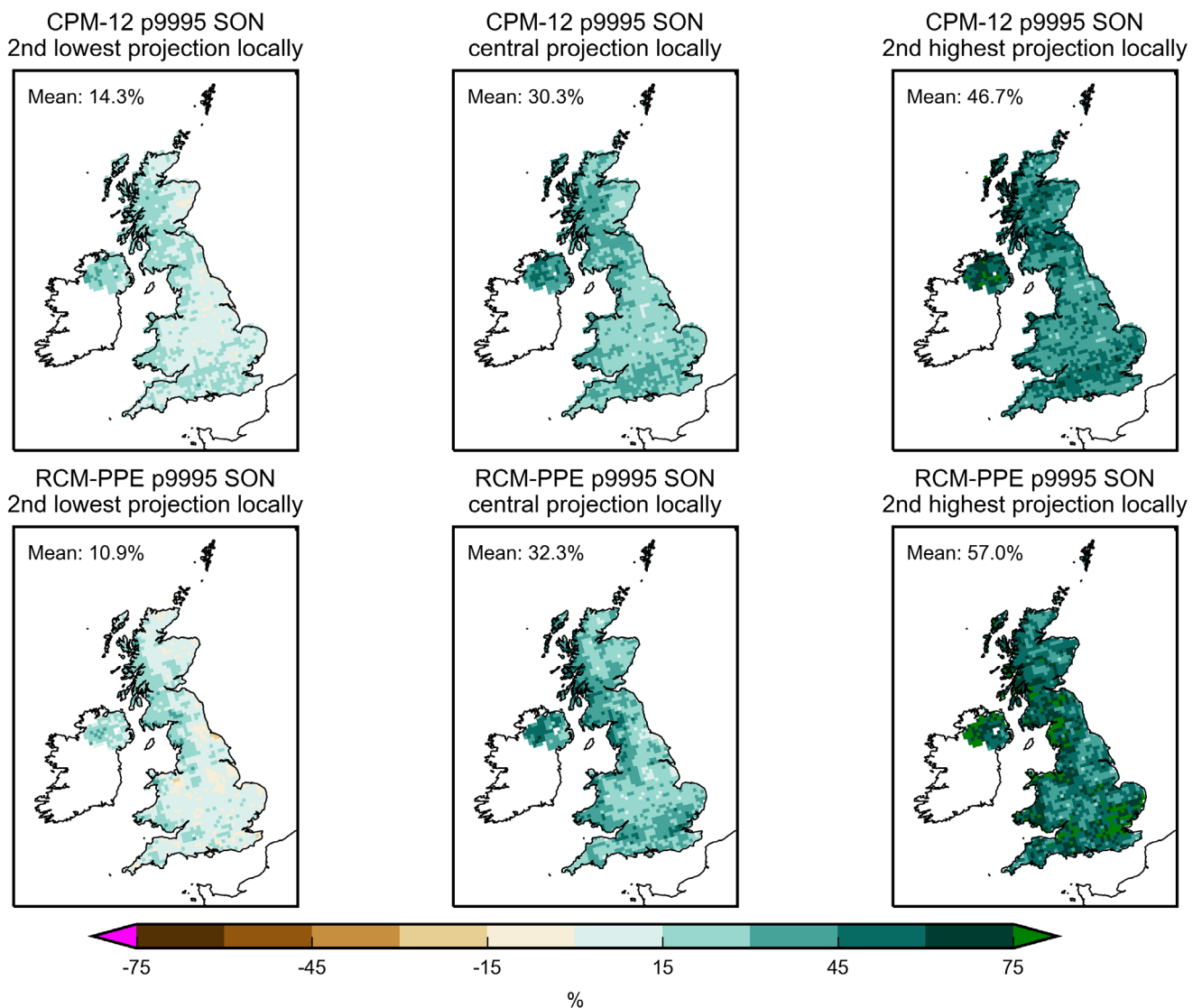
Figure 4.4.7. Future change in heavy hourly precipitation in autumn. As Fig 4.4.1 but for heavy hourly precipitation defined as the 99.95th percentile of hourly precipitation (for all hours) in SON.

Changes in precipitation intensity distribution

Future changes in the shape of the hourly precipitation distribution are shown in Fig 4.4.8. In this case, we are considering only wet values (>0.1mm/h), but note that the key results are the same if fractional contribution changes are plotted for all (wet and dry) values. This shows evidence of an intensification of hourly rainfall in all seasons in both models, and for all ensemble members. In autumn and winter, changes in the shape of the wet value distribution are very similar between the CPM and RCM, although there is a much greater decrease in winter (and smaller increase in autumn) in the percentage of dry days in the CPM (as shown above). Notably in winter, changes in the standard member are smaller than the changes in all other ensemble members. The greatest difference in changes between the models is seen in summer, where there is a much greater increase in the fractional contribution from high intensities in the CPM (consistent with Kendon et al, 2014). This is consistent with the greater increases in the 99.95th percentile (of all hours) in the CPM compared to the RCM shown in Fig 4.4.6.
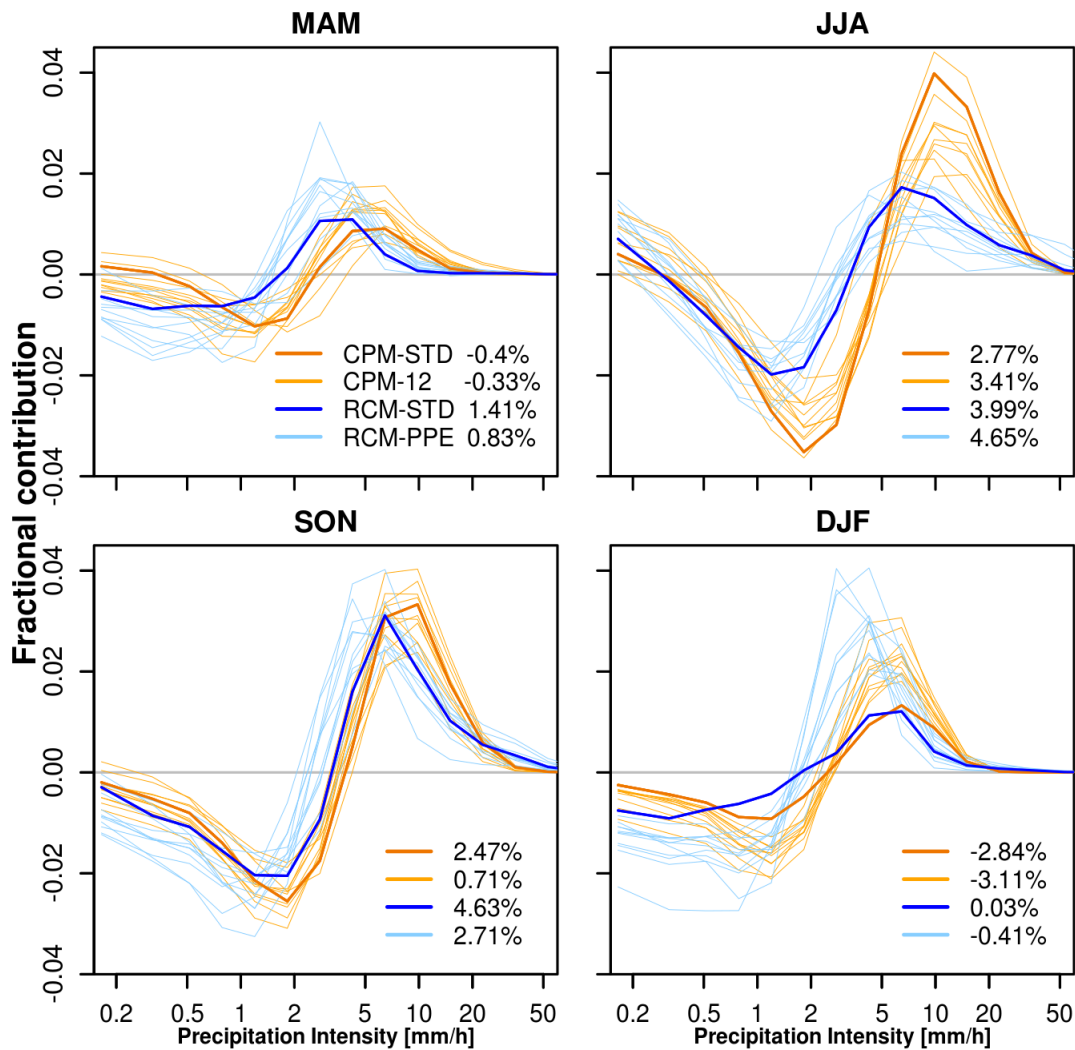
Figure 4.4.8. Future change in fractional contribution of hourly precipitation intensities to total precipitation. Plotted is the future change in the fractional contribution of hourly precipitation events within 17 different intensity bins to total UK rainfall, for wet events only (>0.1mm/h), in different seasons. The contributions were calculated by assigning each wet hour from every 12km UK grid box to the relevant intensity bin, and multiplying the number of counts in each bin by the average intensity; these contributions are then divided by the total precipitation across all bins to give the fractional contribution. Future changes are differences between 2061-80 and 1981-2000 periods, for (orange) CPM-12 and (blue) RCM-PPE members, with dark lines for the standard member. Future changes in the percentage of dry hours (in %) are indicated in the figure legends (corresponding to standard members and ensemble-average value for CPM-12 and RCM-PPE). Intensity bin boundaries are: 0.1, 0.23, 0.41, 0.62, 0.95, 1.4, 2.2, 3.4, 5.1, 7.8, 11.9, 18.1, 27.5, 42.0, 63.9, 97.4,148 and 500 mm/h.

Maps looking in more detail at changes in the intensity distribution of hourly precipitation in winter are shown in Figs 4.4.9-4.4.15. These provide insights into the differences in winter mean precipitation changes between the CPM and RCM shown earlier (Section 4.2). We firstly examine the number of historical events in 4 different intensity bins: 0.0-0.005 mm/day (dry), 0.005-10.0 mm/day (light), 10-50 mm/day (moderate) and >50 mm/day (heavy), where the hourly intensity has been multiplied by 24 to give units of mm/day. It can be seen that about 50% of events are "dry" (<0.005 mm/day or equivalently <0.0002 mm/h) in the CPM, whereas there are many fewer dry events in the RCM with instead more than 50% of hourly events in the light intensity category (Figs 4.4.9-4.4.10). In both models there are fewer dry events and more light/moderate events over the sea to the NW of the UK. Heavier events (>50 mm/day or equivalently >2mm/h) are largely confined to regions of high orography in the west. Future changes in the number of dry events

show quite different behaviour between the CPM and RCM (Fig 4.4.11). In both models there is a large decrease in the number of dry hours over the sea. This decrease is larger in the CPM, with a greater increase in the number of light events compared to the RCM, however there are still many more low intensity events in the RCM than the CPM in future. This decrease in the number of dry hours over the sea is seen to also extend over the land in the CPM, with an increase in both smaller hourly events and larger hourly totals over land. However, this is not the case in the RCM, where there is actually a future increase in dry hours, at the expense of fewer light events (which is the category of the majority of rainfall events). In the future, we expect an increase in convective showers over the sea, due to the warmer ocean and higher atmospheric moisture. This is seen in both models, however the advection of these showers inland (beyond the coastal region) only occurs in the CPM. In the RCM, it seems convection over land is becoming less favourable in the future (possibly due to a longer time needed for the replenishment of moisture between events). Thus the different representation of wintertime convective showers and their advection inland may explain, at least in part, the different winter mean precipitation changes between the models over land.

Similar to the analysis above, but now looking at the actual contribution of hourly events in different intensity bins to the total precipitation in winter (Figs 4.4.12-4.4.13, note the contribution from "dry" events, <0.005mm/day, is not shown), it can be seen that the largest contribution comes from moderate intensity events (10-50 mm/day or equivalently 0.4-2.0 mm/h) rather than the more numerous light events (0.005-10 mm/day category above). In both models, the largest contributions are seen over orography, for all moderate to heavy rainfall categories. In terms of future changes (Figs 4.4.14-4.4.15), there is an increase in the contribution from moderate and heavy events in both models, consistent with an intensification of rainfall in winter (Fig 4.4.8). The largest increases in contribution are found over orography, with greater increases in contribution from the highest intensities over orography in the CPM than RCM. Although there is a future decrease in light intensity events over land in the RCM (Fig 4.4.11), these are seen to only have a small contribution to the overall change in rainfall (Fig 4.4.15).

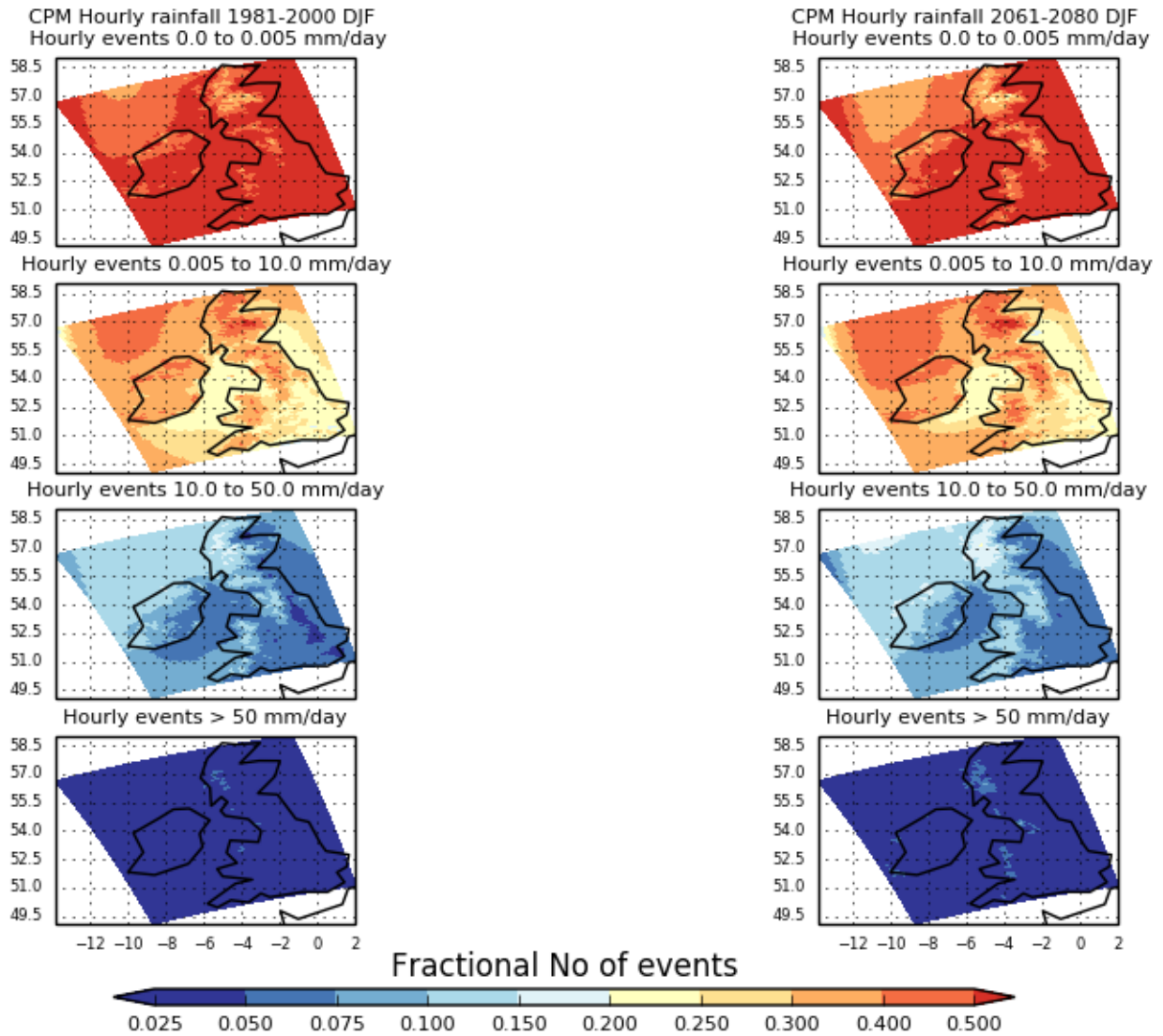## Histogram of fractional no. of rainfall events

Figure 4.4.9. Fractional number of hourly events in different intensity bins in winter in CPM-12. Maps of the ensemble-mean fractional number of events in 4 intensity bins (0.0-0.005, 0.005-10.0, 10-50 and >50 mm/day) in CPM-12 for (left) present-day (1981-2000) and (right) future (2061-80) winters. The hourly intensity has been multiplied by 24 to give units of mm/day
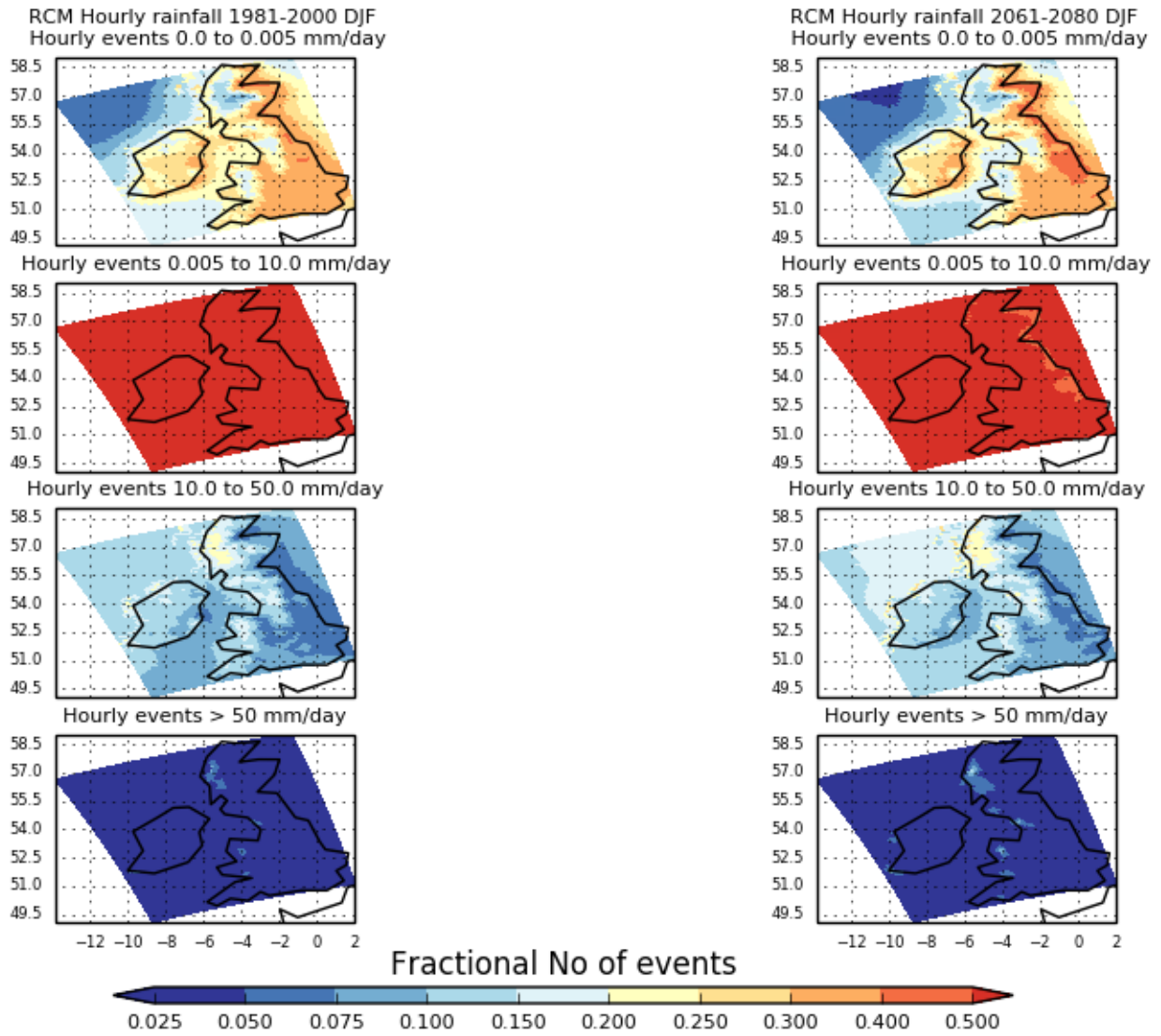
Histogram of fractional no. of rainfall events

Figure 4.4.10. Fractional number of hourly events in different intensity bins in winter in RCM-PPE. As Fig 4.4.9, but for RCM-PPE.

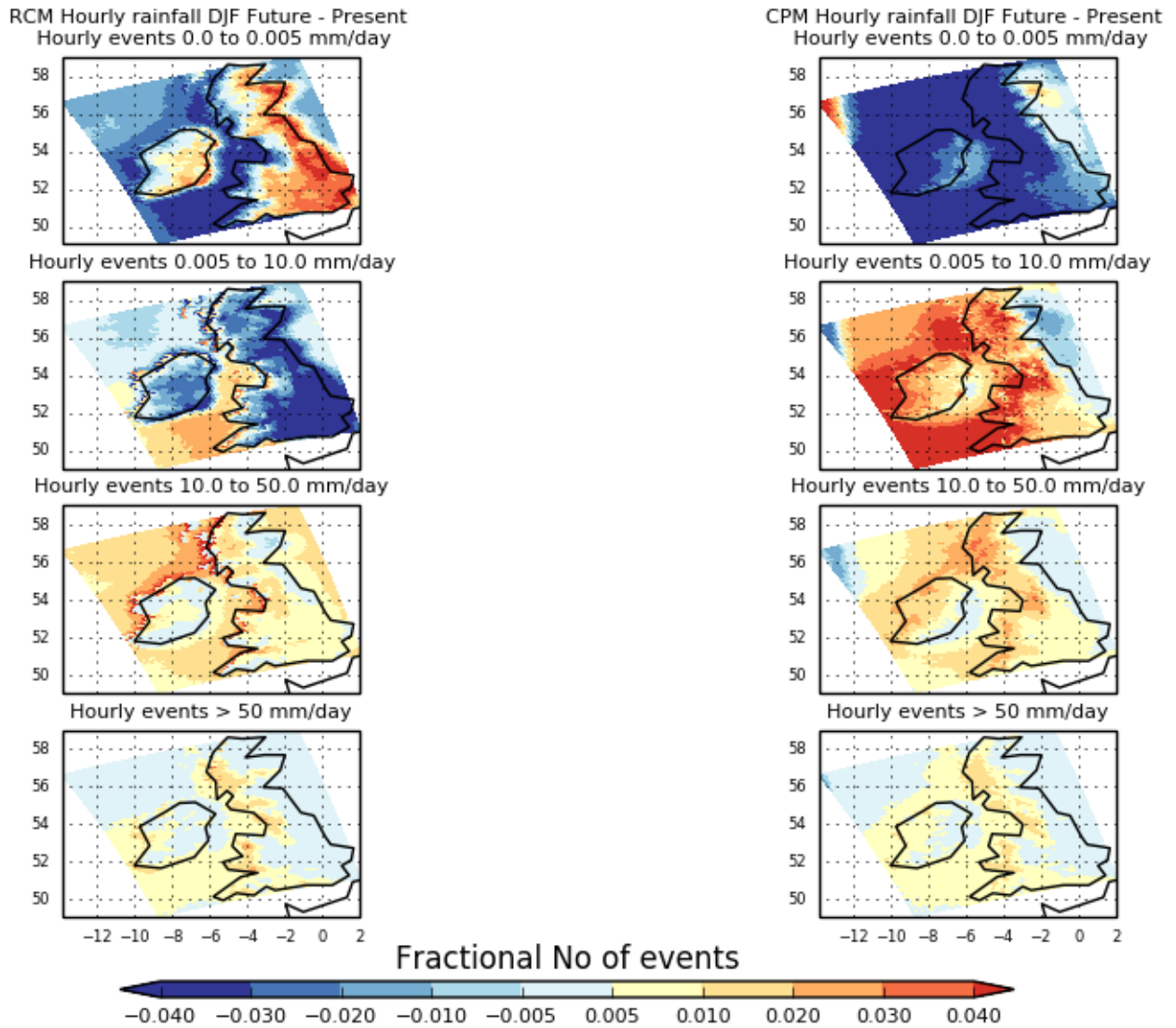## Histogram of fractional DIFFERENCE in total rainfall events

Figure 4.4.11. Future change in the fractional number of hourly events in different intensity bins in winter. Maps of the future change in the ensemble-mean fractional number of events in 4 intensity bins (0.0-0.005, 0.005-10.0, 10-50 and >50 mm/day) in winter in (left) RCM-PPE and (right) CPM-12. Future changes correspond to the difference between the future (2061-80) minus present-day (1981-2000). The hourly intensity has been multiplied by 24 to give units of mm/day.
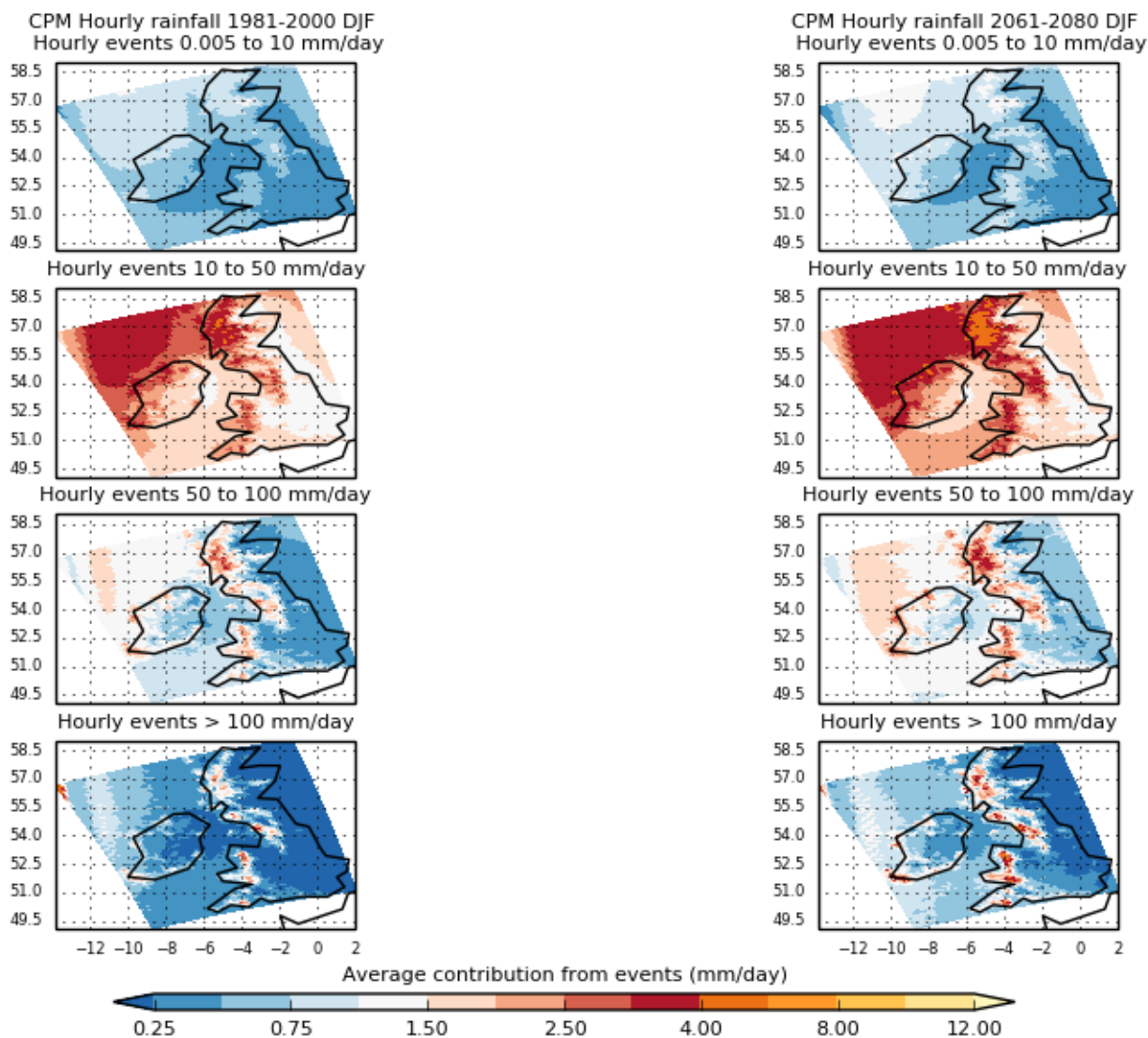
Figure 4.4.12. Contribution of hourly events in different intensity bins to total winter precipitation in CPM-12. As Fig 4.4.9, but showing the contribution from events from 4 different intensity bins (0.005-10.0, 10-50, 50-100 and >100 mm/day). The <0.005 mm/day bin is not shown. Contribution (mm/day) is given by the average bin intensity multiplied by the fractional number of events in each bin.
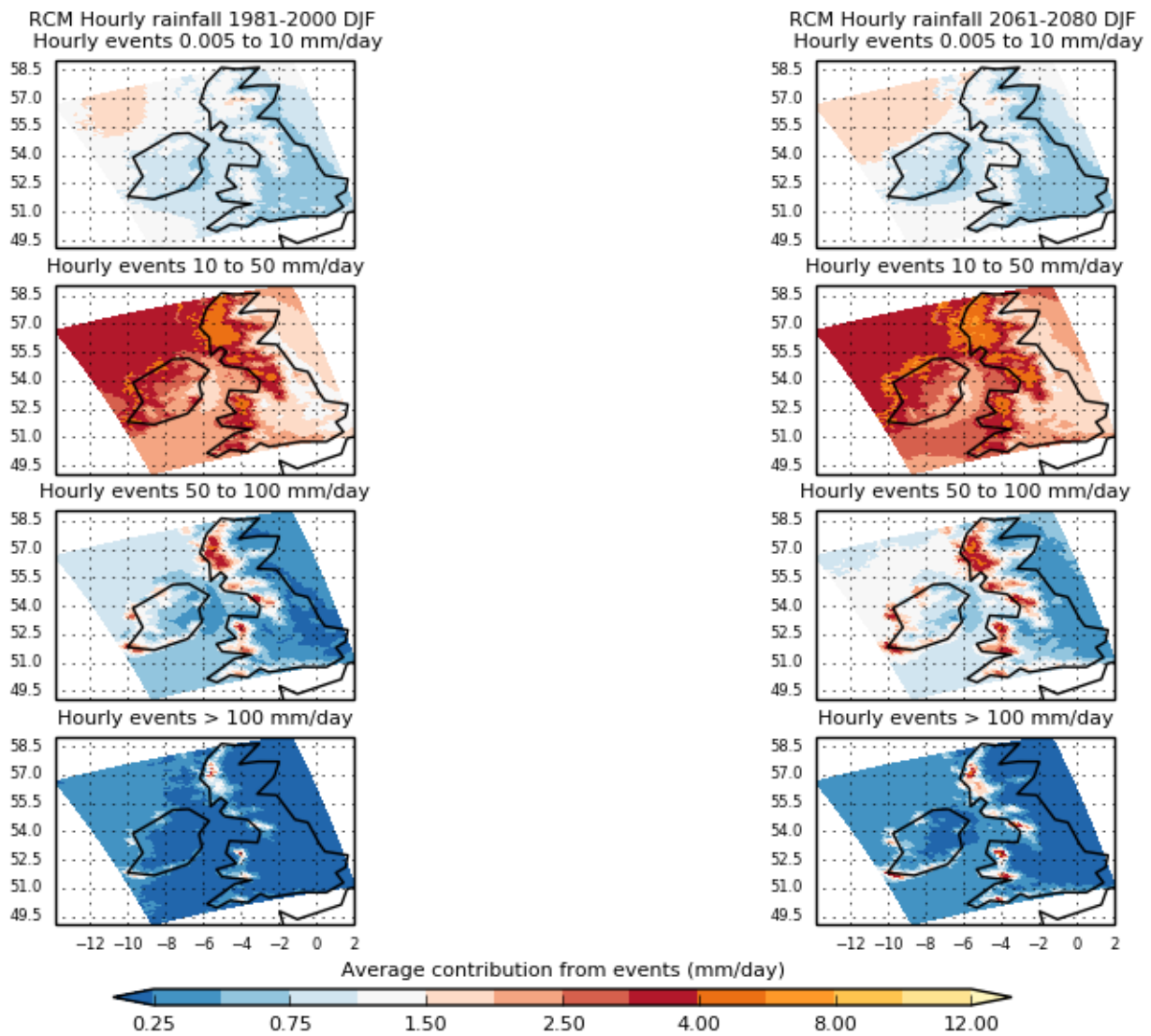
Figure 4.4.13. Contribution of hourly events in different intensity bins to total winter precipitation in RCM-PPE. As Fig 4.4.12, but for RCM-PPE.
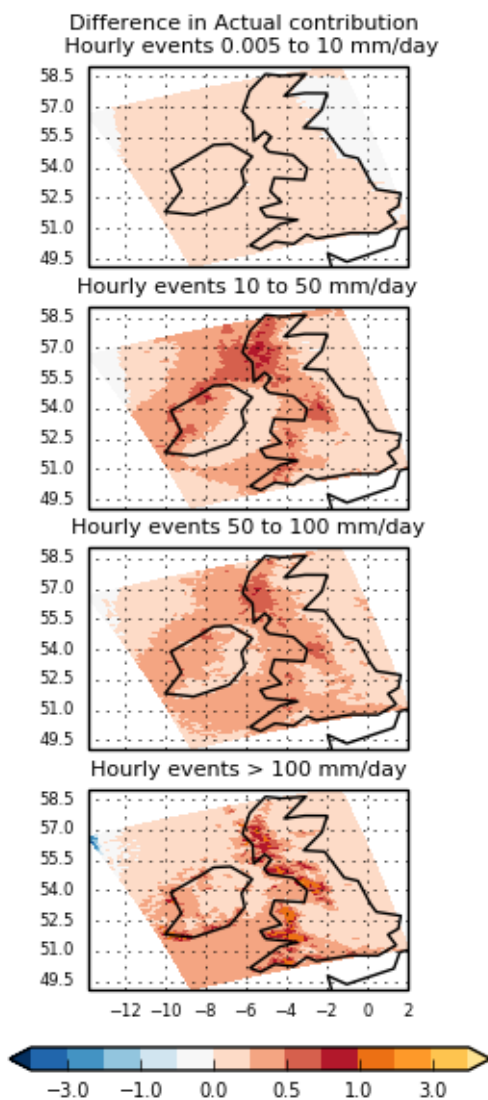
Figure 4.4.14. Future change in the contribution of hourly events in different intensity bins to total winter precipitation in CPM-12. Maps of the future change in the CPM-12 ensemble-mean actual contribution from hourly events in 4 intensity bins (0.005-10.0, 10-50, 50-100 and >100 mm/day) in winter. Actual contribution (mm/day) is given by the average bin intensity multiplied by the fractional number of events in each bin. Future changes correspond to the difference between the future (2061-80) minus present-day (1981-2000). The hourly intensity has been multiplied by 24 to give units of mm/day.
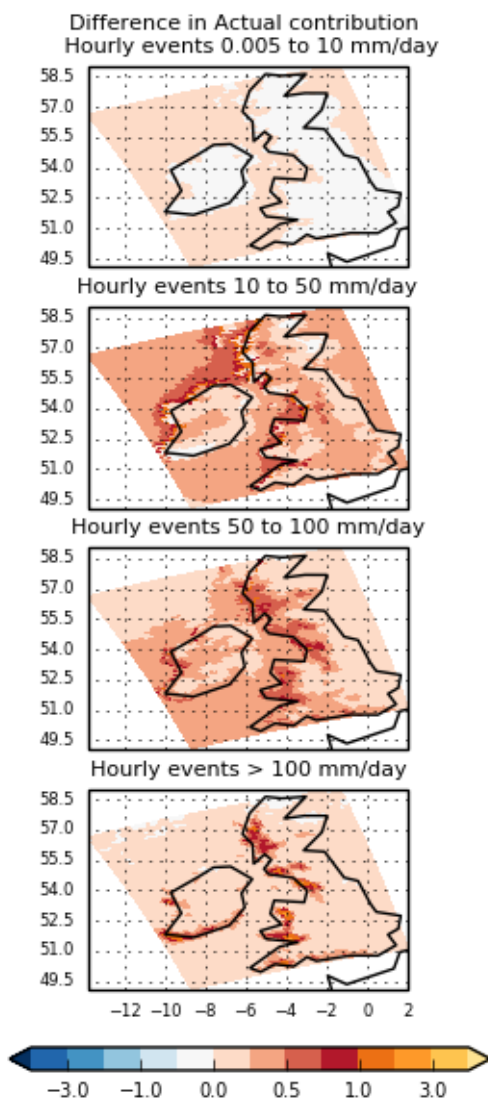
Figure 4.4.15. Future change in the contribution of hourly events in different intensity bins to total winter precipitation in RCM-PPE. As Fig 4.4.14 but for RCM-PPE.

We look now at future changes in the precipitation-amount and duration distribution of events across Great Britain. In summer, both CPM-12 and RCM-PPE show a shift to a relatively greater contribution from short-duration higher-intensity events (Fig 4.4.16). This shift is however more pronounced in the CPM, with a significantly greater increase in the fractional contribution from short-duration intense events in the CPM than RCM. Interestingly Fig 4.4.16 also shows evidence of a greater fractional increase in longer duration events of moderate mean intensity in the CPM than RCM in summer, potentially indicating that there is more organised convection or slower-moving convection. In winter, both models show a future intensification of events, with the shift to higher-intensity events similar in the CPM and RCM. Differences in CPM-RCM responses are instead more significant for longer duration moderate intensity events, with a greater increase in these events in the CPM.

It should be noted that present-day biases in the CPM in Fig 3.4.7 are similar in sign and magnitude to future changes in Fig 4.4.16. Further work is needed to assess the importance of the known tendency of the CPM to overestimate the intensity of heavy events for future projections, and in particular whether it would lead

to smaller or larger increases in summer rainfall intensity. Nevertheless, the improved representation of convective processes in the CPM means it is able to provide plausible projections of changes in hourly rainfall characteristics, unlike the RCM (which shows greater biases in Fig 3.4.7).
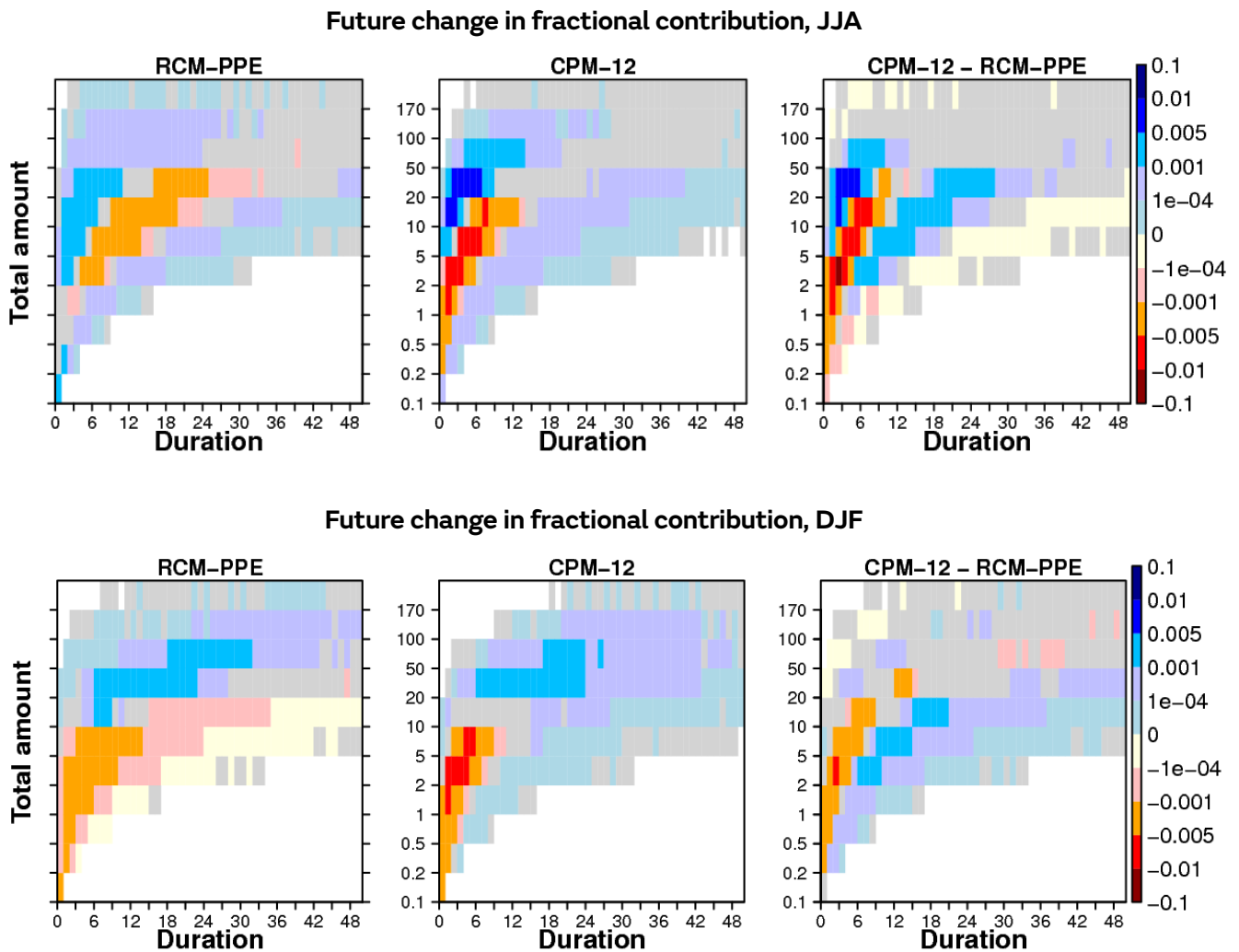

Figure 4.4.16. Future change in the precipitation amount and duration of rainfall events. Plotted is the ensemble mean future change (2061-80 minus 1981-2000) in the fractional contribution of each amount-duration bin in the (left) RCM-PPE, (centre) CPM-12 and (right) the CPM-RCM difference, for (top) summer and (bottom) winter. Amount is the total precipitation accumulated over the event, where events are continuous periods of precipitation exceeding 0.1mm/h. Fractional contribution is given by (joint probability of a given amount-duration bin) x (mean bin precipitation amount) / (total precipitation over all bins), pooling all grid cells over Great Britain. Future changes or differences that are not significant at the 1% level are masked in grey. Significance is tested using a 1000 member bootstrap applied to each ensemble member (by choosing 20 years at random with replacement from the 20-year time series, done identically for the present and future periods) to give 1000 estimates of the future change for each ensemble member; the ensemble mean is then found for each bootstrap sample to give 1000 estimates of the ensemble mean future change; the ensemble mean future change is significant if the 0.5-99.5[th] confidence interval does not overlap zero.

Scaling of hourly precipitation changes

In this section we examine how future increases in hourly precipitation intensity relate to increased atmospheric moisture with warming, across the CPM-12 and RCM-PPE ensembles. The amount of moisture the atmosphere can hold increases with temperature at 6-7%/K, following the Clausius-Clapeyron (CC) relation. However changes in moisture availability may be much less than this temperature dependent maximum, and so here we consider changes in near-surface dew point temperature, which is a measure of specific humidity translated to temperature using the CC relationship (Chan et al, 2016). Results looking at the scaling between changes in the 99th percentile of wet values of daily maximum hourly precipitation and changes in mean dew point temperature, across UK grid points, for the different ensemble members, are shown in Figs. 4.4.17-4.4.18.

In summer, we find that increases in extreme hourly precipitation intensity are on average higher than CC scaling in the CPM (ensemble mean UK-average scaling of 7.8 %/K) but lower than CC-scaling in the RCM (5.2%/K, Fig 4.4.17). Higher scaling rates in a CPM have been found previously over the UK (Kendon et al, 2014) and elsewhere (Kendon et al, 2019), and are consistent with the hypothesis that local dynamical feedbacks within storms, captured by convection-permitting (but not conventional convection-parameterised) models, amplify increases in rainfall extremes on hourly timescales (Lenderink and van Meijgaard, 2008). In winter, increases in hourly precipitation intensity approximately follow CC scaling, with similar scaling rates in the CPM and RCM (Fig 4.4.18). This is consistent with increasing atmospheric moisture with warming (which is captured by both models) being the dominant factor controlling increases in extreme precipitation in winter.

There is a large range of UK-average scaling values across the CPM ensemble in summer (of 5.4-9.3 %/K). This suggests that differences in extreme precipitation changes between members are not just explained by differences in changes in temperature or moisture availability (with the range of UK-average dew point temperature changes being 2.5-4.0K). Some members have different precipitation responses for a given change in moisture availability. We note that the range of scaling values across the CPM ensemble is smaller in winter (4.9-8.1%/K).
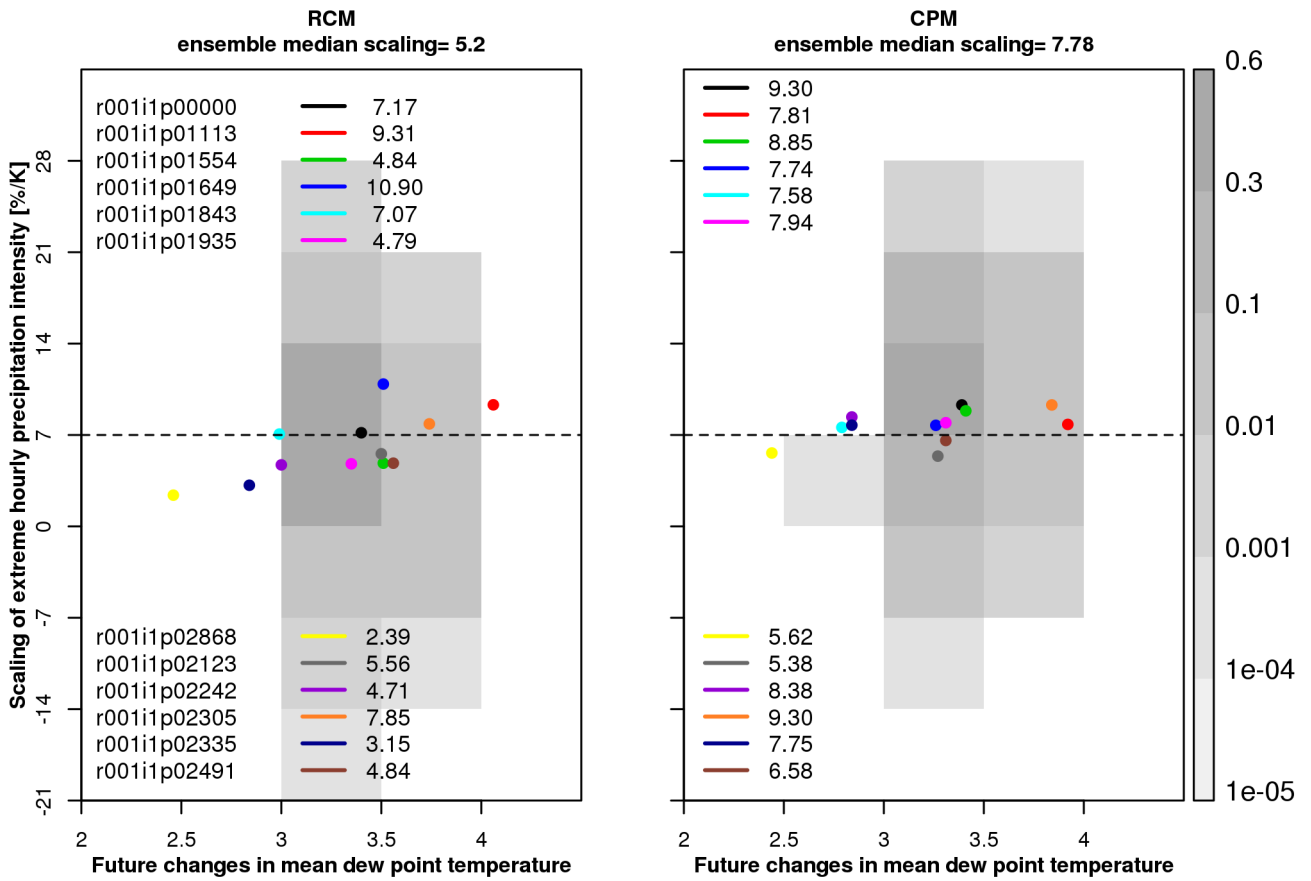
Figure 4.4.17. Scaling between future changes in extreme hourly precipitation intensity and dew point temperature, in summer. Grey shading shows the joint probability distribution of the scaling coefficient (%/K) versus change in mean dew point temperature, for summer, across UK grid boxes, for the standard member of (left) RCM-PPE and (right) CPM-12. The scaling coefficient (%/K) is given by the change in the logarithm of extreme precipitation intensity divided by the change in mean dew point temperature. The circles show the UK-average scaling relationship plotted against the UK-average dew point temperature change, across the ensemble. The UK-average scaling relationship (in %/K) is also quoted for each member in the legend. The dashed black line shows the Clausius-Clapeyron scaling relationship of 7%/K. Extreme precipitation intensity is defined as the 99th percentile of wet values (>0.1mm/h) for daily maximum hourly precipitation.
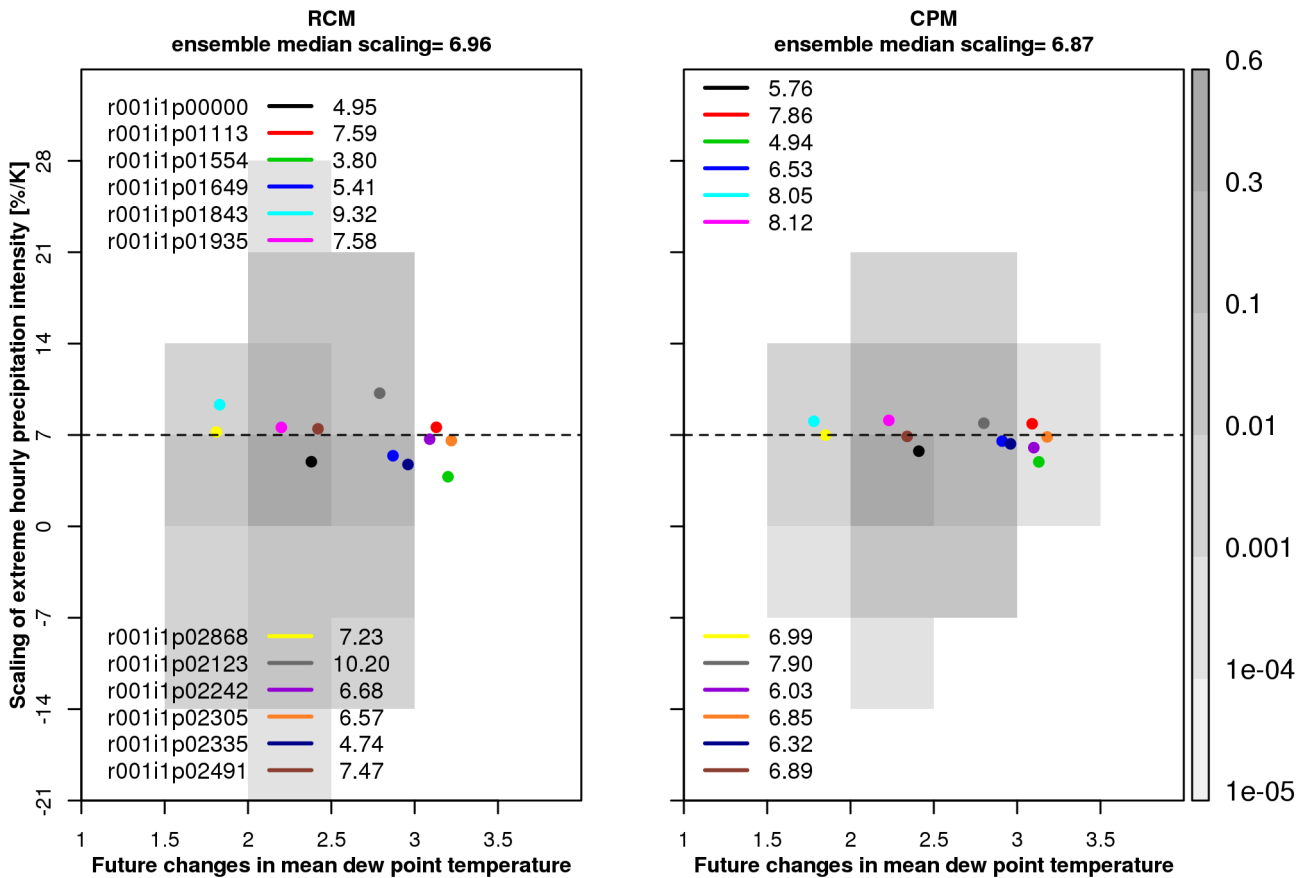
Figure 4.4.18. Scaling between future changes in extreme hourly precipitation intensity and dew point temperature, in winter. As Fig 4.4.17, but for winter.

4.5 Changes in high impact events

Extreme hourly precipitation

Both CPM-12 and RCM-PPE show future increases in the 2 year return level of annual precipitation extremes, with UK-averaged central estimates of 25% and 31% increase respectively (Fig. 4.5.1). Increases in hourly extremes are projected in all seasons and for all regions, except for the S-UK in summer where some members show a decrease in the 2-yr return level (Figs. 4.5.2-4.5.4). Changes in the 2-year return level reflect changes in both the intensity and frequency of precipitation, and decreases for the S-UK in summer are due to large decreases in rainfall occurrence (Fig. 4.4.4), which in this case override increases in rainfall intensity. Changes here are consistent with results reported previously for a 1.5km simulation over the southern UK, using an older version of the Unified Model. In particular, for the 10 year return level of annual extremes the future increase (under RCP8.5) was 33% for SUK for 2080s in the 1.5km model (Dale et al, 2018) compared to 27% for UK for 2060-80 in CPM-12 (central estimate).

CPM-12 gives a similar central-estimate of the projected change in the 2-year return level of annual extremes to RCM-PPE (Fig 4.5.1). However, CPM-12 consistently shows a smaller ensemble spread. The high-end estimate of the change is considerably higher in RCM-PPE (70% compared to 47% increase for annual extremes), but we would have low confidence in this high-end change in the RCM as it likely reflects unphysical grid point storms.

The RCM-PPE also shows a future strengthening in the rate at which return level increases with return period. This occurs in all seasons and regions, and most notably in the S-UK in autumn and winter. This behaviour is much less apparent in the CPM-12, so although the changes for the 2-year return level may be comparable between RCM-PPE and CPM-12, changes for rarer extremes are typically larger in the RCM-PPE particularly in autumn and winter. In particular, increases in high return period events in autumn and winter can be almost a factor of 2 larger in the RCM than CPM for some members (Fig 4.5.2). Ensemble spread is seen to be much smaller than uncertainty in future changes due to uncertainty in the GPD fit, suggesting that differences between ensemble members largely reflect uncertainty in the sampling of extremes. Moving to higher return periods, ensemble spread is seen to increase especially for the RCM-PPE (Figs. 4.5.2-4.5.4). We have low confidence in these results from the RCM-PPE for rare extremes, which are likely due in some cases to unphysical grid point storms (Section 3.5). The maximum value in the RCM-PPE in future in autumn (summer) is 150 mm/h (128 mm/h) compared to a maximum value in the CPM-12 of 74 mm/h (87 mm/h) for precipitation averaged over a 12km grid box. These high values in excess of 100mm/h, at the 12km scale, in the RCM are physically implausible (see Section 3.5).

It is interesting to note the changing seasonality of hourly extremes, with greater increases in SON leading to SON becoming the season with the greatest occurrence of high threshold exceedances (as opposed to JJA for the present-day, Fig 4.5.5). This changing seasonality is evident in both CPM-12 and RCM-PPE, but is especially apparent in RCM-PPE. In RCM-PPE, SON becomes predominantly the season of hourly precipitation extremes in future; whereas in CPM-12, JJA and SON are similarly important. The changing seasonality of extremes may be explained by warming leading to an increase in convective activity in the autumn, and thus effectively an extension of the convective season. Hourly extremes are projected to increase in both seasons with increasing atmospheric moisture. However, the increases are larger in autumn than summer mainly due to the greater increases in moisture availability in autumn (UK-average ensemble-mean dew point temperature increase of 3.7K in SON compared to 3.2K in JJA). However, we do also find higher scaling of extreme precipitation increases with increased moisture in autumn (CPM-12 ensemble-mean UK-average scaling of 8.2%/K in SON compared to 7.8%/K in JJA, Section 4.4), which may be explained by differences in the atmospheric stability or nature of storms, compared to summer.
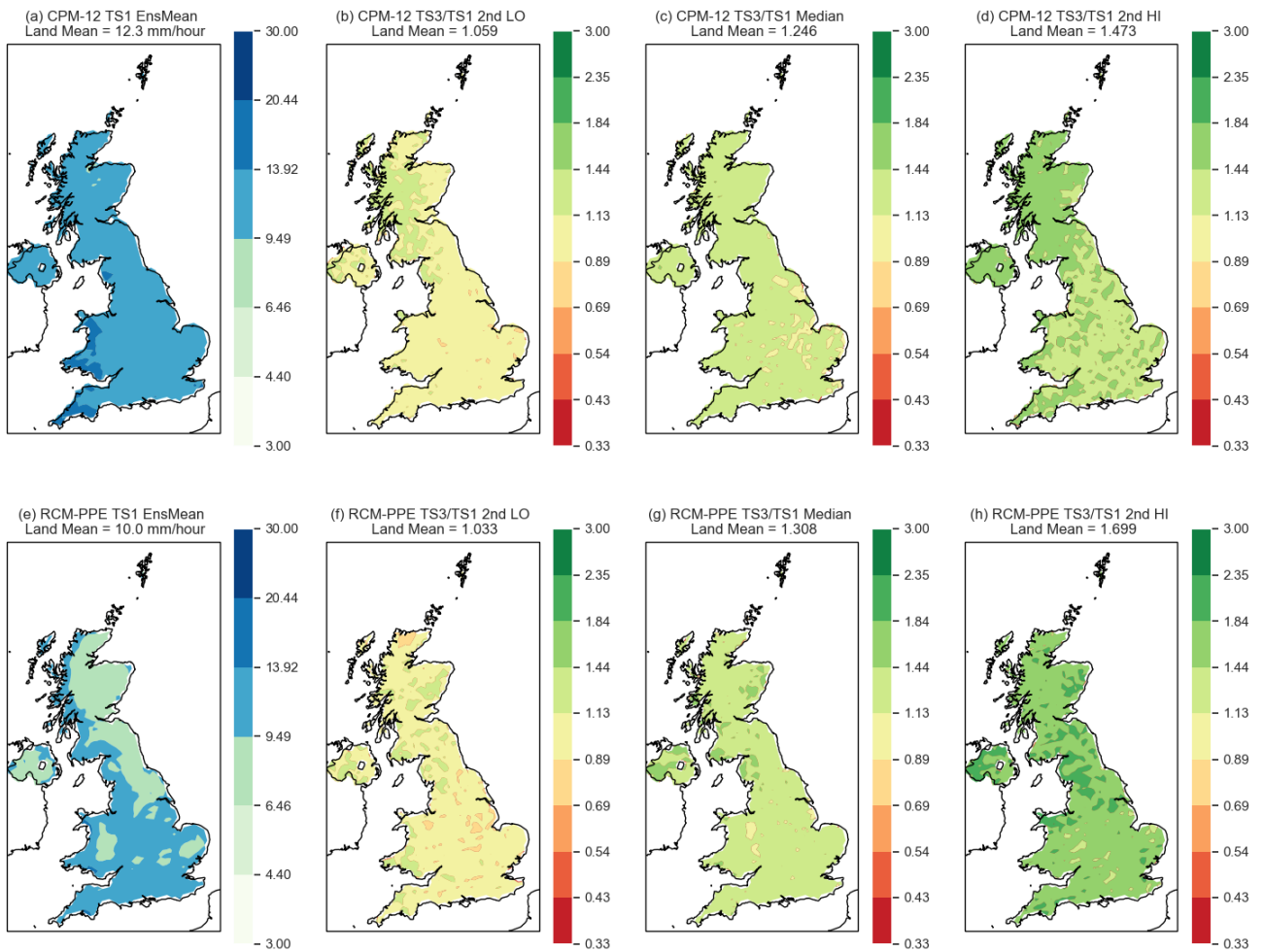
Figure 4.5.1. Future change in 2 year return level of daily maximum hourly precipitation. Shown are (a,e) ensemble-mean estimates of present-day return level (mm/h) for TS1 (Time slice 1, 1981-2000) and the ratio of future (TS3, 2061-80, RCP8.5) to present-day return levels for (b,f) 2nd lowest member locally, (c,g) central estimate and (d,h) 2nd highest member locally, for CPM-12 and RCM-PPE. This is for hourly precipitation data from all seasons, regridded to a common 12km grid before calculation of return levels.

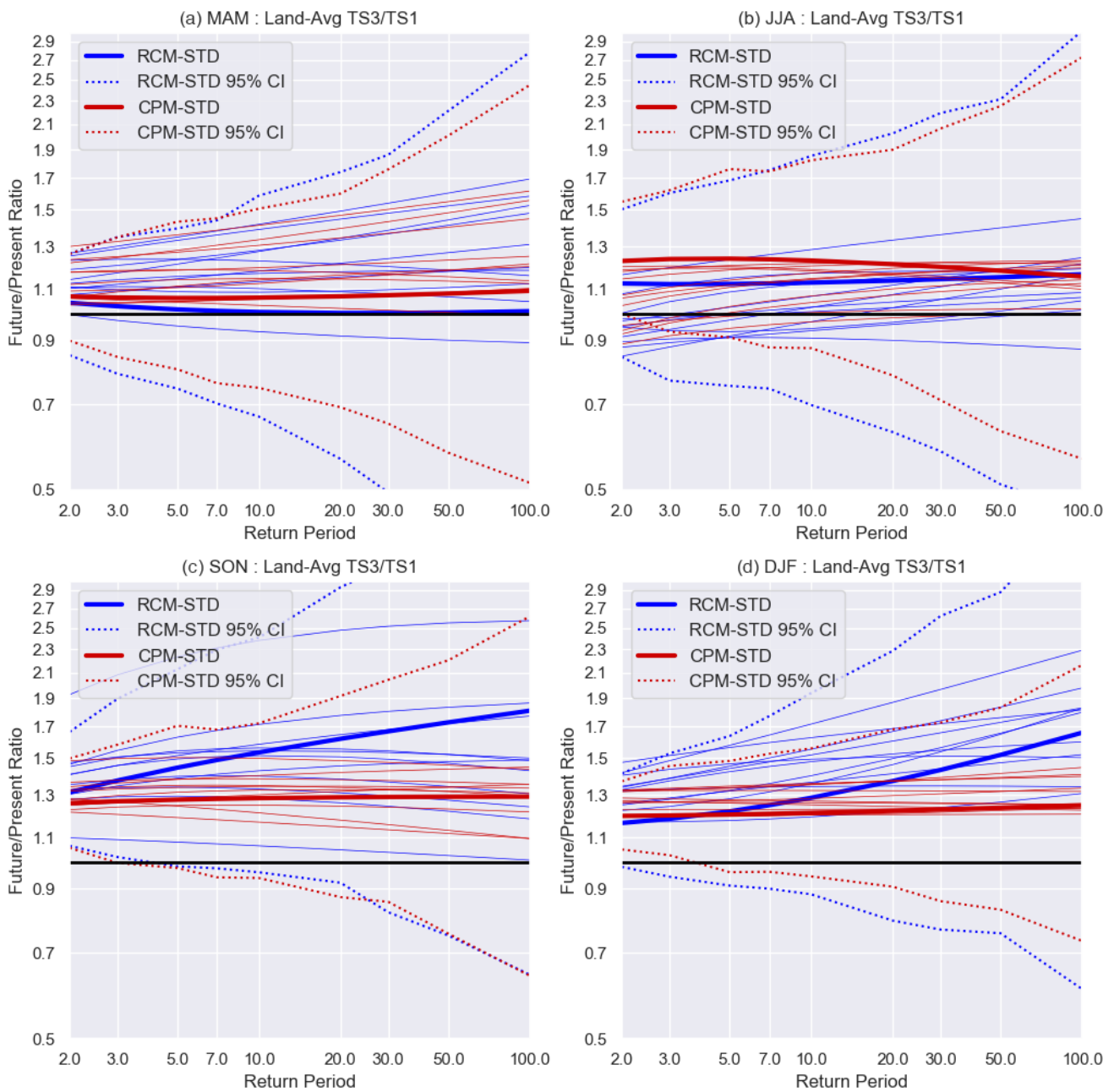**Figure 4.5.2.** Future change in South UK return levels of daily maximum hourly precipitation as a function of return period, for individual seasons. Shown is the ratio of the return level for Time Slice 3 (TS3, 2061-2080) under RCP8.5 to that for the baseline period (TS1, 1981-2000) for the twelve CPM-12 and RCM-PPE ensemble members. The South UK average return levels have been calculated using the regional frequency analysis method. The future changes for the standard member CPM-STD and RCM-STD are shown in bold, and the 95% confidence intervals for these changes due to uncertainty in the GPD fit are shown as dotted. Uncertainty in the GPD fit for each of the present and future periods is calculated by generating random data from the original fit, refitting the GPD, and recomputing the return levels 1000 times. These are then used to give 1000 estimates of the future change.

Figure 4.5.3. Future change in North West UK return levels of daily maximum hourly precipitation as a function of return period, for individual seasons. As Fig 4.5.2 but for NW region.

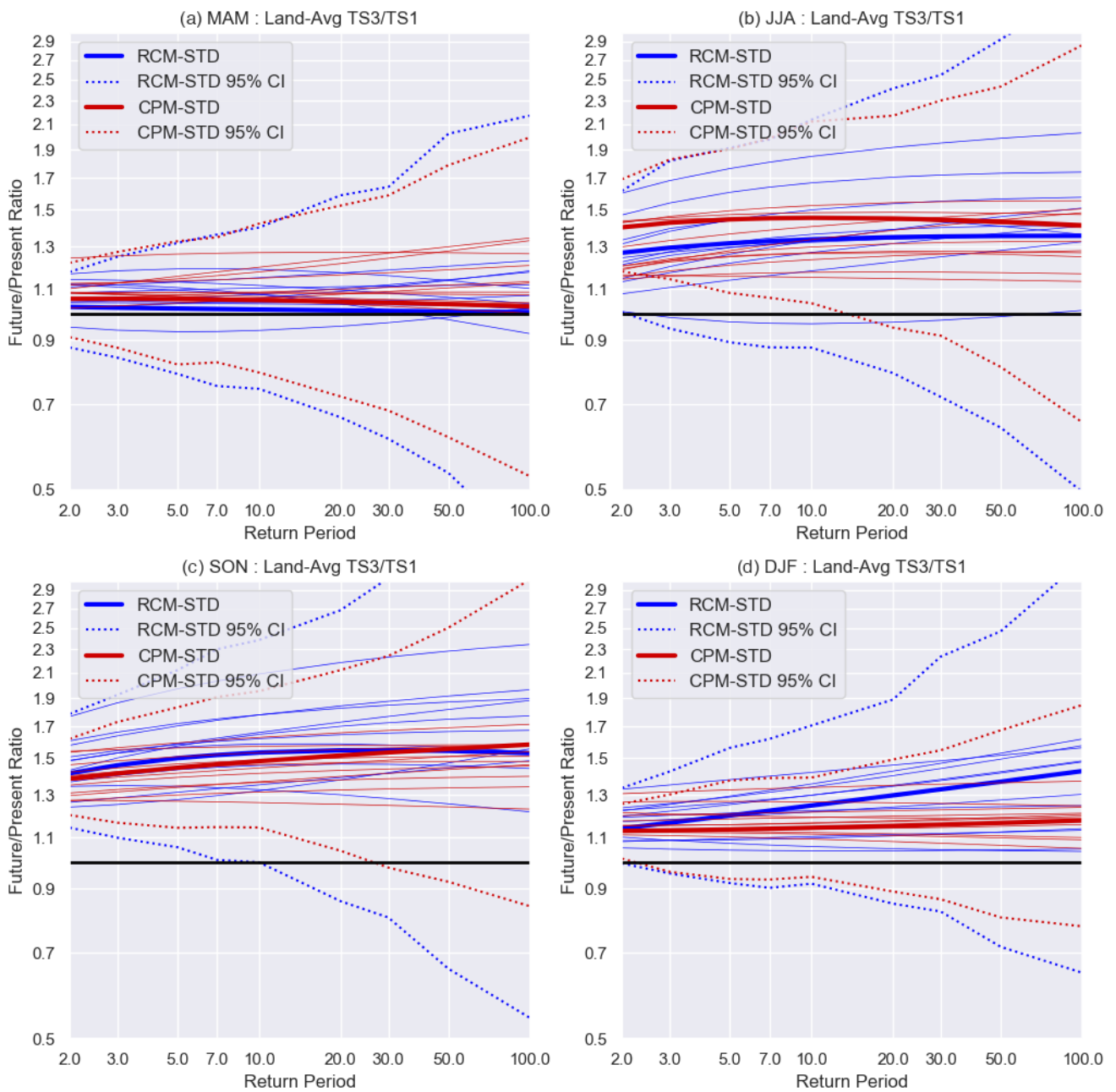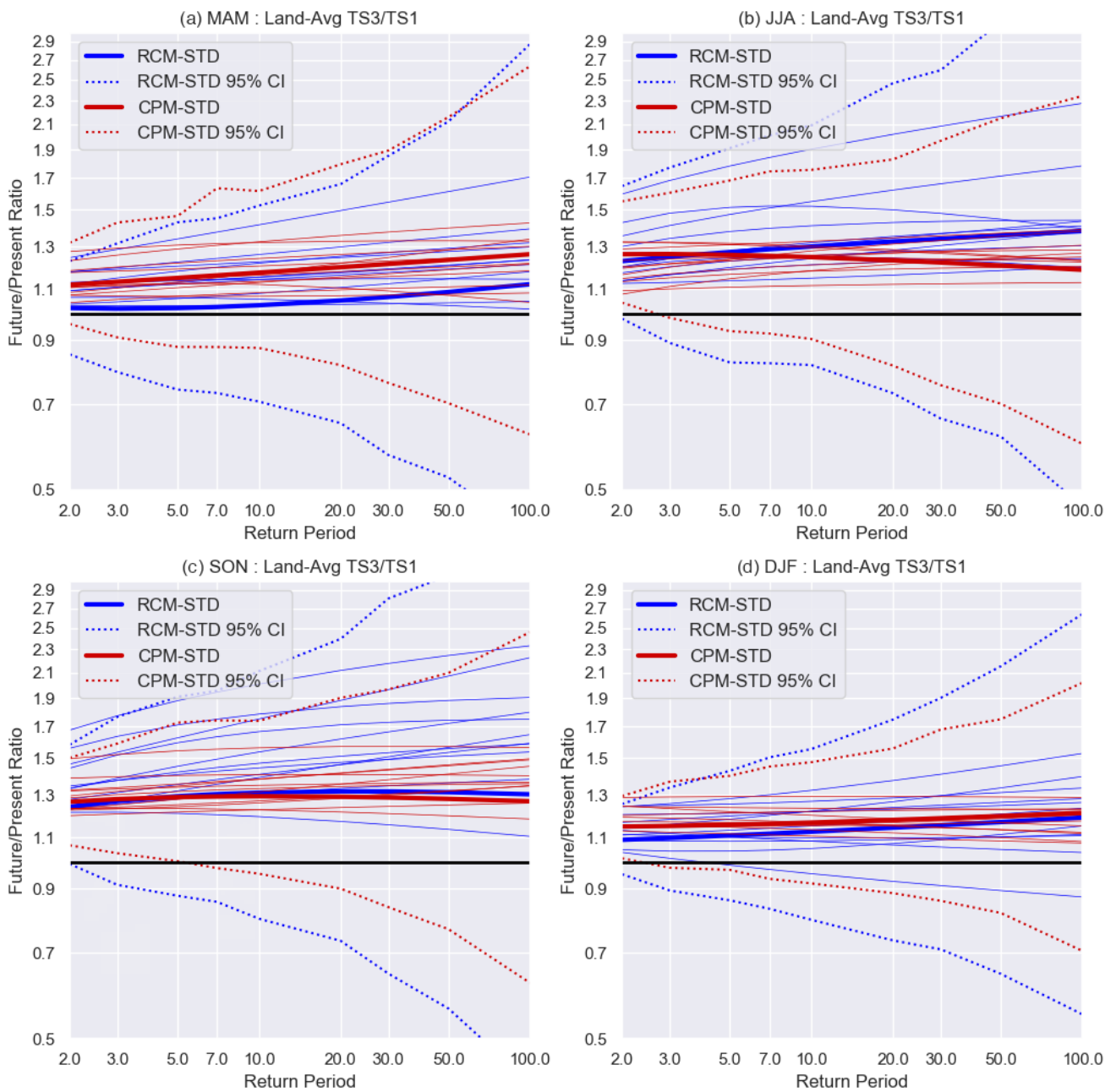**Figure 4.5.4.** Future change in North East UK return levels of daily maximum hourly precipitation as a function of return period, for individual seasons. As Fig 4.5.2 but for NE region.

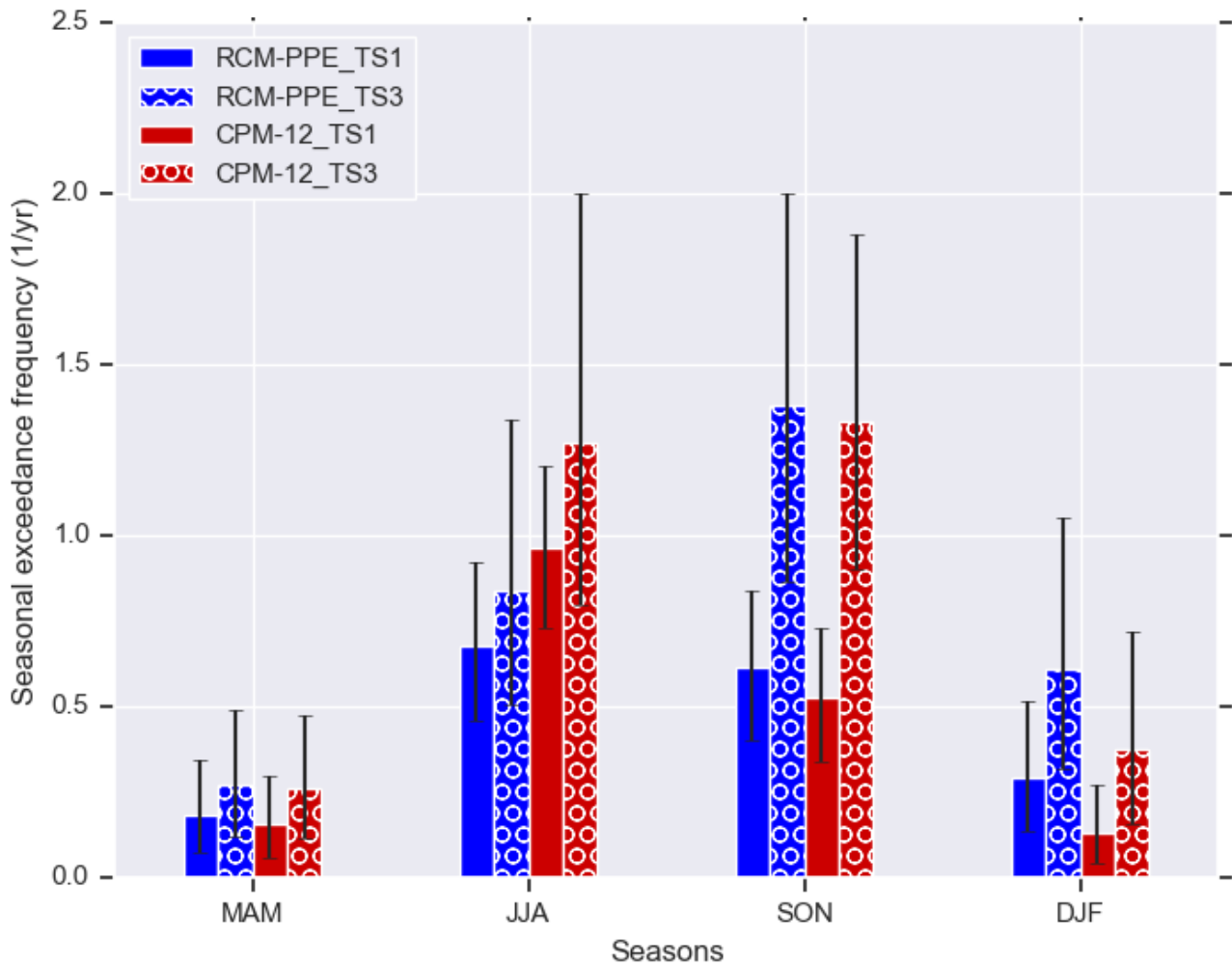## TS1 annual daily-1h-max P99.5 seasonal exceedance frequencies

Figure 4.5.5. Future change in seasonality of hourly precipitation extremes. Seasonal occurrence of annual threshold exceedances, across the UK, in the baseline (TS1) and future (TS3) periods, for CPM-12 and RCM-PPE. The annual threshold corresponds to the 99.5th percentile of all daily-maximum hourly values in the baseline simulation, calculated at each grid box. The bars correspond to the UK-average of the central estimate across the ensemble, whilst the black lines indicate the 2nd lowest to the 2nd highest estimate.

Hot and cold spells

In this section we consider changes in cold spells over the northern UK and hot spells over the southern UK, corresponding to the regions being most strongly affected by the relevant events in the present-day (Section 3.5). Both CPM-12 and RCM-PPE show a decrease in the frequency of cold spells over the northern UK, as expected in a warming climate (Fig. 4.5.6). The decrease in intense cold spells (-2ºC threshold) is significantly smaller in the CPM than the RCM (although larger in relative terms, there being fewer cold spells in the CPM). The smaller decrease in intense cold spells is consistent with the CPM showing less of an increase in temperature in this region in winter.

Both models show an increase in the frequency of hot spells over the southern UK (Fig. 4.5.7). The increase is slightly (but not significantly) larger in the CPM than RCM in absolute terms and very similar in relative terms (there are more hot spells in the CPM in the present-day, Section 3.5). Future increases in hot spells will be driven by large-scale warming (seen by both models), but will also be influenced by other, regionally-specific factors, such as changes in circulation or changes in soil moisture, including the extent to which soil moisture falls below the critical threshold for limiting evaporation (see below).

tas NUK Cold Spells - Future Changes
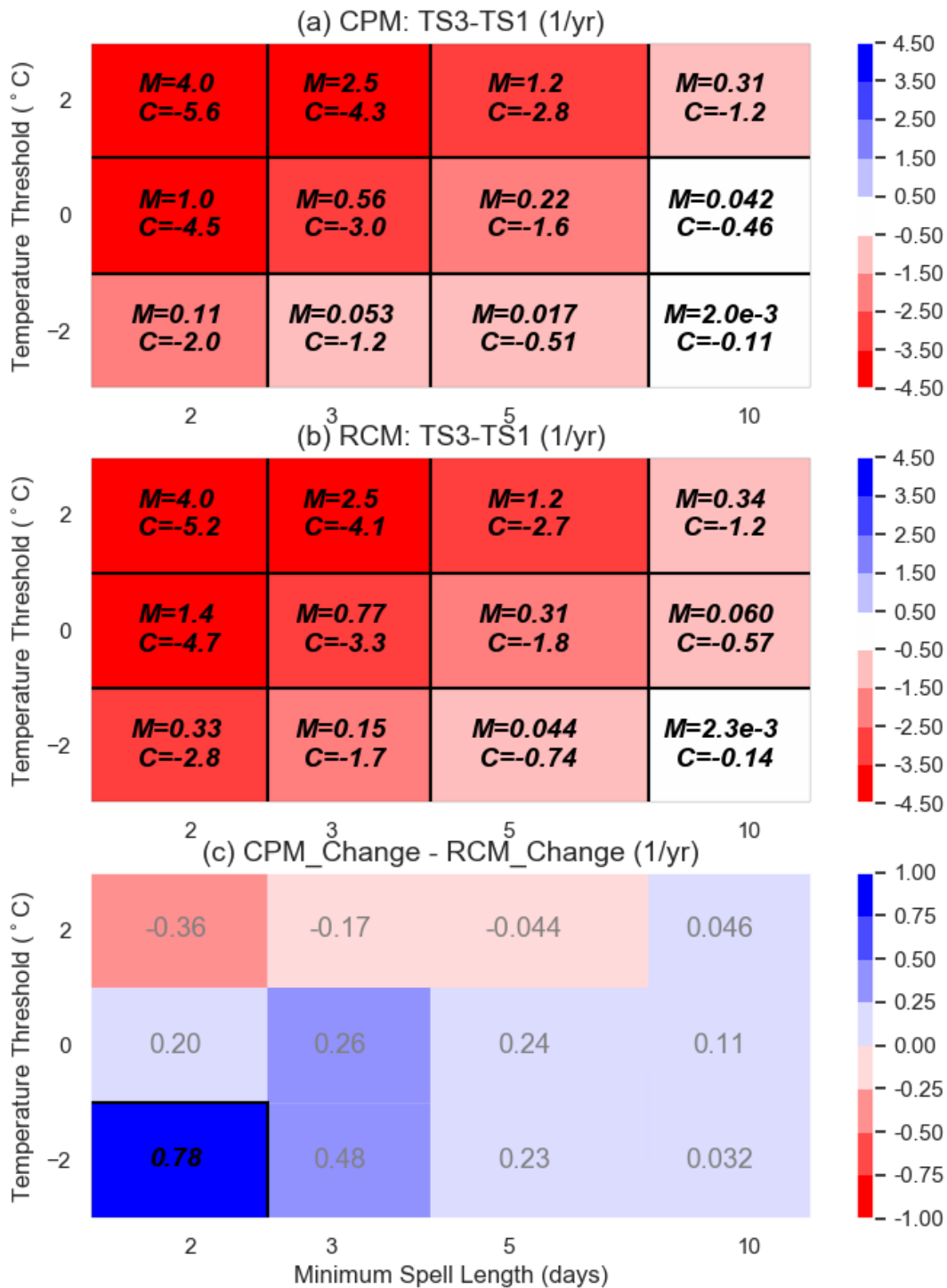
Figure 4.5.6. Future changes in the frequency of cold spells over the northern UK. Ensemble mean future changes in the frequency of cold spells over the northern UK for the (a) CPM-12 and (b) RCM-PPE; and (c) the CPM minus RCM difference in the future changes. TS1 refers to Time Slice 1 (1981-2000) and TS3 refers to Time Slice 3 (2061-2080) of the model simulations. Results are shown for cold spells defined using a range of daily mean surface temperature thresholds (-2°C, 0°C and +2°C) and minimum spell lengths (2, 3, 5, and 10 days). The northern UK region is as defined in Fig 3.5.9. The mean frequency (M) in the model for the future is quoted, along with future change (C). Differences that are significant compared to variability across the ensemble at the 5% level are indicated with a black border and bold black italic text.

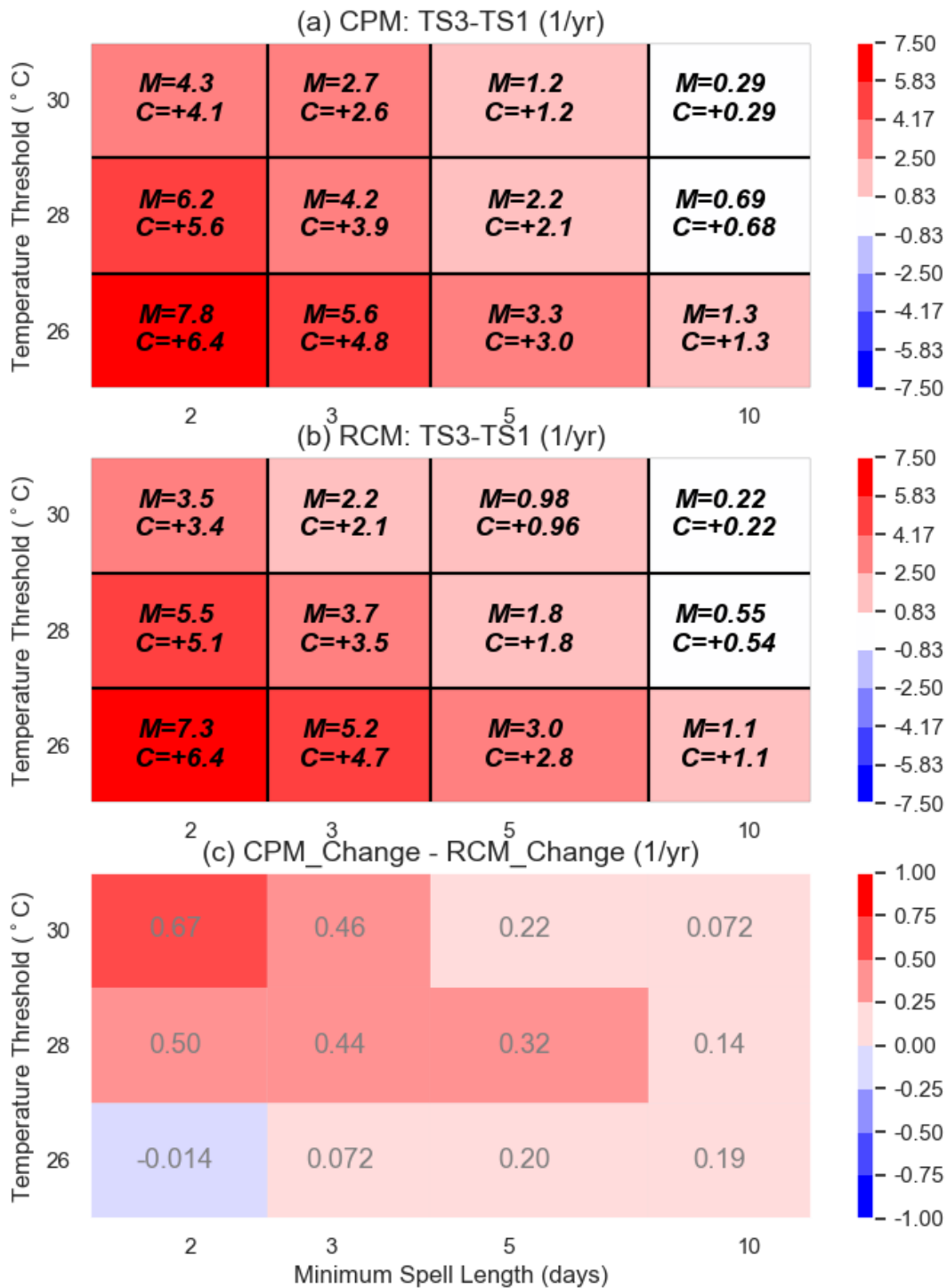**Figure 4.5.7.** Future changes in the frequency of hot spells over the southern UK. As Fig. 4.5.6 but for hot spells over the southern UK defined using a range of daily maximum surface temperature thresholds (26ºC, 28ºC and 30ºC) and minimum spell lengths (2, 3, 5, and 10 days). The southern UK region is as defined in Fig 3.5.9.

Soil moisture stress

In future, there is a decrease in soil moisture during summer (Fig 4.5.8), consistent with the reduction in summer mean precipitation. In RCM-PPE, this results in the majority of members moving into a regime of evapotranspiration being soil-moisture limited over the southern-UK in summer, whilst soil moisture remains above the critical point over the northern-UK. In CPM-12, evapotranspiration becomes soil moisture limited in all members in the future over the northern-UK, as is already the case in the present-climate over the southern-UK (Section 3.5).

The frequency of hot spells is expected to be primarily controlled by large-scale warming and the occurrence of favourable synoptic conditions (large-scale circulation patterns), which are expected to be similarly captured by both the CPM and RCM. Nevertheless, local soil moisture conditions may exacerbate or otherwise the severity of hot spells. In particular, future drying of the soils may lead to more severe hot spells, but only where soil moisture is not already below the critical threshold in the present-day. In the future, there is a greater decrease in precipitation occurrence in the CPM than RCM in summer, however since CPM-12 members are already in the regime of evapotranspiration being soil-moisture limited over the southern-UK in summer, future decreases in soil moisture will have relatively less impact here. This may explain why future increases in hot spells over the southern UK are similar in the CPM and RCM (see above).

Maps (Fig 4.5.9) show the soil moisture stress factor (β) during September, which is the driest point in the annual cycle. This shows the degree to which evapotranspiration is limited by soil-moisture, where β=1 indicates no restriction, β=0 that no root-zone moisture is available to sustain plants, and intermediate values indicate varying levels of water stress. Over Scotland there is no significant water stress in RCM-PPE, with little change in the future. The highest water stress occurs in the south-east, with greater stress in CPM-12 than RCM-PPE. In CPM-12, β is less than 0.3 over much of south-east England, indicating a high degree of moisture restriction during the present-climate. In future, these differences between the models persist. Both models show a similar future decrease in β (increasing water stress) of 20% or more over the southern UK, but with the model differences dominating over the climate change signal. In the CPM, locally large percentage decreases occur where near-zero stress factors are seen in the present-day.
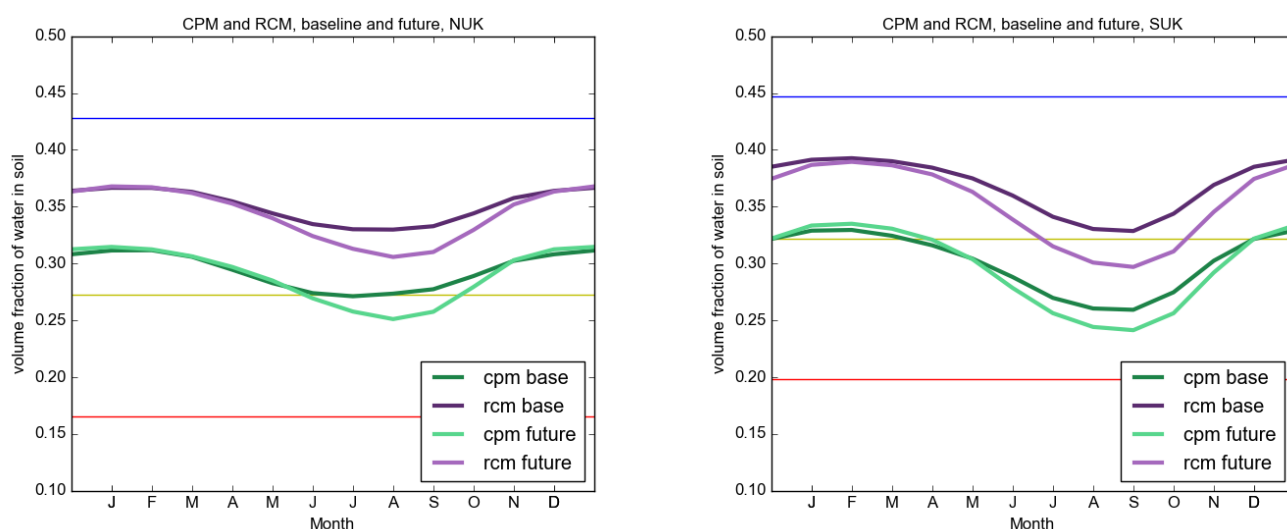
Figure 4.5.8. Future change in the annual cycle of soil moisture in the top 1m of soil. Ensemble-mean volume fraction of water in the soil (m³/m³) in the base (1981-2000) and future (2061-80) periods, in the (green) CPM-12 and (purple) RCM-PPE, for the (left) northern-UK and (right) southern-UK. The blue line indicates soil moisture saturation; yellow line the critical point below which evapotranspiration becomes soil-moisture limited; and red line the wilting point.
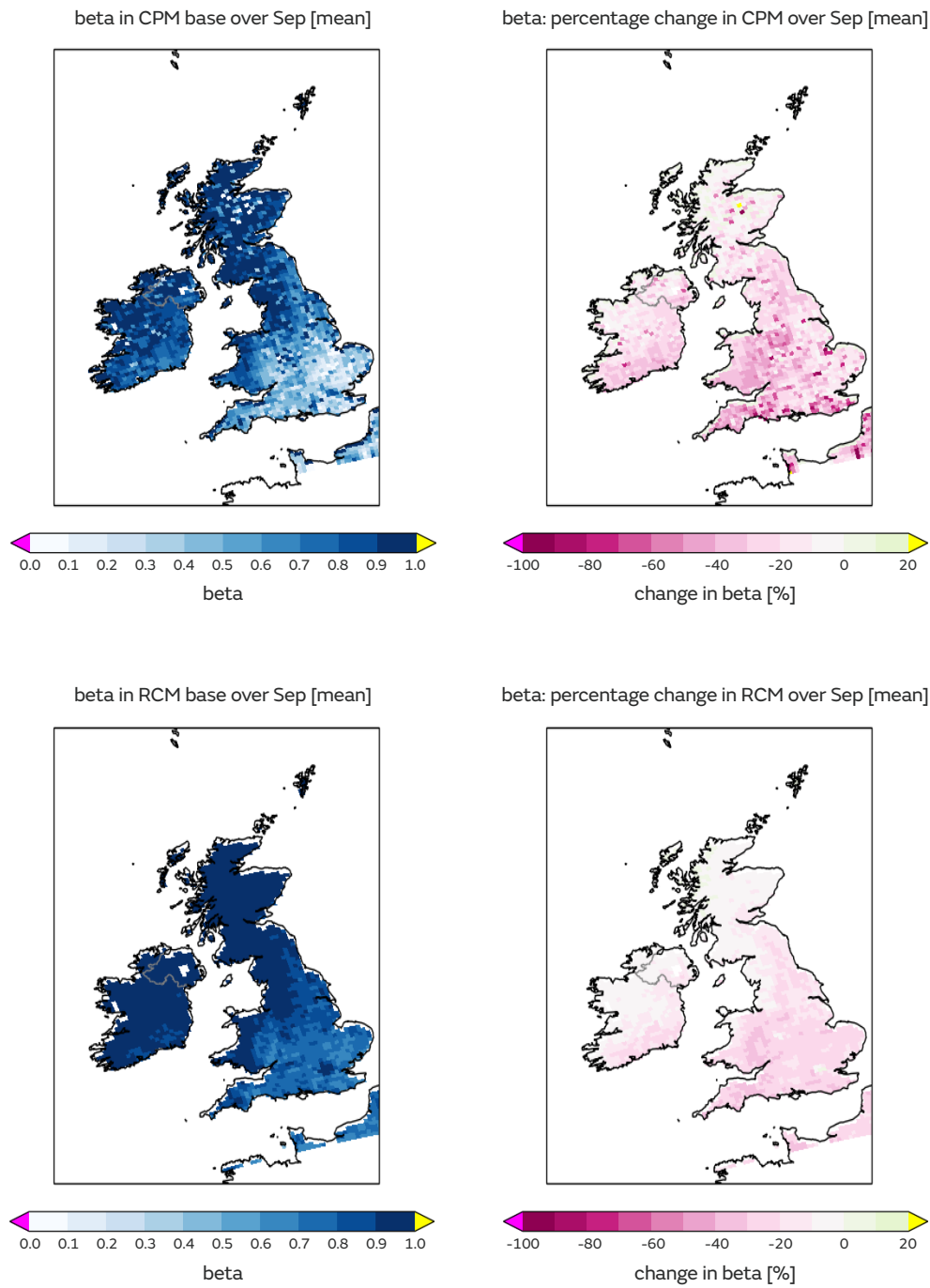
Figure 4.5.9. Future change in the soil moisture stress factor (β) in the top 1m of the soil. Shown is (left) the ensemble-mean stress factor during September in the baseline (1981-2000), and (right) the future percentage change (2061-80 minus 1981-2000, in %), for (top) CPM-12 and (bottom) RCM-PPE. β=1 indicates soil moisture at or above a critical value at which no restriction is placed on transpiration from vegetated surfaces; β<1 indicates limitations in moisture availability that result in reductions in evaporation from both vegetated and bare soil surfaces; β=0 indicates root-zone soil moisture at or below a wilting point at which there is no water available to sustain plants.

Snow

Both CPM-12 and RCM-PPE show a decrease in falling snow in future winters, but this decrease is less in the CPM (Fig 4.5.10). This is consistent with there being a greater increase in precipitation and less of an increase in temperature over Scotland in winter in the CPM. The fact that snowfall includes graupel in the CPM, but not the RCM, may also contribute to the difference.

Both models show a future decrease in lying snow of almost 100% over lowland areas, but smaller decreases over mountains (where some lying snow remains in future, Fig 4.5.11). The decreases are larger in the RCM over the Scottish mountains, and this may explain the greater increase in temperature over Scotland in winter in the RCM (Section 4.2) due to albedo feedback.

Figure 4.5.10. Future change in mean snow fall in winter. Ensemble-averaged future percentage change (%) in winter mean snowfall flux in (left) RCM-PPE, (centre) CPM-12 and (right) the difference. The future change is the difference between 2061-80 and 1981-2000 periods.
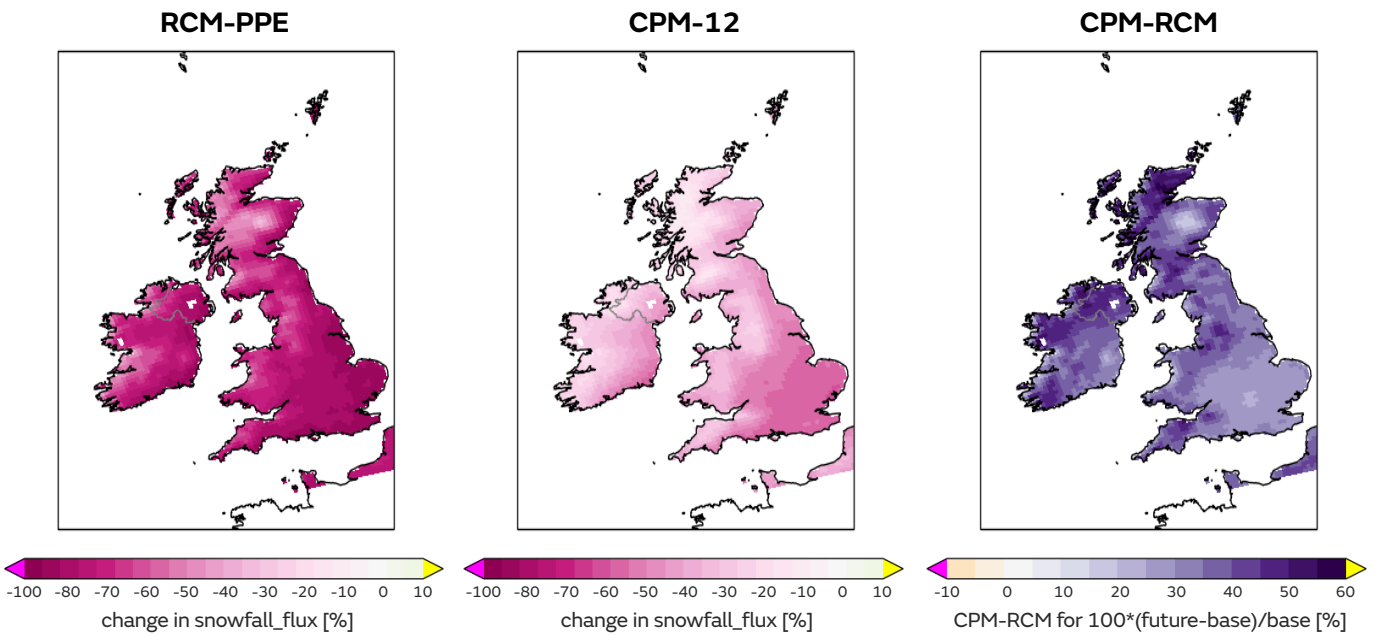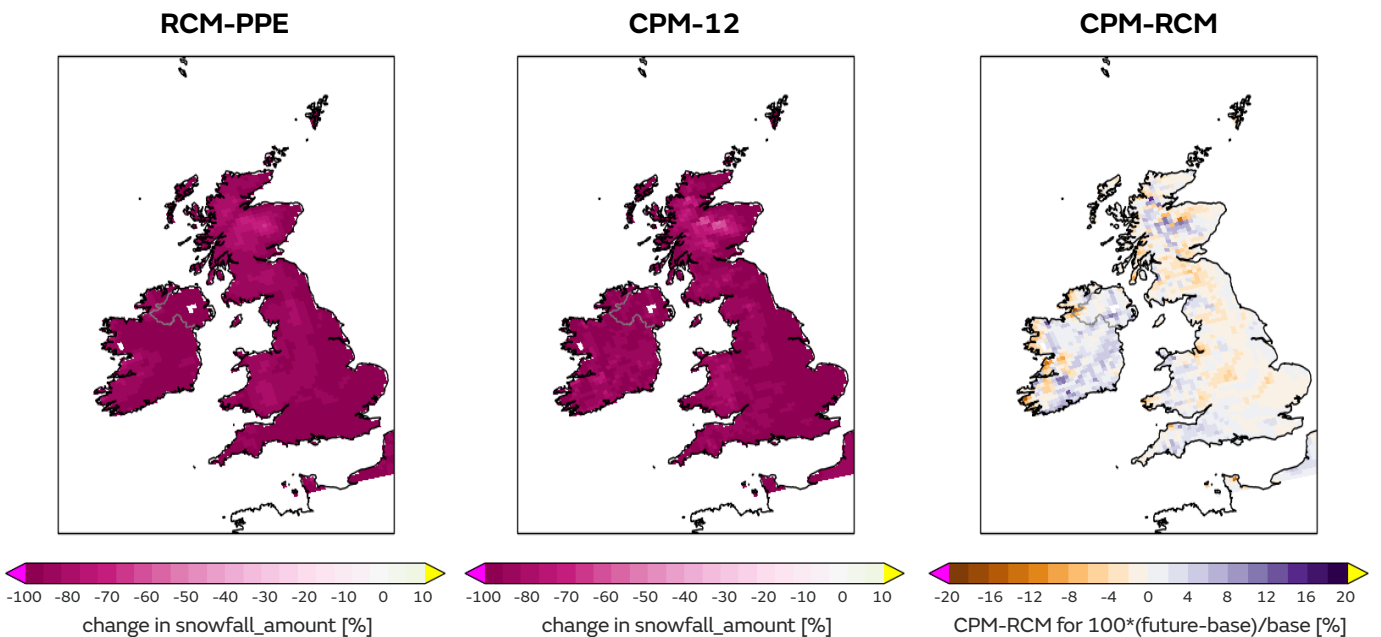

Figure 4.5.11. Future change in mean snow amount in winter. Ensemble-averaged future percentage change (%) in winter mean snow amount in (left) RCM-PPE, (centre) CPM-12 and (right) the difference. The future change is the difference between 2061-80 and 1981-2000 periods.

Cloud

CPM-12 shows an increase in cloud cover in winter in future, although with decreases over the south-east UK (Fig 4.5.12). By contrast, RCM-PPE shows decreases everywhere in winter, with a greater tendency for cloud to decrease over the south-east. These differences between the models are consistent with the greater increase in the number of wet days in winter in the CPM (Section 4.3).

In summer, both CPM-12 and RCM-PPE show decreases in cloud cover in future, with greatest decreases in the south (Fig 4.5.13). These decreases in cloud are consistent with the decreases in rainfall in this season, seen in both models (Section 4.2). The decreases in cloud (absolute changes in a percentage cloud cover) are consistently smaller in the CPM compared to the RCM, which may simply reflect the fact that there is less cloud cover in the CPM in the present-day (Section 3.5).
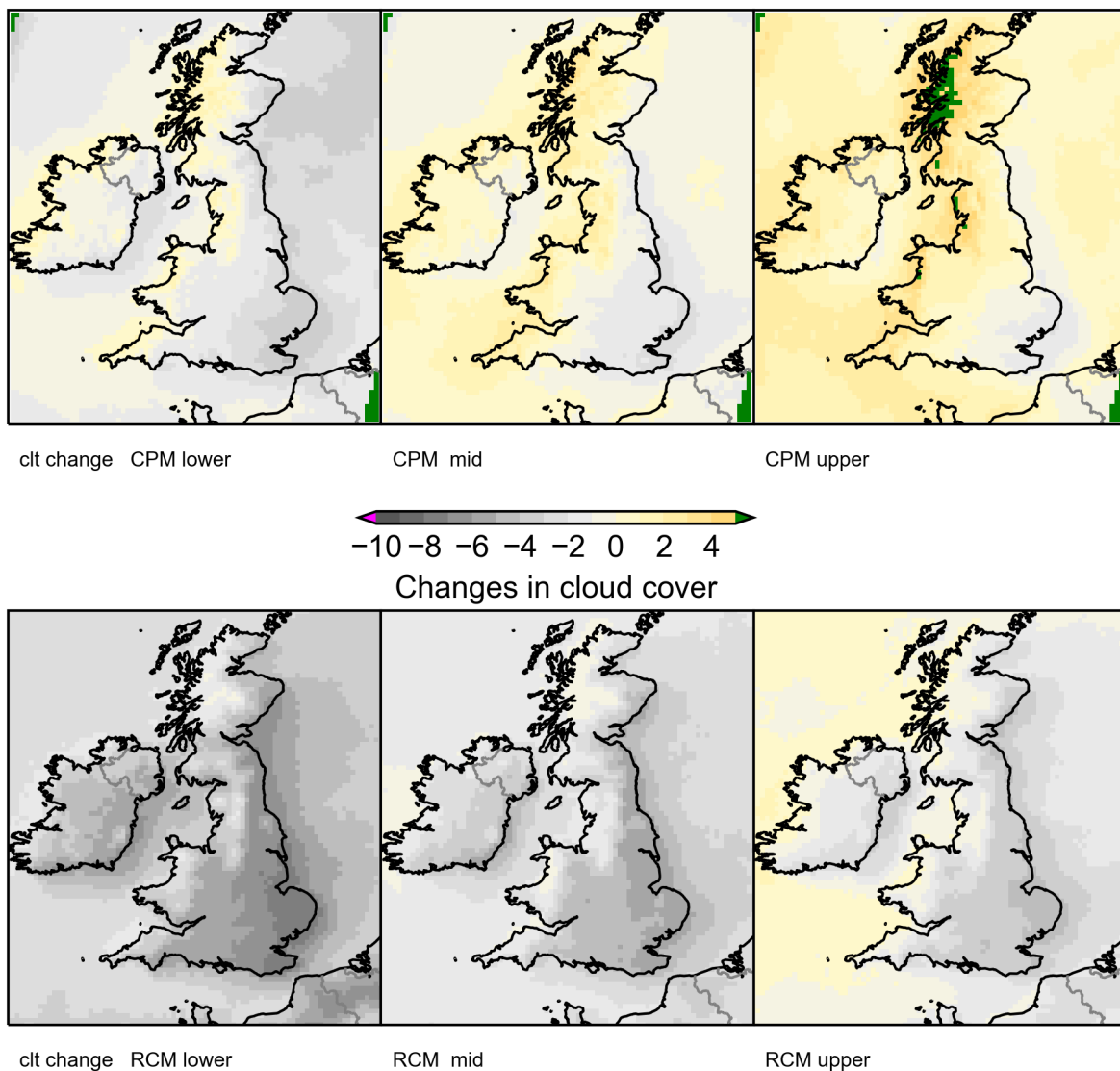
Figure 4.5.12. Future change in cloud cover in winter. Changes for (left) 2nd lowest, (centre) central and (right) 2nd highest member locally, for (top) CPM-12 regridded to 12km RCM grid and (bottom) RCM-PPE. Changes in cloud cover (absolute change in percentage cloud cover, %) correspond to the difference between the future (2061-2080) and baseline (1981-2000) periods.
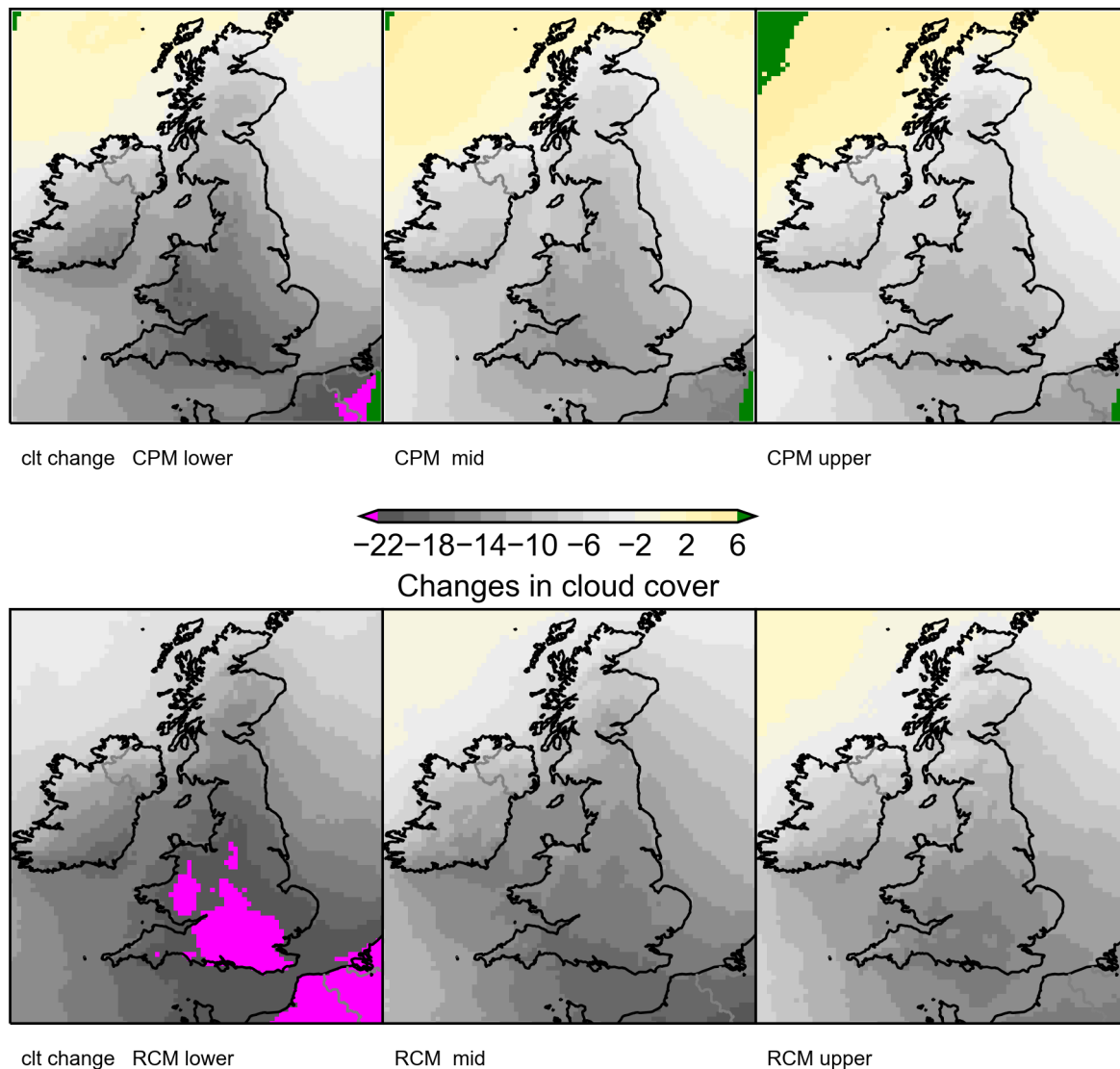
Figure 4.5.13. Future change in cloud cover in summer. As Fig 4.5.12, but for summer.

Lightning

The CPM-12 gives some suggestion that lightning may decrease in the future in summer. However, given the difficulties in evaluating the lightning output for the present-day and the potential deficiencies identified (Section 3.5), we have little confidence in the future lightning projections.

We note that most previous studies (e.g. Price et al, 1994) of the impacts of climate change on lightning have projected a future increase in flash rates, but they used simple parameterisations of lightning based on cloud heights and convective available potential energy (CAPE), and neglect cloud ice fluxes that are fundamental to thunderstorm charging. For example, Boorman et al (2010) found future increases in numbers of lightning days, in the RCM simulations carried out for UKCP09. A recent paper by Finney et al (2018) projected a 15% decrease in flash rate globally when a parameterisation based on ice fluxes was used, although the simulated decreases over the UK are not significant. The UKCP18 CPM uses a similar scheme (Section 2.3), but further work is needed to establish whether decreases predicted for summer (when more lightning reaches the ground) are indeed robust, and to better understand the mechanisms involved. A future decrease in lightning however is not inconsistent with an increase in heavy summer rainfall, due to the role of ice fluxes in lightning generation.

4.6 Summary

We have presented projected changes for the UK, for 2061-2080 compared to 1981-2000 under high emission scenario RCP8.5. We have mainly examined changes in temperature and precipitation, comparing projections from CPM-12 with those from RCM-PPE. We have also shown results for selected high-impact events including hourly precipitation extremes, hot and cold spells, and snow.

Mean temperature increases everywhere and in all seasons. The UK-average central estimate of temperature change is 3.1ºC in winter and 4.6ºC in summer, with the greatest increases occurring in the south. Changes are broadly consistent between CPM-12 and RCM-PPE, although with some local differences. In winter, there is a smaller increase in temperature over Scotland in the CPM and similarly a smaller increase in the temperature of cold winter days and a smaller decrease in the frequency of intense cold spells in the northern UK, compared to the RCM. These differences are likely related to differences in the treatment of lying snow, with more lying snow in the present-day and a greater decrease in lying snow in the future in the RCM. For hot summer days and the frequency of hot spells, CPM-12 and RCM-PPE show similar increases (UK average central estimate of 5.9ºC increase for hot summer days).

Precipitation increases in winter, with the possible exception of northern Scotland. CPM-12 shows significantly greater increases in winter precipitation than RCM-PPE (UK-average central estimate of 27% increase in CPM compared to 16% in RCM). There are similar increases in the intensity of precipitation in winter in the CPM and RCM, with the different response in mean winter precipitation instead due to a greater increase in the number of wet days in the CPM. This may be explained by a number of possible contributing factors. Firstly, given the large number of wet days in the present-day, there is less scope for this to increase in the future in the RCM. Secondly, changes over orography are the main contributor to total precipitation change, and the high frequency of orographic precipitation in the RCM in the present-day means there is less scope for this to increase in future. Thirdly, future changes in the triggering of convective showers over the sea and their advection inland is more realistically represented in the CPM.

Precipitation decreases in summer, again with the possible exception of northern Scotland. The UK-average central estimate is about 28% decrease in summer precipitation. The CPM and RCM show similar decreases in mean precipitation in summer, although there are differences between the models in the underlying changes in the frequency and intensity of precipitation. In particular, there is a greater increase in summer rainfall intensity in the CPM than RCM. Increases in extreme hourly precipitation intensity in the CPM are higher than would be expected solely from increasing atmospheric moisture. This may be explained by local dynamical feedbacks within storms amplifying increases in rainfall extremes on hourly timescales; a process captured neither by the RCM nor coarser resolution climate models more generally.

In terms of high impact events, CPM-12 and RCM-PPE show similar future increases in the 2-year return level of annual extremes of hourly precipitation (25% and 31% increase respectively). For rarer extremes, the RCM shows greater future increases, likely due to unphysical "grid point storms". Both models also show increases in soil moisture stress of about 20% or more over the southern UK for the driest month in the annual cycle. For cloud, the CPM shows increases in cloud cover in winter, whilst the RCM shows decreases. Greater decreases in cloud in absolute terms are also seen in the RCM in summer. For lightning, further work is needed to establish whether decreases predicted for summer are robust and more generally, for other variables of interest to users, additional material will be provided in journal papers.

5 Interpretation and use of the projections

In this section we draw on the assessment of present-day model performance (Section 3) and our understanding of the representation of underlying processes (from differences in model physics, Section 2), to assess the relative confidence we have in the future projections of CPM-12 compared to those of RCM-PPE. Where CPM-12 and RCM-PPE projections (Section 4) agree, due to these being driven by large-scale processes common to both models, we suggest that the CPM and RCM results provide equally plausible projections of future change. Where CPM-12 and RCM-PPE projections disagree, we examine the underlying processes that are likely to be responsible, and hence the extent to which the CPM may or may not provide a more reliable estimate of future change. This assessment then has implications for deciding which of the UKCP18 data products (CPM-12, RCM-PPE and also Strand 1 and Strand 2) may be most appropriate to use for a given application.

For several key temperature and precipitation metrics, Table 5.1 summarises the extent to which present-day biases are reduced in CPM-12 compared to RCM-PPE, whether the future changes are different between the models, and our understanding of these differences in terms of the key processes that are represented differently in the CPM. In this we are primarily considering differences in the central estimates of future change. However, although the central estimates may be similar, CPM-12 and RCM-PPE may provide somewhat different estimates of the uncertainty in future changes. In particular RCM-PPE samples parameter uncertainty in the regional model and uncertainty in the large-scale driving conditions, whilst CPM-12 samples local conditions given uncertainty in the large-scale driving conditions only (with no parameter perturbations applied to the CPM itself). Importantly, neither of these ensembles samples structural model uncertainty (due to different parameterisation schemes or model architectures), and a wider sampling of uncertainty (including multi-model ensemble information) is provided in Strands 1 and 2 of UKCP18 (Murphy et al, 2018). Later in this section we compare the sampling of uncertainty across the different UKCP18 products, for some key variables, and discuss this in the context of user requirements.

Phenomenon	CPM improved present-day biases?	CPM different future changes?	Understanding of CPM-RCM projection differences and implications for reliability
	✔ (improved) or ✘ (made worse) or ∼ (similar) compared to RCM-PPE	✚ (enhanced) ━ (weakened) or ∼ (equivalent) compared to RCM-PPE	Where projections differ, key processes represented differently in CPM, and implications for reliability (✔, ✘ or ■ unknown) - denotes similar projections
Temperature			
Winter mean temperature	✔ Reduced cold bias in north and reduced warm bias in south in CPM.	━ Smaller increase in CPM over Scotland. ∼ Similar increases elsewhere.	Differences in N likely related to missing graupel in the snowpack and different snow scheme in CPM, which lead to much less lying snow in the present-day and a smaller decrease in lying snow in the future in the CPM. ■ Reduced temperature biases in present-day, but treatment of lying snow less sophisticated in CPM. Both CPM and RCM projections plausible, but deficiencies in both cases.
Summer mean temperature	✔ CPM is warmer, with reduced biases except in S.	∼ Similar increases	━ Reduced biases in present-day likely related to less cloud in CPM, but future changes driven by large-scale warming seen by both models.
Cold winter days	✔ Reduction of cold bias in N in CPM.	━ Smaller increase in temperature in CPM in N.	(See above for winter mean temperature) ■ Reduced temperature biases in N in present-day, but treatment of lying snow less sophisticated in CPM. Both CPM and RCM projections plausible, but deficiencies in both cases.
Hot summer days	✔ Biases reduced in N in CPM ✘ CPM too hot in S.	∼ Similar increases in temperature	━ Models have different present-day biases, but future changes dominated by large-scale warming seen by both models.
Cold spells	✔ Reduced biases in the number of intense cold spells in N in CPM (with too many in RCM).	━ Smaller decrease in frequency of intense cold spells in N in CPM	(See above for winter mean temperature) ■ Reduced biases in present-day, but treatment of lying snow less sophisticated in CPM. Both CPM and RCM projections plausible, but deficiencies in both cases.
Hot spells	✔ Reduced biases in the number of hot spells in S in CPM (with too few in RCM).	∼ Similar increase in frequency of hot spells	━ Models have different present-day biases possibly related to drier soils in CPM, but future changes dominated by large-scale warming seen by both models.
	✚ (enhanced) ━ (weakened) or ∼ (equivalent) compared to RCM-PPE		

Phenomenon	CPM improved present-day biases?	CPM different future changes?	Understanding of CPM-RCM projection differences and implications for reliability
	✓ (improved) or ✗ (made worse) or ∼ (similar) compared to RCM-PPE	✚ (enhanced) ▬ (weakened) or ∼ (equivalent) compared to RCM-PPE	Where projections differ, key processes represented differently in CPM, and implications for reliability (✓, ✗ or ■ unknown) ▬ denotes similar projections
Precipitation			
Winter mean precipitation	✓ Reduced wet bias in CPM.	✚ Substantially greater increase in CPM	Improved representation of daily precipitation occurrence in explicit convection model, with greater increase in precipitation occurrence in the future. Large-scale processes common to both models also driving increases in mean precipitation. ✓ Increased confidence in CPM projections due to improved representation of daily variability, but more work needed to understand present-day biases and the relevance of these for future changes.
Summer mean precipitation	✓ Reduced wet bias in CPM, except in S.	∼ Similar decreases in mean ✚ Enhanced changes in underlying frequency and intensity in CPM	▬ Similar changes in mean precipitation. Improved representation of daily rainfall occurrence in CPM, linked to better representation of convective processes, so increased confidence in CPM projections of changes in frequency/intensity components.
Heavy daily events in winter	✓ Improved biases over mountains in CPM (where RCM underestimates heavy events).	∼ Similar increases in intensity of heavy events.	▬ Higher resolution and explicit convection in CPM improves precipitation intensity, especially over mountains. However future changes in daily precipitation intensity are driven by large-scale changes captured by both models.
Heavy daily events in summer	∼ CPM overestimates and RCM underestimates intensity of heavy events	✚ Greater tendency for increase in summertime rainfall intensity in CPM	CPMs give better representation of convection, but tendency for heavy events to be too intense is known bias in CPMs due to convection not being fully resolved. RCM tends to underestimate heavy events due to deficiencies in convection parameterisation. ✓ CPM better represents convective processes, but further research is needed to establish the importance of known biases in the heaviest events for future projections.
Hourly precipitation variability (all seasons)	✓ RCM rainfall is too frequent and low intensity, with biases improved in CPM. ✓ CPM better captures afternoon peak in convection.	✚ Enhanced changes in hourly rainfall occurrence in CPM ✚ Greater increase in summer rainfall intensity in CPM ∼ Similar increase in intensity in winter and autumn	Improved representation of hourly rainfall characteristics in explicit convection model; although convection not fully resolved resulting in heaviest events being too intense. ✓ Improved realism of hourly rainfall in the CPM gives us greater confidence in CPM changes. RCM projections of hourly precipitation change considered unreliable.
Hourly precipitation extremes (all seasons)	∼ CPM overestimates the intensity of hourly extremes, but better represents the rate at which extremes increase with increasing return period.	∼ Similar increases in 2yr return level ▬ Smaller increases in CPM for 10yr (and longer) return level in autumn and winter	Convection-parameterised model underestimates intensity of moderate extremes, and has unphysical grid point storms leading to high values >100mm/h in the far extreme tail. Explicit convection gives more realistic extremes, but overestimates intensity due to convection not being fully resolved. ✓ CPM projections plausible, but further work needed to understand the importance of known biases for future projections. RCM projections for hourly precipitation extremes considered unreliable.

Table 5.1. Summary of present-day biases and future changes in CPM-12 compared to RCM-PPE, and our understanding of the model differences.

For temperature, both for seasonal means and daily variability, there is no evidence to suggest that the CPM projections are more or less plausible than those from the RCM (Table 5.1). In some cases there are differences in the projections between the models, most notably for temperature changes over the northern UK in winter. In this case we understand the reason behind the differences, specifically missing graupel in the snowpack and the zero-layer snow scheme in the CPM. This results in less lying snow in the present-day and a smaller decrease in lying snow in the future compared to the RCM. Despite having a more sophisticated snow-scheme, however, the RCM has larger biases in the baseline climate. This cold bias in the RCM is in part inherited from the driving GCM, but still remains in ERA-Interim driven simulations suggesting it is also an inherent bias in the RCM itself. Although the CPM has reduced biases, given the less sophisticated treatment of lying snow, we do not have greater confidence in its projections. In this case the sets of model projections from CPM-12 and RCM-PPE are both assessed as plausible, but with deficiencies in both cases.

Across the UK in general, there is no evidence of added value from the CPM compared to the RCM in projected changes in temperature. However this will not always be true locally, for example over cities the CPM is expected to better represent changes due to the higher spatial resolution and the use of the more sophisticated urban scheme (MORUSES, Section 2). Also in other regions of high spatial heterogeneity, such as mountains and coastlines, the CPM will provide added spatial detail to the RCM projections which may be important for some users. A further consideration is the relative sampling of uncertainty, with RCM-PPE providing a slightly broader uncertainty range (although still limited compared to Strands 1 and 2) than CPM-12.

For precipitation, we find more evidence of added value from the CPM (Table 5.1). In winter, mean precipitation changes are different between the CPM and RCM, with these differences mainly arising from wet day frequency changes. Since the CPM represents wet day frequency better, we have more confidence in the CPM projections. In particular, wet day frequency is too high in the RCM, with less scope for this to increase in future. In addition, although convective precipitation is not a dominant factor in winter, the CPM and RCM do pick up the influence of events triggered over the sea in unstable airstreams. Early analysis suggests that the more realistic representation of these convective showers in the CPM, and its ability to advect them over the land, may contribute to differences in the response of winter mean precipitation. However, more work is needed to confirm this, and analyse other potential contributions to the differences. In due course, these will inform more detailed assessments of confidence in the changes seen in the two prediction systems. Although we may have greater confidence in the central estimate of the change from the CPM-12, this is not true for the uncertainty range. The uncertainty range is likely to be underestimated in both CPM-12 and RCM-PPE due to the small ensemble size and lack of information from other international climate models, but additionally in CPM-12 due to no parameter perturbations being applied to the CPM itself. The implications of the CPM results for our confidence in winter mean precipitation changes from Strands 1 and 2 are discussed below.

For summer mean precipitation, CPM-12 and RCM-PPE provide similar central estimates of the projected change. Thus in this season the improved representation of daily variability in the CPM does not impact future changes in the mean, with the latter instead driven by large scale changes (such as warming and accompanying humidity changes) seen by both models. This agreement with the CPM provides additional evidence that the RCM projections of decreasing summer mean precipitation over the UK, which follow the driving GC3.05-PPE simulations from Strand 2, are plausible. However, as noted above, locally there may be added value from the CPM, especially in regions of high spatial heterogeneity such as cities, mountains and coastlines.

For heavy daily precipitation events in winter, we similarly find no evidence to suggest that the CPM projections are more or less plausible than those from the RCM. Although present-day biases are improved in the CPM, future changes in daily precipitation intensity are driven by large-scale changes (specifically increasing atmospheric moisture with warming) captured by both models.

For heavy daily precipitation events in summer, and hourly precipitation variability and extremes in all seasons, we have greater confidence in the CPM projections of future change. This is based on the much more realistic representation of convective processes and present-day hourly rainfall characteristics in the CPM, compared to the parameterised model. There are deficiencies in the CPM, in particular the tendency for the heaviest events to be too intense, which is due to convective plumes and smaller convective showers not being well resolved at the 2.2km grid scale. Further research is needed to establish the importance of this known bias for future projections, and in particular whether it would lead to smaller or larger increases in summer rainfall intensity. Nevertheless, the CPM provides a step change in our ability to represent convective processes and local storm feedbacks, to the extent it is able to provide plausible projections of future change in hourly rainfall and convective extremes. Due to inherent limitations of the convection parameterisation scheme, RCM projections of hourly precipitation change are considered unreliable, and for high return period events may differ from CPM projections by almost a factor of 2. We note in the case of hourly precipitation extremes, the RCM-PPE projections span a greater range than CPM-12. However, this is not "real" uncertainty but instead likely reflects unphysical grid point storms in the RCM.

Use of projections in context of wider UKCP18 information

We now move on to consider the use of the downscaled regional projections (from the RCM-PPE or CPM-12) in the context of the wider sampling of uncertainty from Strands 1 and 2.

The Strand 1 projections are designed to provide a broad view of uncertainties, for a set of key variables. They can be interpreted as probabilistic estimates, conditional upon the climate modelling information and methodological choices used. The Strand 2 GCM projections provide a more flexible dataset, for spatially coherent, multi-variate impacts studies. They are plausible climate outcomes that include multi-model ensemble information alongside PPE results, and also support understanding of mechanisms driving future changes, for Europe and other worldwide regions (Section 1.2, Murphy et al, 2018). These Strands offer alternative sources of information for UK impacts, useful in applications where the higher horizontal resolution of Strand 3 products is not required, or to provide context relating to uncertainty and/or understanding that may inform the interpretation of studies based mainly on Strand 3.

For Scotland and England, Fig 5.1 shows a comparison of seasonal mean changes from Strands 1 and 2, with those from the downscaled regional projections. This highlights the differences between the ranges of future change produced by the different Strands. In all cases, the Strand 1 probability distributions provide the widest spread of potential outcomes. In winter, the two ensembles in Strand 2 (GC3.05-PPE and CMIP5-13) show considerable overlap in their responses, with the combined set of Strand 2 projections lying within the 5-95% probability range of the Strand 1 projections. For summer, however, GC3.05-PPE and CMIP5-13 show substantial offsets, with GC3.05-PPE sampling greater levels of summer warming and drying compared to the multi-model ensemble. For summer temperature, GC3.05-PPE samples outcomes exclusively above the median Strand 1 values, whilst for summer precipitation, most GC3.05-PPE members project changes drier than the Strand 1 median. This is also the case for RCM-PPE and CPM-12. In contrast, most CMIP5-13 members give changes below the Strand 1 median for summer temperature, and above

the Strand 1 median for precipitation. This highlights the importance of including structural modelling uncertainty, sampled by the multi-model ensemble information included in Strands 1 and 2, especially for changes in summer.

For applications specifically requiring information at fine spatial scales, Murphy et al (2018) point out that users can consider augmenting the Strand 3 RCM information with results from EURO-CORDEX simulations (Jacob et al, 2014). These include a multi-model ensemble of RCMs run at 12km resolution, and driven by a subset of CMIP5 global models using the RCP8.5 scenario. For example, at the time of writing the EURO-CORDEX archive (see https://euro-cordex.net) contains RCM simulations driven by five of the CMIP5-13 models. Two of these (CNRM-CM5 and EC-EARTH, see Table 3.1 of Murphy et al, 2018) simulate levels of UK summer warming below the coolest response found in any of the Strand 3 simulations. These global models are each used to drive a selection of alternative RCMs, which could potentially be used to explore downscaled outcomes below the envelope of national-scale changes projected in Strand 3. Regarding summer precipitation, Raczjak and Schär (2017) studied 15 EURO-CORDEX simulations, finding that three produced small increases in average summer precipitation over the British Isles, in contrast to the strong drying shown in all the Strand 3 projections. These could be used to augment Strand 3 results, in studies of future impacts of changes in the hydrological cycle. For example, outcomes for extreme daily rainfall events could be studied in cases where projected increases in wet-day intensity are offset to a lesser degree by compensating reductions in wet-day frequency, compared to the Strand 3 projections.

In general the Strand 3 projections (RCM-PPE and CPM-12) show a similar range of changes to the driving GC3.05-PPE for seasonal mean changes at national scales. This is true in both Scotland and England, for temperature changes in both seasons and for precipitation changes in summer. For these, we found no evidence to suggest that the CPM projections are more or less plausible than those from the RCM and driving GCM simulation (see above). Thus, for these changes we suggest Strand 1 and Strand 2 should be the primary source of information, as these provide a more comprehensive view of uncertainties. For applications, where fine spatial detail in seasonal mean changes is required the Strand 3 downscaling projections will be needed. However, in this case it is important to consider the range of Strand 3 projections within the wider context of Strand 1 and 2 projections, and also potentially to consider augmenting the UKCP18 RCM-PPE or CPM-12 results with multi-model information (see above).

Regarding ranges of change, an exception to the discussion above occurs for mean precipitation changes in winter. In this case, CPM-12 projects upper-end increases that are considerably above those in RCM-PPE, and also above any of those in the Strand 2 projections (GC3.05-PPE and CMIP5-13). For Scotland, CPM-12 winter precipitation projections are within the 5-95% probability range of the Strand 1 projections, with members both above and below the median change from Strand 1; but for England, all the CPM-12 projections lie above the Strand 1 median value, with 1 member above the 95% probability level. As discussed above we have greater confidence in the CPM projections for mean winter precipitation, due to the improved representation of daily variability which impacts biases in the seasonal mean.

Figs. 5.2 and 5.3 show the relationship between present-day biases and future changes, for seasonal mean temperature and precipitation, in the Strand 2 and Strand 3 ensembles. Internal climate variability and the effects of different representations of physical processes will both contribute to the spread of points, but the latter are likely to explain any systematic relationships, because the effects of internal variability should be random. For winter precipitation there is a negative relationship between present-day biases and future changes in CPM-12 for England, and in RCM-PPE and CPM-12 for Scotland (although only the latter is significant). Thus a large wet bias is associated with a smaller future increase in mean precipitation in winter.

This is consistent with the possibility mentioned in Section 4.2, that too many wet days in the present-day may limit the scope for future increases in wet day frequency. In particular, this is suggested as one of the possible contributing factors to the different responses in winter mean precipitation between the CPM and RCM. We note that intensity differences will also contribute to the slope in Figs 5.2 and 5.3. The different relationships seen between CPM-12 and RCM-PPE, and also the considerable scatter of points in Figs 5.2 and 5.3, show however that the present-day bias is not the only factor controlling the different future responses. This is underlined further by comparison of the relationships between historical biases and future changes in Strand 2, which reveal some substantial differences between GC3.05-PPE and CMIP5-13.

In summer, the relationship between present-day biases and future changes is positive in the PPEs, with a very similar relationship seen in GC3.05-PPE, RCM-PPE and CPM-12 for England. Thus in this case, drier ensemble members in the present-day tend to give larger decreases in precipitation in the future. This contrast with the winter results is likely explained by differences in the driving processes between the two seasons. In winter, the atmosphere is closer to saturation (with many more wet days). In summer, showers are triggered over the land by surface heating and use the local moisture sources more directly (whereas showers in winter may be more dependent on the advected moisture from the sea). Future changes in summer are however dominated by convergence changes (with evaporation hardly changing). Specifically, over land a switch occurs from a modest net convergence of moisture during the historical time slice, to a net divergence in the future simulations, in both RCM-PPE and CPM-12 (Section 4.2). This suggests that large-scale circulation changes, and not changes in the local soil moisture state, are driving future decreases in summer rainfall. For example, Murphy et al (2018) note a shift towards the positive phase of the summer North Atlantic Oscillation (SNAO) in the future simulations of GC3.05-PPE members. This is correlated with the strength of the projected summer drying, due to the strong relationship between the SNAO and summer rainfall. In the present-day, the extent to which showers (and local moisture recycling) occur may be conditioned by the large-scale circulation patterns (e.g. fewer showers where there is more dry continental flow). If so, such large-scale circulation controls could potentially explain the similarity of the relationship between the GC3.05-PPE, RCM-PPE and CPM-12 in Fig. 5.2, since the global model circulation strongly constrains the regional simulations under both present-day and future conditions. However, further work is needed to understand why a positive correlation emerges between historical biases and future changes in summer rainfall. This may depend, for example, on whether both can be traced to the influence of common circulation types. We also note that CMIP5-13 shows a negative rather than positive relationship, underlining that the factors influencing historical biases and future changes can vary significantly, between different climate model ensembles. In winter, CMIP5-13 shows a positive relationship, in contrast to the negative relationship in the PPE experiments, further underlining this point.

For temperature in winter, there is a negative relationship across the PPE ensembles, which is similar between the CPM-12, RCM-PPE and GCM-PPE (Figs. 5.2-5.3). So if a model is very cold in the present-day, it tends to have a greater increase in temperature in the future. A possible explanation is snow-cover: for models with a lot of snow, there is more scope for this to melt in the future thus enhancing temperature increases through albedo feedbacks. However, we note that a variety of factors can potentially exert a strong influence over UK temperature changes, including the level of the global temperature response, changes in AMOC, and regional changes in cloud and atmospheric circulation. Many of these factors may not be related to regional historical temperature biases, and the relative influence of different drivers may differ between different climate model ensembles. In winter, for example, the CMIP5-13 ensemble does not replicate the negative relationship seen in the PPE simulations.

For temperature in summer, there are no significant relationships between present-day biases and future changes in any of the ensembles.

More work is needed to understand present-day biases and their relative importance for future changes compared to other large-scale processes, which will then inform more detailed assessments of confidence in the changes across the different prediction systems. Early analyses suggest that projections based on convection parameterised models may underestimate "upper-end" responses in winter mean precipitation. However the CPM-12 range will also considerably underestimate uncertainty since this does not include either model structural uncertainties or uncertainties in the CPM physics parameters.
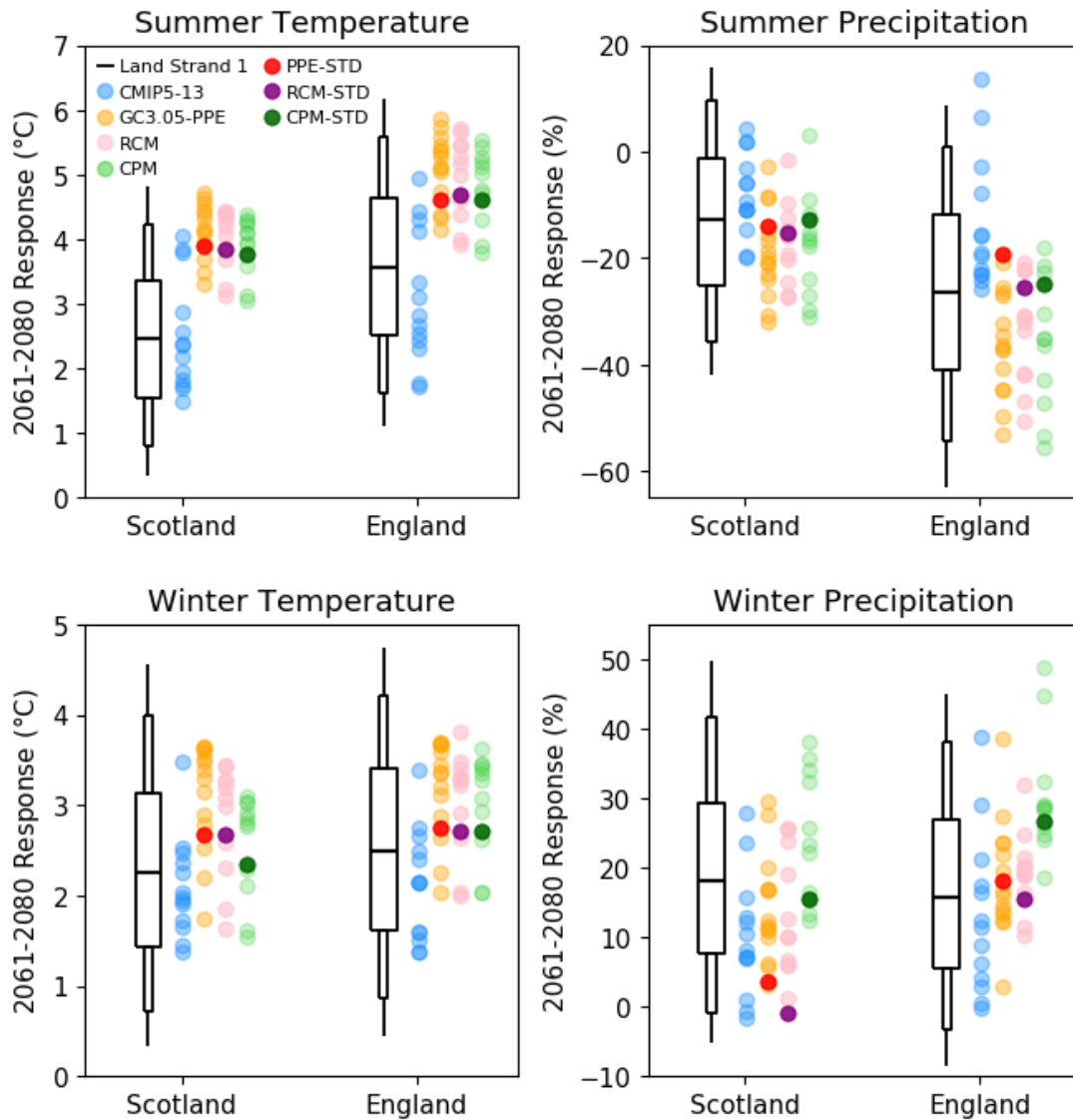

Figure 5.1. Comparison of seasonal mean changes across UKCP18 Strands 1, 2 and 3. Projected changes for 2061-2080 relative to 1981-2000 for Scotland and England in (top) JJA and (bottom) DJF, under RCP8.5 emissions. Results are shown for surface air temperature (left, °C) and precipitation (right, %). Box and whiskers denote the 5, 10, 25, 50, 75, 90 and 95% probability levels of the Strand 1 probabilistic projections. Orange dots (with STD in red) denote members of GC3.05-PPE and blue dots those of CMIP5-13, which together comprise Strand 2. Pink dots (with STD in purple) show members of RCM-PPE and green dots (with STD in dark green) those of CPM-12 (Strand 3).
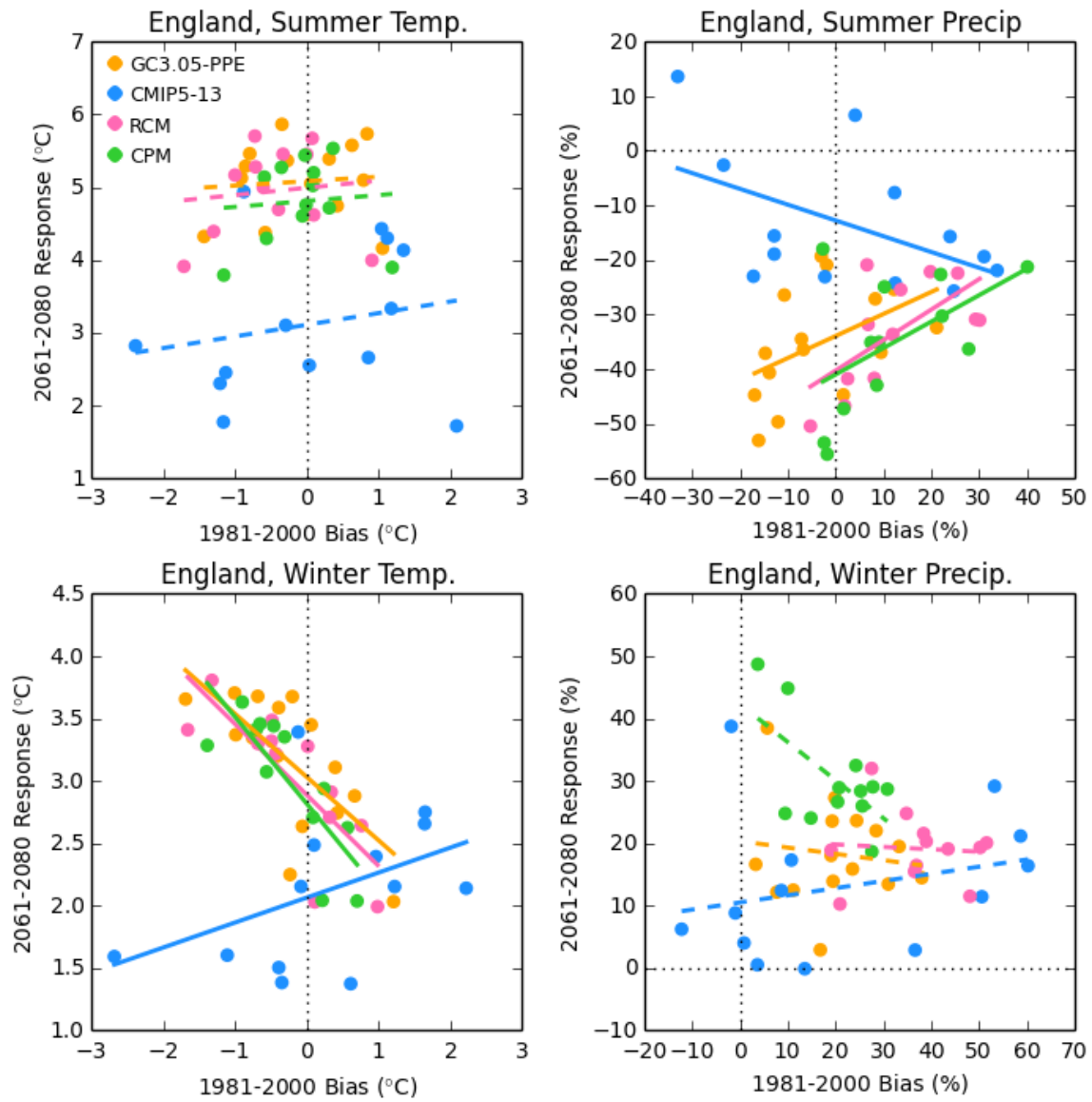
Figure 5.2. Relationship between present-day biases and seasonal mean changes, for England, for UKCP18 Strands 2 and 3. Scatter plot of present-day biases with respect to NCIC observations for 1981-2000 versus projected changes for 2061-2080 relative to 1981-2000, for seasonal mean temperature (left, ºC) and precipitation precipitation (right, %), for England, for (top) JJA and (bottom) DJF. Orange dots denote members of GC3.05-PPE and blue dots those of CMIP5-13 (Strand 2). Pink dots show members of RCM-PPE and green dots those of CPM-12 (Strand 3). Lines show the linear regression relationships, and are shown as dashed where they are not significant at the 10% level assessed using bootstrap resampling.
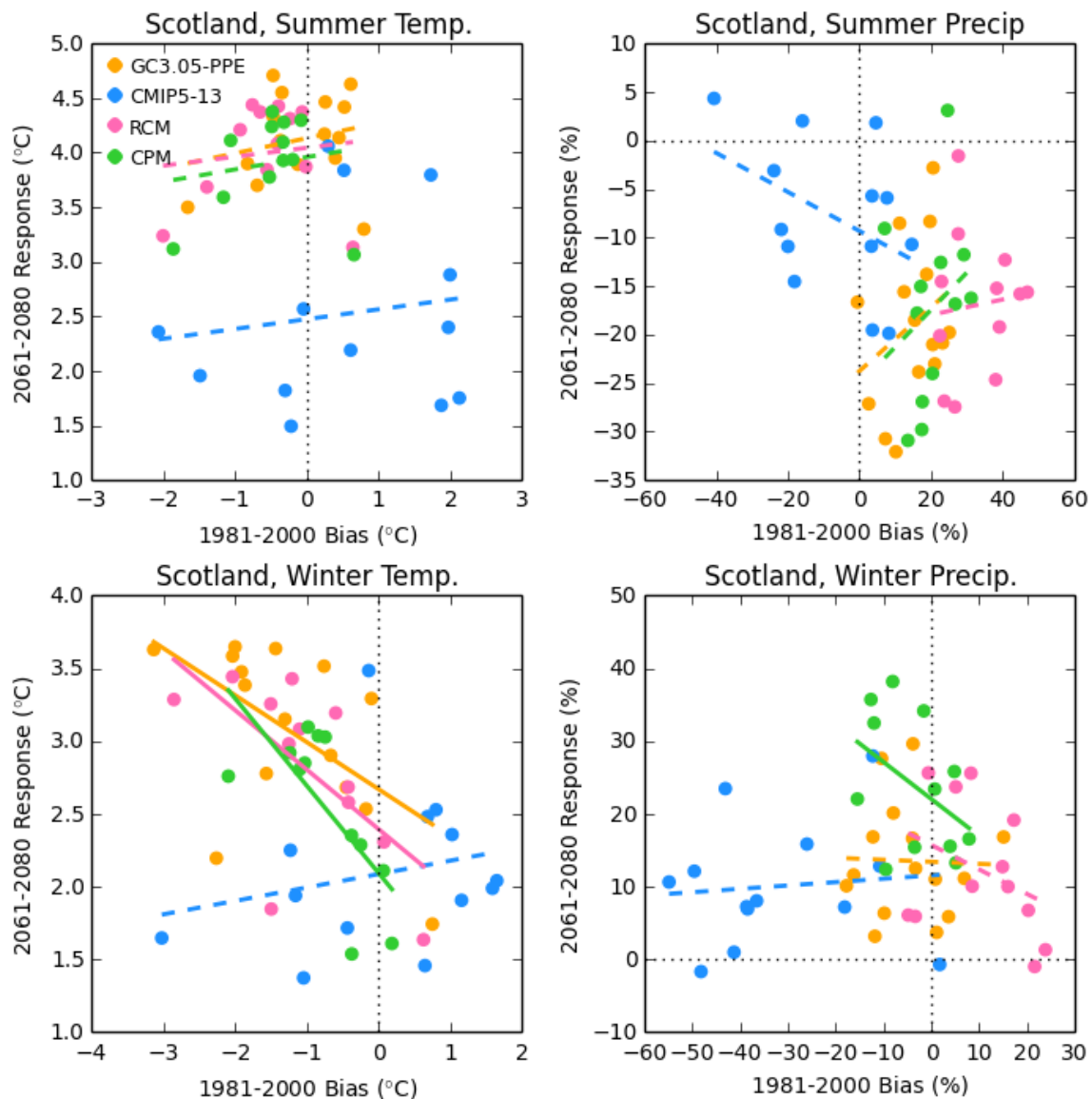
Figure 5.3. Relationship between present-day biases and seasonal mean changes, for Scotland, for UKCP18 Strands 2 and 3. As Fig. 5.2 but for Scotland.

The above discussion is related to seasonal-mean projections. As shown in Murphy et al (2018) the downscaled projections from Strand 3 give an improved simulation of daily extremes as well as enhanced spatial detail. So for applications focussing on extremes, the RCM-PPE or CPM-12 products are expected to be the primary source of information, preferably supplemented by a comparison with Strand 2 to reveal deficiencies in the sampling of uncertainty. For the case of daily rainfall extremes in summer or changes on hourly timescales, projections from convection parameterised models are unreliable and so users should use the CPM-12 projections, although with the caveat that the ensemble does not sample the full uncertainty range.

Differences in CPM and RCM responses are found here mainly for convectively-related phenomena. In particular, the CPM shows different future changes for heavy daily precipitation events in summer and hourly precipitation variability and extremes. A possible exception is winter mean precipitation changes, but again the representation of convective showers may be a contributing factor to the differences. Since the representation of convective processes is very different in the explicit convection model, and this model includes local dynamical feedbacks on future changes (not included in parameterised models), it is unlikely

to be possible to simply predict the CPM response from the RCM response. This can be seen from Fig 5.1, where the smallest response in winter precipitation over Scotland in the RCM is for the STD member, whereas this is not the case for the CPM. However, for temperature, a scaling approach to determine CPM changes from RCM or GCM changes (where CPM downscaling is not available) may be more valid. Fig 5.1 shows a similar relationship between the CPM and RCM response across different ensemble members, for summer and winter temperature. Thus in this case the CPM change is dominated by the large-scale warming in the driving RCM, but with some local differences. Where these local differences are due to the better representation of topography, for example, these will be similar across different CPMs and local temperature changes may be reasonably approximated by a local scaling factor applied on top of the large-scale change.

The Strand 3 projections are intended to be useful for impacts assessments (e.g. relating to extremes or requiring enhanced spatial detail) and the development of storylines. These can potentially take a number of different forms, including narratives of how impacts related to particular types of weather event might change in future (Hazeleger et al, 2015), or characterisations of simulated regional changes that promote understanding in terms of specific remote circulation drivers (Zappa and Shepherd, 2017). One specific role of Strand 3 information, for example, could be to investigate the localised consequences of future flooding events, perhaps conditioned on synoptic flow conditions similar to cases that led to costly impacts in the past (e.g. Huntingford et al, 2014). However, the Strand 3 projections do not support a probabilistic interpretation, and provide a narrower sampling of uncertainty compared to Strands 1 and 2. For applications using Strand 3 downscaling projections, we would recommend augmenting the RCM-PPE or CPM-12 results with multi-model information. This would, for example, create a broader range of projections from which to sub-select a limited but diverse set of storylines. At the 12km scale, multi-model RCM projections can be obtained from the EURO-CORDEX archive (Jacob et al 2014, Kjellstrom et al, 2018), which consists of a partly-filled matrix of RCM simulations contributed by several European regional modelling groups, driven by a selection of CMIP5 global models. At the 2.2km scale, multi-model CPM simulations over European regions are being carried out as part of the CORDEX-FPS (Coppola et al, 2018) and Horizon 2020 EUCP (Hewitt and Lowe, 2018) projects, and the data once available will provide an indication of CPM structural uncertainties.

6 Summary and forward look

For the first time an ensemble of climate projections has been carried out at convection-permitting (2.2km) resolution. This is similar to the horizontal scale currently used for weather forecasting, and represents a big step forward in the approach to climate projection. National climate scenarios have previously been based on information from conventional coarser resolution climate models. Compared to these, the convection-permitting model (CPM) provides a much more realistic representation of convective processes and hourly rainfall characteristics, and as a result provides plausible projections of future change on hourly timescales. The CPM also provides detailed information on changes on local scales, better representing mountains, coastlines and urban areas.

In this report, we have provided the evidence base to establish the credibility of the new ensemble of CPM projections. We have also compared the CPM projections with those from the driving 12km RCM-PPE, and have assessed their relative reliability, drawing on our understanding of their representations of the underlying processes. We have focused on temperature and precipitation, and for almost all metrics examined here we find that the CPM gives reduced present-day biases compared to the RCM. The CPM however does have a tendency to be too hot in the south of the UK in summer, which leads to an increase in the bias compared to the RCM, likely due to drier soils. The CPM also has a known tendency to overestimate intense precipitation events, due to convection not being fully resolved at 2.2km resolution. Nevertheless, this represents an improvement over the RCM, which like other convection-parameterised models more generally, tends to underestimate heavy rainfall and also suffers from grid point storms, leading to unphysically high values at the far tail of the precipitation distribution.

For temperature, future increases in summer are in good agreement between the CPM and RCM, both for the seasonal mean and daily extremes. However, in winter, there are smaller increases in temperature and a smaller decrease in the frequency of intense cold spells over the northern UK in the CPM compared to the RCM. This difference is likely due to the different treatment of graupel and snow-schemes in the CPM and RCM. Since the CPM uses a less sophisticated treatment of lying snow, we do not have greater confidence in its projections in this case, even though present-day biases are reduced. Thus overall for temperature, both for seasonal means and daily variability, there is no evidence to suggest that the CPM projections are more or less plausible than those from the RCM at the regional scale. Locally, particularly in the vicinity of mountains or coastlines, or in urban areas, the CPM will provide added spatial detail. Note, however that the CPM shares the same caveat that applies to all climate downscaling products, that the downscaled scenarios remain subject to the effects of systematic biases, and related process errors, present in the driving global simulations that affect the large-scales (and hence impact the boundary conditions). We also recommend that users interested in results at specific 2.2km locations consider information from other grid boxes in the surrounding region, which may provide useful indications of the level of confidence that can be placed in localised changes.

For precipitation, future decreases in summer mean rainfall are similar between the CPM and RCM. For winter mean precipitation, there is a significant degree of overlap between the ranges of change seen in the two ensembles, however the CPM-12 envelope is shifted to wetter responses, with examples of substantially larger changes than seen in any of the RCM-PPE projections. This result was not expected, with previous studies showing the CPM following the driving model for changes in winter. Early analysis suggests that the more realistic representation of wintertime convective showers and their advection inland in the CPM may contribute to the difference in winter mean precipitation responses found here. The fact that wet-day frequency is too high in the RCM, with less scope for this to increase in future, is also

another possible contributing factor. However more work is needed to confirm this, and analyse other potential contributors to the difference. In due course, this work will inform more detailed assessments of the confidence in the different projection systems. Comparison of projected changes across the different UKCP18 Strands, however, suggests that projections based on convection parameterised models, as in Strands 1 and 2 and the RCM in Strand 3, may underestimate "upper-end" responses in winter mean precipitation.

For changes in daily precipitation, the CPM shows greater increases in rainfall intensity compared to the RCM in summer, but similar changes in winter. This is consistent with previous CPM studies, and is explained by local convective processes being important for changes in summer. In winter, changes in intensity are driven by increasing atmospheric moisture with warming, which is well captured by both models. The improved representation of convective processes in the CPM means it is able to provide plausible projections of future changes on hourly timescales, including for extremes; whilst RCM projections for hourly precipitation extremes are considered unreliable.

Overall, the CPM results here do not change the UKCP18 headline message of a greater chance of warmer wetter winters and hotter drier summers across the UK in future (Lowe et al, 2018). For 2061-80 under a high emissions scenario (RCP8.5), the CPM suggests winters will be warmer by 3.1ºC (1.8-3.3 ºC) and wetter by 27% (16-42%), whilst summers will be hotter by 4.6ºC (3.6-5.0ºC) and drier by 28% (16-46%), for the UK-average central (low-high) estimate. The CPM results however do provide higher estimates of changes in winter mean precipitation, and new information in terms of changes in heavy daily precipitation events in summer (which intensify more in the CPM) and hourly precipitation extremes (UK average estimate of 25% increase in the 2-year return level).

The CPM ensemble projections sit alongside a number of other UKCP18 tools to look at climate change (Murphy et al, 2018, Lowe et al, 2018). These include probabilistic projections (Strand 1), a set of 28 global 60km climate simulations (Strand 2) and a set of twelve regional 12km simulations (Strand 3). The Strand 1 and 2 projections provide a wider sampling of uncertainty, including multi-model information; whilst the Strand 3 projections provide finer spatial detail and a better representation of extremes. It is important that users should look at the different UKCP18 tools together, be informed of the advantages of the different tools and choose a tool or tools that best matches their application (see Fung et al, 2018, for further guidance). The CPM projections are intended to be useful for impacts assessments that require enhanced spatial detail or changes on hourly timescales, but they provide a narrower sampling of uncertainty than the other UKCP18 products and do not support probabilistic interpretation. Note, in particular, that Strands 1 and 2 reveal a wider range of potential outcomes for changes in summer, sampling changes with lower increases in average temperature, and smaller reductions, or even small increases, in summer precipitation. This is due to the inclusion of information from CMIP5 models. As discussed in Murphy et al (2018), users wishing to explore impacts consistent with outcomes outside the envelope of Strand 3 results have a number of potential options, dependent on the requirements of specific applications. These may include direct usage of Strand 2 output (for applications in which information at space and time scales skilfully represented in global climate model output is sufficient), or use of other dynamical downscaling products such as EURO-CORDEX (e.g. Raczjak and Schär, 2017), which includes RCM projections driven by CMIP5 models using the same horizontal resolution (12km) and emissions scenario (RCP8.5) as the Strand 3 RCM simulations. In particular, use of EURO-CORDEX simulations would allow access to spatially-detailed projections consistent with the lower levels of future warming or future summer drying seen at the national scale in some CMIP5 models. Further possibilities to explore a wider set of plausible outcomes include use

of statistical tools, such as scaling or time-shifting methods (e.g. Herger et al, 2015) or weather generators (e.g. Jones et al, 2010).

It is important for users to be aware that, although we have confidence that the UKCP18 projections represent a significant improvement on UKCP09, there are still limitations in our ability to project 21st century weather and climate. For example, although the CPM provides a big step forward in the realism of simulated rainfall, there are still deficiencies, with heavy rainfall being too intense. Furthermore, all simulations of the future are conditioned on the chosen scenario of future greenhouse gas emissions (RCP8.5) and the particular models and methodologies we employ in UKCP18. In particular, in the Strand 3 projections, we are only using variants of the Hadley Centre climate model, with no multi-model information. Additionally, no parameter perturbations have been applied to the CPM, and so the CPM ensemble samples uncertainties in its driving data due to natural climate variability and parametric uncertainties in the physics of the driving models, but not uncertainty in the convective-scale model physics itself. For applications using the CPM projections, we recommend where possible augmenting the UKCP18 results with multi-model information, for example using CPM simulations becoming available as part of the CORDEX-FPS and EUCP projects.

The inclusion of multi-model information within the Strand 3 downscaled projections, and hence the sampling of structural uncertainty, will be considered as a potential future update to UKCP18. One option could be to downscale a selected subset of CMIP5 global models with the standard variant of the RCM and CPM (RCM-STD and CPM-STD), which would add the sampling of structural uncertainty in the global driving model. The effects of structural uncertainty in the downscaling model could potentially be added by using data from the EURO-CORDEX archive of multi-model RCM simulations, available (as noted above) for RCP8.5 at 12km resolution. This archive consists of a partly-filled matrix of RCM simulations contributed by several European regional modelling groups, driven by a selection of CMIP5 global models. These simulations could be screened based on historic performance to identify which are appropriate for inclusion. Similarly multi-model CPM simulations from the EUCP project, for which domains overlap the UK, could potentially be included once available. Augmenting the available regional modelling information could be particularly helpful for assessments of future risks relating to extremes, as the influence of downscaling is a major source of uncertainty in the projected changes.

Parameter perturbations in the CPM were not implemented here as it was not possible to mirror the full set of RCM parameter perturbations, given structural differences between the models. However, work is underway at the Met Office to develop a scale-aware convection scheme. Once available this will allow the same convection scheme to be used across all model resolutions, and thus will facilitate the consistent sampling of parametric uncertainties between the CPM and the driving RCM. Therefore future UKCP18 enhancements on the 5-10 year timescale may include a CPM-PPE, allowing an estimate of uncertainties in projections due to the convective-scale model physics. An important additional benefit of the scale-aware convection scheme is that this is expected to alleviate many deficiencies in the explicit convection model due to convection not being fully resolved at kilometre scales, including the overestimation of intense precipitation events.

Proposed enhancements to UKCP18 CPM projections in the shorter term include additional simulations to fill the gaps between the three 20-year time-slices (1981-2000, 2021-40 and 2061-80) presented here. In particular, this would result in a 12-member CPM ensemble being provided for continuous time series covering 1980 to 2080. This will improve the ability of users to analyse the changing contributions of forced climate change and internal variability through the 21st century, and improve sampling of extreme events for studies of climate impacts.

This report is a first look at projected changes in the CPM, focussing on temperature and precipitation, and provides initial guidance on the use of these projections in the light of other information from UKCP18. Changes in soil moisture, snow, cloud and lightning have also been considered. However, this is not a comprehensive assessment of the added value of the CPM projections. Further work is planned to assess the CPM ensemble performance for other variables and other specific applications. However, it is clear from the results here that the CPM ensemble opens up new information for decision-making. In particular, for the first-time in any national climate scenarios, these results provide an indication of uncertainties in changes at kilometre and hourly scales using physical climate modelling, and plausible projections of future changes in convective extremes. Therefore, these new climate projections will have important implications for risk assessments for a number of impact sectors.

Acknowledgment

References

Anderson G. and D. Klugmann (2014) A European lightning density analysis using 5 years of ATDnet data. Nat. Hazards Earth Syst. Sci., 14, 815-829,

Argueso, D., J.P. Evans, L. Fita, K.J. Bormann (2014) Temperature response to future urbanization and climate change, Clim Dyn, 42:2183–2199, doi 10.1007/s00382-013-1789-6

Argueso, D., J. P. Evans, A. J. Pitman, and A. Di Luca (2015) Effects of city expansion on heat stress under climate change conditions. PLoS One, 10, e0117066, doi: https://doi.org/10.1371/journal.pone.0117066.

Ban, N., J. Schmidli, and C. Schar (2014) Evaluation of the convection-resolving regional climate modeling approach in decade-long simulations. J. Geophys. Res. Atmos., 119, 7889–7907, doi: https://doi.org/10.1002/2014JD021478.

Ban, N., J. Schmidli, and C. Schar (2015) Heavy precipitation in a changing climate: Does short-term summer precipitation increase faster? Geophys. Res. Lett., 42, 1165–1172, doi: https://doi.org/10.1002/2014GL062588

Belušić A., Telišman P.M., Güttler I., Ban N., Leutwyler D., Schär C. (2018) Near-surface wind variability over the broader Adriatic region: insights from an ensemble of regional climate models, Clim. Dyn., 50 (11-12), 4455–4480, http://dx.doi.org/10.1007/s00382-017-3885-5

Bennett, A. J., C. Gaffard, J. Nash, G. Callaghan, and N. C. Atkinson (2011) The Effect of Modal Interference on VLF Long-Range Lightning Location Networks Using the Waveform Correlation Technique, Journal of Atmospheric and Oceanic Technology, doi: 10.1175/2011JTECHA1527.1

Berthou, S., E.J. Kendon, S.C. Chan, N. Ban, D. Leutwyler, C. Schär, G. Fosser (2018) Pan-European climate at convection-permitting scale: a model intercomparison study. Clim. Dyn., https://doi.org/10.1007/s00382-018-4114-6

Best, M. J., Pryor, M., Clark, D. B., Rooney, G. G., Essery, R. L. H., Ménard, C. B., Edwards, J. M., Hendry, M. A., Porson, A., Gedney, N., Mercado, L. M., Sitch, S., Blyth, E., Boucher, O., Cox, P. M., Grimmond, C. S. B., and Harding, R. J. (2011) The Joint UK Land Environment Simulator (JULES), model description – Part 1: Energy and water fluxes, Geosci. Model Dev., 4, 677–699, doi:10.5194/gmd-4-677-2011.

Beven, K. and Kirkby, M. J. (1979) A physically based, variable contributing area model of basin hydrology, Hydrol. Sci. B., 24, 43–69.

Bond T.C., Bergstrom R.W. (2006). Light absorption by carbonaceous particles: An investigative review. Aerosol Sci. Technol. 40, 27–67, https://doi.org/10.1080/02786820500421521

Boorman, P., G. Jenkins, J. Murphy, K. Burgess (2010) Future changes in lightning from the UKCP09 ensemble of regional climate model projections, UKCP09 technical note, Met Office Hadley Centre, Exeter, UK.

Boutle, I. A., S. J. Abel, P. G. Hill, and C. J. Morcrette (2014) Spatial variability of liquid cloud rain: Observations and microphysical effects. Quart. J. Roy. Meteor. Soc., 140, 583–594, https://doi.org/10.1002/qj.2140.

Boutle, I.A., Finnenkoetter, A., Lock, A. P., and Wells, H. (2016) The London Model: forecasting fog at 333 m resolution, Q. J. Roy. Meteor. Soc., 142, 360–371, https://doi.org/10.1002/qj.2656

Brockhaus, P. and Lüthi, D. and Schär, C. (2008) Aspects of the diurnal cycle in a regional climate model Meteorol. Z.,17, 433-443, doi: 10.1127/0941-2948/2008/0316

Brooks R.H., Corey A.T. (1964). Hydraulic properties of porous media. Hydrol. Pap. 3, Colorado State University, Fort Collins, 27 pp.

Brown, A. R., Derbyshire, S. H., and Mason, P. J. (1994) 'Large-Eddy Simulation of Stable Atmospheric Boundary Layers with a Revised Stochastic Subgrid Model', Quart. J. Roy. Meteorol. Soc. 120, 1485–1512.

Burke E.J., Perry R.H.J., Brown S.J. (2010). An extreme value analysis of UK drought and projections of change in the future. J. Hydrol. 388:131-143

Bush, M., T. Allen, C. Bain, I. Boutle, J. Edwards, A. Finnenkoetter, C. Franklin, K. Hanley, H. Lean, A. Lock, J. Manners, M. Mittermaier, C. Morcrette, R. North, J. Petch, C. Short, S. Vosper, D. Walters, S. Webster, M. Weeks, J. Wilkinson, N. Wood and M. Zerroukat (2019) The first Met Office Unified Model/JULES Regional Atmosphere and Land configuration, RAL1. Geoscientific Model Development Discussions, https://doi.org/10.5194/gmd-2019-130

Chan S.C., E.J. Kendon, H.J. Fowler, S. Blenkinsop, C.A.T. Ferro, D.B. Stephenson (2013) Does increasing spatial resolution improve the simulation of United Kingdom daily precipitation in a regional climate model? Clim Dyn. Doi: 10.1007/s00382-012-1568-9

Chan S.C., E.J. Kendon, H.J. Fowler, S. Blenkinsop, N.M. Roberts, C.A.T. Ferro (2014) The value of high-resolution Met Office regional climate models in the simulation of multi-hourly precipitation extremes. J Climate, 27, 16, 6155-6174, doi 10.1175/JCLIM-13-00723.1

Chan S.C., E.J. Kendon, N.M. Roberts, H.J. Fowler and S. Blenkinsop (2016) Downturn in scaling of UK extreme rainfall with temperature for future hottest days, Nature Geoscience, doi: 10.1038/NGEO2596

Coles, S. (2001) An introduction to statistical modeling of extreme values. Springer, London.

Coppola, E, S. Sobolowski, E. Pichelli, F. Raffaele, B. Ahrens, I. Anders, N. Ban, S. Bastin, M. Belda, D. Belusic, A. Caldas Alvarez, R. M. Cardoso, S. Davolio, A. Dobler, J. Fernandez, L. Fita, Q. Fumiere, F. Giorgi, K. Goergen, I. Güttler, T. Halenka, D. Heinzeller, Ø. Hodnebrog, D. Jacob, S. Kartsios, E. Katragkou, E. Kendon, S. Khodayar, H. Kunstmann, S. Knist, A. Lavín Gullón, P. Lind, T. Lorenz, D. Maraun, L. Marelle, E. van Meijgaard, J. Milovac, G. Myhre, H. J. Panitz, M. Piazza, M. Raffa, T. Raub, B. Rockel, C. Schär, K. Sieck, P. M. M. Soares, S. Somot, L. Srnec, P. Stocchi, M. H. Tölle, H. Truhetz, R. Vautard, H. de Vries, K. Warrach Sagi (2018) A first-of-its-kind multi-model convection permitting ensemble for investigating convective phenomena over Europe and the Mediterranean. Climate Dynamics. doi: https://doi.org/10.1007/s00382-018-4521-8

Dai A. (2016) Precipitation Characteristics in Eighteen Coupled Climate Models, J Climate, 19, 4605-4630

Dale, M., A. Hosking, E. Gill, E. Kendon, H. J. Fowler, S. Blenkinsop, S. Chan (2018) Understanding how changing rainfall may impact on urban drainage systems; lessons from projects in the UK and USA. Water Practice and Technology, 13 (3): 654-661. https://doi.org/10.2166/wpt.2018.069

Dale, M., B. Luck, H. J. Fowler, S. Blenkinsop, E. Gill, J. Bennett, E. J. Kendon, and S. C. Chan (2016) New climate change rainfall estimates for sustainable drainage. Proc. Inst. Civ. Eng.: Eng. Sustainability, doi: https://doi.org/10.1680/jensu.15.00030

Dee D.P., and co-authors (2011). The ERA-Interim reanalysis: configuration and performance of the data assimilation system. Q. J. R. Meteorol. Soc. 137:553-597

Done, J., C. A. Davis, and M. L. Weisman (2004): The next generation of NWP: Explicit forecasts of convection using the weather research and forecasting (WRF) model. Atmos. Sci. Lett., 5, 110–117, doi: https://doi.org/10.1002/asl.72.

Edwards, J. M., and A. Slingo (1996) Studies with a flexible new radiation code. I: Choosing a configuration for a large-scale model. Quart. J. Roy. Meteor. Soc., 122, 689–720, https://doi.org/10.1002/qj.49712253107.

Enno, S-E., G. Anderson, and J. Sugier (2016) ATDnet Detection Efficiency and Cloud Lightning Detection Characteristics from Comparison with the HyLMA during HyMeX SOP1, Journal of Atmospheric and Oceanic Technology, doi:10.1175/JTECH-D-15-0256.1

Fierro, A. O., E.R. Mansell, D.R. MacGorman, and C.L. Ziegler (2013) The Implementation of an Explicit Charging and Discharge Lightning Scheme within the WRF-ARW Model: Benchmark Simulations of a Continental Squall Line, a Tropical Cyclone, and a Winter Storm, Mon. Weather Review, doi:10.1175/MWR-D-12-00278.1

Finney D.L., R. M. Doherty, O. Wild, D. S. Stevenson, I. A. MacKenzie & A. M. Blyth (2018) A projected decrease in lightning under climate change, Nature Climate Change, 8, 210–213

Forbes, R., and C. Halliwell (2003) Assessment of the performance of an enhanced microphysics parametrization scheme in the Unified Model at 1 km resolution. Met Office Internal Rep., 40 pp.

Fosser, G., S. Khodayar, and P. Berg (2015) Benefit of convection permitting climate model simulations in the representation of convective precipitation. Climate Dyn., 44, 45–60, doi: https://doi.org/10.1007/s00382-014-2242-1

Fosser, G., S. Khodayar, and P. Berg (2017) Climate change in the next 30 years: what can a convection-permitting model tell us that we did not already know? Climate Dyn., doi: https://doi.org/10.1007/s00382-016-3186-4

Fosser, G., E. Kendon, S. Chan, A. Lock, N. Roberts and M. Bush (submitted) Optimal configuration and resolution for the first convection-permitting ensemble of climate projections over the UK. Submitted to Int. J. Climatol.

Fuller, R.M., Groom, G.B. and Jones, A.R. (1994). The Land Cover Map of Great Britain: an automated classification of Landsat Thematic Mapper data. Photogrammetric Engineering ∓ Remote Sensing, 60, 553-562.

Fung F. and Gawith M. (2018). UKCP18 for UKCP09 Users, UKCP18 Guidance. Met Office, Hadley, Centre, Exeter. Available from https://www.metoffice.gov.uk/binaries/content/assets/metofficegovuk/pdf/research/ukcp/ukcp18-guidance-ukcp18-for-ukcp09-users.pdf

Fung F., Lowe J., Mitchell J.F.B., Murphy J., Bernie D., Gohar L., Harris G., Howard T., Kendon E.J., Maisey P., Palmer M. and Sexton D. (2018). UKCP18 Guidance: How to use the UKCP18 Land Projections. Met Office Hadley Centre, Exeter.

Giorgi F., Jones C., Asrar G. (2009) Addressing climate information needs at the regional level: the CORDEX framework. WMO Bull., 58:175–83.

Gregersen, I.B., H.J.D. Sorup, H. Madsen, D. Rosbjerg, P.S. Mikkelsen and K. Arnbjerg-Nielsen (2013) Assessing future climatic changes of rainfall extremes at small spatio-temporal scales Clim. Change, 118, 3-4, 783-797, doi: 10.1007/s10584-012-0669-0

Gregory, D., and P. R. Rowntree (1990) A mass flux convection scheme with representation of cloud ensemble characteristics and stability-dependent closure. Mon. Wea. Rev., 118, 1483–1506.

Hanel M. and T. Adri Buishand (2010) On the value of hourly precipitation extremes in regional climate model simulations, J. Hydrol., 393, 265-273, doi:10.1016/j.jhydrol.2010.08.024

Hanley, K. E., R. S. Plant, T. H. M. Stein, R. J. Hogan, J. C. Nicol, H. W. Lean, C. Halliwell, and P. A. Clark (2015) Mixing length controls on high resolution simulations of convective storms. Quart. J. Roy. Meteor. Soc., 141, 272–284, doi: https://doi.org/10.1002/qj.2356

Harrison D.L., S. J. Driscoll and M. Kitchen (2000) Improving precipitation estimates from weather radar using quality control and correction techniques, Meteorol. Appl. 6, 135–144, doi: 10.1017/S1350482700001468

Hazeleger, W., B.J.J.M. van den Hurk, E. Min, G.J. van Oldenborgh, A.C. Petersen, D.A. Stainforth, E. Vasileiadou & L.A. Smith (2015) Tales of future weather, Nature Climate Change, 5, 107–113

Herger N., B.M. Sanderson, R. Knutti (2015) Improved pattern scaling approaches for the use in climate impact studies: Improved Pattern Scaling Approaches, GRL, doi: 10.1002/2015GL063569

Hewitt C.D. and J.A. Lowe (2018) Toward a European Climate Prediction System, BAMS, doi: 10.1175/BAMS-D-18-0022.1

Hosking, J. R. M., and J. R. Wallis (1993) Some statistics useful in regional frequency analysis. Water Resources Research, 29, 271–281, doi:10.1029/92WR01980.

Huntingford, C., T Marsh, A. A. Scaife, E. J. Kendon, J. Hannaford, A. L. Kay, M. Lockwood, C. Prudhomme, N. S. Reynard, S. Parry, J. A. Lowe, J. A. Screen, H. C. Ward, M. Roberts, P. A. Stott, V. A. Bell, M. Bailey, A. Jenkins, T. Legg, F. E. L. Otto, N. Massey, N. Schaller, J. Slingo & M. R. Allen (2014) Potential influences on the United Kingdom's floods of winter 2013/14, Nature Climate Change, 4, 769–777

Hurtt G.C., Chini L.P., Frolking S., Betts R., Feddema J., Fischer G., Fisk J.P., Hibbard K., Houghton R.A., Janetos A., Jones C., Kindermann G., Kinoshita T., Klein Goldewijk K., Riahi K., Shevliakova E., Smith S., Stehfest E., Thomson A., Thornton P., van Vuuren D.P. and Wang Y. (2011) Harmonization of land-use scenarios for the period 1500-2100: 600 years of global gridded annual land-use transitions, wood harvest, and resulting secondary lands. Clim Change, 109, 117-161.

Jacob, D., J. Petersen, B. Eggert, A. Alias, O. B. Christensen, L. M. Bouwer, A. Braun, A. Colette, M. Déqué, G. Georgievski, E. Georgopoulou, A. Gobiet, L. Menut, G. Nikulin, A. Haensler, N. Hempelmann, C. Jones, K. Keuler, S. Kovats, N. Kröner, S. Kotlarski, A. Kriegsmann, E. Martin, E. van Meijgaard, C. Moseley, S. Pfeifer, S. Preuschmann, C. Radermacher, K. Radtke, D. Rechid, M. Rounsevell, P. Samuelsson, S. Somot, J-F. Soussana, C. Teichmann, R. Valentini, R. Vautard, B. Weber and P. Yiou (2014) EURO-CORDEX: new high-resolution climate change projections for European impact research, Regional Environmental Change, 14, 2, 563-578, https://doi.org/10.1007/s10113-013-0499-2

Jenkins G.J., Murphy J.M., Sexton D.M.H., Lowe J.A., Jones P., Kilsby C.G. (2009). UK Climate Projections: Briefing Report. Met Office Hadley Centre, Exeter, UK.

Jones P., Kilsby C., Harpham C., Glenis V., Burton A. (2010). UK Climate Projections Science Report: Projections of Future Daily Climate for the UK from the Weather Generator. University of Newcastle, UK. Available from https://webarchive.nationalarchives.gov.uk/20181204111018/http://ukclimateprojections-ukcp09.metoffice.gov.uk/

Karlsson, K.-G., Anttila, K., Trentmann, J., Stengel, M., Meirink, J. F, Devasthale, A., Hanschmann, T., Kothe, S., Jääskeläinen, E., Sedlar, J., Benas, N., van Zadelhoff, G.-J., Schlundt, C., Stein, D., Finkensieper, S., Håkansson, N., and Hollmann, R. (2017) CLARA-A2: the second edition of the CM SAF cloud and radiation data record from 34 years of global AVHRR data, Atmos. Chem. Phys., 17, 5809-5828, doi:10.5194/acp-17-5809-2017.

Kay A., Jones R. (2012). Comparison of the use of alternative UKCP09 products for modelling the impacts of climate change on flood frequency. Clim. Change 114:211-230.

Kendon, E. J., N. M. Roberts, C. A. Senior, and M. J. Roberts (2012) Realism of rainfall in a very high resolution regional climate model. J. Climate, 25, 5791–5806, doi: https://doi.org/10.1175/JCLI-D-11-00562.1

Kendon E.J., N.M. Roberts, H.J. Fowler, M.J. Roberts, S.C. Chan and C.A. Senior (2014), Heavier summer downpours with climate change revealed by weather forecast resolution model, Nature Climate Change, 4, 570-576, doi: 10.1038/NCLIMATE2258

Kendon E.J., N. Ban, N.M. Roberts, H.J. Fowler, M.J. Roberts, S.C. Chan, J.P. Evans, G. Fosser and J. M. Wilkinson (2017) Do convection-permitting regional climate models improve projections of future precipitation change? BAMS, 98 (1), 79-, doi: 10.1175/BAMS-D-15-0004.1

Kendon E.J., R.A. Stratton, S. Tucker, J.H. Marsham, S. Berthou, D.P. Rowell and C.A. Senior (2019) Enhanced future changes in wet and dry extremes over Africa at convection-permitting scale. Nature Comms. doi: 10.1038/s41467-019-09776-9

Kirchner-Bossi, N., Kendon E.J., Fowler H.J., Dawson R.J., Wilkinson S.M. (submitted) Present and Future Wind Gust Climatology using a Convection-Permitting Climate Model over the Southern UK, submitted to IJOC

Kjellström, E., Nikulin, G., Strandberg, G., Christensen, O. B., Jacob, D., Keuler, K., Lenderink, G., van Meijgaard, E., Schär, C., Somot, S., Sørland, S. L., Teichmann, C., and Vautard, R. (2018) European climate change at global mean temperature increases of 1.5 and 2 °C above pre-industrial conditions as simulated by the EURO-CORDEX regional climate models, Earth Syst. Dynam., 9, 459-478, https://doi.org/10.5194/esd-9-459-2018.

Knote, C., G. Heinemann, and B. Rockel (2010) Changes in weather extremes: Assessment of return values using high resolution climate simulations at convection-resolving scale. Meteor. Z., 19, 11–23, doi: https://doi.org/10.1127/0941-2948/2010/0424.

Kotlarski, S., Keuler, K., Christensen, O. B., Colette, A., Déqué, M., Gobiet, A., and Wulfmeyer, V. (2014). Regional climate modeling on European scales: A joint standard evaluation of the EURO-CORDEX RCM ensemble. Geoscientific Model Development, 7(4), 1297–1333. https://doi.org/10.5194/gmd-7-1297-2014

Lean, H., and K. Browning (2013) Quantification of the importance of wind drift to the surface distribution of orographic rain on the occasion of the extreme Cockermouth flood in Cumbria, QJRMS, 139, 1342-1353.

Lean, H. W., P. A. Clark, M. Dixon, N. M. Roberts, A. Fitch, R. Forbes, and C. Halliwell, (2008) Characteristics of high-resolution versions of the Met Office Unified Model for forecasting convection over the United Kingdom. Mon. Wea. Rev., 136, 3408–3424, doi: https://doi.org/10.1175/2008MWR2332.1.

Lenderink G. and E. van Meijgaard (2008) Increase in hourly precipitation extremes beyond expectations from temperature changes, Nature Geosci., 1, 511-514

Lewis, E., N. Quinn, S. Blenkinsop, H. J. Fowler, J. Freer, M. Tanguy, O. Hitt, G. Coxon, P. Bates, R. Woods (2018) A rule based quality control method for hourly rainfall data and a 1 km resolution gridded hourly rainfall dataset for Great Britain: CEH-GEAR1hr, Journal of Hydrology, 564, 930–943

Lilly D.K. (1962) On the Numerical Simulation of Buoyant Convection, Tellus, 14, 2, pp.148-172.

Lind, P., Lindstedt, D., Kjellström, E., and Jones, C (2016) Spatial and Temporal Characteristics of Summer Precipitation over Central Europe in a Suite of High- Resolution Climate Models. J Clim, 3501-3518. doi:10.1175/JCLI-D-15-0463.1.

Liu C., Ikeda K., Rasmussen R., Barlage M., Newman A.J., Prein A.F., Chen F., Chen L., Clark M., Dai A., Dudhia J., Eidhammer T., Gochis D., Gutmann E., Kurkute S., Li Y., Thompson G., Yates D. (2016) Continental-scale convection-permitting modeling of the current and future climate of North America. Clim Dyn. https://doi.org/10.1007/s00382-016-3327-9

Liu Y., Daum P.H., Guo H., Peng Y. (2008). Dispersion bias, dispersion effect, and the aerosol-cloud conundrum. Environ. Res. Lett. 3:045021, doi:10.1088/1748-9326/3/4/045021.

Lock, A. P., A. R. Brown, M. R. Bush, G. M. Martin, and R. N. B. Smith (2000) A new boundary layer mixing scheme. Part I: Scheme description and single-column model tests. Mon. Wea. Rev., 128, 3187–3199, https://doi.org/10.1175/1520-0493(2000)128%3C3187:ANBLMS%3E2.0.CO;2

Lowe J.A., Bernie D., Bett P., Bricheno L., Brown S., Calvert D., Clark R., Eagle K., Edwards T., Fosser G., Fung F., Gohar L., Good P., Gregory J., Harris G., Howard T., Kaye N., Kendon E., Krijnen J., Maisey P., McDonald R., McInnes R., McSweeney C., Mitchell J.F.B., Murphy J., Palmer M., Roberts C., Rostron J., Sexton D., Thornton H., Tinker J., Tucker S., Yamazaki K., Belcher S. (2018). UKCP18 Science Overview Report. Available from https://www.metoffice.gov.uk/research/collaboration/ukcp/guidance-science-reports

McCaul, E. W., S. J. Goodman, K. M. LaCasse, and D. J. Cecil (2009) Forecasting lightning threat using cloud-resolving model simulations. Wea. Forecasting, 24, 709–729, doi: https://doi.org/10.1175/2008WAF2222152.1.

McColl L., Palin E.J., Thornton H.E., Sexton D.M.H., Betts R., Mylne K. (2012) Assessing the potential impact of climate change on the UK's electricity network. Clim. Change 115:821-835.

Moore, R. J. (2007) The PDM rainfall-runoff model. Hydrol. Earth Syst. Sci. 11 (1) 483-499.

Murphy, J.M., G.R. Harris, D.M.H. Sexton, E.J. Kendon, P.E. Bett, R.T. Clark, K.E. Eagle, G. Fosser, F. Fung, J.A. Lowe, R.E. McDonald, R.N. McInnes, C.F. McSweeney, J.F.B. Mitchell, J.W. Rostron, H.E. Thornton, S. Tucker and K. Yamazaki (2018) UKCP18 Land Projections: Science Report. Available from https://www.metoffice.gov.uk/research/collaboration/ukcp/guidance-science-reports

Palin E.J., Thornton H.E., Mathison C.T., McCarthy R.E., Clark R.T., Dora J. (2013) Future projections of temperature-related climate change impacts on the railway network of Great Britain. Clim. Change 120:71-93.

Perry, M. and Hollis, D. (2005) The generation of monthly gridded datasets for a range of climatic variables over the UK. Int. J. Climatol., 25: 1041-1054. doi:10.1002/joc.1161

Perry, M.C., Hollis, D.M., and Elms, M.I. (2009) The generation of daily gridded data sets of temperature and rainfall for the UK, NCIC Climate Memorandum No. 24. Met Office: Exeter, UK.

Porson A., Clark P.A., Harman I.N., Best M.J. and Belcher S.E. (2010) Implementation of a new urban energy budget scheme in the MetUM. Part I: Description and idealized simulations. Quarterly Journal of the Royal Meteorological Society, 136, 1514–1529

Price, C. & Rind, D (1994) Possible implications of global climate change on global lightning distributions and frequencies. J. Geophys. Res. 99, 10823–10831

Prudhomme C., Young A., Watts G., Haxton C., Crooks S., Williamson J., Davies H., Dadson S., Allen S. (2012) The drying up of Britain? A national estimate of changes in seasonal river flows from 11 Regional Climate Model simulations. Hydrol. Proc. 2:1115-1118.

Rajczak J. and Schär C. (2017) Projections of future precipitation extremes over Europe: A multimodel assessment of climate simulations. J Geophys Res Atmos, 122, 10773-10800

Rasmussen, R., and co-authors, (2014) Climate change impacts on the water balance of the Colorado headwaters: High-resolution regional climate model simulations. J. Hydrometeor., 15, 1091–1116, doi: https://doi.org/10.1175/JHM-D-13-0118.1

Reynolds R.W., Rayner N.A., Smith T.M., Stokes D.C., Wang W. (2002) An improved in situ and satellite SST analysis for climate. J. Clim. 15:1609-1625

Roberts, N. M. (2003) The impact of a change to the use of the convection scheme to high-resolution simulations of convective events. Met Office Tech. Rep. 407, 30 pp.

Roberts, N. M., and H. W. Lean (2008) Scale-selective verification of rainfall accumulations from high resolution forecasts of convective events. Mon. Wea. Rev., 136, 78–97.

Sanderson M.G., Wiltshire A., Betts R.A. (2012). Projected changes in water availability in the United Kingdom. Water Resources Res. 48:W08512

Smagorinsky, J. (1963) General circulation experiments with the primitive equations. Part 1: The basic experiment. Mon. Wea. Rev., 91, 99–164, https://doi.org/10.1175/1520-0493(1963)091%3C0099:GCEWTP%3E2.3.CO;2

Smith, R. N. B. (1990) A scheme for predicting layer clouds and their water content in a general circulation model. Quart. J. Roy. Meteor. Soc., 116, 435–460, https://doi.org/10.1002/qj.49711649210

Stephens, G.L., T. L'Ecuyer, R. Forbes, A. Gettlemen, J-C. Golaz, A. Bodas-Salcedo, K. Suzuki, P. Gabriel and J. Haynes (2010) The dreary state of precipitation in global models. J. Geophys Res, doi: 10.1029/2010JD014532

Stevens, B., S. Fiedler, S. Kinne, K. Peters, S. Rast, J. Müsse, S. J. Smith, and T. Mauritsen (2017) MACv2-SP: a parameterization of anthropogenic aerosol optical properties and an associated Twomey effect for use in CMIP6, Geosci. Model Dev., 10, 433-452, doi: 10.5194/gmd-10-433-2017

Tang, Y., H. Lean, and J. Bornemann (2013) The benefits of the Met Office variable resolution NWP model for forecasting convection. Meteor. Appl., 20, 417–426, https://doi.org/10.1002/met.1300

Tennant, W. (2015) Improving initial condition perturbations for MOGREPS-UK. Quart. J. Roy. Meteor. Soc., 141, 2324–2336, doi: 10.1002/qj.2524.

Van Genuchten, M.T. (1980). "A closed-form equation for predicting the hydraulic conductivity of unsaturated soils". Soil Science Society of America Journal. 44 (5): 892–898. doi:10.2136/sssaj1980.03615995004400050002x.

Walters, D., I. Boutle, M. Brooks, T. Melvin, R. Stratton, S. Vosper, H. Wells, K. Williams, N. Wood, T. Allen, A. Bushell, D. Copsey, P. Earnshaw, J. Edwards, M. Gross, S. Hardiman, C. Harris, J. Heming, N. Klingaman, R. Levine, J. Manners, G. Martin, S. Milton, M. Mittermaier, C. Morcrette, T. Riddick, M. Roberts, C. Sanchez, P. Selwood, A. Stirling, C. Smith, D. Suri, W. Tennant, P. L. Vidale, J. Wilkinson, M. Willett, S. Woolnough, and P. Xavier (2017) The Met Office Unified Model Global Atmosphere 6.0/6.1 and JULES Global Land 6.0/6.1 configurations, Geosci. Model Dev., 10, 1487–1520, doi:10.5194/gmd-10-1487-2017

Walters, D., A. Baran, I. Boutle, M. Brooks, P. Earnshaw, J. Edwards, K. Furtado, P. Hill, A. Lock, J. Manners, C. Morcrette, J. Mulcahy, C. Sanchez, C. Smith, R. Stratton, W. Tennant, L. Tomassini, K. Van Weverberg, S. Vosper, M. Willett, J. Browse, A. Bushell, M. Dalvi, R. Essery, N. Gedney, S. Hardiman, B. Johnson, C. Johnson, A. Jones, G. Mann, S. Milton, H. Rumbold, A. Sellar, M. Ujiie, M. Whitall, K. Williams and M. Zerroukat (2019) The Met Office Unified Model Global Atmosphere 7.0/7.1 and JULES Global Land 7.0 configurations, Geosci. Model Dev., 12, 1909-1963, doi: 10.5194/gmd-2017-291

Weedon, G. P., G. Balsamo, N. Bellouin, S. Gomes, M. J. Best, P. Viterbo (2014) The WFDEI meteorological forcing data set: WATCH Forcing Data methodology applied to ERA-Interim reanalysis data, Water Resources Research, doi: 10.1002/2014WR015638

Weisman, M. L., C. Davis, W. Wang, K. W. Manning, and J. B. Klemp (2008) Experiences with 0-36-h explicit convective forecasts with the WRF-ARW model. Wea. Forecasting, 23, 407–437, doi: https://doi.org/10.1175/2007WAF2007005.1.

Weusthoff, T., F. Ament, M. Arpagaus, and M. W. Rotach (2010): Assessing the benefits of convection-permitting models by neighborhood verification: Examples from MAP D-PHASE. Mon. Wea. Rev., 138, 3418–3433, doi: https://doi.org/10.1175/2010MWR3380.1.

Wilkinson, J. M. and Bornemann, F. J. (2014) A lightning forecast for the London 2012 Olympics opening ceremony, Weather, 69: 16–19 doi: 10.1002/wea.2176

Williams K.D., Copsey D., Blockley E.W., Bodas-Salcedo A., Calvert D., Comer R., Davis P., Graham T., Hewitt H.T., Hill R., Hyder P., Ineson S., Johns T.C., Keen A.B., Lee R.W., Megann A., Milton S.G., Rae J.G.L., Roberts M.J., Scaife A.A., Schiemann R., Storkey D., Thorpe L., Watterson I.G., Walters D.N., West A., Wood R.A., Woollings T., Xavier P.K. (2018). The Met Office Global Coupled model 3.0 and 3.1 (GC3.0 & GC3.1) configurations. J. Adv. Model. Earth. Sys. 10:357-380.

Wilson, D. R., and S. P. Ballard (1999) A microphysically based precipitation scheme for the UK Meteorological Office Unified Model. Quart. J. Roy. Meteor. Soc., 125, 1607–1636, https://doi.org/10.1002/qj.49712555707

Wilson D.R., Bushell A.C., Kerr-Munslow A.M., Price J.D., Morcrette C.J. (2008). PC2: A prognostic cloud fraction and condensation scheme. I: Scheme description. Q. J. R. Meteorol. Soc. 134:2093-2107, doi:10.1002/qj.333.

Wood N., Staniforth A., White A., Allen T., Diamantakis M., Gross M., Melvin T., Smith C., Vosper S., Zerroukat M., Thuburn J. (2014). An inherently mass-conserving semi-implicit semi-Lagrangian discretisation of the deep-atmosphere global nonhydrostatic equations. Q. J. R. Meteorol. Soc. 140:1505–1520, doi:10.1002/qj.2235.

Zappa G. and T.G. Shepherd (2017) Storylines of Atmospheric Circulation Change for European Regional Climate Impact Assessment, J Climate, doi: https://doi.org/10.1175/JCLI-D-16-0807.1

Zerroukat, M. and B. Shipway (2017) ZLF (Zero Lateral Flux): A simple mass conservation method for semi-Lagrangian based limited area models, Quarterly Journal of the Royal Meteorological Society, Vol. 143, 2578-2584

Appendix A: Regional frequency analysis of extremes

To allow a more robust calculation of return levels for higher return periods, we carry out a regional frequency analysis following Hoskins and Wallis (1993). For this we divide the UK into three sub-regions, chosen to be approximately uniform in terms of their precipitation climatology. We fit a Generalised-Pareto Distribution (GPD) to extremes of daily maximum hourly precipitation at each grid box (see Section 3.5). Then for each UK sub-region and each ensemble member, we take the GPD scale and shape parameters obtained from each grid box in the region. The shape parameter is averaged over the entire region to give a single regional value. The locally fitted scale parameter is normalised by the 2-year return level minus the local percentile threshold (which is either 99.5th percentile for annual data or 99.0th percentile for seasonal data). This normalised scale parameter is then averaged over the entire region. Using the regional normalised scale and shape parameter values, the regional growth curve (the rate of increase in extremes with return period) is computed. The return level at each grid box is then obtained by first multiplying the growth curve by the local normalisation value (2-year return level less the local threshold), and then secondly adding the local threshold back. The return levels obtained using this regional frequency analysis method are then spatially averaged across the region.
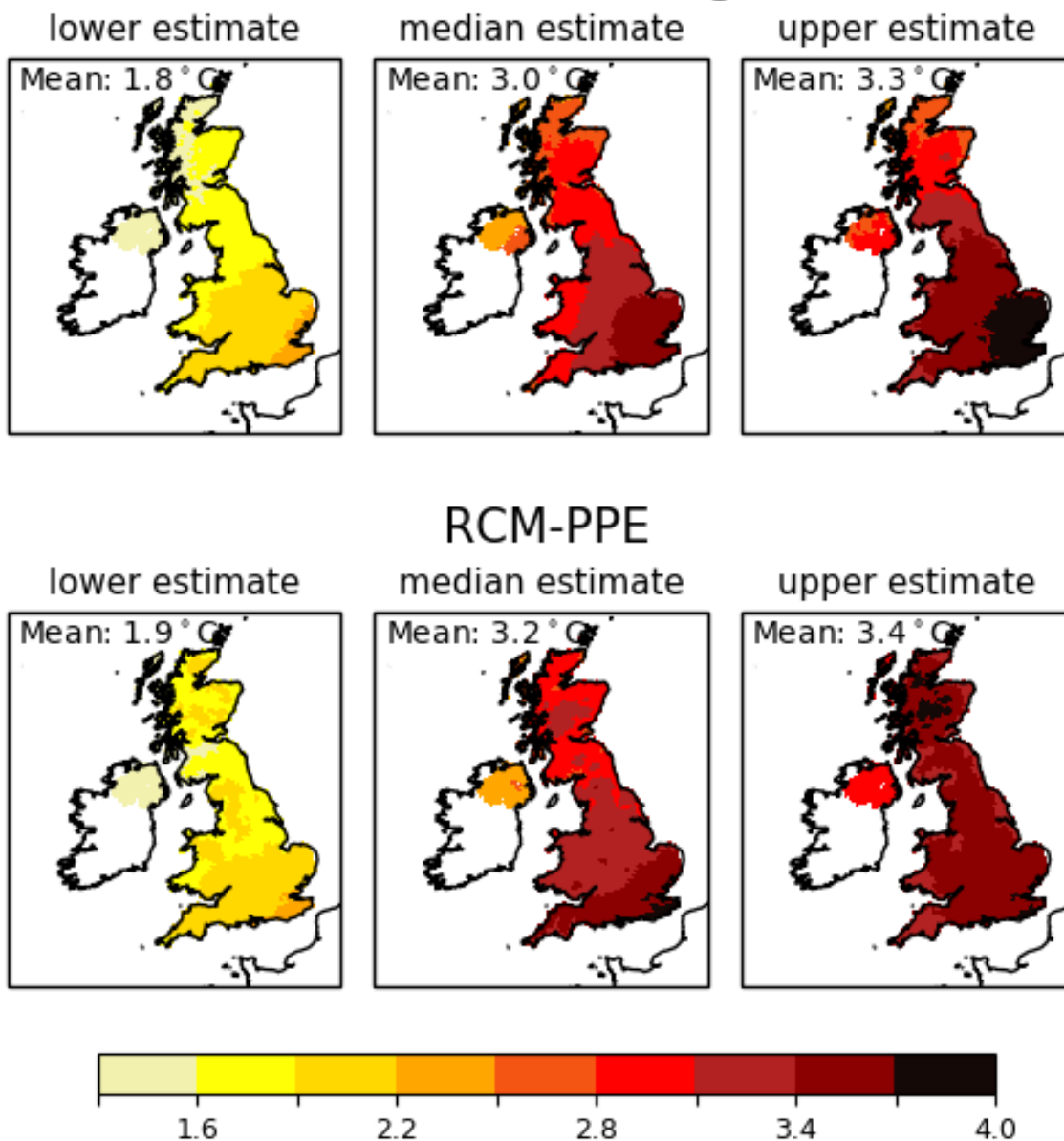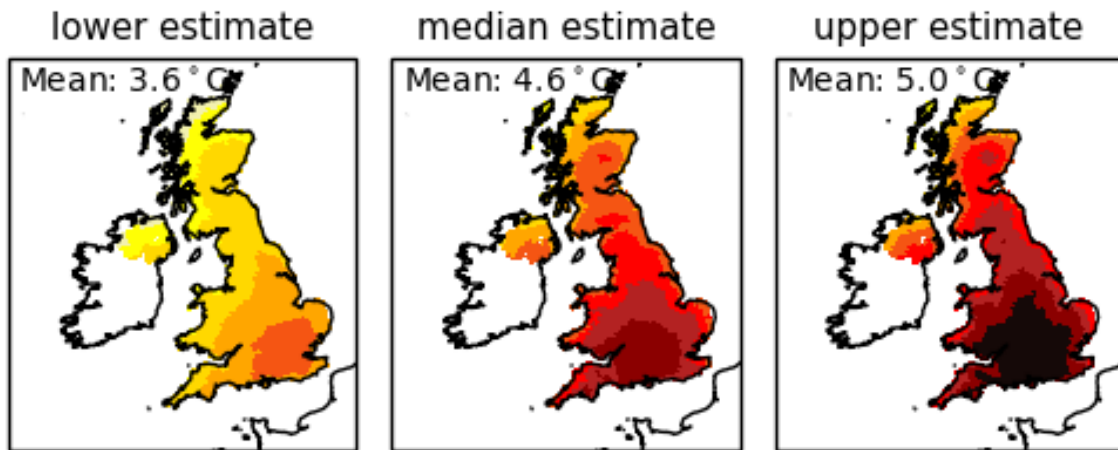
Appendix B: Individual member responses

Figure B1.1. Future change in winter mean temperature for individual members. Maps of changes in winter surface air temperature for 2061-2080 relative to 1981-2000 under RCP8.5 emissions, from individual projections selected from (top) CPM-12 regridded to 12km RCM grid and (bottom) RCM-PPE. The projections are selected by ranking the UK-average changes, and selecting those giving the (left) 2nd lowest, (centre) central and (right) 2nd highest values within the set of 12 members.

TS3 MINUS TS1 seasonal mean tas jja tas (˚C)
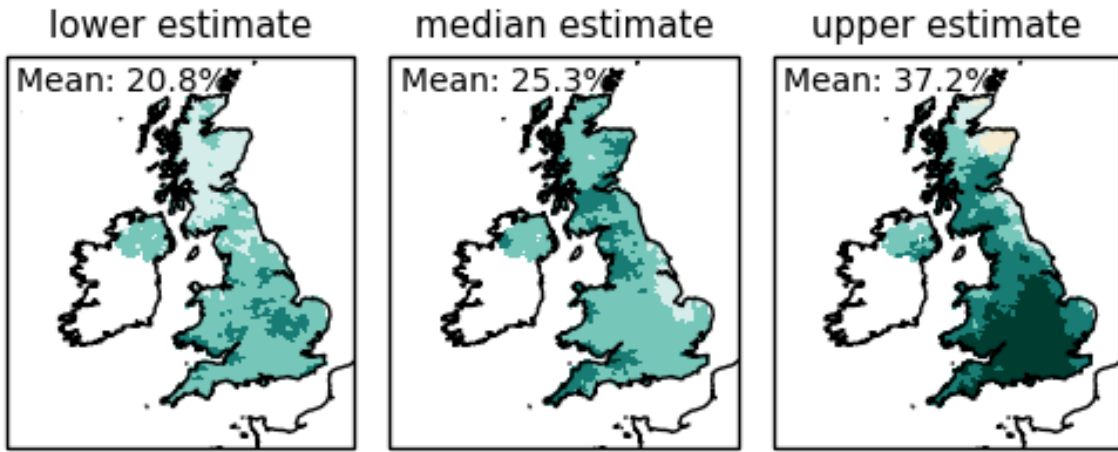upper, median & lower estimates across PPE

Figure B1.2. Future change in summer mean temperature for individual members. As Fig B1.1, but for summer mean temperature.

TS3 MINUS TS1 seasonal mean pr djf pr (%)
upper, median & lower estimates across PPE
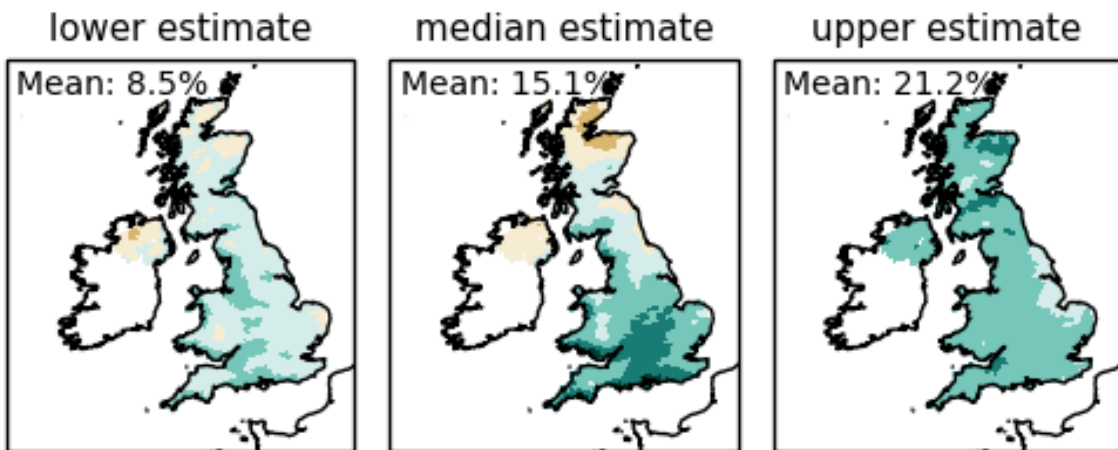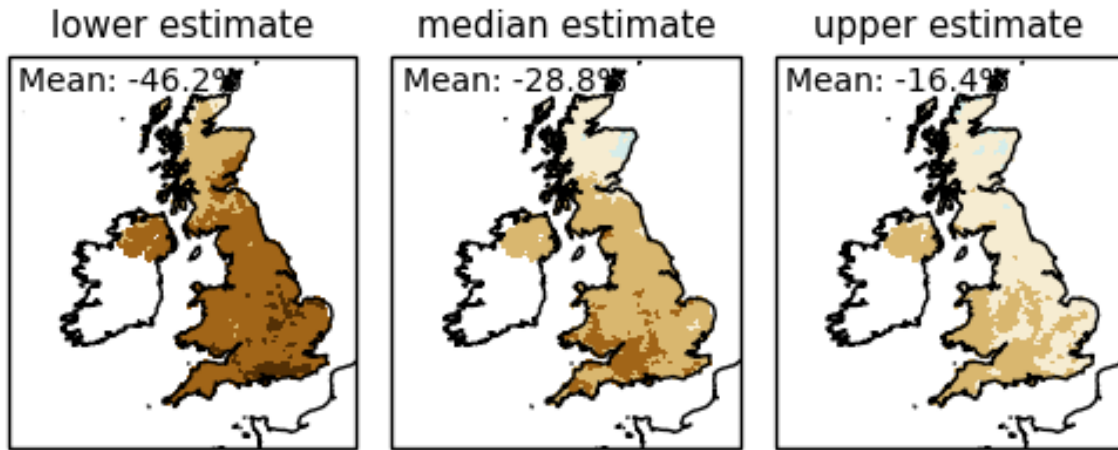
CPM-12 on 12km grid

lower estimate	median estimate	upper estimate
Mean: 20.8%	Mean: 25.3%	Mean: 37.2%

RCM-PPE

lower estimate	median estimate	upper estimate
Mean: 8.5%	Mean: 15.1%	Mean: 21.2%

−45   −15   15   45

Figure B1.3. Future change in winter mean precipitation for individual members. As Fig B1.1, but for winter mean precipitation.
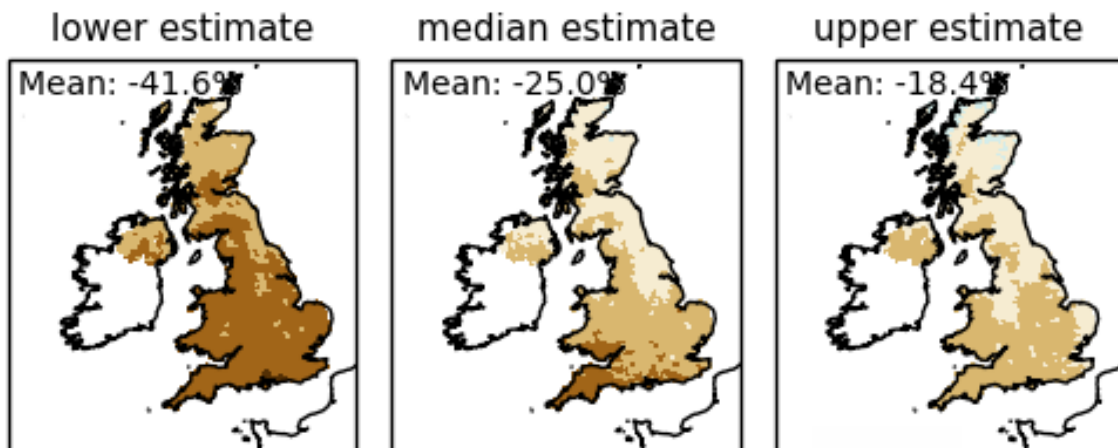
Figure B1.4. Future change in summer mean precipitation for individual members. As Fig B1.1, but for summer mean precipitation.

01048